

UNITED STATES DEPARTMENT OF THE INTERIOR  
GEOLOGICAL SURVEY

METHODS OF SIMULATION ANALYSIS APPLIED TO QUESTIONS OF  
GEOLOGICAL STABILITY OF A RADIOACTIVE WASTE DEPOSITORY IN  
BEDDED SALT

Herbert R. Shaw, Anne E. Gartner, Charlene Sontag Eng, and Leslie Casey

1980

Open-File Report

80-705

This report is preliminary and  
has not been edited or reviewed  
for conformity with  
Geological Survey standards or nomenclature

## CONTENTS

	page
AR.1. <u>Introduction</u> -----	1
AR.2. <u>Reference System for DYNAMO Simulation</u> -----	6
AR.3. <u>System Diagrams</u> -----	8
AR.4. <u>Physical Content of System Equations</u> -----	16
AR.5. <u>Computer Runs for Dissolution with and without</u> <u>Crack Closure</u> -----	31
AR.6. <u>Conclusions and Recommendations</u> -----	45

## TABLES

AR.3.1.    List of Acronyms and Initialisms in DISSCC-----	49
AR.3.2.    Annotated Listing of Equations in DISSCC-----	50
AR.3.3.    Breakdown of Equations by Type-----	51
AR.3.4.    (A-D) DYNAMO Equation Lists 4(X2) Modes of DISSCC-----	52
AR.5.1.    Example of Printout of all Variables; DISSCC OPTION 1----	53
AR.5.2.    (A,B) Examples of Printout of all Variables; DISSCC OPTION 2-----	54
AR.5.3.    Numerical Values of Constants in DISSCC-----	55
AR.5.4.    (A,B,C) Tabulation of Penetration and Overrun Times varying RCW from 1E-2 to 1E-5, other parameters held constant-----	56
AR.5.5.    (A-G) Tabulation of Penetration and Overrun Times; from Sensitivity Analysis-----	57
AR.5.6.    DYNAMO Equation Test List-OPTION 1 for Thermal Expansion Feedback-----	58
AR.5.7.    DYNAMO Equation List-OPTION 1(CLTST) CL Loop Test Program	59

## FIGURES

AR.3.1.    System Diagram for DISSCC-----	60
AR.3.2.    Schematic of Equation Ordering for DISSCC-----	61
AR.5.1.    Plot from DISSCC OPTION 1-----	62
AR.5.2.    Plots from DISSCC OPTION 2-----	63
AR.5.3.    (A-H) Computer plots of dissolution Variables versus Time, varying the Reference Crack Width, RCW from 1E-2 to 1E-5-----	64
AR.5.4.    (A and B) Penetration and Overrun Times versus Reference Crack Width, RCW; (A, B) OPTION 1, RPST 1 and 2-----	65
AR.5.5.    (A and B) Penetration and Overrun Times versus Reference Crack Width, RCW; OPTION 2, RPST 3 and 4-----	66
AR.5.6.    (A, B and C) Example of Sensitivity Result Using Raw Data; SCDIA versus CC, RCW and CC <sup>2</sup> -----	67
AR.5.7.    (A and B) Example of Sensitivity Result using Ranked Data; (A, B) SCDIA versus RCW and DCP*BMCL-----	68
AR.5.8.    (A) Threshold times as functions of SHLROM in OPTION 1(TEF)-----	69
(B) Threshold times in DISSCC OPTION 1(CLTST)-----	69
(C) Composite diagram of relative effects of initial values of heat and compaction parameters-----	69

# OPEN FILE REPORT

80-705

## TABLES

- AR.3.1. List of Acronyms and Initialisms in DISSCC-----
- AR.3.2. Annotated Listing of Equations in DISSCC-----
- AR.3.3. Breakdown of Equations by Type-----
- AR.3.4. (A-D) DYNAMO Equation Lists 4(X2) Modes of DISSCC-----
- AR.5.1. Example of Printout of all Variables; DISSCC OPTION 1----
- AR.5.2. (A,B) Examples of Printout of all Variables;  
DISSCC OPTION 2-----
- AR.5.3. Numerical Values of Constants in DISSCC-----
- AR.5.4. (A,B,C) Tabulation of Penetration and Overrun Times  
varying RCW from 1E-2 to 1E-5, other parameters  
held constant-----
- AR.5.5. (A-G) Tabulation of Penetration and Overrun Times;  
from Sensitivity Analysis-----
- AR.5.6. DYNAMO Equation Test List-OPTION 1 for Thermal  
Expansion Feedback-----
- AR.5.7. DYNAMO Equation List-OPTION 1(CLTST) CL Loop Test Program

# OPEN FILE REPORT 80-705

## FIGURES

- AR.3.1. System Diagram for DISSCC-----
- AR.3.2. Schematic of Equation Ordering for DISSCC-----
- AR.5.1. Plot from DISSCC OPTION 1-----
- AR.5.2. Plots from DISSCC OPTION 2-----
- AR.5.3. (A-H) Computer plots of dissolution Variables versus  
Time, varying the Reference Crack Width,  
RCW from  $1E-2$  to  $1E-5$ -----
- AR.5.4. (A and B) Penetration and Overrun Times versus  
Reference Crack Width, RCW; (A, B) OPTION 1,  
RFST 1 and 2-----
- AR.5.5. (A and B) Penetration and Overrun Times versus  
Reference Crack Width, RCW; OPTION 2, RFST 3 and 4-----
- AR.5.6. (A, B and C) Example of Sensitivity Result Using Raw  
Data; SCDIA versus CC, RCW and  $CC^2$ -----
- AR.5.7. (A and B) Example of Sensitivity Result using Ranked  
Data; (A, B) SCDIA versus RCW and  $DCP \cdot BMCL$ -----
- AR.5.8. (A) Threshold times as functions of SHLROM in  
OPTION 1 (TEF)-----  
(B) Threshold times in DISSCC OPTION 1 (CLTST)-----  
(C) Composite diagram of relative effects of initial  
values of heat and compaction parameters-----

METHODS OF SIMULATION ANALYSIS APPLIED TO QUESTIONS OF  
GEOLOGICAL STABILITY OF A RADIOACTIVE WASTE DEPOSITORY IN  
BEDDED SALT

Herbert R. Shaw, Anne E. Gartner, and Charlene Sontag Eng\*  
U.S. Geological Survey, Menlo Park CA 94025

Leslie Casey\*\*  
Nuclear Regulatory Commission, Washington D.C. 20555

AR.1. Introduction

This report comprises a revision, update, and elaboration of the numerical aspects of the geological simulation methods of Appendix 2A of the Sandia Laboratories report, "Risk Methodology for Geologic Disposal of Radioactive Waste: Interim Report" (Campbell and others, 1978). That report in general, and specifically Appendix 2A, forms the principal reference for the present report, and it is both assumed and expected that a copy of that report will be available for cross reference concerning aspects of the methodology not discussed here. In order to facilitate comparison with Appendix 2A of the Sandia report we have also attached it as an appendix to this report.

---

\*Present address: Dept. of the Navy, Naval Facility Engineering  
Command, San Bruno, California 94066

\*\*Present address: Department of Energy, 505 King Ave., Columbus, Ohio  
43201

For convenience, the present report is organized in a manner that is directly parallel to Appendix 2A (e.g. section AR.4.2.4 corresponds to the subject matter of IR2A.4.2.4, where AR refers to the present Annual Report and IR2A refers to Appendix 2A of the Interim Report). Comparison of the descriptions in the respective sections should provide the reader with an overall grasp of the methodology and specifically what is new or revised in the present report.

Appendix 2A of the Interim Report gives a broad geological and conceptual overview of the problems of geological analysis leading to a specific set of simulation models for aspects of depository stability, namely the access of ground water to the depository and the vulnerability of the salt layer to dissolution by ground water. The present Annual Report, on the other hand, begins with description of a specific revised simulation model for the dissolution of salt and refers general questions about the approach and philosophy of analysis to the Interim Report, except as arise in discussion of specific aspects of the problem (e.g. compare this section with section IR2A.1.).

#### AR.1.1. Simulation Models and Geological Perspectives

See IR2A.1.1. It is recommended that the user thoroughly study Forrester (1961) because the philosophy of feedback systems analysis described there is analogous to the approach used here for geological feedback.

AR.1.1.1. Questions of Geological Stability -- The present report addresses aspects of item (3) of IR2A.1.1.1: analysis of the behavior in the immediate vicinity of the waste depository environment. Furthermore, the analysis is limited to questions of gross thermal

effects, compaction of porosity existing or created in the salt horizon, and the creation of fracture pathways by which ground water gains access to the salt.

AR.1.1.2. Strategies of Systems Analysis -- Feedback systems analysis has proved to be an effective exploratory tool and stimulus that has expanded the viewpoints of investigators in several aspects of risk methodology. The basic strategy remains the same as in IR2A, and in this report we explore effects of increased degrees of freedom in the choice of fundamental relationships used in these sets of simulation equations.

AR.1.1.3. Role of Approximations in Systems Analysis -- One of the principal results of this report concerns the effect of approximations used in functional relationships describing phenomena affecting dissolution of salt. The admonition concerning "belief" in models is the same.

AR.1.1.4. Conceptual Importance of Feedback Phenomena -- See IR2A.1.1.4. Sets of equations are given in the present report that demonstrate the competing effects of functional relationships involving both positive and negative feedback.

#### AR.1.2. Numerical Simulation Methods

AR.1.2.1. Choice of Simulation Language -- The languages DYNAMO and GASP IV were mentioned in IR2A.1.2.1. The operational procedures for DYNAMO are described in Forrester (1961) and Pugh (1976), and for GASP IV they are given in Pritsker (1974).

In principle, GASP IV can be used for any calculation performed by DYNAMO, and many others. It is written in FORTRAN and therefore it can be more individually tailored to a problem than can DYNAMO. DYNAMO, on

the other hand, is much simpler to use.

AR.1.2.2. Characteristics of DYNAMO -- Both DYNAMO and GASP IV are codes for the solution of sets of linear ordinary differential equations. GASP IV uses a Runge-Kutta code (Pritsker, 1974). The internal programming of DYNAMO is proprietary and can not be described in detail (see Pugh, 1976), although it also uses standard techniques for solving sets of differential equations. In practice the main advantages of DYNAMO found in this study are its ability to automatically order the sets of equations written by the user and to test them for internal consistency and redundancy. Usually, specific error messages are given that quickly identify inappropriate equations, inconsistent constants, incorrectly coupled equations and so on. These features of DYNAMO have often saved much time in searching for errors and in avoiding hand calculations in search of redundancies. DYNAMO certainly is recommended for anyone not already experienced in the use of simulation languages, although the availability of DYNAMO is not essential to the study of feedback models as discussed here.

At this point it is suggested that the user thoroughly study the DYNAMO User's Manual (Pugh, 1973) and to study the applications and principles discussed by Forrester (1961). When that is done, glance through the nomenclature, schematic system diagrams, and equation lists given in the present report and the Interim Report. It should then be a simple matter to follow the later descriptions of specific equations and to implement parallel or analogous simulation calculations.

With experience and ingenuity, DYNAMO can be applied to many kinds of physical problems. For example, we have used DYNAMO for the approximate solution of problems in transient heat flow with



intermittent heat sources and boundary conditions. Use of DYNAMO for all sorts of trial calculations can greatly assist the development of more sophisticated models which may be written independently in FORTRAN or solved with other codes like GASP IV. Specific FORTRAN models may be desirable for intricate problems where the need is to perform many repeated calculations with the same basic model. Our purpose, however, is to explore system structures for diversity and variability of functional interactions, and so far DYNAMO has served that purpose admirably.

## AR.2. Reference System for DYNAMO Simulation

See the Interim Report (Campbell and others, 1978, Figure 1.2.2. and Chapter 1) for specific descriptions of the Sandia Reference System. Subsequently the cross section in Figure 1.2.2. was revised so that the Middle and Lower Sandstones meet near the position of River L; that is, there is no intervening shale layer in the Sandia Reference System currently applied to questions of regional ground water flow. The distinction does not affect the hydrologic assumptions of the present report.

### AR.2.1. Rudimentary Geometric Structure

DYNAMO simulation in IR2A was performed relative to a Simulation Reference Volume shown in figure IR2A.1. This was done so that properties could be averaged over a specified control volume, and inputs and outputs of heat and mass could be similarly averaged over that control volume, or over specifically defined subvolumes such as the depository horizon, the backfill horizon, and so on. The same basic control volume is used in the present report.

The DYNAMO model differs from finite difference or finite element models such as Figures IR3.3.3 and IR2A 7 in that the calculated balances refer to specified control volumes rather than to a geometric grid of cells with rigidly defined dimensions. This means that many parameters can be lumped together to roughly describe overall behavior, but detail in terms of local values within the control volume is not available without additional modeling.

The above distinction between the DYNAMO models and finite difference or finite element models represents a trade-off. In DYNAMO simulation we sacrifice geometric detail to obtain information on

functional relationships that are interdependent, that is that involve feedback. In the finite difference/element models, detail is available in terms of constant properties per cell or properties that are changed iteratively according to some predetermined scheme. Fully implicit, finite differences or finite element models that incorporate feedback effects, however, are exceedingly difficult to program though they are conceivable in principle. Such codes are being explored, but so far they are much too cumbersome for practical applications.

#### AR.2.2. Capabilities of Increased Geometric Complexity Using DYNAMO

DYNAMO simulation can be used in a manner directly analogous to finite difference calculations by subdividing the control volume and writing parallel sets of equations for each subvolume. We have used this technique to solve some simple problems in transient heat transfer, using a 3 x 3 array, or 9 control subvolumes. In principle, this could be done with the equations lists given in this report if it were necessary to specify local behavior in more detail. The number of equations and the length of computations, however, increase in proportion to the number of subvolumes to be described. It is suggested, however, that this technique should be attempted if it becomes necessary to simultaneously describe behavior at different horizons in a reference system such as figure IR2A.1.

### AR.3. System Diagrams

Study Forrester (1961, chapter 8) in detail. Those conventions were used in IR2A and are followed here.

#### AR.3.1. Descriptive System

See IR2A.3.1.

##### AR.3.1.1. System Structure -- Read section IR2A.3.1.1.

Figure IR2A.2. is a schematic overview of the system structure. That diagram is not an operational diagram and is intended only to identify the general progression of interacting states and processes, beginning with quantities involving heat and mechanical work at the bottom, through terms involving fracture pathways and ground water in the center, to terms involving transport of radionuclides at the top. The purpose of the diagram is to demonstrate the types of relationships and their interactions that would be required to create an overall feedback systems analysis of the depository, even in the most rudimentary terms. It is simply a mnemonic device to stimulate thoughts about physico-chemical relationships and processes and how they may relate to one another from the standpoint of feedback.

In figure IR2A.2 any one of the terms in the auxiliary and rate equations, or in the system states of the level equations may be in a feedback relationship with any other or all other terms and states. Only a few of the possible feedback connections are shown by dashed lines. A closed path connected by dashed lines with a direction shown by the arrows is a feedback loop. A thermomechanical example is shown by a dashed line connecting the heating rate  $dH/dt$  through auxiliary equations HA to the mechanical work rate  $dMW/dt$ , hence to the mechanical work states MW, and through mechanical work auxiliary

equations MWA (involving terms that identify components of the work dissipated as heat) back to the rate equation for the rate of heat generation  $dH/dt$ .

This is only one of many possible ways to schematically describe a thermomechanical feedback loop. It serves as a reminder, however, that no entity in a feedback system (and all natural systems are feedback systems) can be evaluated a priori independently from all others.

The quantitative analysis in IR2A did not consider the functions and states for radionuclide transport, nor does the present report. Such an analysis is specific to the waste form, the specific inventory as a function of time and distribution, and the distribution in terms of hydrologic pathways leading outside the control volume. Bookkeeping functions can be written to include radionuclide transport as the nature of the system structure evolves. These functions would also involve whatever retardation factors are characteristic of the radionuclide species and media present.

In the present report worst case scenarios for radionuclide loss from the control volume can be calculated directly from the mass balances of brine transport rates out of the control volume following the time the waste horizon is breached or overrun, depending on the type of scenario it is assumed will apply. Transport times for arrival of radionuclides at any other location, within aquifers or on the surface, can then be estimated on the basis of regional hydrologic data and/or hydrologic models.

Unfortunately, there is some ambiguity in the Acronyms and Initialisms of section IR2A.3.1.1. They are not operating functions, however, and are irrelevant to the nomenclature of the present report.

The user is nonetheless advised to study the intent of figure IR2A.2 and to consider the appropriate functions relating the respective level, rate, and auxiliary functions.

#### AR.3.2. Specific Diagram and Equations for Dissolution Feedback

The name of this section is changed from that in IR2A.3.2 because we have eliminated the confusing term "sector." That term is appropriate if it is used in a manner like that of Forrester (1961) where the system can be subdivided into distinguishable domains of behavior. In the system of figure IR2A.2, however, it is difficult to clearly define sectors.

Although the organization of the following sections in AR.3.2 is parallel to IR2A.3.2 there are major changes in nomenclature and equations. In that sense we have attempted to define completely all names and equations used in this report. A glossary of the names we have defined is given in table AR.3.1 "LIST OF ACRONYMS AND INITIALISMS USED IN DISSCC." The name DISSCC is an abbreviation for the master equation list of this report "DISSOLUTION WITH AND WITHOUT CRACK CLOSURE." An annotated listing of these equations, and terms named in the equations, is given in table AR.3.2. When in doubt about names used in this report, refer directly to tables AR.3.1 and AR.3.2.

DISSCC actually refers to a series of master equations which contain options for eight different modes of calculation as follows:

##### I. No Crack Closure

##### A. Number of cracks defined according to flexural crack coefficient.

Mode I.A.1--Maximum brine pressure head.

Mode I.A.2--Decaying brine pressure head.

B. Number of cracks defined by ratio of compaction volume to reference crack volume.

Mode I.B.1--Maximum brine pressure head.

Mode I.B.2--Decaying brine pressure head.

## II. Crack Closure

A. Number of cracks defined according to flexural crack coefficient.

Mode II.A.1--Maximum brine pressure head.

Mode II.A.2--Decaying brine pressure head.

B. Number of cracks defined by ratio of compaction volume to reference crack volume.

Mode II.B.1--Maximum brine pressure head.

Mode II.B.2--Decaying brine pressure head.

The reason we have included several different modes is heuristic. It is sometimes not possible to determine the most realistic mode of behavior of a geological system. By exercising different assumptions and studying the system behavior in different modes, insight is gained on the nature of feedback relationships. In many instances the system behavior is similar in all of the eight modes; in other instances there are combinations of parameters that identify sets of critical conditions for either relatively slow or fast rates of dissolution.

The remainder of this report specifically addresses the above sets of equations. This implies some repetition and redundancy, which are included so that the user will become increasingly familiar with adjusting the physical assumptions and modifying the manipulations of

equations. Another purpose is to provide an example of the problems of sensitivity analysis when the best choices of functional relationships are not known and several variants are possible.

Figure AR.3.1 replaces figure IR2A.3 and is the Systems Diagram showing the relationships among the equations of DISSCC. Table AR.3.3 gives a breakdown of the equations according to type: Level, Rate, Auxiliary, and Supplementary equations. Figure AR.3.2 shows the schematics of the ordering of equations in DISSCC more or less according to the sequence of actual calculations. This schematic ordering is not necessarily accurate in the sense that DYNAMO automatically determines the order of equations required for numerical solution. Comparisons of table AR.3.3, figure AR.3.1 and figure AR.3.2 should clarify questions about the role of any function and the way in which all the functions are interrelated.

Table AR.3.4 (A through D) gives actual DYNAMO listings for each of the eight modes outlined above for calculations with DISSCC. Each equation listing simultaneously calculates results with and without crack closure in one of the four modes above. Thus there are only four equation sets for DISSCC representing the four modes of computation, each one giving a result assuming that cracks remain open once formed and a result assuming that cracks tend to close according to a specified rate function. Therefore there are eight sets of dissolution rates.

The above sets of tables and figures are self explanatory, but for completeness each of the functions specifically described in the Interim Report is reiterated. Where appropriate we describe differences between the previously used functions and those defined in



the present report.

AR.3.2.1. Heat Level--identical to IR2A.3.2.1.

AR.3.2.2. Thermal Expansion Level -- This is identical to IR2A.3.2.2. except that the average heat capacity is introduced as a numerical constant in the TER equation (see tables AR.3.2 and AR.3.3).

AR.3.2.3. Compaction Level -- This level is conceptually the same as described in IR2A.3.2.3. The working equations, however, are different and will be described in detail in section AR.4. Basically, we are interested in the initial volume of pores or openings in the control volume, the volume of pores or openings produced by dissolution, and the volume of pores or openings closed by collapse owing to the superincumbent load (see Table AR.3.3).

AR.3.2.4. Net Displacement -- In IR2A.3.2.4 this section was described as a Level. In the present report the same numerical function is described as an Auxilliary equation representing the algebraic sum of the Thermal Expansion and Compaction Levels (see figure AR.3.1 and table AR.3.3).

AR.3.2.5. Fracturing -- In this report functions describing the numbers of cracks initially existing and created in the control volume are described as Auxilliary equations (see figure AR.3.1 and table AR.3.3). Two modes are considered; in one the numbering of cracks is assumed to be proportional to the net vertical displacement (see figure IR2A.4, p. 114), and in the other the number of cracks is determined from the compacted volume relative to the volume of a reference crack. These functions are defined in section AR.4.2.5.

AR.3.2.6. Solution Openings Level -- This section is almost completely revised from IR2A.3.2.6. All calculations are referred to a

U-tube syphon effect connecting the upper aquifer and salt layer. The scenario is geometrically like the setup for ORSCUA, "Opening Rate from Solutioning by Convection to the Upper Aquifer" (see figure IR2A.9, p. 123), but the equations for flow rates are different. In the ORSCUA function, the aquifer flow rate and fracture flow rate were coupled because flow through cracks was assumed to be proportional to the aquifer flow rate and number of cracks. The present equations are governed by the same limit in the steady state, but up to that time flow in cracks is calculated independently on the basis of crack dimensions and pressure differences across the U-tube. This means that there are more functions to consider; the dominant functions involve the Reference Crack Width, RCW, and the function used to compute the number of cracks. Additional functions are included to explore the effects of crack closure and decreasing pressure head across the U-tube as the steady state is approached (see figure AR.3.1 and table AR.3.3).

As before, it is assumed that the brine is saturated instantly on contact with the salt, but that dissolution is distributed over the entire salt layer. This assumption is artificial. A more realistic calculation will require a multicell version of the DYNAMO simulation including kinetic factors in each cell for the dissolution rate.

**AR.3.2.7. Dominant Feedback Loops** -- See IR2A.3.2.7. The only feedback loop investigated in the present report concerns dissolution via the U-tube scenario of figure IR2A.9 (Interim Report, p. 123). Included, however, are additional components involving negative feedback resulting from crack closure and decay of the brine pressure head as the steady state is approached.

One of our principal aims is to identify conditions where either

positive (accelerating) or negative (decelerating) feedback will dominate.

#### AR.4. Physical Content of System Equations

##### AR.4.1. The Basic Assumptions

Our interest in using simulation methods is to learn the principles of the behavior of feedback systems. Therefore, we emphasize the nature of interactions of physico-chemical mechanisms rather than the rigorous analytical description of each individual mechanism. The results map out categories or regimes of behavior that can be refined as the requirements for detail evolve out of the understanding that accrues from the analysis itself. The refinements may involve other modeling techniques and/or a multicell version of DYNAMO simulation.

##### AR.4.2. Simplified Physical Relationships

Rock properties for numerical analyses are listed in table IR2A.1 (Interim Report, p. 106).

We have used the properties of rock salt for heat capacity and thermal expansion because the maximum thermal effects occur in the vicinity of the depository horizon. On the other hand, we have used an average thermal conductivity of  $5 \times 10^{-3} \text{ cal cm}^{-1} \text{ sec}^{-1} \text{ }^{\circ}\text{C}^{-1}$  because overall heat losses are largely determined by properties of the superincumbent rocks. In refined calculations each of these properties would be functions of time, temperature, porosity, fluid flux, and position in the Control Volume.

Because we describe overall volumetric changes in terms of the Depository Area (DA) times a depth factor, terms involving porosity, compaction or expansion are defined as a length. Numerical volumes are determined from the appropriate length times the constant  $DA = 7.9 \times 10^{10} \text{ cm}^2$ . For numerical work the depth to the depository is taken as 600 meters.

AR.4.2.1. Heat Input -- The total heat production of high-level waste over a million years is given in Figure IR.1.4.2 (Interim Report, p. 31) for the depository design described in Chapter 1 of the Interim Report. This gives an initial thermal power of about 61 kw/acre for a 1000 acre site, though values as high as 150 kw/acre have been mentioned (Parsons and others, 1976).

The DYNAMO equation for heat input is the same as in the Interim Report (p. 105 ff.; also see table AR.3.3). The Dimensional Coefficient of Power,  $DCP=0.094$  cal/gm/yr, is the value of initial thermal power (61 kw/acre) divided by the depth to the source and the average density of the rock, in cgs. units (IR2A, p. 105). The heat input rate (HINR) is this value multiplied by the Fractional Decay function (FD); this function is expressed as a numerical table of values taken directly from the total inventory of Figure IR.1.4.2 (Interim Report, p. 31). The curve of Figure IR.1.4.2 is divided into twelve intervals, but it could be expressed in as much detail as desired by expanding the TABLE Function, FDTAB.

AR.4.2.2. Heat Output -- Calculation of heat transfer is, rigorously, very complex. It is an example of a mechanism that requires sophisticated finite element or finite difference modeling to evaluate accurately (see IR2A.4.2.5.1 for discussion of finite element analysis). Approximations for heat transfer, however, are very simple. We are principally interested in the maximum temperature reached and the timing of the thermal peak. Because the DYNAMO simulation model refers to a single Control Volume, ostensibly making it impossible to describe the temperature distribution, we have used a trick to estimate the conductive heat loss. First an equation was

written that defines what the heat loss rate would be if a steady heat flow were established for each value of heat content H. This equation is called the Steady Heat Loss Rate (SHLR). Because the rate of heat loss lags in time behind the rate of heat input, the steady rate of heat loss is adjusted by introducing a delay time which is evaluated by introducing SHLR as an argument of a DYNAMO Delay Function. Experience has shown that a Third Order Delay (see Forrester, 1961, Chapt. 9) with a delay time of 100 years is adequate to approximate the more rigorous finite element analysis of Section IR2A.4.2.5.1. The delay time is termed Delay of Surface Heat Flux (DSHF). Other delay functions or a multicell subroutine could be used to improve the temperature estimates.

The parameters defining SHLR are given explicitly in IR2A.4.2.2. Using a thermal conductivity of  $5 \times 10^{-3} \text{ cal}^{-1} \text{ cm}^{-1} \text{ sec}^{-1} \text{ } ^\circ\text{C}^{-1}$ , a heat capacity of  $0.2 \text{ cal gm}^{-1}$ , a density of  $2.2 \text{ gm cm}^{-3}$ , a depth to source of  $6 \times 10^4 \text{ cm}$  and a background geothermal flux of  $1 \times 10^{-6} \text{ cal cm}^{-2} \text{ sec}^{-1}$  (corresponding to an undisturbed geothermal gradient of  $20^\circ\text{C/km}$ , fairly typical in the western U.S.) we obtain the DYNAMO equation:

$$\text{R} \quad \text{SHLR.KL} = 2.0\text{E-}4 * (\text{H.K-}4.0) - 2.4\text{E-}4 \quad \text{STEADY HEAT LOSS RATE} \\ (\text{CAL/GM/YR})$$

Numbers calculated from this equation differ from those in IR2A.4.2.2 by about 5 percent because of slight differences in rounding.

The term (H.K-4.0) is required by the assumption that the surface temperature is  $20^\circ\text{C}$  and the initial thermal gradient is  $20^\circ\text{C/km}$ . That is, the initial temperature at 600 meters depth is  $32^\circ\text{C}$ ,  $12^\circ\text{C}$  above

the surface temperature; the initial mean temperature is 26°C, 6°C above the surface temperature, corresponding to an initial mean heat content of 5.2 cal gm<sup>-1</sup>.

The Supplementary Equation SURFLX is not included in the present analysis because the calculated values are not realistic with an aquifer existing between the surface and the depository depth. Heat transfer into the aquifer can be approximated from the estimated rate of heat loss, Heat Output Rate (HOUTR), given by the DYNAMO equation:

R     HOUTR.KL = DELAY 3 (SHLR.JK, DSHF)     HEAT LOSS RATE (CAL/GM/YR).

AR.4.2.3. Thermal Expansion -- The values of thermal expansion are estimated using a linear thermal expansion coefficient of  $1.5 \times 10^{-3} \text{ } ^\circ\text{C}^{-1}$ ; the Unit Expansion Coefficient (UEC) is this value multiplied by  $6 \times 10^4$  cm, the depth to the depository horizon giving  $\text{UEC} = 0.9 \text{ cm } ^\circ\text{C}^{-1}$ . The Thermal Expansion Rate (TER) is UEC times the mean rate of change of temperature per time step, given by the net rate of change of heat content (HINR-HOUTR) for that time step divided by the heat capacity of  $0.2 \text{ cal gm}^{-1} \text{ } ^\circ\text{C}^{-1}$ .

These are the same relationships given in IR2A.4.2.3. They assume that expansion is dominated by heating in the salt layer.

AR.4.2.4. Compaction -- Beginning with this section there are some major changes in the derivation of DYNAMO Equations between this report and the Interim Report. Acronyms and Initialisms are not identical, and therefore definitions should always be checked against the Glossary and Equation Descriptions of this report (see tables AR.3.1 and AR3.2). The principles of analysis remain the same, so the

corresponding sections of the Interim Report still should be studied for concepts and background.

The main difference in calculations of compaction concern the detailed form of the compaction rate equations. Conceptually we are concerned with compaction of any porosity that exists at the time the analysis begins and any porosity created during the time interval considered in the analysis. The term "porosity" refers generically to any form of open space, including interstitial pores between mineral grains and any cavern-like voids that existed or are created. Simplistically, we are mainly concerned with the porosity of the backfilled region of the depository, assumed to be salt, and with the volume of salt dissolved by access of ground water.

The initial backfill porosity is termed the Backfill Maximum Compaction Length (BMCL), because it defines the maximum vertical subsidence in the absence of dissolution.

The salt removed by dissolution is converted to an apparent layer thickness termed the Average Compaction Length from Solution (ACLS). Physically, this value would be literally accurate only if the U-tube flow system removed salt uniformly from the top of the salt layer over the total area of the repository. This assumption is dynamically unrealistic, but it is the simplest scenario consistent with the concept of the Control Volume. More realistically, salt would be removed progressively beginning at the upstream end of the U-tube. This means that the radionuclide canister horizon would be reached sooner than is calculated by the time required to dissolve the entire superincumbent salt layer. We allow for this discrepancy by also calculating the dissolved volume as though it were concentrated at a single spherical locus, described by the Single Cavity Diameter



(SCDIA). The resulting time required for the cavity to reach the canister horizon is assumed to be the shortest time for penetration of the salt layer by ground water according to the U-tube scenario.

The Compaction Length (CL) simply represents the linear subsidence of the superincumbent rock as salt is removed. The characteristic time a cavity can remain open in salt is taken to be the response time for collapse of an empty void in a viscous medium, as defined in the Interim Report (IR2A.4.2.1, p. 112). The nature of the overall deformation depends on the relative rates of subsidence of the superincumbent nonsalt rock strata versus the convergence of the salt laterally and from below. Therefore, the assumption of viscous collapse is oversimplified, but whatever form the deformation may take, it is assumed that ultimately there will be disturbances in the overlying shale layer within the depository area and concentrated near the depository perimeter.

In section IR2A.4.2.4 the compaction rate was determined by the dissolution rate, with a lag determined from the equation for the rate of viscous flow of salt, the Linear Pore Volume Compaction Rate (LPVCR), according to the functions:

L	$CL.K = MCL.K - LPV.K$	COMPACTION LENGTH (CM)
L	$LPV.K = LPV.J + DT*LPVCR.JK$	LINEAR PORE VOLUME (CM)
N	$LPV = BMCL$	
N	$CL = 0$	INITIAL COMPACTION REFERENCE STATE (CM)
C	$BMCL = 60$	BACKFILL MAXIMUM COMPACTION LENGTH (CM)
R	$LPVCR.KL = LPV.K*EXP (-2.303*ELP*3E7*DT/EVISC.K)/DT - LPV.K/DT$	

		LINEAR PORE VOLUME
		COMPACTION RATE (CM/YR)
C	ELP = 1.3E8	EFFECTIVE LOAD PRESSURE (DYNE/SQ CM)
A	EVISC.K = TABLE (EVTAB, BFTEMP. K, 0, 250, 25)	EFFECTIVE VISCOSITY (POISE)
		Note: See table AR.3.1 for definition of EVTAB and BFTEMP.

Algebraically, this set of equations expresses the volume balances correctly, but because of the definitions of LPV and LPVCR the value of Linear Pore Volume simply decreases from the initial value given by BMCL. This means that the compaction rate is essentially forced to follow the dissolution rate with very little lag.

Subsequently we defined the same balances by the equations

L	CL.K = MCL.J - LPV.J	COMPACTION LENGTH (CM)
N	CL = 1	INITIAL VALUE CL (CM)
A	LPV.K = BMCL + PVPS.K - PVDC.K	LINEAR PORE VOLUME (CM)
C	BMCL = 60	BACKFILL MAXIMUM COMPACTION LENGTH (CM)
L	PVPS.K = PVPS.J + DT*(BDRUA.JK)/DA	(LINEAR) PORE VOLUME PRODUCED BY SOLUTIONING (CM)
N	PVPS = 0	INITIAL VALUE OF PVPS (CM)
R	BDRUA.KL = FIFGE (MBFA, ACDR.K, ACDR.K, MBFA)	BRINE DISCHARGE RATE TO UPPER AQUIFER (CU CM/YR)

Note: FIFGE defines BDRUA as  
ACDR if BDRUA is less than  
MBFA; if not, BDRUA is set  
equal to MBFA.

C MBFA = 3E12

MAXIMUM BRINE FLOW IN  
AQUIFER (CU CM/YR)

A ACDR.K = RCVR.K\*NC.K

(TOTAL) APPARENT CRACK  
DISCHARGE RATE (CU CM/YR).

Note: RCVR and NC are,  
respectively, the REFERENCE  
CRACK VOLUME RATE, and  
NUMBER OF CRACKS.

L PVDC.K = PVDC.J - DT\*(LPVCR.JK)

PORE VOLUME DESTROYED BY  
COMPACTION (CM)

In both sets of equations LPVCR is the same rate equation (see tables AR.3.2 and AR.3.3 for complete definitions of all terms). The difference is that in the second set, LPV is calculated from the independently computed terms PVPS and PVDC so that it can take any value greater than zero and can either increase or decrease, depending on the balance of these two terms. Because LPV is not constricted in range, the compaction rate, LPVCR, and compacted volume, PVDC, can be arbitrarily large, depending on the dissolution rate.

For example, say the dissolution rate is initially very rapid and, because of the viscous lag, compaction does not initially keep pace. Eventually, however, the magnitude of LPVCR increases as LPV increases so that it eventually matches PVPS. If any factor causes PVPS to eventually decrease with time, changes in PVDC can exceed those in PVPS,

resulting in a decreasing Linear Pore Volume, LPV. Such factors are described in subsequent sections as forms of negative feedback affecting cracking functions and brine flow equations.

The viscosity term (EVISC) remains identical to that in IR2A. The TABLE function EVTAB defines the actual values of viscosity used, at intervals of 25°C from 0 to 250°C. Interpolation and limited extrapolation can be accomplished by constructing a graph of that function. The viscosity values for salt were determined uniquely for this study by comparison of the Salt Vault data of Bradshaw and McClain (1971) with the viscous compaction function of Shaw and Swanson (1970); temperature dependence was determined from the data in Heard (1976).

AR.4.2.5. Cracking -- Two different assumptions are used in this report to calculate the numbers of cracks. One of them is identical to the estimate in IR2A.4.2.5 though the names of terms are new:

A	$NC.K = CC * FIFGE(1E4, AVNEC.K, AVNEC.K, 1E4)$	NUMBER OF CRACKS FROM NET VERTICAL DISPLACEMENT
C	$CC = 5$	CRACK COEFFICIENT (PER CM)

This equation is numerically equivalent to NECC in IR2A.4.2.5, (p. 115); note that the initials NECC are used for a different function in the present report. The function FIFGE limits the maximum number of cracks to  $1E4 * CC$ .

The other method of computing numbers of cracks is to assume that the volume of compaction at the depository level allows an

approximately equivalent volume of cracks to open up in the overlying rocks. This possibility was mentioned in IR2A but was not employed. In the present analysis the master equation list DISSCC is written with both options. The new volumetric estimate is called OPTION 1 and the old version is called OPTION 2. OPTION 1 overestimates the numbers of cracks and can be considered to give the worst case scenario, other stated assumptions being the same. OPTION 2 was written to give a maximum number of cracks of  $5E4$  for a Reference Crack width (RCW) of 0.1 cm. Geologically this width may be excessive and our Reference Set of example calculations uses values of  $RCW = 1E-2$  CM. In order to maintain the same volume ratio in OPTION 2 as in OPTION 1 with  $RCW = 1E-2$  the maximum number of cracks would have to be increased by a thousand. In that case the two options would give similar results for brine flow. Therefore we chose to retain OPTION 2 with the original proportionality as a geologically skeptical estimate of cracking, and to use OPTION 1 as the conservative (worst case) estimate of cracking. OPTION 1 has the advantage of being written explicitly so that the dimensions and numbers of cracks are evident in each computer calculation. Each dimension, therefore, could also be expressed as a function of TIME, though for simplicity we have kept them constants within each calculation of this report. The equations for OPTION 1 are written:

A	$NC.K = DA * PVDC.K / (RCW * CTL * CPL)$	NUMBER OF CRACKS FROM VOLUME OF REFERENCE CRACK
N	$NC = 1$	INITIAL NUMBER OF CRACKS
C	$DA = 7.9E10$	DEPOSITORY AREA (SQ CM)
C	$RCW = 1E-3$	REFERENCE CRACK WIDTH (CM)
C	$CTL = 6E5$	CRACK TRACE LENGTH (CM)

C

CPL = 1E4

CRACK PATH LENGTH (CM)

PVDC, of course, is the compacted volume defined before for the potential volume of crack openings. An initial value of NC = 1 is assigned to avoid the possibility of terms with zero in the denominator, and also because some amount of initial fracture permeability is geologically more realistic than none.

In addition to these two options for cracking, we have written a parallel set of equations that is simultaneously built into the master equation list DISSCC that allows some proportion of the cracks to close during compaction. In other words, a single set of equations calculates results both with and without the assumption of crack closure. The physical reasoning is that cracks may initially open as described above in either OPTION 1 or 2 and then eventually close up again as all of the superincumbent rock strata subside and compact into the openings created by dissolution. In order to give a numerical sense of that effect, we calculate a new term called the Active Number of Cracks with Closure (ANCC) which represents the number of cracks calculated by either OPTION 1 or 2 normalized by the ratio of the Linear Pore Volume, LPVC, to the maximum compaction length, MCLC (C is added to names otherwise the same to refer to the crack closure mode). When the available pore space is entirely collapsed, this ratio is zero and the number of cracks, hence dissolution rate, falls to zero. When LPVC is large those cracks that do form according to PVDCC remain open and active. The detailed equations are given in table AR.3.2.

We do not consider fault-related cracking in this report. It will contribute to either the initial numbers of cracks or to the number

existing at a later time. In either case some variant of the U-tube scenario will eventually dominate the flow unless hydrologic conditions are totally modified by faulting. Fault related cracks will usually increase the dissolution rates and the effects can be estimated with DISSOC by varying the initial number of cracks or the numbers introduced at any specified values of TIME. See IR2A.4.2.5, pp. 116 and 117 for discussion of faulting.

Note: Section IR2A.4.2.5.1, Digression on Two-Dimensional Stress Analysis Calculation, remains unchanged and stands as a comparative reference for calculations of temperature and potential strain patterns. Figure IR2A.8 can be compared with outputs of DYNAMO calculations of temperature and thermal expansion.

AR.4.2.6. Openings from Effects of Dissolution -- Each of the mechanisms described in IR2A.4.2.6 exists as a possible mode of dissolution. The general spectrum of rates, however, resembles that of the U-tube scenario, and numerous exploratory calculations have shown that other scenarios often evolve into variants of the U-tube scenario. We chose to concentrate on the one scenario in this report so the user can get a clear sense of its ramifications. Setting up other scenarios is then a relatively simple matter if some physical picture of a scenario can be written in even a crudely numerical format.

The equations describing the rates of dissolution for DISSOC are partly described in the foregoing discussion of compaction and cracking. The approach differs significantly from that derived for the function ORSCUA, the Opening Rate from Solutioning by Convection to the Upper Aquifer. Although we derived an equation in IR2A for brine flow

in cracks, we did not use it. Instead the function ORSCUA simply proportioned the maximum potential rate, as defined by a fraction of the total discharge rate of the Upper Aquifer (see IR2A.4.2.6.2, p. 124-125).

ORSCUA has two deficiencies: (a) it lumps the cracking rate coefficient with the aquifer flow rate so that independent variations are obscured, and (b) it underestimates the initial rates of flow through cracks. In the present report we separate these effects.

For a given pressure head the rate of flow in an individual crack is defined by the dimensional equation given in IR2A.4.2.6.2 (p. 124). In DYNAMO format it is expressed:

A	$RCVR.K = (3E7 * BPH * RCW * RCW * RCW * CTL) / (12 * BV * CPL)$	REFERENCE CRACK VOLUME RATE (CU CM/YR)
C	BPH = 2E6	BRINE PRESSURE HEAD (DYNE/SQ CM)
C	RCW = 1E-3	REFERENCE CRACK WIDTH (CM)
C	CTL = 6E5	CRACK TRACE LENGTH (CM)
C	BV = 1E-2	BRINE VISCOSITY (POISE)
C	CPL = 1E4	CRACK PATH LENGTH (CM)

Because this rate (RCVR) multiplied by the number of cracks can exceed the Maximum Brine Flow in the Aquifer (MBFA), the Brine Discharge Rate to the Upper Aquifer (BDRUA) is written so it does not exceed the limit  $MBFA = 3E12$  (CU CM/YR). MBFA is the calculated capacity of the aquifer to carry away brine discharged from the



U-tube. Incidentally, this value is based on a balance of buoyancy forces involving a head difference between the inlet and outlet of the U-tube of 20 meters (see figure IR2A.9). We have retained this value, though it is roughly 30 percent smaller than the exact gradient of the aquifer in the Sandia Reference System (see Interim Report, Chapters 1 and 3).

Though equations involving RCVR, NC, ACDR, and BDRUA are more realistic than ORSCUA, there are still significant artificialities. One is that the dimensions are considered constants. This deficiency is easily corrected by making all terms in the crack dimensions variables if there is a physical reason to do so. We have retained them as constants in this report so we can more easily separate the relative effects. A more serious deficiency is that the Brine Pressure Head has been defined as a constant. Clearly, as the brine builds up in the aquifer the pressure head decreases. Application of the limit MBFA artificially truncates the rate so this is not a serious problem, but it is of interest to demonstrate how yet another negative feedback cycle, in addition to crack closure, can enter the analysis.

In order to allow the Brine Pressure Head to effectively decrease with brine discharge, we have written equations for the total flow, ACDR, so that the pressure term is decreased by factors involving the ratio of total flow to maximum flow MBFA. When these are equal the acting pressure head has reached a steady value. The normalizing equations are written:

$$A \quad ACDR.K = DCBPHA.K * NBPH * NC.K / (1. + (DCBPHA.K * DCBPHB.K * NC.K))$$

(TOTAL) APPARENT CRACK

DISCHARGE RATE (CU CM/YR)

$$A \quad DCBPHA.K = (3E7*RCW*RCW*RCW*CTL)/(12*BV*CPL)$$

DIMENSIONAL COEFFICIENT  
FOR BRINE PRESSURE HEAD  
PART A (CU CM\*SQ  
CM/DYNE/YR)

$$A \quad DCBPHB.K = NBPH/MBFA$$

DIMENSIONAL COEFFICIENT  
FOR BRINE PRESSURE HEAD  
PART B (DYNE\*YR/CU CM\*SQ  
CM)

$$C \quad NBPH = 2E6$$

INITIAL VALUE OF BRINE  
PRESSURE HEAD (DYNE/SQ  
CM)

These equations adjust the brine pressure in the following way:  
When the Number of Cracks, NC, is small the value of ACDR is nearly identical to the product RCVR\*NC as in the case for constant pressure head; when NC is large the value of ACDR simply approaches the limit MBFA, Maximum Brine Flow in Aquifer. This limit represents the situation where the pressure head and consequent brine discharge rate precisely balance the rate that the brine layer in the aquifer can be carried away by the regional flow.

The effect of decaying brine pressure head depends on the regime of overall behavior. In some instances where dissolution feedback progresses rapidly, the effect of decaying brine pressure has negligible effect on the outcome. In other cases where dissolution is relatively slow at constant BPH, decreasing pressure has a major effect on further slowing the rate of salt removal.

## AR.5. Computer Runs for Dissolution with and without Crack Closure

Note: This section condenses material equivalent to subsections IR2A.5.1 through IR2A.5.3; subsection AR.5.4 is added to describe Sensitivity Analysis, which was not performed in the Interim Report.

In this section we describe a Reference Set (RFST) of calculations for the U-tube scenario using DISSCC in all modes described in this report. These consist of four basic equation lists (OPTIONS 1 and 2, WITH AND WITHOUT DECAY OF BRINE PRESSURE HEAD) each of which calculates dissolution WITH AND WITHOUT CRACK CLOSURE. Therefore, we have eight sets of results describing different regimes of dissolution feedback. We give all eight so the user can see the variations that result from contrasting assumptions concerning the form of the equations.

The results are described primarily in terms of the time required for dissolution to reach the canister horizon of the Depository either at a single locus, expressed as the SINGLE CAVITY DIAMETER (SCDIA and SCDIAC), or in a wholesale manner, expressed as the time the ABSOLUTE VALUE OF NET EXPANSION MINUS COMPACTION (AVNEC and AVNECC) attain a value of 100 meters ( $1E4$  cm) representing the thickness of salt above the canister horizon.

First we give examples of results for OPTION 1 and 2 using the most complete sets of equations, with a printout of all variables and a plot of selected variables for a Reference Crack Width,  $RCW = 1E-3$  CM, (tables AR.5.1, AR.5.2; figures AR.5.1, AR.5.2). In the printout, the variables appear as rows in the heading, and the respective numerical

values of the variables appear at each value of TIME also arranged in rows in the same respective positions; a set of scaling factors appears immediately following the names of variables. Particularly note the behavior of the variables BACKFILL TEMPERATURE (BFTEMP), NUMBER OF CRACKS (NC), ACTIVE NUMBER OF CRACKS WITH CLOSURE (ANCC), ABSOLUTE VALUE OF NET EXPANSION MINUS COMPACTION WITH AND WITHOUT CLOSURE (AVNECC and AVNEC), and SINGLE CAVITY DIAMETER WITH AND WITHOUT CLOSURE (SCDIAC and SCDIA). The values of brine discharge rates are given by BDRUAC and BDRUA, and the total volumes of salt removed are given by SOC and SO; BDRAT gives the ratio of brine discharge rate with closure to brine discharge rate without closure. PVRAT and PVRATC give the ratios of collapsed pore volume to maximum pore volume with and without closure; these two ratios give a measure of the lag of compaction rates relative to dissolution rates. This lag is also seen in the time required for the volume of dissolved salt to approach the limit SO or  $SOC = 1E4 \cdot DA = 7.9E14$  CU CM, versus the time required for the subsidence, measured by AVNEC or AVNECC, to approach the limit  $1E4$  CM. We repeat this statement for emphasis in the following examples.

From the printout in table AR.5.2, OPTION 2 WITH DECAY OF BRINE PRESSURE HEAD we obtain sets of values representing nearly complete dissolution of salt above the cannister horizon; the corresponding value of TIME is referred to as the "OVERRUN TIME:"

TIME	=	65,000 YRS
SOC	=	789.1E12 CU CM
AVNECC	=	8,882 CM
BDRAT	=	0.1448

PVRATC = 0.8856  
  
 TIME = 5,000 YRS  
 SO = 924.E12 CU CM  
 AVNEC = 8.2E3 CM  
 BDRAT = 0.0000  
 PVRAT = 707.06

In the equilibrium situation Overrun would occur when SOC and SO have the exact value 790E12 CU CM and AVNECC and AVNEC have exactly the value 1E4 CM. In the tabulated results the values of SOC and SO respectively, equal and exceed the theoretical limit, whereas AVNECC and AVNEC have not attained the value 1E4 CM. These results reflect the dynamic lag of compaction relative to dissolution; the lag is relatively greater without crack closure because the rates are faster. The values of TIME corresponding to the exact limits are obtained by interpolation. The contrast in lag is also shown in the ratios BDRAT, PVRAT and PVRATC. At 65,000 years the brine discharge rate with closure is about 15 percent of the value without closure, and the compacted pore volume is nearly 89 percent of the maximum possible. On the other hand, at 5,000 yrs the brine discharge rate with closure is less than 0.00 percent of the rate without closure, and the compacted pore volume is only 71 percent of the maximum possible. This means that dissolution rates without closure are very high so that compaction rates have major lags relative to dissolution rates and the lag with closure greatly exceeds the lag without closure (i.e., feedback is weak in the closure model at the earlier times, whereas it is strong in the

model without closure).

By comparative study of the tables, considerable insight can be obtained about the behavior of the respective models. Insight is increased by comparing sets of calculations with varying crack widths, RCW, which clearly plays a dominant role. Yet more insight is gained by simultaneously varying several of the significant variables. This aspect of the study is described in the section on Sensitivity Analysis. In the present section, however, we demonstrate how the results are affected by varying RCW over a range of 3 decades, from  $1\text{E-}2$  CM to  $1\text{E-}5$  CM. The other variables are held constant in this section and are listed in table AR.5.3.

In principle, all of these "constants" should be varied in sensitivity analyses. We demonstrate the principles of variation, however, by first looking at simple variations, beginning with only RCW in this section, and then considering the combinations DCP, BMCL, CC, and RCW. These four variables represent the dominant initial forcing functions for heat, porosity, intensity of fracturing, and crack width (the primary influences on potential flow rates).

Table AR.5.4 gives a listing of results for a variation of RCW from  $1\text{E-}2$  to  $1\text{E-}5$  CM. Figure AR.5.3 illustrates the corresponding dissolution curves of contrasting form and duration as functions of time. Figures AR.5.4 and AR5.5 show the respective regimes of behavior in terms of PENETRATION TIME and OVERRUN TIME.

Figures AR.5.4 and AR.5.5 demonstrate some valuable generalizations about flow in cracks. RFST 1 and 2 represent OPTION 1, and RFST 3 and 4 represent OPTION 2 for calculating numbers of cracks. OPTION 2 determines the number of cracks independently of the crack width, RCW,

whereas in OPTION 1 the number of cracks depends directly on RCW. At values of RCW below  $10^{-3}$  CM, OPTION 2 always gives much longer dissolution times than OPTION 1 because of the rapid decrease in overall conduit volume. On the other hand, for values of RCW  $> 10^{-3}$  CM dissolution according to OPTION 2 may go to completion in times comparable to OPTION 1; the numbers of large cracks are not automatically normalized by the value of RCW in OPTION 2.

The results for OPTION 1 show the interesting characteristic that dissolution times are not greatly increased with decreasing RCW until RCW falls below about  $10^{-4}$  CM, and then at critical values in the neighborhood of  $10^{-5}$  CM dissolution times become infinitely long. We reserve additional comment until the sensitivity results are described, but clearly dissolution times are extremely sensitive to the mode of cracking mechanisms.

Comparison of figures AR.5.4 and AR.5.5 show that crack closure and decay of brine pressure head affect the limits of the respective flow regimes but do not change the form of behavior. These negative feedback effects, however, become very important for OPTION 1 near the critical value of RCW.

#### AR.5.4. Computer Runs for DISSCC: Demonstration of Sensitivity Analysis

Our approach is to simplify in the extreme so that essentials of the analysis are conspicuous. Accordingly, the number of parameters chosen are the fewest that represent the principal source factors for heat, compaction and brine flow (to clarify this point go back to section 5.3 and the comments concerning "constants" in table AR.5.3). Therefore we selected for variation DCP, BMCL, RCW and CC.

Numerical ranges were chosen for each parameter that represent

maximum plausible limits as follows:

$$0 < \text{DCP} < 0.376$$

$$0 < \text{BMCL} < 540$$

$$10^{-4} < \text{RCW} < 10^{-1}$$

$$0 < \text{CC} < 5$$

For example, the range of DCP represents thermal loads from 0 to about 250 kW/acre; the range of BMCL represents total porosities of the mined region ranging from 0 to 30 percent; the range of RCW represents cracks from submicron widths to a tenth of a millimeter; and CC ranges from zero to 5 reference cracks per centimeter of vertical displacement (see section IR2A.4.2.5, p. 115).—

Within these ranges each parameter was assigned 20 values using the Latin Hypercube Sampling technique, LHS (McKay and others, 1978). These twenty values were chosen as a number that is manageable and yet gives a reasonable test of the statistical approach (R. Iman, oral communication, September, 1979). Even with this small a sample per reference set, a minimum of 80 runs are required to calculate the corresponding ranges of penetration and overrun times. Tests involving different choices for the parameter ranges increase this number. Our conclusions are based on about 140 runs.

---

—The ranges of these parameters is based on inference and hearsay. By "hearsay," we mean that the ranges of DCP and BMCL represent values mentioned in verbal discussions with many participants in evaluations of Depository Design (see Interim Report, Chapt. 1). By "inference," we mean that we have chosen ranges of RCW and CC based on our particular subjective evaluations of geologic plausibility.



The results of sensitivity calculations essentially confirm that RCW is the dominant parameter and that the form of behavior is anticipated by the results illustrated in AR.5.4 and AR 5.5.

Regression analyses were done for two models. The dependent variables were the times of termination of the runs, i.e., the Penetration and Overrun Times as illustrated in figures AR.5.4 and AR.5.5. The first model used the DYNAMO results directly ("raw data") and the second used a ranked set, as defined below. The data basically represent times when the waste horizon is breached either at a point, as defined by the single cavity diameter (penetration time), or in a wholesale manner, as defined by the total amount of salt removed; a related time represents completion of subsidence over the entire repository area. Thus, regressions for each reference set of calculations were done for each of the variables SCDIA, SCDIAC, AVNEC, AVNECC, SO and SOC.

Figures AR.5.6 and AR.5.7 give examples of plots of Penetration Time, determined from SCDIA, versus each of the parameters chosen by the regression to fit the output (raw data and ranked data). The regression chooses the minimum number of parameters that fit at least fifty percent of the output range. It then continues to choose additional variables until an optimum combination is achieved as determined by the variation of the predicted error of the sum of the squares (PRESS value). In this instance two sets of three combinations were chosen successively by the computer code: CC, CC and RCW, and CC, RCW and CC<sup>2</sup>.

In each iteration, regression equations are derived for the output in terms of the chosen variables. We do not give these equations

because they apply only to the appropriate range and must be viewed in terms of the full array of statistical tests, which we do not have space to reproduce. Out of context, the equations can give grossly misleading results. The significant results are the sequences of variables chosen in the two modes to fit the scatter shown by figures AR.5.6 and AR.5.7.

Comparison of the raw data and ranked data (compare figure AR.5.6 with figure AR.5.7) shows an interesting statistical result that was discovered accidentally. This set of results used equation sets for the OPTION 1 cracking mode (numbers of cracks calculated from the crack width) for which the dominant sensitivity parameters should be RCW, DCP, and BMCL; the parameter CC applies only to the other cracking mode. Inadvertantly, however, the regressions were performed including CC as a sensitivity variable, and, by chance, the sampling of CC happens to correlate so strongly with the other variables that it was chosen as the dominant variable in regressions on the raw data (figure AR.5.6). The correlation, however, is inverse to what would be expected if CC were a variable parameter, and the regressions are totally spurious. The strong correlation occurs because the result is weighted by a large value of CC which happened to be combined in sampling with a small value of RCW. Even such a highly spurious result, however, was corrected by the ranked regressions.

Ranking of data is based on choosing an artificial scale in which each value of input and output is ranked sequentially from 1 to 20 and given that number as its numerical value. In terms of the rank scale, RCW is the dominant variable and shows an almost linear proportionality to all the output variables (i.e., end times calculated from SCDIA,

SCDIAC, AVNEC, ANECC, SO and SOC), as illustrated in figure AR.5.7 for SCDIA. The strongest secondary correlation is with the product DCP\*BMCL, though the scatter of values is much greater.

Regression by rank agrees with our physical interpretation of parameter importances. It is clear that statistical results without knowledge of expected correlations can be misleading or totally spurious. With knowledge of expected correlations, however, the statistical method can quantify both the ranges of uncertainty and the appropriate hierarchy of parameter importances. In order to place the statistical results on a sound footing, however, it is advisable to test various sample ranges and distributions and to increase the sample size within the final distributions chosen. The output of such repeated trials is much too voluminous to attempt to include in this report.

Refinement of the sensitivity results should also be performed by testing the parameter sequences as a function of time. This means performing the regressions at several time intervals. Our exploration of such sequences, to date, has directly supported our interpretation of physical importance based on the results of selected simulation exercises. That is, the process of exploration of system behavior using simulation methods contains an implicit "sensitivity analysis" which, though not based formally on statistics, is confirmed by rigorous statistical methods.

In the present instance the dominance of RCW in the statistical and simulation tests is clear, and we can evaluate the separate effects of DCP and BMCL from the physical equations themselves (see AR.5.4.1). Time series regressions are more useful if the variables are less

obviously correlated or if there are more variables with possibilities of combined effects of less obvious nature. Like the simulation analyses, sensitivity analyses represent methods for learning more about system behavior by studying the evolution of the results themselves. In that sense, the statistical methods described represent a powerful complement to simulation analysis.

In fact, we suggest that the philosophy of analysis, whether by simulation or statistical methods, is basically the same; that is, the aim is to create an evolving methodology that leads to an understanding or a knowing about how a prescribed system will behave when subjected to variation of any of the system parameters. This "knowing" is essentially a function of experience, and we suggest that this experience should be based on as wide an array of analytical techniques as can be brought to bear on the problem, including subjective, statistical, simulation, probabilistic and specifically deterministic methods of analysis. In this context we distinguish "simulation" and "deterministic" methods because simulation methods, while physically deterministic in the prescription of equations, contain an implicitly statistical element by virtue of the repetitively exploratory strategy of its application to system behavior.

AR.5.4.1 Single-Parameter Sensitivity -- The purpose of the general sensitivity analyses was to establish ranges of simulation response time and relative importances of parameters without having to compute the limitless combinations possible. The Latin Hypercube Sampling technique reduces the problem to manageable size within the specification of ranges and forms of parameter variations. There are situations, however, where the correlations may not be clear, or where

there are abrupt changes or discontinuities beyond the upper or lower bounds of the sample range. In order to check these possibilities, we found it necessary to make a variety of runs in which only one parameter at a time was varied, in a manner analogous to figures AR.5.4 and AR.5.5.

Another purpose of single-parameter variations is to test individual functions or groups of functions to verify that they are, in fact, operating correctly with the ensemble of other equations. A related test is to check the internal consistency of initial values of all equations.

We illustrate these points by reference to the behavior of DISSCC, OPTION 1. Recall that Option 1 defines the number of cracks, NC., as the ratio of collapsed volume PVDC, to the volume of a reference crack (given by the product RCW\*CPL\*CTL). The activating equation is (see Table AR.3.4.A):

$$A \quad NC.K = DA*PVDC.K/(RCW*CTL*CPL)$$

Physically, this form of the relation assumes that cracking responds to an actual collapse of openings, SO; thermal expansion or contraction does not produce openings and therefore does not contribute to cracking. Option 2, on the other hand, calculates the number of cracks from the vertical displacement, and therefore thermal effects are directly included. A more complete formulation would combine aspects of compaction cracking and flexural cracking.

The point is, in testing single-parameter variations, there is no dissolution in Option 1 when all of the porosity parameters (BMCL, PVDC, PVPS, CL, SO) are initially set to zero, regardless of the magnitude of thermal input, DCP. In Option 2, the thermal input

triggers cracking and initiates dissolution over similar time spans even if porosity is initially zero.

In order to obtain a qualitative test of a coupled response in Option 1, we replaced PVDC with AVNEC in the cracking equation:

$$A \quad NC.K = DA*AVNEC.K/(RCW*CTL*CPL)$$

This equation is inconsistent with the physical assumptions, unless it is assumed that thermal expansion actually creates some pore space that can then begin to collapse to induce cracking. We illustrate this version in Table AR.5.6. as Option 1 (TEF), where (TEF) refers to the component of Thermal Expansion Feedback.

We have also modified Option 1 (TEF) in other ways to facilitate testing single-parameter variations. One of these is the addition of a constant term permitting an independent specification of the initial number of cracks, as follows:

$$A \quad NC.K = NCN + DA*AVNEC.K/(RCW*CTL*CPL).$$

Another modification is the introduction of a multiplier constant in the equation for steady Heat Loss Rate; the constant is SHLROM and the equation is written:

$$R \quad SHLR.KL = (2E-4*(H.K-4.0)-2.4E-4)*SHLROM$$

The purpose of SHLROM is to permit an arbitrary and independent reduction of the heat loss rate, for test purposes only. Other changes are the removal of terms that result in division by zero, such as ANCC, or the logarithm of zero, such as LNVFU, when initial values are set to zero.

We emphasize, therefore, that OPTION 1 (TEF) IS A CHECK LIST ONLY AND DOES NOT GIVE PHYSICALLY CORRECT RESULTS. It does, however, illustrate some important points about simulation analysis:

- (1) It is important to learn the numerical behavior of a simulation model when the equations are deactivated by specifying zero values, or values that give zero result.
- (2) Because of rounding by the computer, it may be impossible to "zero" some equations; this is true of the SHLR equation that involves differences of small numbers.
- (3) There may be threshold effects of numerical origin that might be interpreted as physically valid if the single-parameter tests are not made.

The smallest initial value of SHLR that can be computed is of the order  $E-270$ . Even this small a value, however, activates the dissolution feedback equations in a time of the order of  $1E4$  years (see figure 5.8). Physically, the initial numbers of cracks and dimensions of flow are far below the limits of validity of the transport equations. This observation identifies two important points: (a) simulation analysis may calculate sets of internally consistent results that include physically inadmissible numerical regimes, and (b) in DISSCC OPTION 1 there is some threshold condition that determines the effective starting time of dissolution feedback.

The implication of (a) is that a general or multiparameter sensitivity analysis may be misleading if inadmissible numerical ranges are included. The implication of (b) is that some form of additional physical assumption or modeling is required to determine the inception of cracking that can then grow according to the feedback relations. For example, the hypothetical curves of figure 5.8A could be viewed as nucleation functions for the inception of macroscopic cracking rates. Unfortunately, we do not know what form those functions should take.

Therefore, all we can do is to specify some arbitrary nonzero initial condition. According to OPTION 1 (TEF), virtually any such choice that is physically plausible leads to overrun in times comparable to the results in figure AR.5.4. as functions of RCW.

The same effect is true whether or not we are including thermal expansion as a factor (compare figures AR.5.8.A, B and C).

AR.5.4.2 Threshold Effects -- The preceding exploration has very interesting conceptual implications that could have been overlooked if we had taken either OPTION 1 or OPTION 2 at face value (a combined model would give results essentially like OPTION 1, because it represents the dominant rate-determining feedback).

The interesting conclusion is that the process of exploring combinations of simulation options focuses on and virtually demands resolution of the factors, or threshold effects, that create the inception of feedback. In this case we have proceeded as far with the analyses as is meaningful until we can discover the processes that govern nucleation rates for crack growth and hence the threshold times for dissolution feedback.



#### AR.6. Conclusions and Recommendations

The principal conclusion of this study is that the mechanisms controlling the number of cracks and/or the crack widths are the crucial determinants of the dissolution rate. Maximum potential rates of dissolution are very high if crack widths can exceed about  $10^{-4}$  cm and if an unrestricted U-tube scenario as described here is operative. The reality of that scenario depends on statistical tests of geologic observations and on refinement of deterministic mechanical models not addressed in this report. On the other hand, if likely scenarios exist that indicate small crack widths (of order  $10^{-5}$  cm) then mechanisms involving crack closure and decreasing pressure head in the brine column can result in very slow dissolution rates. In fact, below a certain range of crack widths the corresponding dissolution rates are negligible. Extensive simulation and sensitivity studies, however, are required to establish this limit in any specific case.

On the basis of these results it is recommended that studies of cracking mechanisms be expanded both geologically and by deterministic modeling and that more attention be given to scenarios involving detailed analyses of the geometry of flow paths coupled with the information gained on cracking mechanisms. With such information, the statistical techniques of sensitivity analysis described in this report should give a very quantitative picture of the expected ranges of dissolution effects. On the basis of present information, potential mechanisms for dissolution of salt must be considered a major deterrent to any affirmative conclusions about the suitability of bedded salt environments as sites of radioactive waste storage or disposal.

## Tables

- AR.3.1. List of Acronyms and Initialisms in DISSCC
- AR.3.2. Annotated Listing of Equations in DISSCC
- AR.3.3. Breakdown of Equations by Type
- AR.3.4. (A-D) DYNAMO Equation Lists 4 (X2) Modes of DISSCC
- AR.5.1. Example of Printout of all Variables; DISSCC OPTION 1
- AR.5.2. (A,B) Examples of Printout of all Variables; DISSCC  
OPTION 2
- AR.5.3. Numerical Values of Constants in DISSCC
- AR.5.4. (A,B,C) Tabulation of Penetration and Overrun Times  
varying RCW from  $1E-2$  to  $1E-5$  CM, other parameters held  
constant
- AR.5.5. (A-G) Tabulation of Penetration and Overrun Times; from  
Sensitivity Analysis
- AR.5.6. DYNAMO Equation Test List-OPTION 1 for Thermal Expansion  
Feedback
- AR.5.7. DYNAMO Equation List-OPTION 1 (CLTST) CL Loop Test Program

## Figures

- AR.3.1. System Diagram for DISSCC
- AR.3.2. Schematic of Equation Ordering for DISSCC
- AR.5.1. Plot from DISSCC OPTION 1
- AR.5.2. Plots from DISSCC OPTION 2
- AR.5.3. (A-H) Computer plots of dissolution Variables versus Time, varying the Reference Crack Width, RCW from  $1E-2$  to  $1E-5$  CM
- AR.5.4. (A and B) Penetration and Overrun Times versus Reference Crack Width, RCW; (A, B) OPTION 1, RFST 1 and 2
- AR.5.5. (A and B) Penetration and Overrun Times versus Reference Crack Width, RCW; OPTION 2, RFST 3 and 4
- AR.5.6. (A, B and C) Example of Sensitivity Result Using Raw Data; SCDIA versus CC, RCW and  $CC^2$
- AR.5.7. (A and B) Example of Sensitivity Result using Ranked Data; (A, B) SCDIA versus RCW and  $DCP \cdot BMCL$
- AR 5.8. (A) Threshold times as functions of SHLROM in OPTION 1 (TEF)  
(B) Threshold times in DISSCC OPTION 1 (CLTST)  
(C) Composite diagram of relative effects of initial values of heat and compaction parameters

## References

### Annual Report

1. R. L. Bradshaw and W. C. McClain (eds.), 1971, Project Salt Vault: A Demonstration of the Disposal of High-Activity Solidified Wastes in Underground Salt Mines, ORNL-4555, 360 p.
2. J. W. Forrester, 1961, Industrial Dynamics, Cambridge, Mass., M.I.T. Press, 464 p.
3. H. C. Heard, 1976, "Comparison of the Flow Properties of Rocks at Crustal Conditions," Phil. Trans. Royal. Soc. Lond., A., Vol. 283, pp. 173-186.
4. R. L. Iman and W. J. Conover, 1979, The use of the rank transform in regression, *Technometrics*, vol. 21, p. 499-509.
5. M. D. McKay, W. J. Conover and R. J. Beckman, 1978, A comparison of three methods for selecting values of input variables in the analysis of output from a computer code, *Technometrics*, Vol. 21, p. 239-245.
6. A. A. B. Pritsker, 1974, The GASP IV Simulation Language, New York, Wiley and Sons, 451 p.
7. A. L. Pugh III, 1976, DYNAMO II User's Manual, 5th Edition, Cambridge, Mass., M.I.T. Press, 131 p.
8. H. R. Shaw and D. A. Swanson, 1970, "Eruption and Flow rates of Flood Basalts; in E. H. Gilmour and D. Stradling (eds.) *Proceedings of the Second Columbia River Basalt Symposium*, Eastern Wash. State College Press, Cheney, WA, pp. 271-299.

**TABLE AR.3.1. List of Acronyms and Initialisms in DISSCC.**

**TABLE AR.3.2. Annotated Listing of Equations in DISSCC.**

Table AR.3.3. Breakdown of Equations by Type.

TABLE AR.3.4(A-D). DYNAMO Equation Lists 4(X2) Modes of DISSCC.



TABLE AR.5.1. Example of Printout of all Variables: DISSCC OPTION 1  
(results are identical with and without crack closure for this set of  
parameters); selected interval (see figure AR.5.1).

**TABLE AR.5.2(A,B).** Examples of Printout of all Variables; DISSOC  
OPTION 2, With Decay of BPH; Selected intervals (see figure AR.5.2)

- A.** Tabulation of numerical results for first 10,000 years.
- **B.** Tabulation of numerical results for first 100,000 years.

TABLE AR.5.3. Numerical Values of Constants in DISSCC: these constants were used in computations varying the Reference Crack Width, RCW (see table AR.5.4 and figures AR.5.3, AR.5.4 and AR.5.5).

TABLE AR.5.4 (A,B,C). Tabulation of Penetration and Overrun Times, varying RCW from  $1E-2$  to  $1E-5$  CM; other parameters held constant (see table AR.5.3).

A. Data from results for  $LENGTH = 1E4$  YEARS.

B. Data from results for  $LENGTH = 1E5$  YEARS.

C. Data from results for  $LENGTH = 1E6$  YEARS.

Legend: PT - Penetration Time, based on time when either SCDIA or SCDIAC reaches  $1E4$  CM.

TCT - Total Compaction Time, based on time when either AVNEC or AVNECC reaches  $1E4$  CM.

OT - Overrun Time, based on time when either SO or SOC reaches  $7.9E14$  CU CM.

TDT - Termination of Dissolution Time, based on time when crack closure is effectively complete, ANCC = 0 and dissolution has stopped.

(L) - Values based on linear interpolation.

Note: Numerical values cited from these results should be for the shortest value of  $LENGTH$  that gives the result sought. Results read from the longer runs have larger errors at the shorter times because of the larger value of the time step, DT.

**TABLE AR.5.5(A-G). Tabulation of Penetration and Overrun Times; from  
Sensitivity Analysis.**

**Note:** Numerical values are tabulated according to run length, as in  
table AR.5.4. Results used for regression analysis, however, are from  
the runs of shortest length that gave results for PT, TCT or OT (see  
caption of table AR.5.4).

TABLE AR.5.6. DYNAMO Equation Test List-OPTION 1 for Thermal Expansion  
Feedback.

**TABLE AR.5.7.   Dynamo Equation List-OPTION 1 (CLTST)CL Loop Test  
Program.**

-

FIGURE AR.3.1. System Diagram for DISSCC. The diagram gives a layout of the Level, Rate and Auxilliary functions (see Legend for symbols) used to describe Dissolution With and Without Crack Closure. Names are identified in table AR.3.1 and equations are annotated in table AR.3.2; abbreviated equations are shown for identification only. The lower part of the diagram (below the Thermal Expansion box) refers to the sets of functions that describe dissolution with time-dependent closure of cracks.



FIGURE AR.3.2. Schematic illustration of the approximate sequence of calculations using DISSCC. Lines with arrows indicate the connections of constants, initial values and functions with the equations they feed. Self-contained portions of feedback loops are identified by heavy dashed lines. Blocks of directly coupled equations are identified by the symbol of their active function.

FIGURE AR.5.1. Example of computer plot for DISSCC, OPTION 1; results are identical with and without crack closure. The functions plotted are identified by single letter symbols shown at the top of the diagram. The numerical scale for each symbol is listed immediately below the list of identifications; where more than one function symbol is indicated, the numerical values are the same for each symbol. The scale symbols are given in the DYNAMO User's Manual (PUGH, 1976; Appendix A).

$B = 10^9$  (billions)

$M = 10^6$  (millions)

$T = 10^3$  (thousands)

**FIGURE AR.5.2.** Example of computer plot for DISSCC, OPTION 2 WITH DECAY OF BRINE PRESSURE HEAD (see FIGURE AR.5.1 caption for symbols); intervals identified by braces are tabulated (TABLE AR.5.2-A).

- A.** Plot of first 10,000 years illustrating behavior without crack closure.
- B.** Plot of first 100,000 years illustrating behavior with crack closure. Note that there is no sign of an instability for functions A and C (compaction and numbers of active cracks, respectively, with closure) during the first 30,000 years or so and then a wholesale instability develops between about 50,000 to 65,000 years.

FIGURE AR.5.3 (A-H). Computer plots of Dissolution With and Without Crack Closure, allowing for decay of brine pressure for different values of reference crack width (RCW), holding other parameters constant.

- A, B, C, and D: Results for OPTION 1 with RCW of  $10^{-2}$ ,  $10^{-3}$ ,  $10^{-4}$  and  $10^{-5}$  CM.

E, F, G, and H: Results for OPTION 2 with RCW of  $10^{-2}$ ,  $10^{-3}$ ,  $10^{-4}$  and  $10^{-5}$  CM.

Note: Run lengths were determined according to time required to achieve the result sought; in some instances these results were not achieved in a million years.

Penetration Time, PT (see tables AR.5.4 and AR.5.5), is identified by the time for SCDIA or SCDIAC to reach  $1E4$  CM; Total Compaction Time, TCT, is given by the time for AVNEC or AVNECC to reach  $1E4$  CM. Overrun Time, OT, is not plotted explicitly and is somewhat shorter than TCT in each instance.

FIGURE AR.5.4. Penetration Time, PT, and Overrun Time, OT, versus Reference Crack Width for OPTION 1 With and Without Crack Closure, holding other parameters constant (see table AR.5.4). Penetration Times are defined by SCDIA (without crack closure) and SCDIAC (with crack closure). Overrun Times are defined by SO (without crack closure) and SOC (with crack closure). The dependent variables AVNEC (without crack closure) and AVNECC (with crack closure) define times for the net subsidence compensating the dissolved volumes (includes thermal expansion), called the Total Compaction Time, TCT.

- A. Constant pressure head of brine (BPH).
- B. Pressure head of brine decreasing with time.

**FIGURE AR.5.5. Penetration Time and Overrun Time versus Reference Crack Width for OPTION 2 With and Without Crack Closure (see FIGURE AR.5.4 for definition of variables), other paramteres held constant.**

- A. Constant pressure head of brine (BPH).**
- B. Pressure head of brine decreasing with time.**

**FIGURE AR.5.6.** Sensitivity results (raw data) plotted in terms of dependent variables (ordinate) versus independent variables (abscissa) chosen from regression analysis using the Latin Hypercube Sample given in TABLE AR.5.5. The dependent variable represents actual values of either Penetration Time or Overrun Time as identified by the name on the ordinate.

- A.** Penetration Time, determined from SCDIA, versus Crack Coefficient,  $CC$ .
- B.** Penetration Time, determined from SCDIA, versus Reference Crack width,  $RCW$ .
- C.** Penetration Time, determined from SCDIA, versus the square of the Crack Coefficient,  $CC^2$ .

**FIGURE AR.5.7.** Sensitivity results (ranked data) plotted in terms of dependent versus independent variables (see caption FIGURE AR.5.6).

The data of TABLE AR.5.5 are assigned values ranging in relative rank from 1 to 20 for each variable, and these rank values are the plotted values in the figures. Conversions between "raw" and "rank" data are described by Iman and Conover (1979).

- A.** Penetration Time, determined from SCDIA, versus the Reference Crack Width, RCW.
- B.** Penetration Time, determined from SCDIA, versus the product of Dimensional Coefficient of Power, DCP, and Backfill Maximum Compaction Length, BMCL.



**FIGURE AR.5.8. Threshold times for dissolution feedback.**

**A.** Threshold times for dissolution feedback as functions of SHLROM in DISSCC OPTION 1(TEF). The horizontal dashed lines identify limits of dissolution for complete release.

**B.** Threshold times for dissolution feedback in DISSCC OPTION 1 based on CL Loop Test Program (Table AR.5.7.) in which the block of thermal equations is deleted to suppress thermal expansion threshold effects, as in figure AR.5.8.A.

**C.** Composite diagram showing relative effects of initial values of heat and compaction parameters. Other things equal, dissolution is triggered faster by the initial thermal input than the initial value of backfill porosity relative to the test forms of DISSCC: OPTION 1(TEF) and OPTION 1(CLTST).

APPENDIX

James E. Campbell, Richard T. Dillon, Martin S. Tierney,  
Herbert T. Davis, Peter E. McGrath, F. Joe Pearson, Jr.,  
Herbert R. Shaw, Jon C. Helton, Fred A. Donath

1978

Risk Methodology for Geologic Disposal  
of Radioactive Waste: Interim Report

NUREG/CR-0485, SAND78-0029  
Albuquerque, Sandia Laboratory, 264 pp;  
Appendix 2A\*, p 87-160

\* Text and Calculations in Appendix 2A were responsibility of H.R. Shaw,  
assisted by F. Lusso

## APPENDIX 2A

### Methods of Simulation Analysis Applied to Questions of Geological Stability of the Reference System

#### 2A.1 Introduction

At the present stage of development there is relatively little cohesion between the model types described earlier in this chapter. Need exists to integrate the several modeling efforts to: (a) quantify their implications in a comprehensible format, and (b) test for interactions between different models and for feedback loops connecting two or more process models.

Toward this goal several integrating methodologies are available, in principle to define the scope of such relationships. One of these consists of various forms of fault tree analysis, in the broad sense discussed by Barlow and Lambert<sup>(2A.1)</sup>; another is simulation analysis using some form of the many computer simulation languages available today.\* The analysis in previous parts of this chapter explores some of the difficulties in trying to describe a geologic system in probabilistic terms. These difficulties include: (a) problems of scale-- i.e., what are the physical and temporal bounds of the system which must be analyzed? (b) problems of knowledge -- there is a lack of rigorous numerical constitutive relations for geologic behavior and a lack of geophysical data and time series to generate probabilities, (c) problems of coupling and feedback-- there is usually no simple way to take account of complicated interactions using probabilistic methods, and (d) probabilistic methods often obscure some of the common sense physical relationships in the system. Point (b) is analogous to problems of weather predictions, except that we have the additional problem of analyzing both the geological system (the geological "weather" system) and an engineered structure that interacts with and affects geological "weather" changes. With respect to probability analysis, we also have the problem of generating the geological analog of the performance characteristics normally supplied for the analysis of engineered structures. Simulation methods seem necessary to make any substantial progress toward that goal in the foreseeable future. Geological data collection is notoriously slow and difficult by comparison with engineered systems because of the limited accessibility and long times involved.

---

\* We have chosen in this report to use the language, DYNAMO, distributed and maintained by Pugh-Roberts Associates, Inc., Five Lee Street, Cambridge, Mass., 02139; see references 2A.4 and 2A.11.

#### 2A.1.1 Simulation Models and Geological Perspectives

The method of simulation used in this report was chosen because it is highly developed in many fields of systems analysis<sup>(2A.4)</sup> and is particularly useful in problems where boundary conditions and system variables are poorly known - e.g., as in applications to economic models.<sup>(2A.5)(2A.9)</sup> Application to natural systems is not known to us, but the method is promising in that context because of the ability to simplify system behavior both conceptually and mathematically. To us, this approach to geological simulation has the following advantages:

1. It does not obscure common sense relations or mask the identity of simplified functions,
2. It is very easily modified or completely rearranged as experience accrues on boundary conditions or as other research modifies various constitutive relations,
3. It provides a united framework against which to view total system behavior,
4. It allows for feedback loops of conceptually any length or complexity;
5. By its physical simplicity it keeps the analyst aware of model limitations that are sometimes lost in a more mathematical format.

This last point cannot be overemphasized. We are dealing with idealogical models that simply reproduce relationships that are either known or reasonably suspected and are permitted to interact in ways that suggest, but do not predict, how the real world may behave. We repeat this for emphasis.

Simulation calculations of the sort described remind us by their very simplicity that they are just idealized models. They only reproduce phenomena already known or reasonably suspected and suggest, but do not predict, how the real world may behave.

2A.1.1.1 Questions of Geological Stability -- Three types of questions challenge our ability to evaluate the containment potential of a repository site: (1) How accurately can we describe the natural changes that affect the integrity of a given volume of rock over specified intervals of time from tens of years to a million years? (2) With what confidence can we state how these natural changes will be modified by the disturbances invoked by a radioactive waste repository? (3) How comprehensively can we describe and analyze the behavior of the waste repository facility -- an engineered structure which presents problems somewhat analogous in difficulty to those of nuclear reactor safety studies.

2A.1.1.2 Strategies of Systems Analysis -- We view the methodology development as an evolving process dependent on interaction of many analytical methods. The examples cited above indicate that geological analysis is a key phase without which others may be meaningless exercises. There may be stages at which analytical progress will be directly contingent on the laborious process of geological data collection. In the meantime, however, the array of problems that may have to be addressed geologically can be sorted and organized by the artificial creation of system structures involving simulation analyses. These may take the form of detailed geochemical transport modeling, thermochemical-mechanical interaction simulation, simulations of multiple dynamic feedback processes, or possibly even some forms of fault-tree/event-tree analyses when there develops a sufficient understanding of processes to warrant them. Though feedback simulation is addressed in this part of the chapter, there is no recommendation that it supersede any other, except in the sense of exploring new terrain for study and in the possibility of providing a communications medium for coordinating other techniques.

2A.1.1.3 Role of Approximations in Systems Analysis -- Approximations are implicit, though often hidden, in all analytical efforts however sophisticated the final product may appear. To address analytical goals of system behavior, the system must be defined in terms of consistent relationships between the dimensional scales of the phenomena involved. For instance, in petrography we do not go directly to the oil immersion lens or scanning electron microscope. First we examine the rock in the field setting, in hand specimen, in rough cut, in binocular field, petrographic microscope, etc., sometimes winding up with highly focused and sophisticated x-ray structure analysis of one of the mineral grains. There are many levels of meaning and information at all stages of this process which interact and potentially form part of what we call our knowledge of that rock. Even this multistage process is a small part of the total effort. There are chemistry, geochronology, physical property measurements, other field surveys (such as provided by mapping, paleontological and geophysical techniques), and so forth.

The point is that numerical simulation analysis consists of similar hierarchies of effort. The reconnaissance survey is often of crucial importance in either the actual or simulation cases to the value of any highly sophisticated analysis.

Taken together, these questions pose a problem of incredible intricacy. No unequivocal statement seems possible concerning the precise nature of future system states. With respect to question (1) alone, our understanding of the composite history of any given geological site on this dynamic planet is insufficient to give evaluations other than by educated opinion or assertion. Entire continents are postulated to move distances commensurate with their half-widths on time scales of the order of 100 million years. To be sure, old rocks of relatively undisturbed character exist, but the rocks that are now of entirely different character or have been chemically broken down, dispersed and reconstituted in various ways were once represented by states resembling these so-called stable rock types. The problem is that usually we are not able to say exactly where and when these changes have taken place or will take place. An example pertinent to this

report is shown by 200 million-year-old salt beds that still exist today, except for those beds that have been partly or totally dissolved away. This would be a conundrum but for the traces derived from indirect geological deductions based on local and regional studies of structural, geochemical, stratigraphic, and geochronological continuity.

Another case in point is the phenomenon of the 1.8 billion-year-old "fossil nuclear reactor" Oklo in the Republic of Gabon. <sup>(2A.3)</sup> This natural situation demonstrates the potential retention capacity of some geological settings. Oklo, however, also illustrates some of the above questions. With what assurance can we state that another site has exactly the same characteristics? Although "most" of the fission products generated at Oklo have been retained, what precisely is that amount and what is the geometric scale of dispersal of the percentage lost? Is it possible to say what percentage of the radionuclides reached surface waters? Is there any major distinction between 10 percent, 1 percent, etc., from the standpoint of potential pathways to humans? An event of major chemical alteration apparently affected some of the Oklo rocks about 10 million years ago (Ref. 2A.3, p. 257). Could that have been predicted at a million years or less before its occurrence?

The point concerning Oklo is that evidence of radionuclide retention does not necessarily answer the more relevant questions concerning conditions and mechanisms of fractional loss. It does demonstrate, however, that geological data, if extensive enough, can delimit a time-space framework against which evaluations of dispersal mechanisms can be tested.

Another aspect of geological stability is that macroscopic chemical integrity is possible even though there has been extensive chemical exchange at the levels of trace element concentrations (e.g., less than parts per thousand; see Ref. 2A.15). The fact that a rock has existed with mineralogical and textural integrity for a long time is not in itself admissible testimony to its chemical integrity. Documentation of the sort partially compiled for Oklo is essential to such claims. The opportunity to document analogous cases for other geological media exists at the sites of past underground nuclear explosions (e.g., the Gnome Site near Carlsbad, N.M., which is in rocks similar to those of another site in that vicinity which is being considered for a possible radioactive waste facility).

In our view the most important, and seemingly contradictory, value of approximate ("lumped parameter") analyses, is that the very nature of the simplifications used for numerical relationships enforces the reminder that numerical simulation under any circumstance is an approximation technique. We are continuously warned against believing the result simply because

we know that the primary relationships themselves are incomplete approximations. "Belief" is often a subtle and powerful tendency when great effort and intricacy has gone into building a sophisticated model.\*

It is usually easier to change or abandon parts of a DYNAMO simulation, for example, than it is to change or abandon results of sophisticated finite difference or finite element modeling. Reconnaissance calculations also are many times faster and much cheaper. A hundred DYNAMO runs involving many coupled phenomena can be made probably with less expenditure of time and money than one relatively refined (but still incomplete) three-dimensional heat conduction calculation (presupposing similar levels of prior analytical experience and insight in the two cases). In either case the greatest time, effort, and importance goes into "setting up the problem" or formulating the ideas and numerical content of the system structure. Once a question can be addressed hypothetically or approximately, however, simulation languages like DYNAMO can give conditional answers very quickly.

2A.1.1.4 Conceptual Importance of Feedback Phenomena -- There are three general categories of functional relationships important to system behavior: (a) independent phenomena, (b) directly coupled phenomena, and (c) phenomena that are part of feedback cycles. These categories are artificial in the sense that (b) may partly imply (a), and (c) usually involves aspects of both (a) and (b).

Independence was assumed, for example, in the probabilistic discussion of this report (Section 2.5) and requires no further explanation here. However, one qualification is offered. Events or processes that can be treated in isolation from other events or processes in one time-space framework may be influenced by feedback mechanisms on other scales of behavior. A patently distorted, but graphic, example of this sort of effect can be imagined relative to meteorite impact. Suppose that the current incidence of impacts were sufficient to effect changes in the earth's orbital parameters so as to bring it into more direct intersection with asteroid orbits which resulted in much higher incidences of meteorite impacts? The independence of the event is no longer defined only by external conditions. In this case the energy and time scales indicate that the effect is inappropriate to the scale of our problem, but the existence of this type of behavior requires diligent searching for analogous cases that may be relevant. Other large-scale examples can be found in relationships between atmospheric circulation, climate, and vegetation zones.

---

\* There is a major distinction between building an isolated sophisticated model and a sophisticated numerical scheme that is capable of rigorous calculations involving many variables. The latter is used in conjunction with reconnaissance techniques and field observations to force part of the analysis to its logically rigorous conclusion if justification exists. This capability (like the transport modeling capability described in the main report) will be of crucial importance to any future abilities to make more specific statements. The rougher structural framework, however, remains as a check on tendencies to follow this special path to the exclusion of others.

Coupled phenomena represent the class of problems most often encountered in engineered systems. For example, flow of the working fluid in some sort of chemical reactor may influence the behavior of other parts of the system by heat and/or chemical transfers, but the resulting changes in behavior may have no reciprocal influence on the thermal or chemical sources. Evaluation of the consequences is in practice often difficult and intricate, but it is relatively straightforward.

Feedback phenomena exist in a variety of forms. There are types involving phenomena that are also highly coupled and types involving remote and circuitous paths. We can never say that we have discovered all of the latter, but we must continue to look for their existence if we are to operate by other than blind faith in functional independence. Feedback may be positive (or regenerative) leading to unstable system states, or negative tending toward steady or equilibrium states.

An example of a highly coupled feedback phenomenon that is easily grasped and documented, and is of potentially major concern to the behavior of mechanical systems, consists of the relation between mechanical work, dissipation as heat, and thermal effects on system properties. In many cases a feedback loop is established in which the mechanical work rate itself becomes influenced by this chain of events, thereby perpetuating the cycle. The situation is easily visualized in the flow of viscous liquids, particularly as it has been placed in dimensional perspective by Gruntfest.<sup>(2A.6,7)</sup> Here the heat generated by frictional resistances in viscous flow decreases the viscosity and thereby increases the flow rate, the local heat generation rate, and the rate of decrease of viscosity for a given driving potential. This sort of positive feedback cycle is highly unstable.

Positive thermal feedback phenomena have been shown to be important to the flow behavior of rocks at high temperatures and pressures by several workers (see Ref. 2A.12 for relationships between melting and deformation phenomena). Since we are concerned with rock deformation in connection with repository stability, a simple test of this sort of feedback was performed relative to possible stresses and deformation rates that could be encountered in a repository in a bedded salt deposit. At shallow depths, low stress differences and temperatures in the neighborhood of 100°C ( $\pm 10^\circ\text{C}$ ), energy balance calculations indicate that the time scale of a possible thermal feedback instability is much greater than the time scale of interest (i.e.,  $\gg 1$  million years). Hence we conclude that the laboratory and the in situ field measurements concerning behavior of salt deformation are applicable to salt deposits at shallow depths and low stress concentrations to the extent that other sorts of phenomena are not involved.\*

---

\* Thermal feedback effects become enhanced at higher pressures and temperatures, hence further analyses are indicated relative to behavior of large-scale salt diapirism.



Several other phenomena in salt deposits appear to call for feedback analyses which we have not performed. Important among these are the behavior of fluid inclusions and possible interactions between the chemical stability of mineral hydrous phases and the mechanical properties of the rocks.

The migration of fluid inclusions in salt caused by thermal gradients is known to represent a form of feedback (Ref. 2A.2, p. 164). Without going into details, the temperature dependence of the solubility of salt in liquid water leads to inclusion migration up the thermal gradient. This effect is countered by an inverse solubility relation if temperatures become high enough to form a vapor phase. In that case the migration tendency is reversed and inclusion distributions in principle would become stabilized. This would seem to represent a form of negative feedback tending toward dynamic equilibrium and quasisteady inclusion distributions. In our opinion, however, the reality of this conclusion is not completely established, and further work is needed from the standpoint of mechanical interactions and relation to temperature histories. This report has given attention only to some questions of potentially greater whole-sale consequences.

#### 2A.1.2 Numerical Simulation Methods

2A.1.2.1 Choice of Simulation Language -- Several simulation languages are in widespread use. We have chosen DYNAMO as the initial vehicle because of immediate availability, simplicity, and convenience of operation. We plan to explore the possibility of using GASP IV<sup>(2A.10)</sup> or other such languages, that offer greater options for handling discrete and discontinuous phenomena.

2A.1.2.2 Characteristics of DYNAMO -- DYNAMO is a computer technique for the ordering and approximate solution of sets of ordinary differential equations. Its advantages stem from many years of widespread use and consequently many built-in conveniences involving automatic equation ordering, internal tests for consistency and redundancy, automatic or specified plotting limits, relatively complete and convenient error messages, speed, and flexibility. The equations are essentially statements concerning quantities (Level Equations), their rates of change (Rate Equations), and statements concerning any other relationships required to define the Rate and Level Equations (Auxiliary Equations).

The calculation consists of evaluation of all Auxiliary Equations at a given time based on previous statements for the Levels (obtained either from specified initial values or previous calculations) followed by calculations of the Rate Equations and their inputs to the Level quantities over some specified time change. The output is in a form displaying the continuous

functions (ten functions at a time can be plotted). \* Depending on purpose, it may be desired to compare different functions on the same plot or the same function with several choices of parameter variations. In the latter case one need only be sure that the equations are uniquely specified for the different choices. Equation listings for examples of the two modes are given in the section on results.

Although time is plotted linearly, the effect of logarithmic variation can be examined by means of repeated calculations with lengths and plotting periods progressively increasing, for example, by factors of ten. A time sequence can thereby be pieced together which simultaneously illustrates on the same plot contrasts of short-term and long-term variations of the prescribed sets of quantities.

More complete descriptions and instructions for DYNAMO are given in Refs. 2A.4 and 2A.11. With these guides in hand, the more specific characteristics of DYNAMO are quickly picked up by making test runs of functional behavior using test problems with real or invented equations.

## 2A.2 Reference System for DYNAMO Simulation

The reference system used for DYNAMO calculations is similar to that described in Chapter 1. Any differences reflect approximations assumed for the sake of illustrating numerical capability. All numerical quantities and relationships in this report are subject to review, correction, or revision.

### 2A.2.1 Rudimentary Geometric Structure

The simplified reference system is shown in Figure 2A.1. The approach is to portray as many physically meaningful relationships as possible with the fewest possible geometric constraints. In other words, as many parameters as possible are lumped into relationships that approximate general behavior as though describing a one-cell model. For example, heat distributions are treated only in terms of conservative input-output balances for a single volume element. As will be shown, considerable information is obtained from such a simplistic "model" even though little spatial detail is available. The latter sort of information is independently available from the multi-cell modeling techniques (thermal-elastic modeling and transport modeling). Comparison with DYNAMO results shown later illustrates the degree of approximation available from the one-cell approach and reinforces our position that several different integrated techniques are needed to build understanding of system performance.

---

\*The fact that the functions are continuous is sometimes an apparent drawback. It is possible, however, by judicious consideration of system structure to simulate discontinuities by continuous but rapidly changing functions. Many kinds of variation can be considered so long as care is used in choices of time steps and in checks for physical plausibility, etc.

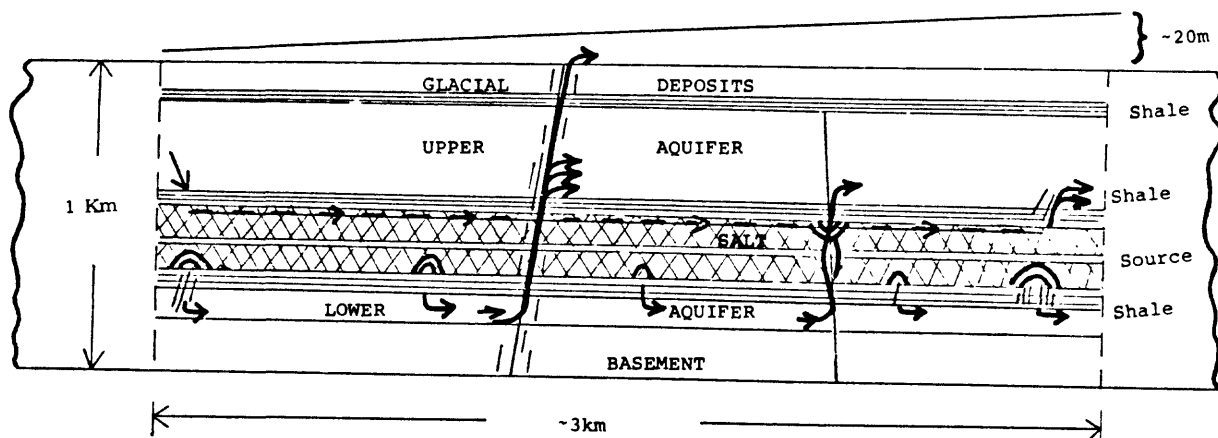


Figure 2A.1. Simulation Reference Volume for DYNAMO

Other relationships such as thermal expansion uplift, compaction, subsidence, cracking and so forth are also lumped or averaged over the same volume element. The form of these approximations will be evident when the system equations are defined.

The several groundwater pathways schematically portrayed in Figure 2A.1 are used only to guide the form of potential access of water to the salt horizons. Mass transport mechanisms appropriate to a given path are then examined for their potential magnitude limits. The potential reality of these conditions are subject to other considerations (further modeling, geological data synthesis, etc.). Our general aim will be revealed more clearly when we describe flow diagrams of functional system structure.

#### 2A.2.2 Capabilities of Increased Geometric Complexity Using DYNAMO

There is no theoretical restriction on the number of cells that might be defined for feed-back calculations. We feel that such refinements should only be attempted, however, when the system interactions of interest are well known in the lumped parameter mode so that deviations originating in geometric factors (including variations of physical properties, etc.) can be meaningfully isolated. Therefore, we restrain our calculations to aspects that are, or may be, generically meaningful in the absence of spatial detail, recognizing that greater detail is obtainable at a price. The price is not primarily computer time and money, but the potential distraction of analysis from pursuit of unexplored causal relationships for the sake of numerical precision in relationships that are only partially understood.

There are times, however, when detail may be very important to other aspects of feedback approximation if system responses are sensitive to, or triggered by, small fluctuations in some specific variable (e.g., temperature). Recognition of such situations inevitably depends on the insight of the analyst. Again, this emphasizes the need for parallel and simultaneous analytical tools.

### 2A.3 Systems Diagrams

The beginning of any numerical simulation consists of organizing the active functional relationships. For consistency with DYNAMO and previous practice, we have used the form of systems diagram and symbols described by Forrester. (2A.4)

#### 2A.3.1 Descriptive System

An attempt is made to verbally describe the nature of the reference system structure as it is viewed from the standpoint of potential feedback relationships. The terms described in Section 2A.3.1.1 are given no quantitative values. Explicit terms for numerical work are defined in Section 2A.3.2.

2A.3.1.1 System Structure -- Figure 2A.2 shows a schematic diagram of system structure as it pertains to questions addressed to the reference system shown in Figure 2A.1. Minimum complexity is again emphasized. An effort is made to involve the fewest possible level and Rate Equations that still might be capable of identifying processes in the schematic system affecting geological stability and radionuclide dispersal. Actual mechanisms of dispersal, however, have not been addressed in the numerical demonstrations subsequently described, because considerably more effort is desirable in probing the kinds of behavior symbolized in the lower portions of the diagram. Currently, we have only studied some questions relevant to possible access of groundwater to the salt horizons of Figure 2A.1.

The Levels of Figure 2A.2 (rectangles) are mostly self-explanatory and simply represent conservation statements concerning the respective quantities. Most of the Levels are composite. For example, the mechanical work (MW) Level represents several effects such as thermal expansion (TE), compaction (C), work of earthquakes and faulting (EF), and other mechanical work terms (OMW).

The ways in which the levels are organized depends on the aim of the analysis. Our idea in this particular scheme is to explore various effects on potential groundwater access to the repository. Levels labeled FRACTURES and OPENINGS are separated because, in principle, fracturing does not necessarily create porosity (in fact, it could create barriers to flow with consequent major changes in flow paths).

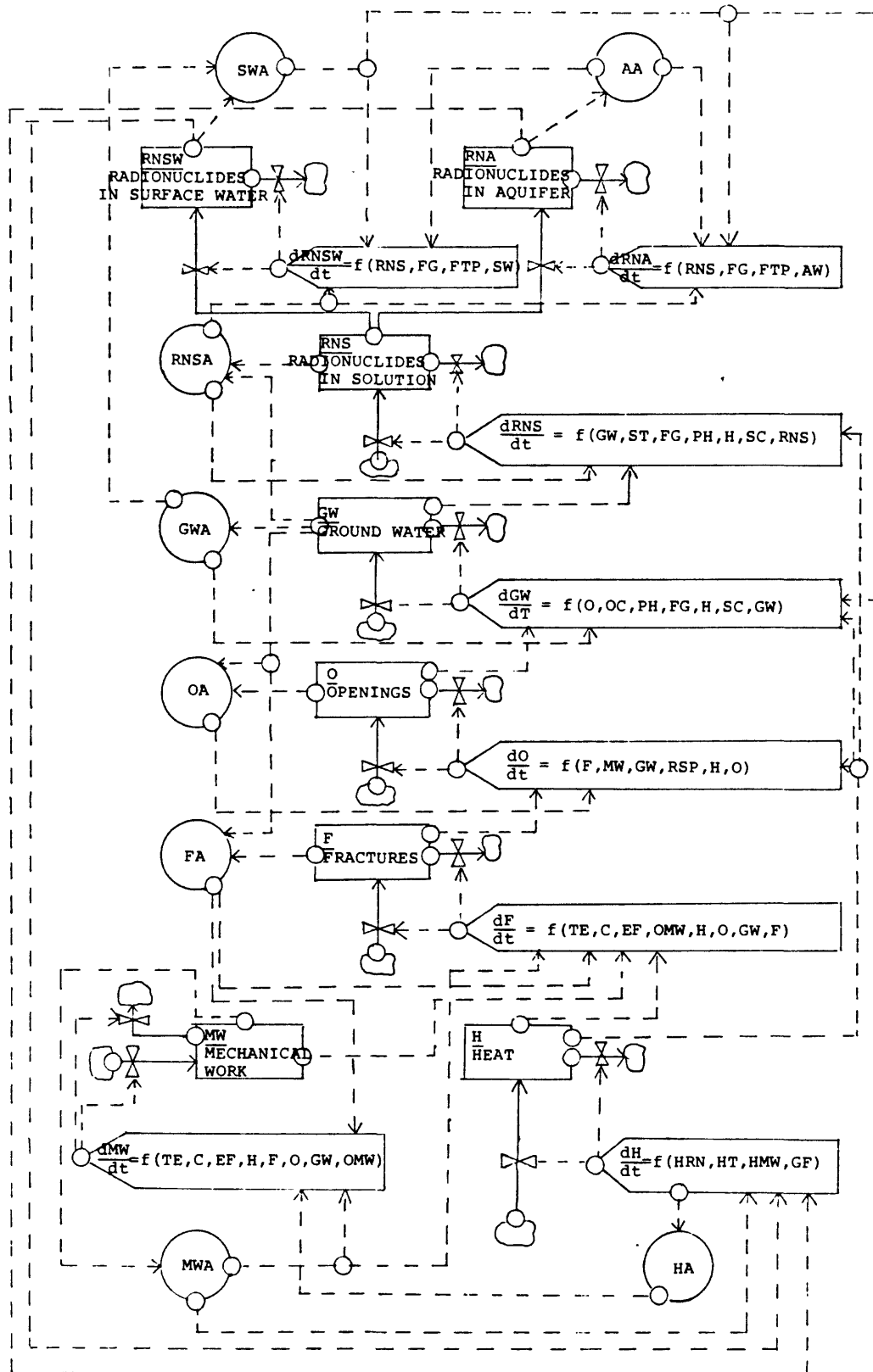


Figure 2A.2. System Structure Diagram

The interactions portrayed in Figure 2A.2 involve effects of the following general kinds: (1) effects of radionuclide decay on thermal mechanical and chemical states, (2) effects of mining and backfill properties on lithologic integrity, porosity and compaction, (3) effects of these work mechanisms and faulting mechanisms on fracturing, (4) the above composite effects on rock openings, (5) composite effects on groundwater quantities and flow states, (6) effects of groundwater on rock openings via influences on mechanical and chemical properties (particularly salt solubility in the context of the reference system), (7) effects of all processes on the potential access of groundwater to radionuclides and rates of their incorporation in the groundwater system, and (8) net effects on dispersal of radionuclides out of the system via either aquifer or surface water pathways.

Changes in the above relations are schematically described by a series of rate equations that govern input-output balances via the schematic valve symbols. The source-sink "cloud" symbols simply indicate that the quantity may relate to mass and energy reservoirs of different kinds that are defined outside the system; physically, they remind us of various possible initial conditions, boundary conditions, and time dependent influences of external origins (changes in geothermal flux, tectonic effects, and so on). Some types of point events (e.g., meteorite impact) and intermittent or pulse events (e.g., earthquakes) might be crudely approximated as to very simplified consequences using DYNAMO, but this is an area of simulation technique that needs innovative research attention.

Level and Rate Equations are related by sets of Auxiliary Equations. In a completed diagram the interrelationships are displayed by a network of dashed Information Lines. In Figure 2A.2, the Auxiliary Equations are completely lumped in one general symbol for each Level; many different kinds of functions are implied by each symbol. Here the Information Lines are shown only to indicate their purpose; i.e., the Information Lines of Figure 2A.2 are not complete and are not necessarily even rigorously correct. We have included some improbable connections to emphasize that fact. It is suggested that other persons involved in the analysis of radioactive waste management study this diagram or reconstruct others of their own in terms of attempts to identify functional dependencies.\*

---

\* The Information Line between RNSW and SWA, for example, may be misleading in the present physical context. The amount of radionuclides in surface waters is not expected to have an effect on the hydrology, unless there is a bizarre effect like influence on growth of massive algae deposits that influence stream flow. Effects of radionuclide interactions on aquifer properties are possibly less farfetched (e.g., as regards heat).

The symbols for the Auxiliaries in Figure 2A.2 are simply the Level symbols followed by A. Later on, the terms included in the various equations will be assigned specific descriptive name symbols. Symbols in the schematic Rate Equations are also the same as the Level symbols, with the following additions:

- HRN - Heat produced by RadioNuclides as originally placed in the repository.
- HT - Heat Transfer by conduction and convection.
- GF - Geothermal Flux balances.
- HMW - Heat produced by dissipation of Mechanical Work.  
Note: Dissipation is included as an example of an input that might be overlooked; as discussed in the text, this term probably is not significant in the context of the general balances relative to the conditions of the reference system.
- TE - Thermal Expansion (in context of reference system, this takes the form of uplift).
- C - Compaction of pore space (such as produced by residual porosity of mining activities, salt dissolution, etc.).
- EF - Tectonic energy induced by Earthquakes and/or Faulting.
- OMW - Other Mechanical Work (e.g., induced by buoyancy forces of various origins).
- RSP - Rock Solubility Parameters (mineralogical phases present, their stabilities, solution properties, etc.).
- OC - Openings Connectivity (in part overlaps with FG).
- PH - Pressure Head (in present context defined externally by reference to hydrologic modeling; see discussion in Chapter 3).
- FG - Flow Guides (in present context, identified by geometric structure and specified assumptions relative to Figure 2A.1; repetitive modeling of hydrologic options is essential to sorting the relative importances of artificially imposed flow conditions).
- SC - Solute Concentration (as it affects solubility, hydraulic properties of water, thermodynamic stabilities of minerals and so on).
- ST - Source Terms (local conditions of water access to canisters, canister stability, leaching, etc.).

- FTP - Fluid Transport Properties (relative to hydrology, radionuclide distributions influenced by distribution coefficients, etc.).
- AW - Aquifer Water (hydrologic factors in aquifer flows).
- SW - Surface Water (hydrologic factors in surface flows).

Inspection will show that this is not a comprehensive list of the Rate Equations and variables. It is given to indicate the general idea and to stimulate searches for the relevant variables and their interdependencies.

Closer inspection of Figure 2A.2 will disclose various types of potential Feedback Loops. Possibly, the most conspicuous type of feedback is of the sort already described (e.g., mechanical work-heat cycles). Another fundamental kind is the effect of a Level quantity on the rate of change of that quantity. In one way or another this form of feedback affects every Level. For example, the amount of heat stored in the reference system affects the rate of heat loss and hence the subsequent heat quantity. The amount of mechanical deformation (relative to some initial reference configuration) performed on a system influences the mechanical states and properties of the rocks of the system, hence the future mechanical work rates. Similar statements are true of fracturing and production of rock openings. Groundwater quantities influence future Level states via consequent hydrologic flow rates. Radionuclide quantities in solution influence future rates of incorporation by depletion of the finite source, and so on.

Many types of indirect Feedback Loops can be found by careful study of diagrams like Figure 2A.2. Formally, all closed circuits in the directions of Information Arrows represent Feedback Loops. There is virtually an infinity of involutions and convolutions of these possible connections. The problem forced on us by questions of radioactive waste containment in geological media is to find the dominant loops and to understand their magnitude-time relations as regards geological stability. Diligent and repetitive construction of such Systems Diagrams, Information Lines, and Feedback Loops assists these hierarchical sorting processes.

Only two indirect Feedback Loops will be mentioned as type examples. The first of these is very simple to understand, but it is the most indirect and is quantitatively contingent on some form of numerical solution of all system variables which has not been accomplished to this date. Starting with the Heat Level on the lower right of the diagram, Information Lines can be traced through the entire diagram and back to the Heat Level. That is, the amount and distribution of heat generation by radioactivity simply depends on what happens to the radionuclides other than simple decay in their original configurations. From the standpoint of the overall system this represents a Negative Feedback Loop tending toward thermal equilibrium. This conclusion, however, should not encourage complacency concerning other forms of potential thermal feedback.



Local Positive Feedback Loops of thermal origins are conceivable within this system-wide negative feedback cycle (a simple case being thermally induced chemical reactions triggered by transport of hot solutions).

The second specific example considers feedback between Mechanical Work, Fracturing, Openings and Groundwater. The Heat Level is an input via Thermal Expansion (TE) and via the temperature dependence of mechanical properties. Hydrologic parameters, in particular the Pressure Head (PH), can be defined outside this particular subsystem, but it should be possible to incorporate the hydrology as part of the Feedback Loop by judicious iterations in sequence with the Hydrologic Transport Model of this Report (Chapter 3).

The main feedback of this artificial subsystem, which will be referred to as the H-MW-F-O-GW Sector, is a consequence of salt solubility and brine transport. The feedback is strongly positive. The rest of this appendix, other than the section on Recommendations, deals with numerical approximations for this Sector.

#### 2A.3.2 Specific Diagram and Equations for the H-MW-F-O-GW Sector

The bottom half of the system diagram of Figure 2A.2 is redrawn more explicitly in Figure 2A.3. For practical reasons, some Levels, particularly Mechanical Work, were subdivided into several Levels. The remainder of Section 2A.3 identifies the respective equations within a DYNAMO format, without going into their physical content. Section 2A.4 discusses the physical approximations and dimensional content of the equations and attempts to identify their limitations. Section 2A.5 gives the computer results.

2A.3.2.1 Heat Level -- Letter symbols at the left margin for each equation shown in the following paragraphs indicate its type: Level (L), Rate (R), Auxiliary (A), Constant (C), Initial Value (N), Table (T), Supplementary (S), Continuation (X).

$$L \quad H, K, = H, J + DT*(HINR, JK - HOUTR, JK) \quad \underline{HEAT}$$

The indices J, K, L refer, respectively to an immediately preceding time (J), the current time (K) and immediate future time (L). The time step of the calculations is DT and corresponds in length to the past interval (JK) and future interval (KL). Algebraic symbols are standard, except that the asterisk indicates multiplication. For algebraic conventions and other elaborations of equation writing for DYNAMO, see Pugh<sup>(2A.11)</sup> and Forrester.<sup>(2A.4)</sup>

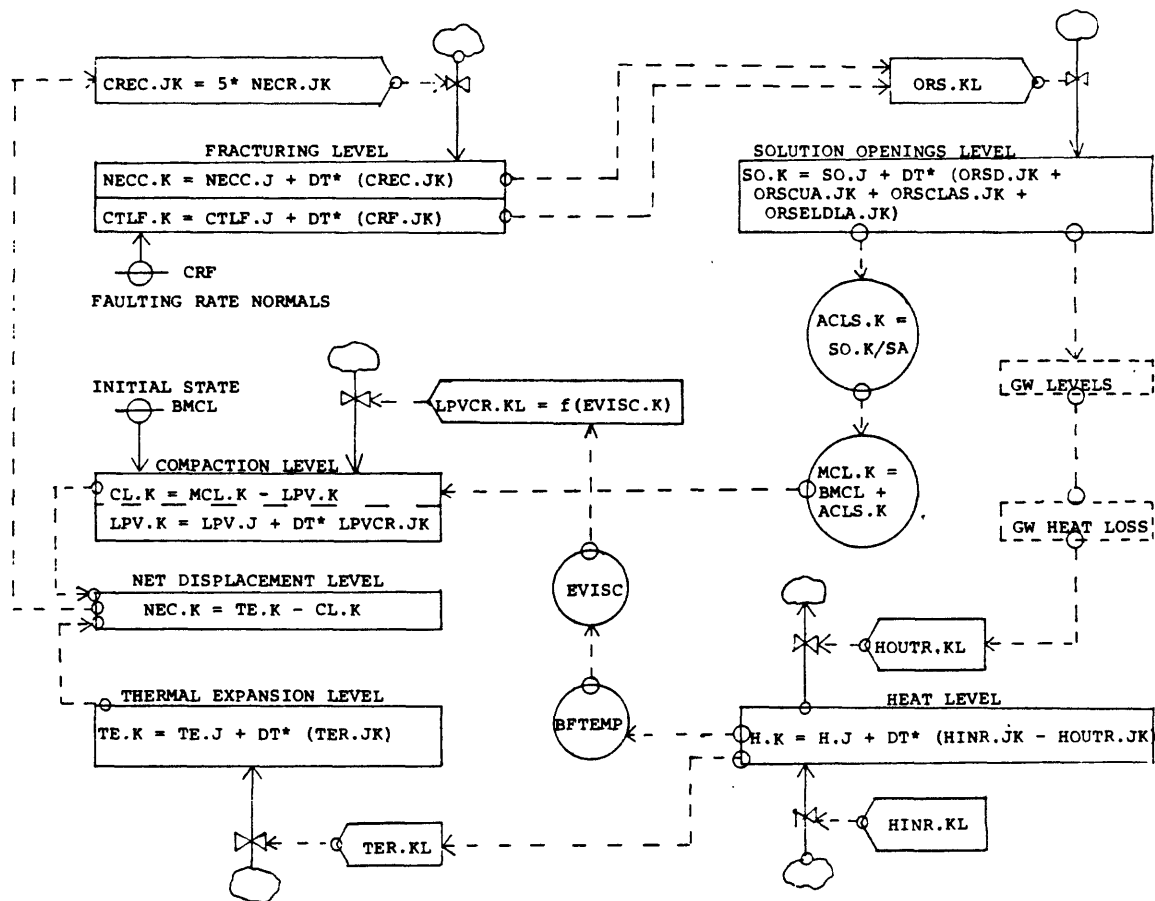


Figure 2A.3. System Diagram for H-MW-F-O-GW Sector

The active equations for the Heat Level are as follows (in this section equations are simply named without derivations or dimensional quantities; where equations could not be completed without discussion of physical principles, their types are indicated parenthetically - see Sec. 4):

- R  $HINR.KL = DCP * FD.K$  HEAT INPUT RATE
- A  $FD.K = (\text{Table function})$  FRACTIONAL DECAY
- C  $DCP = (\text{Constant})$  DIMENSIONAL CONSTANT FOR THERMAL POWER
- R  $HOUTR.KL = \text{DELAY} (SHLR.JK, DSHF)$  HEAT OUTPUT RATE  
(Note: "DELAY" refers to built-in DYNAMO functions that introduce delayed responses of output to input functions; see Ref. 9.4, Chapter 9)
- R  $SHLR.KL = (\text{Analytic function})$  STEADY HEAT LOSS RATE
- C  $DSHF = (\text{Time Constant})$  DELAY OF SURFACE HEAT FLUX

2A.3.2.2 Thermal Expansion Level -- Thermal expansion is, of course, directly coupled with the Heat Level via equations of the following type:

$$\begin{array}{ll}
 \text{L} & \text{TE.K} = \text{TE.J} + \text{DT} * (\text{TER.JK}) \quad \text{THERMAL EXPANSION UPLIFT} \\
 \text{R} & \text{TER.KL} = \text{UEC} * (\text{HINR.JK} - \text{HOUTR.JK}) * \text{HC} \quad \text{THERMAL EXPANSION RATE} \\
 \text{C} & \text{UEC} = (\text{Constant}) \quad \text{UNIT EXPANSION COEFFICIENT} \\
 \text{C} & \text{HC} = (\text{Constant}) \quad \text{HEAT CAPACITY (AVERAGE)}
 \end{array}$$

2A.3.2.3 Compaction Level -- Compaction refers primarily to average vertical displacements caused by collapse of pore space in the salt horizons due to the weight of the overburden strata; the pore space arises from both mining activities and imagined salt solutioning mechanisms. The equations are written for the one-dimensional case as follows:

$$\begin{array}{ll}
 \text{L} & \text{CL.K} = \text{MCL.J} - \text{LPV.J} \quad \text{COMPACTION LENGTH} \\
 \text{A} & \text{MCL.K} = (\text{Constant} + \text{Output of Solution Openings Level}) \\
 & \quad \text{MAXIMUM COMPACTION LENGTH} \\
 \text{L} & \text{LPV.K} = \text{LPV.J} + \text{DT} * (\text{LPVCR.JK}) \quad \text{LINEAR PORE VOLUME} \\
 \text{R} & \text{LPVCR.KL} = (\text{Analytic} + \text{Table Functions}) \quad \text{LINEAR PORE VOLUME} \\
 & \quad \text{COMPACTION RATE}
 \end{array}$$

2A.3.2.4 Net Displacement Level -- This Level represents simple algebraic summation of the Thermal Expansion and Compaction Levels:

$$\text{L} \quad \text{NEC.K} = \text{TE.K} - \text{CL.K} \quad \text{NET EXPANSION MINUS COMPACTION}$$

2A.3.2.5 Fracturing Levels -- In any rigorous analysis, this composite Level involves many intricate and complex phenomena which in themselves depend on other forms of interaction and feedback not explicitly represented in the simplistic system structures of Figures 2A.2 and 2A.3. In order to carry through with the demonstration, these relations have been given conditional roles. For the purposes of the feedback demonstration, the dominant relation appears to be the connection between net vertical displacements (NEC) and fracturing:

$$\text{L} \quad \text{NECC.K} = \text{NECC.J} + \text{DT} * (\text{CREC.JK}) \quad \text{NET EXPANSION COMPACTION} \\
 \quad \text{CRACKING}$$



2A.3.2.7 Dominant Feedback Loops Investigated in the H-MW-F-O-GW Sector -- Two loops are considered. In the first loop, Heat affects Thermal Expansion (TE) directly and Compaction (C) indirectly via influence on the effective viscous response of a porous salt medium (EVISC) to loading. The Net Displacement (NEC) affects Fracturing (F) by directly coupled responses; Fracturing is additionally affected by externally defined inputs from Faulting (CRF). The amount of Fracturing affects Solutioning (SO) which affects the amount of pore space (LPV) available for renewed Compaction (C). At this stage a Positive Feedback Loop is established and the solutioning effects progressively increase.

The second loop considers the effect of the transport cycle on the cooling history (HOUTR) and hence on the TE-NEC-F-SO-C loop. This coupling has not been examined in detail to date, however, because the solutioning feedback is so strong that small perturbations are sufficient to set it in motion. This latter point is explored quantitatively in Section 5 on Computer Calculations. Groundwater effects on cooling have been studied using the Hydrologic Transport Model of Chapter 3. Heat transfer by groundwater is very important to the long term cooling history but does not significantly influence early thermal effects relative to the feedback processes discussed in this section.

#### 2A.4 Physical Content of System Equations

##### 2A.4.1 The Basic Assumption

The working principle adopted for the trial calculations was to keep them simple enough that the roles of the individual effects could be detected when the composite system was permitted to interact. Thus, heat transfer functions, mechanical equations of state, etc., are simplistic without being totally hypothetical. Rock properties are essentially those of the reference site: for convenience, rock properties are listed in Table 2A.1.

##### 2A.4.2 Simplified Physical Relationships

The equation forms are described in words and then in DYNAMO format (i.e., as typed on computer input cards); quantities usually are in c.g.s. (centimeter, gram, second) units which are then scaled to dimensions more suitable to the scope of the problem (meters, kilometers, years, etc). DYNAMO equations are normally labeled with their numerical units.

2A.4.2.1 Heat Input -- Heat input (HINR) is determined from the waste load specifications given in Chapter 1. It is expressed as a Table Function of decay fraction versus time which is multiplied by a dimensional constant representing the assumed initial thermal power:

$$\text{HINR} = \frac{(\text{sec/yr})(\text{Initial Power; watts/acre})(\text{Fractional Decay Table})}{(\text{joules/cal})(\text{sq.cm/acre})(\text{Depth to Source;cm})(\text{Density;gm/cu.cm.})}$$

cal/gm/yr.

TABLE 2A.1  
Physical Properties Assumed for Rocks of the Reference Site

Property	Upper Sand and Gravel	Upper Shale	Middle Sand	Repository (Salt)	Salt (Ambient)	Lower Shale	Lower Sand	Bedrock
Density ( $\text{gm} \cdot \text{cm}^{-3}$ ) of saturated rock at 30% porosity	2.3	2.1	2.3	1.7	2.2	2.2	2.3	2.6
Thermal Conductivity ( $\text{cal} \cdot \text{cm}^{-1} \cdot \text{sec}^{-1} \cdot ^\circ\text{C}^{-1}$ )	"Dry" $5.0 \times 10^{-3} @ 0^\circ\text{C}$ $1.1 \times 10^{-3} @ 400^\circ\text{C}$ (vertical the same)	"Wet" $10^{-2} @ 0^\circ\text{C}$ $4 \times 10^{-3} @ 400^\circ\text{C}$ $5 \times 10^{-3} @ 0^\circ\text{C}$ $1.1 \times 10^{-3} @ 400^\circ\text{C}$	(same as Upper Sand)	(isotropic) $11.7 \times 10^{-3} @ 0^\circ\text{C}$ +0 $5.9 \times 10^{-3} @ 200^\circ\text{C}$	(isotropic) $14.6 \times 10^{-3} @ 0^\circ\text{C}$ +0 $7.4 \times 10^{-3} @ 200^\circ\text{C}$	(same as Upper Sand)	(same as Upper Sand)	$7.0 \times 10^{-3}$ (constant)
Heat Capacity ( $\text{cal} \cdot \text{gm}^{-1} \cdot ^\circ\text{C}^{-1}$ )	0.50 @ $0^\circ\text{C}$	0.50 @ $0^\circ\text{C}$	0.50 @ $0^\circ\text{C}$	0.16 @ $0^\circ\text{C}$	0.21 @ $0^\circ\text{C}$	(same as Upper Shale)	(same as Upper Sand)	0.2 (constant)
Rock + Water	0.54 @ $400^\circ\text{C}$	0.54 @ $400^\circ\text{C}$	0.54 @ $400^\circ\text{C}$	0.19 @ $400^\circ\text{C}$	0.24 @ $400^\circ\text{C}$			
Thermal Expansion ( $^\circ\text{C}^{-1}$ )				(isotropic)	(isotropic)	(same as Upper Shale)	(same as Upper Sand)	(isotropic) $10^{-5}$
Horizontal:	$10^{-5}$	$10^{-5}$	$10^{-5}$	$1.4 \times 10^{-5}$	$4.2 \times 10^{-5}$			
Vertical:	$10^{-5}$	$2.0 \times 10^{-5}$	$10^{-5}$					
Young's Modulus ( $\text{dyne} \cdot \text{cm}^{-2}$ )				(isotropic)	(isotropic)	(same as Upper Shale)	(same as Upper Sand)	(isotropic) $5 \times 10^{11}$
Horizontal:	$10^{11}$	$10^{11}$	$10^{11}$	$6.7 \times 10^{10}$	$2 \times 10^{11}$			
Vertical:	$6.7 \times 10^{10}$	$6.7 \times 10^{10}$	$6.7 \times 10^{10}$					
Modulus of Rigidity ( $\text{dyne} \cdot \text{cm}^{-2}$ )						(same as Upper Shale)	(same as Upper Sand)	$2.3 \times 10^{11}$
	$5 \times 10^{10}$	$5 \times 10^{10}$	$5 \times 10^{10}$	$2.7 \times 10^{10}$	$8 \times 10^{10}$			

For an Initial Power of 61 kw/acre, this function in DYNAMO

is written:

R HINR, KL = 0.094\*FD, K      RN POWER (CAL/GM/YR)

The Dimensional Coefficient of Power (DCP = 0.094 cal/gm/yr) is an amount that would produce an initial average thermal rise in overlying rock of roughly 1/2°C per year, a rate which rapidly decreases with time because of radionuclide decay. This decay is described by the nondimensional ratio:

$$FD = \frac{\text{Thermal Power at TIME}}{\text{Initial Thermal Power}}$$

Note: TIME is the built-in DYNAMO name for the value of time starting from a specified zero, or from a specified initial value.

For the numerical work, a TABLE Function was generated in DYNAMO Language making use of Auxiliary relations for logarithmic transformation (see the DYNAMO User's Manual; Ref. 2A, 11), where N at the left margin indicates an Initial Value Equation and T indicates the values of the TABLE Function; X indicates a Continuation Card when more than one card is needed to list the values.

A FD, K = EXP(2.303\*LOGFD, K)      RN DECAY FRACTION

N FD = 1.0

A LOGFD, K = TABLE(FDTAB, LOGT, K, 0, 6, 0.5)      LOGTEN DECAY FRACTION

Note: The values of FDTAB are  $\text{LOG}_{10}$  values of FD at values of  $\text{LOG}_{10}$  TIME ranging from 1 to  $10^6$  years at intervals of  $\text{LOG}_{10}$  TIME = 0.5.

T FDTAB = 0/-0.03/-0.11/-0.38/-1.00/-1.80/-2.17/-2.51/-2.80/

X -3.84/-4.0/-4.0      LOGTEN DECAY FRACTION TABLE

Note: Any date identifies a particular set of data when more than one set is used in the same context.

A LOGT, K = LOGN(TIME, K)/2.303      LOGTEN TIME (YEARS)

Note: The built-in Log function in DYNAMO, LOGN, is to the Base e.

N LOGT = 0

Note: The starting time for DYNAMO runs as displayed here is at 1 year; initializing the TIME depends on the problem scale of interest.

2A.4.2.2 Heat Output -- If a constant heat source were turned on at TIME = 0 at a specified depth in the earth, a steady-state heat flow from source to surface would be approached in a time given roughly by the ratio  $(\text{depth;cm})^2 / (\text{Avg. Thermal Diffusivity Rock; cm}^2/\text{sec})$ . The source depth of roughly 600 m (see Chapter 1) indicates that this characteristic time would be of the order 10,000 years, although detectable surface loss would begin at a time of the order of 1000 years.

This simple test gives an idea of the time delay involved in the average thermal response, though the actual heat source decreases with time. The response near the repository level is, of course, much faster and requires detailed calculations of transient heat transfer mechanisms. The point is that a range of delay functions is indicated by this kind of relation that will give an idea of thermal responses over different length scales. Some of these choices are displayed later and are compared with the more complete calculations.

For an initial estimate, we let the output be defined as proportional to twice the mean temperature (e.g., as though the steady gradient were linear between a surface at 20°C and the repository source). We also imposed an initial geothermal gradient of 20°C/km and assumed that all radioactive heat is eventually lost to the surface. This means that the initial temperature at the repository depth is 32°C, for a surface temperature of 20°C, and the initial mean temperature is 26°C.

The mean temperature is given by the mean heat content divided by the mean heat capacity. This defines the initial value for the Heat Level:

$$H = (\text{Mean Temperature; } ^\circ\text{C})(\text{Mean Heat Capacity; cal/gm/}^\circ\text{C})$$

$$N \quad H = 5.2 \text{ CAL/GM} \quad \text{INITIAL HEAT (MTEMP} = 26^\circ\text{C)}$$

Thus, the Heat output in the steady state can be written as Steady Heat Loss Rate (SHLR) (note that the geothermal flux is both input and output and therefore cancels out):

$$\text{SHLR} = \frac{(2) (\text{Mean Heat Content; cal/gm}) (\text{Thermal Conductivity; cal/cm/sec/}^\circ\text{C}) (\text{sec/yr})}{(\text{Heat Capacity; cal/gm/}^\circ\text{C})(\text{Depth to Source; cm})^2 (\text{Density; gm/cu cm})}$$

$$= \frac{(\text{Steady Geothermal Flux; cal/sq cm/sec}) (\text{sec/yr})}{(\text{Depth to Source; cm}) (\text{Density; gm/cu cm})}, \text{ cal/gm/yr}$$



which in DYNAMO becomes the approximate equation (using averages of physical properties from Table 2A.1):

R SHLR, KL = 25.0\*(H, K-4, 0)/1.32E5-2.273 E-4  
STEADY HEAT LOSS RATE (CAL/GM/YR)

N SHLR = 0

The Heat Output Rate is then related to SHLR by means of a Delay function. The sharpness of the output wave can be determined by the order of the Delay. For these preliminary purposes a third-order Delay illustrates the general form of the thermal history (The mathematical structure of the Delay function in terms of Levels and Rates is described graphically and numerically by Forrester, Ref. 2A.4, Chapter 9):

R HOUTR, KL = DELAY3 (SHLR, JK, DSHF) HEAT LOSS RATE (CAL/GM/YR)

N HOUTR = 0

Note: The expected initial value is often written only as a reminder to check the numerical printout for internal consistency; DYNAMO automatically initializes if equations are complete.

C DSHF = 1000 YRS DELAY SURFACE HEAT FLUX

Note: We experimented with delays of various lengths and order. The values used are indicated in the equation listings for particular calculations cited later. The terms in parentheses on the right of HOUTR represent the input and delay intervals in three cascaded first-order delays, each with intervals DSHF/3.

The above equations define the Heat Level at subsequent time intervals, from which the updated values of mean temperature are calculated;

A MTEMP, K = (H, K-4, 0)/0.2 +20 MEAN TEMP FOR STEMP = 20°C

N MTEMP = 26 DEG C

Although the implied surface heat flux is already computed by the above equations, it is sometimes convenient to write it (or other output variables) in other forms. For this purpose Supplementary Equations can be written for printing and plotting purposes which otherwise play no active role in the computations. For example, the Surface Heat Flux in units of geological heat flow units (microcalories per square cm per sec) is written as follows:

S SURFLX, K = 1.0 + 1.32E5\*(HOUTR, JK/30)  
SURFACE FLUX (MICROCAL/SQ CM/SEC)

N SURFLX = 1.0 MICROCAL/SQ CM/SEC

2A.4.2.3 Thermal Expansion -- Expansion of the planar slab is simply given by the change of mean temperature times the thermal expansion coefficient times the thickness. The latter two terms are combined as the Unit Expansion Coefficient (UEC). Details of expansion near the repository margins require detailed study by means of two-dimensional thermal stress calculations. The Thermal Expansion Rate (TER) is directly obtained from the Heat Rate equations as follows:

$$\text{TER} = \frac{(\text{Unit Expansion Coefficient; cm/}^\circ\text{C})}{(\text{Heat Capacity; cal/gm/}^\circ\text{C})} \frac{(\text{Heat Input Rate} - \text{Heat Output Rate; cal/gm/yr})}{\text{cal/gm/}^\circ\text{C}}$$

or,

$$\text{R } \text{TER.KL} = \text{UEC} * (\text{HINR.JK} - \text{HOUTR.JK}) / 0.2$$

LINEAR THERMAL EXPANSION RATE (CM/YR)

Note: The Heat Capacity and Thermal Expansion coefficients are averages for relatively dry rock. Effects of the more realistic variations of these coefficients as shown in Table 2A.1, are quite significant and are discussed following presentation of computer results.

$$\text{N } \text{TER} = 0.423 \quad \text{CM/YR}$$

$$\text{C } \text{UEC} = 0.9 \quad \text{CM/DEGC UNIT EXPANSION CONSTANT}$$

The cumulative expansion is computed from the Level Equation:

$$\text{L } \text{TE.K} = \text{TE.J} + \text{DT} * (\text{TER.JK}) \quad \text{LINEAR THERMAL EXPANSION (CM)}$$

$$\text{N } \text{TE} = 0 \quad \text{INITIAL THERMAL REFERENCE STATE}$$

2A.4.2.4 Compaction -- Two principal effects are considered. One is the quantitative settling and compaction of unfilled pore space in the backfill material which is assumed to be salt. We also assume a uniform distribution of voids with bulk porosities ranging from 3 to 30 percent. Since the backfill layer is designed to be about 6 m thick, we assume maximum possible compaction lengths ranging from 20 cm to 180 cm.

The second effect is compaction of porosity caused by solutioning. In order to make the calculation similar to the above mechanism, we assume that solutioning was uniformly distributed. Local compaction or collapse rates (e.g., as occurs in the formation of at least some breccia zones in salt) have not been explicitly simulated, though some estimate of the possible growth rate of a localized cavity is made later in the solutioning calculation.

The simplistic assumption from the mechanical standpoint is that the response to loading is approximately similar to the collapse of cavities in a viscous material. We emphasize that the rheology of salt is highly complex and incompletely known. An assumption such as ours gives, at best, an estimate of gross displacements averaged over long times. The averaging is based on comparisons with effective times for viscous deformation obtained from data given by Heard<sup>(2A.8)</sup> and from the in situ measurements made during Project Salt Vault.<sup>(2A.2)</sup> The validity of the assumption depends on the phenomenon being simulated. Average subsidence rates in a widespread planar layer may be approximated on this basis, whereas it may have no validity at all for the deformation around a single waste canister.

The relationship used is based on some experiments by one of the authors on collapse of cavities in a viscous material simulating molten rock.<sup>(2A.14)</sup> It was found that the approximate compaction rate was exponentially dependent on the time interval multiplied by the ratio of effective pressure acting on the voids to the effective viscosity of the matrix. This relationship was checked against average convergence rates in the Salt Vault experiments using an estimate of viscosity for salt from Ref. 2A.8. The comparison agreed within a factor of about three; this agreement is considered good in terms of the assumptions and the fact that we are dealing with effective viscosities of the order of  $10^{18}$  to  $10^{19}$  dyne/sec/cm<sup>2</sup> (poise). The compaction function was roughly adjusted to the Salt Vault data and a TABLE Function was derived for the effective viscosity. It is emphasized, however, that this "calibration" cannot be considered general, because every site is to a degree structurally and compositionally distinct. We therefore tested variations differing by a factor of ten.

The Compaction Equations involve relations between the three lengths (one-dimensional case): Compaction Length (CL), Maximum Compaction Length (MCL) and Linear Pore Volume (LPV). The latter represents the uncollapsed void space at a given time:

L CL,K = MCL,K-LPV,K    COMPACTION LENGTH (CM)

L LPV,K = LPV,J + DT\*LPVCR,JK    LINEAR PORE VOLUME (CM)

N LPV = BMCL

N CL = 0    INITIAL COMPACTION REFERENCE STATE

C BMCL = 60 CM    BACKFILL MAX COMPACTION LENGTH (CM)

Note: A value of about 10 percent initial porosity was assumed in most calculations as an estimate of the best possible backfill procedures; values two or three times larger are considered likely by many observers.

The Linear Pore Volume Compaction Rate (LPVCR) is based on the function given in Reference 2A.14.

$$\text{LOG}_{10} \frac{\text{Linear Pore Volume at TIME K}}{\text{Linear Pore Volume at TIME J}}$$

$$= \frac{-(\text{Effective Load Pressure; dyne/sq cm})}{(\text{Effective Viscosity; dyne sec/sq cm})} (\text{TIME JK;sec})$$

Rewritten in DYNAMO format this becomes:

R LPVCR.KL = LPV.K\*EXP(-2.303\*ELP\*3E7\*DT/EVISC.K)/DT-LPV.K/DT  
LINEAR PORE VOLUME COMPACTION RATE (CM/YR)

C ELP = 1.3E8 DYNE/SQ CM EFFECTIVE LOAD PRESSURE

A EVISC.K = TABLE (EVTAB,BFTEMP.K,0,250,25) EFFECTIVE  
VISCOSITY (POISE)

T EVTAB = 1.15E19/7.08E18/4.47E18/2.81E18/1.78E18

X 1.26E18/8.91E17/6.61E17/5.01E17/3.80E17/3.02E17

Note: The effective Viscosity is tabulated at intervals of 25°C from 0 to 250°C.

The temperature dependence was estimated from Ref. 2A.8.

A BFTEMP.K = 32 + 2\*(MTEMP.K-26) APPROX BACKFILL  
TEMPERATURE (DEGC)

N BFTEMP = 32 (DEGC)

Note: The temperature near the Repository depth is assumed to dominate the compaction rate. It is taken to be the initial steady state temperature plus twice the change in mean temperature of the overburden.

The Maximum Compaction Length (MCL) is introduced above as a variable because later it is related to the amount of solutioning. We also reiterate that the above equations are of the most simplistic form for the mechanics of compaction. We could, for example, have written a stress-strain-time-temperature function from results like those given by Bradshaw and McClain<sup>(2A.2)</sup>, but the complexity would only add confusion to the demonstration calculations at this stage. When the simulation results are better understood, however, it may well become critically important to simulate the rheology in great detail.

2A.4.2.5 Cracking -- Relationships describing fracturing phenomena are based largely on intuitive guesses constrained by some simple observations of limits. These guesses are required to carry through a numerical example of how such generic functions can be coupled together. It is hoped that they will also serve to encourage more realistic assessment.

The potential multiplicity of cracking phenomena is reduced to two kinds of input functions: (1) cracking caused by bending and layer extensions as consequences of vertical motions, (2) cracking related to existing and created fracture zones produced by any faulting phenomena.

Figure 2A.4 schematically illustrates the reasoning applied to cracking caused by vertical motions of layers. Here, the distributions and orientations of cracks are drawn only in the intuitive sense that some distributed cracking will occur and there are likely to be zones of more concentrated cracking related to regions of greatest flexure. The only quantitative tests made to date are from numerical modeling of maximum elastic stresses caused by thermal expansion. As shown in Figure 2A.5 the loci of maximum tensile stresses are near the repository margins and are concentrated in the shale layers.\* Although some incompetent rocks fail at these stress levels in laboratory tests, most rocks have higher apparent strengths. The view expressed here, however, is that whereas this is true for short-term experiments, most rocks will fail in one way or another under such sustained stresses if the stresses are maintained for periods exceeding 100 years.

The limiting condition for the amount of extension cracking was estimated on the assumption that if the layer is assumed to be "clamped" at some lateral distance from the repository site, then any vertical motion implies a change in length which is compensated by fracture porosity. This does not allow for ductility and a compensating attenuation of thickness, which is one point, among many, that will require detailed analysis of all relevant rheological parameters (stress, strain, time, temperature, mineralogical state, textural state and anisotropy, pore fluid pressure, etc.).

---

\*The calculations behind Figure 2A.5 will be discussed in 2A.4.2.5.1.

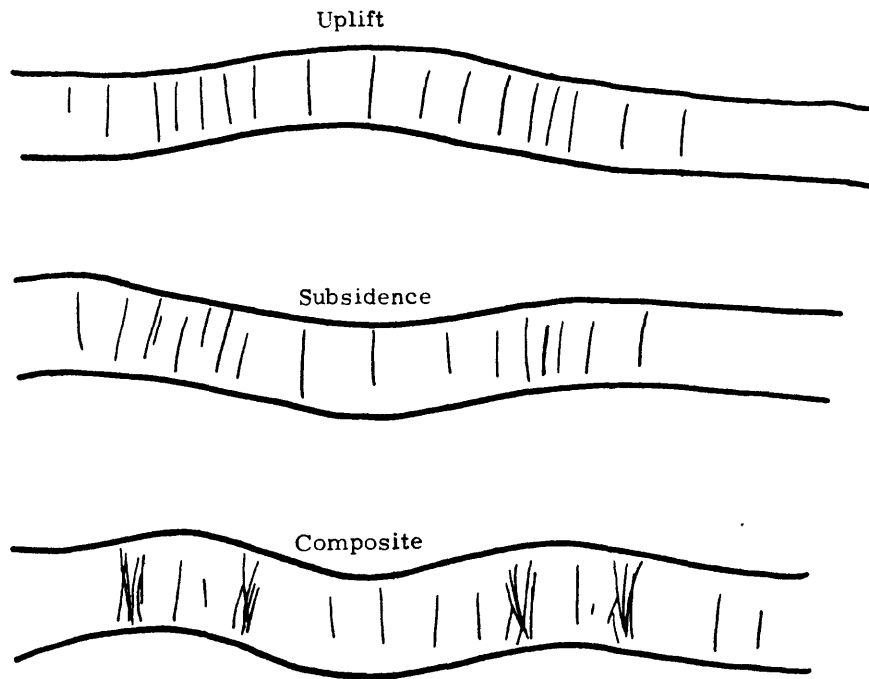


Figure 2A.4. Combined Effects of Uplift and Subsidence

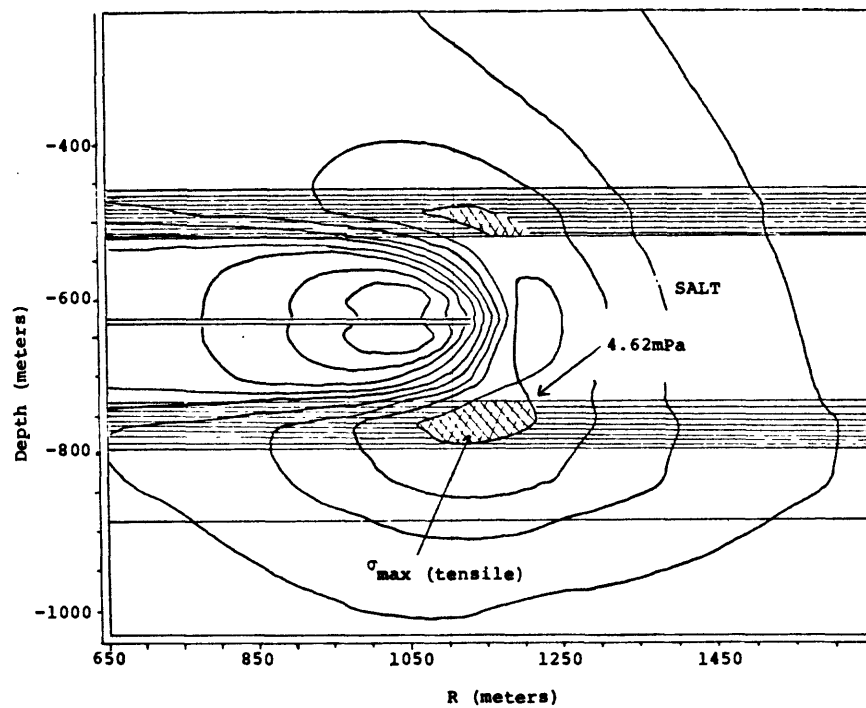


Figure 2A.5. Contours of Maximum Normal Stress Near Repository at  $t = 50$  years

The magnitude of the extensional fracturing can be expressed in terms of numbers of Reference Cracks of trace dimensions 1 millimeter width by about 3 km in length (roughly the diameter of the repository). The volume of fractures depends on the number and depth range of such cracks. During uplift or subsidence, imaginary horizontal lines will be stretched by amounts depending on flexural form and any compensating ductile flow. For example, a simple conical uplift of a meter would produce a change in surface area of a stratigraphic horizon (e.g., change from the area of a plane circular disc to the surface area of a right circular cone) of the order of  $2 \times 10^4 \text{ cm}^2$ . This would correspond to the trace area of roughly one Reference Crack. Convex, concave, or even more abrupt punch-like forms of uplift or subsidence create greater and more localized forms of extension near the margins of the deformation. A change of surface area of a punch-like uplift or depression (which seems likely for such a tabular source horizon, either from thermal expansion or compaction) could produce an areal stretching of some horizontal reference plane by something like  $1 \times 10^8 \text{ cm}^2$  per meter of vertical motion. The volume of cracks formed is impossible to estimate, and their distributions would be complex, but in terms of areal ratios of extension to trace area of a Reference Crack one can estimate about 5000 cracks.

Another way of looking at limits is to consider the displaced volume of one meter vertical displacement over the repository area (a meter is used as a comparison length because of the backfill maximum compaction lengths, BMCL, discussed in the preceding section). This would amount to about  $10^{13} \text{ cm}^3$  volumetric displacement. If even one percent of this volume is not totally compensated by displacements at the ground surface, an internal fracture space amounting to some hundreds of cracks of Reference Volume 50 meters x 3 kilometers x 1 millimeter ( $= 1.5 \times 10^8 \text{ cm}^3$ ) could be formed. Cracks of this dimension are chosen for comparison because they dimensionally represent the scale of cracking that could significantly breach the shale layers above and below the salt horizons of the Reference Site.

These general bounds suggest that cracking may be roughly proportional to vertical displacement with a proportionality constant ranging from about 1 to 1000 Reference Cracks per meter displacement. In later calculations we have usually used the factor  $5 \cdot h$  Reference Cracks, where  $h$  is vertical displacement in centimeters. Intuitively, this factor is probably near the upper bounds of estimate, so we have also made calculations over several decades of decreasing magnitudes.

The corresponding DYNAMO equations are written as follows:

```
L  NECC.K = NECC.J + DT*(CREC.JK)      NUMBER OF REFERENCE CRACKS
    FROM NEC
N  NECC = O      INITIAL STATE OF CRACKING
```

R    CREC.KL = 5\*SQRT(NECR.JK\*NECR.JK)            CRACKING RATE  
FROM NEC RATE (REF CRACK/YR FOR CM/YR)

Note: The square root function is used because NECR may be either positive or negative. One Reference Crack corresponds to  $2 \times 10^8 \text{ cm}^3$  fracture pore space. The coefficient 5 is probably a high estimate, though under special circumstances the value conceivably could be several times larger.

Estimates of cracking produced by fault motions are even more tenuous than the above estimates. Toward this goal we made compilations of fault measurements based on U. S. Geological Survey maps, and also made some preliminary statistical analyses of the results. The results were used to guide our initial assumptions, but they are highly tentative and must be studied in much greater detail. We have chosen high and low estimates of both the initial amount of fracturing related to fault zones and the rate of production of new cracking. In these cases the fracture trace lengths at the ground surface are assumed to represent planes that cut all strata of the Reference Site.

One of the initial states assumes that there are no fault-related fractures at the beginning of the simulation period but that they are created at rates ranging from a millimeter to a tenth of a kilometer trace length per year. Geologically, this might represent the situation in a stable tectonic region adjacent to an actively evolving tectonic province that is encroaching with time on the stable region. The low rate of 1 mm/year is probably imperceptible either by mapping or seismology unless it has been operating for some time. The high rate represents a region of major faulting and earthquakes during a period of very intense activity. The value of 0.1 km/yr, however, does not correspond to single fault plane slips of that magnitude, but represents the integrated trace lengths of fault-related cracks in a complex fault zone. For this purpose we assume that there are roughly 100 times the fracture trace lengths as fault zone length, meaning that the zone itself is growing at a rate of about 1 m/yr (this is many times faster than mean crustal plate motions and therefore represents an episode of abnormally high strain release).

Although the high rate represents a very active fault region that would be seismically conspicuous, it is included to give some insight on solutioning consequences of high faulting rates that are either undetected because of poor historical records or represent unexpected rejuvenation or initiation of major faulting.

The statistical data base for these assumptions is very sensitive to data selection, age biasing and so on. It may be proven in time that the growth rate estimates are partly artifacts of sampling and age criteria. It is important to notice, however, that even if the lowest rate that might be estimated were permitted to proceed very long, there would be a great deal of fracturing already in existence. Anyone who has spent any time in man-made underground openings of various



kinds cannot help but be impressed by this fact. Therefore, whereas our estimates may be incorrect in space-time distributions, there is no doubt that fracture pathways are important even in relatively stable geologic domains. These older fractures may have an important role in that even if the vertical displacement of the previous section caused by combined thermal expansion and compaction are insufficient to cause failure of intact rock, they still may induce extensional opening of existing fractures. Therefore, partly as a reminder of the above importance, we write the following tentative equations including an option for an initial value of 100 km cracking trace length that has accumulated within the repository area over geologic time:

L  $CTLF.K = CRLF.J + DT*(CRF.JK)$  CRACK TRACE LENGTH  
FROM FAULTING (CM)

N  $CTLF = 0$  ASSUMED MIN INITIAL REFERENCE STATE (CM)

N  $CTLF = 1.0E7$  AVERAGE INITIAL REFERENCE STATE (CM)

Note: This last figure is based on an areal averaging of measurements of all mapped faults younger than about 15 million years in the conterminous U. S. normalized to trace length per 100 sq. km. It also assumes 100 fracture lengths per unit fault length (i.e., for the zone of influence).

R  $CRF.KL = 1.0E-1$  MIN CRACK RATE FROM FAULTING (CM/YR)

R  $CRF.KL = 1.0E4$  MAX CRACK RATE FROM FAULTING (CM/YR)

Note: It is assumed that fracturing of given trace length penetrates all strata vertically. The crack volume associated with above faulting depends on faulting style. We have assumed that all cracks have a mean width of 1 millimeter.

2A.4.2.5.1 Digression on Two-Dimensional Stress Analysis Calculations -- Figure 2A.5 shows a representation of the loci of maximum tensile stress near the repository margins. We digress momentarily to explain the source of that figure.

To check some of the results obtained with the present DYNAMO simulation, a two-dimensional transient thermal stress analysis of the reference repository was performed using a finite element computer code. The goals of these calculations were to (1) determine the thermal, stress and displacement response of a reference geological salt formation to a reference nuclear waste decay function, and (2) evaluate the effect of selected unknown variables in order to identify important parameters for future analytical modeling.

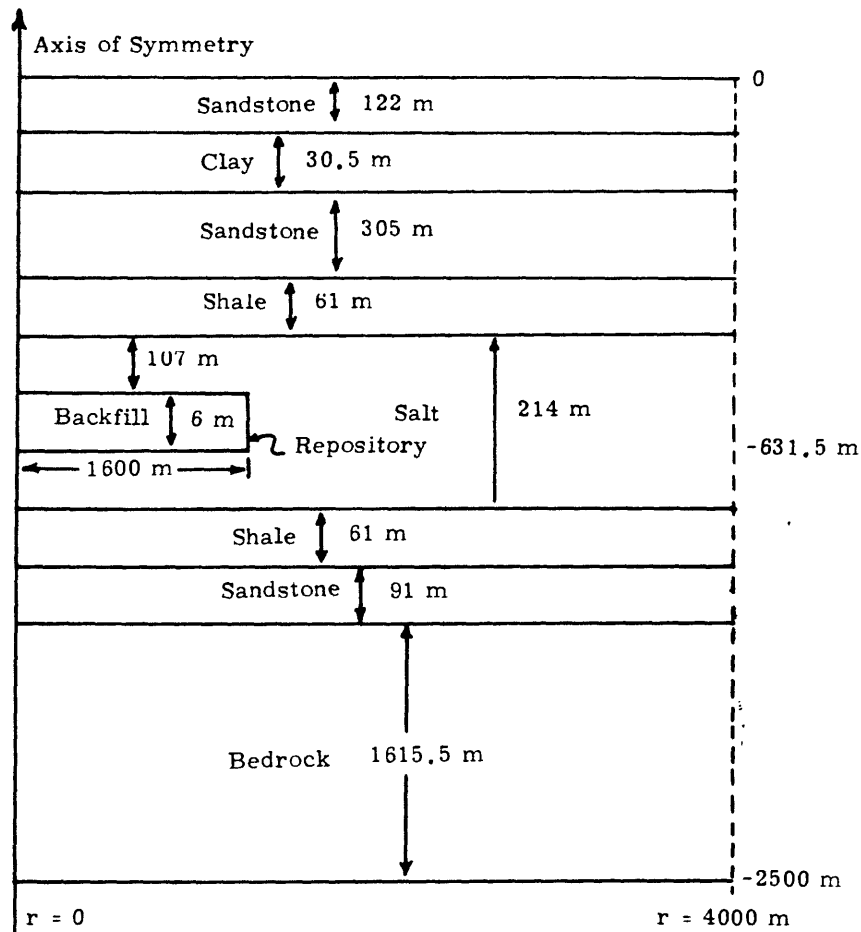


Figure 2A.6. Idealized Site Geometry for Thermal and Structural Calculation

A schematic of the reference geological salt formation used in the calculations is shown in Figure 2A.6. The model of the formation was assumed to be axisymmetric about the z-axis, extending 4000 m in the radial direction and 2500 m in depth. In addition, the waste repository was located at a depth of 631.5 m and had a radius of 1600 m. Of considerable importance are the overall dimensions of the model, which must be large so that the boundary conditions do not affect the thermal and stress states of interest near the repository. This distance can be determined from the thermal diffusion constant of the material and the time of the problem.

A close-up view of the model and the zoning used in the vicinity of the repository is shown in Figure 2A.7.

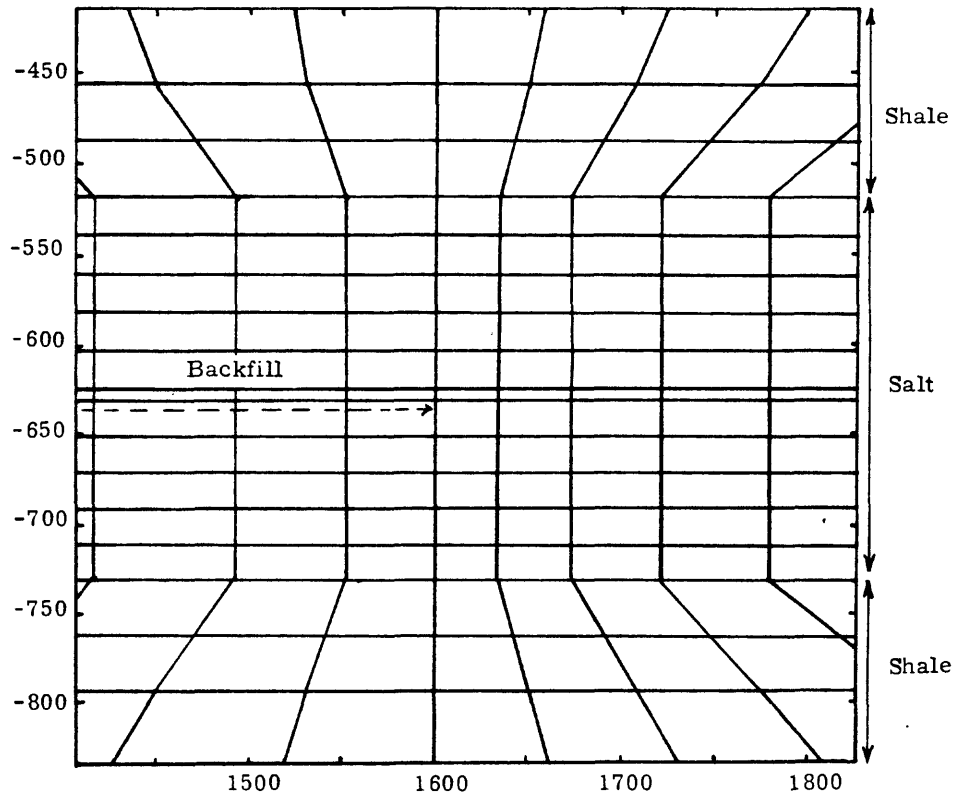


Figure 2A.7. Close-up View of Finite Element Zoning at Edge of Nuclear Waste Repository

For the thermal problem, the boundary conditions are:

1. Prescribed heat flux as a function of time from nuclear waste.
2. Constant temperature at  $20^{\circ}\text{C}$  at top surface and  $70^{\circ}\text{C}$  at bottom surface.
3. Zero heat flux across outer circumferential surface.

The temperature difference between top and bottom surfaces reflects a geothermal gradient of  $20^{\circ}\text{C}/\text{km}$ . The initial condition to the thermal problem is the steady state solution with the geothermal gradient.

The boundary conditions for the stress problem are:

1. Stress-free top surface.
2. Zero normal displacement at bottom surface and outer circumferential surface.

Initially, at  $t = 0$  years, the entire region is considered to be stress-free. Because of the initial thermal gradient and the fixed displacement boundaries, the thermal stresses were not everywhere zero at  $t = 0$ . The stress-free condition was determined by first calculating the initial stresses and displacements and then subtracting these from the same quantities calculated at all subsequent times.

Physical and mechanical properties of the various geological layers are given in Table 2A.1. The effects of temperature and anisotropy have been included; however, all materials were assumed to be linear elastic.

The reference waste heat decay function is given in Table 2A.2. Upon closing the repository, it is required to have an initial heat generation rate of 61.3 kw/acre based upon a 1000-acre site.

TABLE 2A.2

Assumed Thermal Power,  $W(t)$ , of Waste in Repository  
as a Function of Time

<u><math>\log_{10}</math> (time in years)</u>	<u><math>\log_{10} [W(t)/W(1)]</math></u>
0	0
1	-0.3
2	-0.6
3	-1.45
4	-2.2
5	-3.2
6	-3.2

Some of the results of the calculations on the reference geological formation are summarized in Figure 2A.8. From these plots, and other calculations in which selected variables were changed, the following conclusions can be drawn:

1. With regard to the far-field thermal calculations, the maximum temperature occurs at the center of the repository ( $r = 0$ ,  $z = -631.5$  m). This temperature peaks at  $94^{\circ}\text{C}$  at 35 years. Local temperatures near the canisters in the plane of the repository may be higher but were not considered.

2. The largest positive normal stress ( $\sigma_{\max}$ ) occurs in the lower shale layer radially outward from the repository. Stress contours for  $t = 50$  years are shown in Figure 2A.5. The maximum shear stress ( $\tau_{\max}$ ) occurs in the salt layer directly above and below the repository. This is also the location of the maximum compressive stress ( $\sigma_{\min}$ ). The largest value for  $\sigma_{\max}$  is 4.6 MPa, for  $\tau_{\max}$  is 22.5 MPa and for ( $\sigma_{\min}$ ) is -45 MPa. All are a maximum at approximately the same time. Superimposed upon these thermal stresses, however, is a hydrostatic compression stress of 14 MPa. Hence, there are no resultant tensile stresses.
3. The shape of the waste heat decay function, especially for  $t = 100$  years, has considerable effect on the temperature distributions.
4. The maximum ground uplift occurs directly over the center of the repository. Its magnitude and distribution with time is strongly affected by the thermal expansion coefficient of the salt layer, since this is where the largest temperature differences occur.

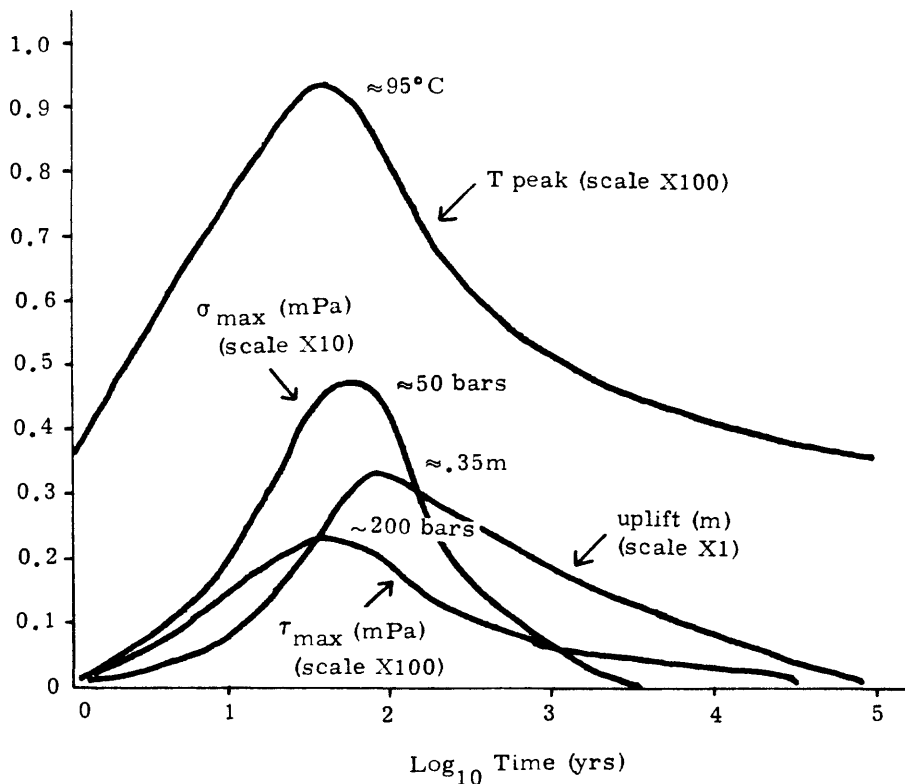


Figure 2A.8. Summary of Results of 2-D Calculation for Reference Repository and Waste Heat Function

2A.4.2.6 Openings From Solutioning Effects -- Only the openings related to the fracturing effects discussed in 2A.4.2.5 are considered numerically. Other openings, such as dilations caused by uplift, subsidence, and deformations of other origins (geothermal effect of igneous phenomena, tectonic block sliding, vertical tectonic motions such as the "Palmdale Bulge" in California, and so on) are not evaluated, though all of such phenomena are candidates for feedback analyses.

First, we write an expression for the volume of solutioning related to various mechanisms and then discuss the assumed limits of the respective rate equations, as follows:

L SO.K = SO.J + DT\*(ORSD.JK + ORSCUA.JK + ORSCLAS.JK + ORSEDLA.JK)  
SOLUTION OPENINGS (CU CM)

N SO = 1 CU CM MIN INITIAL REFERENCE STATE

Note: This latter value is assigned as the minimum limit in case logarithmic transformations or inverse ratios become involved in the calculations (i.e., functions often need checking to see that they do not involve the Log of zero or zero in a denominator). Other initial values are implied by the assumptions on initial fracture states.

The rate equations were previously named and are discussed below.

2A.4.2.6.1 Opening Rate From Solutioning by Diffusion (ORSD) -- This rate is assumed to depend primarily on pathways between the salt horizons and groundwater in aquifers, which depend, according to our assumptions, on intersecting crack volumes.

The calculation supposes that all cracks defined above intersect the aquifers and provide a diffusion path of brine from the salt horizons (we are not considering radionuclide diffusion at this stage).

The mass transfer depends on the following approximate relation:

$$\begin{aligned} (\text{Mass Diffusion Flux; gm/cm}^2/\text{sec}) &= -(\text{Diffusivity; cm}^2/\text{sec}) \\ &\quad *(\text{Gradient of Concentration; gm/cm}^4) \end{aligned}$$

Assuming an average gradient between pure water and saturated brine over a path length of about 50 meters shale thickness, we obtain an order of magnitude estimate of  $10^{-4}$  g/cm<sup>4</sup>, which for a diffusivity of  $10^{-5}$  cm<sup>2</sup>/sec (typical of aqueous solutions at room temperature) gives a mean flux of  $3 \times 10^{-2}$  gm/cm<sup>2</sup>/yr.

There are, of course, factors like concentration and temperature dependence of solubility and diffusion, tortuosity of paths, and so on, but these refinements are masked by the coarseness of the assumptions on fracturing. We note this but also try not to forget that whereas our assumptions may be reasonable for gross transport, the details of diffusion would be important in any situation where a chemical species might act as a catalytic trigger to some other form of instability (e.g., access of even small amounts of water can be of crucial importance to the mechanical stability of glass).

There are three contributions to the integrated mass flux or mean mass transport rate: (a) crack trace lengths from NEC, (b) crack trace lengths from faulting rates, and (c) initial fracture trace lengths. The combined effect leads to the combined proportions:

$$R \quad \text{ORSD, KL} = 1.0\text{E}4 * \text{SQRT}(\text{NEC, K} * \text{NEC, K}) + 1.0\text{E}2 * \text{TIME, K} + 1.0\text{E}5$$

OPENING RATE FROM SOL BY DIFFUSION (CU CM/YR)

Note: We have rounded to the nearest factors of ten and have ignored corrections for the density of brine.

The first term on the right depends on the non-linear history of compaction and expansion, the second term represents the high estimate of constant fault fracturing rate, and the last term represents the high estimate of initial fractures. These terms illustrate that if NEC is of the order of 1 meter, then the second term only becomes more significant than the first term for solutioning after about  $10^4$  years. The last term on the right initially dominates the other two but is exceeded by the first term when NEC exceeds 10 cm. With feedback, however, even if NEC caused by thermal expansion and backfill porosity were initially negligible, the porosity from solutioning by the latter two terms eventually will allow the first term to dominate. It is also noted, and displayed later, that the volumetric magnitudes for diffusion transport are not large (e.g., of the order of one cubic meter per year per meter of NEC for the first term. This value occurs after  $10^4$  years for the second term).

2A.4.2.6.2 Opening Rate From Solutioning by Convective Transfer to Upper Aquifer (ORSCUA) -- Figure 2A.9 shows the assumed pathway. This is a U-tube siphoning effect dependent on the hydraulic gradient of the upper aquifer, the cracking distribution in the shale horizon above the salt, the permeability of the shale-salt interface, and the salt content of interbeds in the shale.

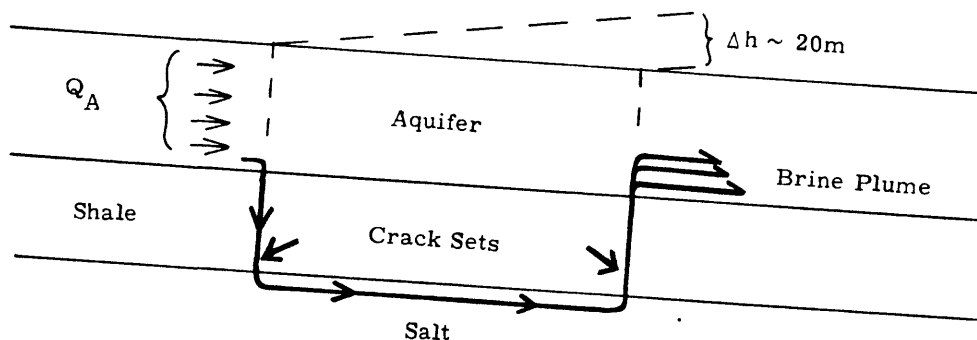


Figure 2A.9. Assumed Water Pathway for Solutioning by Convection to Upper Aquifer

Initially, we assume that the crack sets are localized near the repository margins, that the permeability of the salt-shale interface is not rate determining, and that there is enough salt in the shale sequence to saturate water in fractures. The second assumption is consistent with the existence of fragmented and structurally chaotic zones between shale and salt in at least some evaporite sequences; the last assumption is consistent with the existence of both salt interbeds and salt admixtures in shales of evaporite sequences. The hydraulic gradient is roughly the same as that of the Reference Site (see Chapter 3).

With these conditions outlined, we simply estimated laminar flow in narrow slot-like conduits corresponding to 1 millimeter wide fractures. We did not allow for growth of crack width or for the much higher transport rates of wider cracks. These effects and various forms of channel focussing represent other types of feedback that remain to be included in more detailed calculations.

With these boundary conditions, we applied a relation given in Reference 2A.13 for viscous flow in narrow tabular slots:

$$(\text{Volume rate; cm}^3/\text{sec}) = \frac{(\text{Pressure Difference; dyne/cm}^2)(\text{Width; cm})^3(\text{Trace Length, cm})}{(12)(\text{Viscosity of Fluid; poise})(\text{Transport Length; cm})}$$

Taken literally, this equation gives very high transport rates (water that encounters salt is assumed to be instantly saturated relative to the time scales of interest). Limiting factors, however, are the flow rates of the aquifer and changes of the pressure head. For example, when the effluent of the fracture U-tube is injected into the aquifer at a given rate it will tend to "pile up" to an extent determined by how fast it is swept away by the mean flow. This pile-up occurs to a maximum value equivalent to a factor that compensates the pressure head by the brine density. If the water in the shale is saturated and the aquifer contains pure water, the effluent brine column could grow to about 2/3 the head difference ( $\Delta h$ ). This would be the case if the conduit flow is large for small pressure differences, as it is in the assumed situation.

That is, the brine plume quickly builds up until it approaches hydrostatic equilibrium and thereafter it is replenished at a rate determined by how fast it is carried away by the aquifer flow. Thus, for the hydrology of Chapter 3, the total discharge rate across the width of the repository is of the order of  $0.3(300 \text{ m})(100 \text{ m/yr})(3000 \text{ m}) = 3 \times 10^7 \text{ m}^3/\text{yr}$  ( $= 3 \times 10^{13} \text{ cm}^3/\text{yr}$ ). From the head balances, the height of the brine plume could be about 4 percent of the aquifer thickness, giving a maximum brine discharge of the order of  $10^{12} \text{ cm}^3/\text{yr}$ .



On the basis of this limit, we estimated the transport rate as follows (the maximum possible rate is not reached until  $NEC \approx 100$  m, i.e., when the salt above the repository layer is nearly all removed):

R ORSCUA.KL = 1.0E8\*SQRT(NEC.K\*NEC.K)      OPENING  
RATE FROM SOL BY CONVECT TO UP AQUIF. (CU CM/YR)

Note that we have included only the cracking from vertical motions, because as mentioned in the last section, it is assumed to dominate. If for some reason, however, there is assumed to be negligible thermal expansion or backfill porosity, then additional terms like those included in ORSD must be added. Those terms then provide potential feedback inputs to NEC in ORSCUA as written above.

Note: Numerical calculations with terms of this type have not been carried out as yet in as many combinations as would be desirable. They should be included in future work.

2A.4.2.6.3 Opening Rate From Solutioning by Convective Transfer from Lower Aquifer to Surface (ORSCLAS) -- This solutioning rate depends principally on the number of throughgoing cracks and the pressure head in the aquifer below the salt horizons. Since the minimum rate is zero, we have written a relation only for the maximum rate, in the form

R ORSCLAS.KL = 6.0E10\*TIME    MAX OPEN RATE BY CONVECT L.  
AQUIF TO SURFACE PER ATM HEAD (CU CM/YR)

These rates are potentially very high and are limited only by the potential total discharge rate of the aquifer (e.g., for the above equation this could be achieved in less than 1000 years). They are, however, subject to the difficult question of pressure distributions in fractures relative to the lower aquifer, which may have zero or negative values. The latter implies downward flow. Such a flow regime may be analogous to ORSCUA but with potentially higher rates because they are not limited by the salinity plume effect. Even without the forced convection term, however, there could be a substantial mass transfer to the lower aquifer by free convection. This is examined in the next section.

2A.4.2.6.4 Opening Rate From Solutioning by Eddy Diffusion to Lower Aquifer (ORSEDLA) -- An important reservation and admonition concerning either forced or free convection transport to horizons below the salt is that gravitational forces favor instabilities of various types that may have quite different forms from those associated with strata above the salt. One of these effects relative to brine flow is considered below. A potential major effect, however, that has not been studied in adequate dimensional perspective is the mechanical instability that will occur in the salt strata when solutioning from below occurs. We expect that certain conditions could lead to rapid propagation of breccia zones. These involve

forms of localized fracturing that are not accounted for by any of the equations for fracturing we have discussed so far. Some perspective is given by the time required to form large single cavities. This is shown later in the numerical results. However, feedback leading to even faster local penetration seems possible, because gravity favors higher fracturing potentials, larger fracture spacings and higher local brine transport rates by either free or forced convection. Understanding this problem from the feedback standpoint is an important future goal and should be high on the list of demonstration calculations for all projects related to waste repositories in salt media.

A start on this problem has been made by evaluating the transport in terms of a one-dimensional diffusion analogy. This form is suggested by work in progress by several investigators elsewhere relative to the Solution Mining industry. The assumption also simplifies the calculation in that the discharge rate can be estimated in a manner parallel to that for ORSD, except that because the fracture pathways are below the repository we can't assume the same proportionality to NEC. That is, at present we have no intuitive feel for where the fracture permeability will occur below the repository even though extensional stress concentrations are indicated by Figure 2A.5 in the underlying shale layer. It seems possible, for example, that part of the compaction displacement could be taken up by upward displacements of the floor of the repository by virtue of isostatic and thermally buoyant adjustments in rock immediately around and below this depth.

Our interpretation of this form of transport is that turbulent brine eddies can propagate downward with mean diffusivities at least as great as  $0.1 \text{ cm}^2/\text{sec}$ . At present this must be considered an unsupported assumption until the relevant investigations have been described in detail. On this assumption, transport occurs at a rate  $10^4$  times faster than with the coefficient in ORSD. If there is a relation for NEC analogous to that in the equation for ORSD, the new coefficient is  $1.0\text{E}8$  in the first term of the ORSD equation, which gives a transport rate of the same magnitude as ORSCUA. Though we are not able to document that assumption, the consequence of it is indicated by the ORSCUA output (except for the brecciation mechanisms mentioned above). Therefore, at present we write ORSEDLA only in terms of fractures produced by the faulting equations, as follows:

```
R  ORSEDLA.KL = 1.0E6*TIME + 1.0E9      OPENING RATE SOL
      EDDY DIFF TO L AQUIF (CU CM/YR)
```

Note: This equation does not account for all potentially important mechanical feedback mechanisms. The transport rate assumes constant rates of fracture creation from faulting sources only. See discussion in text.

In concluding the section on salt transport it is appropriate to comment again on the relationships of simulation models and more detailed transport modeling of Chapter 3. The hydrologic model is capable of giving very good estimates of transport rates and geometric distributions of species when the permeability regimes are known. It cannot, however, handle variable rock properties and boundary conditions during a calculation. Therefore, we envisage a coupled mode of calculation in which DYNAMO (or other languages) simulates the time changes of these variable conditions, the transport model then computes the amounts and distributions of chemical transport (salt removal, etc.) for some specified time interval, DYNAMO recomputes changes in system properties, fracture pathways, etc., and the transport model performs another iteration in that mode, and so on. In practice, a set of permeability regimes could be defined by reconnaissance DYNAMO calculations (or prescribed by other modeling or geological constraints). From this set the transport model can generate tables of transport data which then become table functions to be used by DYNAMO whenever a calculation encounters the appropriate conditions. In this way, a large catalog of transport functions could be accumulated and used interactively with a variety of different simulation sequences.

#### 2A.5 Computer Runs: H-TE-C-F-O-GW Sector

It is evident from the repeated warnings in the foregoing text that numerical calculations reported here are strictly test cases designed to provide the flavor of this approach to geological simulation without implying any rigid substantive conclusions. We have made over two hundred computer calculations during the report period in learning by trial and error some of the combinations possible using DYNAMO. The total costs in computer time are trivial (only a few dollars per calculation). We mention this to illustrate that: (a) the present report of work represents a bare beginning on problems of Geological Feedback Simulation using a very simple form of Simulation Language, and (b) rapid progress can be made, however, with inexpensive simulation techniques once a problem is defined.

We cannot display many of the calculations in this report. Therefore we give equation listings and examples of time plots in the form of direct computer outputs for two types of calculations: (1) a composite plot of simultaneous parameter variations, as an example of solutioning feedback, and (2) a series of plots showing results of single parameter variations (we refer to these later as "multiplots"). Because of their length, the time plots representing items (1) and (2) are supplied at the end of Appendix 2A.

The multiplots, shown in Figure 2A.11 (a-1) are computed in the same way as the plot of simultaneous parameter variation shown in Figure 2A.10. However, the multiplots demonstrate the effects of varying some of the parameters individually; these effects are shown sequentially on a series of plots each of which contains outputs for a single type of variable computed from several different choices of input assumptions.

#### 2A.5.1 Equation Listings

In order to compile the equations discussed in Section 2A.4 in one concise format, we show a typical listing from one of the solutioning calculations in Table 2A.3. (The equation list for each plot displayed in Figures 2A.7 and 2A.8 is given in a key that precedes the Tables and Figures at the end of Appendix 2A.

Parallel, but somewhat abbreviated, listings are given for the actual calculations displayed. The names of functions were necessarily modified for multiplots of single variables. The general scheme for the multiplots was to write the same equations repeatedly with similar but unique equation variables. We chose this approach in order to be explicit about data and equation sets, although there are automatic rerun options that can make use of sets of redefined Equation Constants (see Ref. 2A.11).

#### 2A.5.2 Computed Time Series

Examples of computer plots are shown in Figure 2A.10\* and 2A.11(a-l) for the Equation Listings in Table 2A.4 and Table 2A.5. These calculations are shown on a time scale of 10,000 years as a compromise that gives some idea of both short term and long term behavior. Other calculations have been made on time scales ranging from a thousand to a million years.

Generally a short title and other I.D. are shown at the top (or at the left margin if the TIME axis runs from left to right) followed by the correspondence of Equation Variables and Plot Symbols (HINR = P, etc.). The plotting scale is next identified for each plotting symbol for the chosen chart divisions (either by assignment or automatically by DYNAMO); the letter symbol immediately following the number scale represents the order of magnitude: A represents  $10^{-3}$ , T represents  $10^3$ , etc. (see Ref. 2A.11). Symbols that happen to plot at the same point on the chart are listed together at the margin (e.g., E and N plot together at the upper limit of the variable at 1000 years in Figure 2A.10, and P, C and M plot together at the lower limit of the variable at the same value of TIME).

The equation list and function plots for the multiplots (Table 2A.5 and Figures 2A.11) may seem confusing, but a complete explanation would be excessively long. The idea in generating these plots was to pick a set of functions for display and perform the calculations with several different choices of input parameters. The following tables give the choice of functions whose input parameters were varied in Figure 2A.11:

---

\* At end of Appendix 2A.

<u>Function Name</u>	<u>Figure 2A.11</u>
MTEMP	a
HOUTR	b
TE	c
HINR	d
SURFLX	e
EVISC	f
CL	g
NEC	h
NECSD (NEC with solutioning by diffusion)	i
SCDD (SCDIAM with solution- ing by diffusion)	j
NECSC (NEC with solutioning by convection)	k
SCDC (SCDIAM with solution- ing by convection)	l

The functions related to Heat content (Figures 2A.11 a-f) were varied by choosing three different values of thermal loading (roughly 30, 60, and 120 kw/acre) with various Delay times.

The compaction calculations of Figure 2A.11g were included to show comparisons of results using constant viscosities ranging from  $10^{18}$  poise (curve A) to  $10^{19}$  poise (curve C), and using variable viscosities from table functions (curves D, E, F). Curve D in 2A.11g represents a different compaction function from the other curves and has a somewhat lower final value of CL.

The multiplots in Figures 2A.11 i-l show the range of solutioning effects for the range of physical property variations in the preceding multiplots. Particularly, note the small range of times in Figure 2A.11k where NEC goes off scale (exceeds 100 meters of solutioning and compaction) despite the fairly wide range of variations in the input parameters.

Table 2A.6 and Figure 2A.12(a-b) give results for a time scale of one million years to show the long-term behavior of temperature and of solutioning compaction when the solutioning rate is decreased progressively by four orders of magnitude.

### 2A.5.3 Discussion of Computer Calculations

2A.5.3.1 General Summary -- As a guide to examination of the charts, some of the general points are summarized as follows: (1) the thermal steady state is achieved between 10,000 and 100,000 years, at which time temperatures and heat flux are indistinguishable from the normal geothermal gradient at a resolution of  $1^{\circ}\text{C}$ , (2) mean temperatures (MTEMP) quickly rise to maxima, generally less than  $100^{\circ}\text{C}$ , on a time scale of 1000 years or less and fall to below  $50^{\circ}\text{C}$  in the first 10,000 years; the position of the maximum is sensitive to assumed values of heat loss delays and distributions of thermal properties, (3) backfill temperatures (BFTEMP) are shown as roughly twice the mean temperature in order to represent the approximate average temperatures near the repository level ignoring short-term variations relative to canister distributions; the true values and their time distributions are very sensitive to the depth regions of averaging and to differences of thermal properties of the rock strata, (4) thermal expansion is equivalent to uplifts measured in tens of centimeters when compaction is not taken into account; the maximum follows soon after the thermal peak, (5) simple compaction of backfill porosity occurs rapidly in the first few hundred years and has nearly reached equilibrium in times of the order of 1000 years, (6) disturbance of the surface geothermal flux may be detectable within the first 10,000 years or so in dry environments, but convective heat transfer by groundwater probably will obliterate this effect in most systems (see Chapter 3), (7) solutioning effects related to the assumed fracture paths are very large relative to the scales of thermal expansion and backfill compaction because of feedback and may be commensurate with the thickness of the entire salt formation on a time scale of 10,000 years.

These general results are important for comparison with the calculations provided by the multicell model discussed in 2A.4.2.5.1. Figure 2A.8 shows some results of the finite-element thermal stress calculation. The differences emphasize the inaccuracies of the lumped parameter nature of the DYNAMO calculations but confirm the general magnitudes. The sharp contrast of the larger thermal expansion coefficient of halite relative to the rock average (see Table 2A.1) partly explains why the thermal expansion peak occurs much sooner in Figure 2A.8 than in the DYNAMO runs. This contrast combines with the more accurate representation of peak temperature in salt at the repository level (rather than a value based on the mean of average rock properties) to greatly shorten the peak response time. Factors of this type must be watched for continually in thinking about the results of simplified calculations. It is important, however, to have a feel for both this sort of response scale and the average response on the larger scale as represented by the DYNAMO calculations. Apparently, the very simple DYNAMO calculations categorically reproduce the kinds of responses found in much more sophisticated thermal calculations.

The most important general result, however, is that DYNAMO simulation is able to anticipate phenomena, such as item (7) above, that could not be predicted with the more specialized models and which are not intuitively obvious. This conceptual conclusion supports our introductory defense of simulation modeling as the simplest and quickest basis for discovering hidden effects that arise from feedback mechanisms.

2A.5.3.2 Conclusions on Salt Solutioning-Compaction Feedback -- The results of simulation calculations indicate the possibility for removal of a 100-meter layer of salt in less than 5000 years (Figure 2A.10, curve C; Figure 2A.11k) and the local penetration of the entire salt formation in less than 1500 years (Figure 2A.10, curve D; Figure 2A.11l). These are drastic consequences, at face value, and need some explanation.

The reason for this rather dramatic solutioning behavior is two-fold: (1) any mechanism at all that initiates cracking and establishes a convective siphon of the type postulated in Figure 2A.9 catalyzes the rapid acceleration of solutioning rates via the Feedback Loop of Figure 2A.3, and (2) the maximum rate of solutioning is large because of the large capacity and discharge rate of the Upper Aquifer of the Reference System in Figure 2A.1.

This simulation conclusion is made more severe by the fact that liberal variations in thermal loading (Figure 2A.11 a-d), effective viscosities (Figure 2A.11f) and backfill porosity (Figure 2A.13\*) have only minor effects on the solutioning time (Figure 2A.11k and l; Figure 2A.13\*). Figure 2A.13 is the result of a calculation in which the backfill maximum compaction length, BMCL, was reduced to 20 cm (about 4 percent initial porosity) and the thermal load was halved. As shown by curves C, N, and D of that figure, the solutioning times cited above are increased only by 20 to 30 percent. In fact, other calculations were made with zero initial backfill porosity and a low value of thermal load, and the solutioning times were still less than 10,000 years. The main conclusion is that if the conditions permit any cracking of the sort postulated, and if the hydrologic conditions are sufficiently dynamic, solutioning instabilities of layered salt media could occur on short time scales and hence represent major hypothetical threats to release of radionuclides to aquifers.

In order to test these phenomena for less active hydrologic environments, we made several runs on a million year time scale with solutioning rate coefficients (constants in functions like ORSCUA) progressively smaller by factors of ten. One example is shown in Figure 2A.12 (a-b). \* Two main conclusions are indicated: (a) the "incubation time" before the solutioning instability becomes conspicuous increases more or less in inverse proportion to the coefficient (the correspondence is not exact because of the nonlinearities of the various responses; this point needs additional "sorting"), and (b) by the same token, the system may appear stable to solutioning effects for long times (say on the 10,000 or 100,000 year scales), and still it may be susceptible to wholesale solutioning on the million-year time scale.

---

\* At end of Appendix 2A.

Geologically, it is clear even in other kinds of rock (e.g., limestone), that any process that initiates chemical transport along fracture pathways may act as a catalyst to increased transport. This general form of solutioning cycle is consistent with geological phenomena like Carlsbad Caverns of similar volumetric scale to the repository that occurred on a time scale roughly a hundred times longer in less soluble rock. There are, however, major scale differences in depth, deformation rate phenomena, chemistry, and presumably in hydrology so that only qualitative comparisons may be meaningful.

The reality of the higher solutioning rates will require much more careful analysis. The rates depend critically on the criteria of fracturing, which are very difficult to specify with rigor. The ranges of possibilities, however, can be narrowed by making calculations based on other forms of fracturing criteria than the simplistic assumptions used for the sake of demonstrating the simulation method. These refinements combined with a more appropriate rheological equation of state for salt may greatly modify the results.

Much geological evidence exists that can be brought to bear on these apparent conclusions. Unfortunately, geological knowledge of solutioning mechanisms has not been adequately systematized in a form that permits very great restrictions on maximum rates. Also, conditions of the sort artificially catalyzed by the local and rapid thermal loading are not presently known in the geologic record (to our knowledge). It is very difficult to state, however, from the existing statistically small sampling of the vast areas of salt deposits, that such phenomena as described in this report have not taken place at similar rates in some circumstances.

#### 2A.6 Recommendations

There is a major and sometimes confusing distinction between the use of numerical results of simulation analysis and belief in those results. We do not believe the foregoing consequence curves in a context much stronger than confirmation of existing geological knowledge and intuition that such instabilities can happen. We suggest that the results be used to continue building on these combined experiences until some confidence is gained on how likely is the possibility. Here again we need be careful on subjective probabilities versus empirical probabilities, though to some degree they will have to be combined (e.g., as occurs in weather "prediction").

We conclude that simulation analysis adds an important new dimension to methodology development that can be expanded and can add new perspectives to other analytical schemes. However, conclusions drawn from feedback calculations simply mirror and potentially amplify the insight (or lack thereof) of the analyst. Hence, progressive incorporation of greater geological insight is also desired. Feedback systems analysis can in itself provide a form of communications medium if it is used within common sense geological perspectives.



Though we have not tried to do so in the time available for preparation of this report, it is recommended that problems be classified by means of System Diagrams and Feedback Loops of the sorts we have discussed. Several have been mentioned in addition to solutioning processes. In these efforts we particularly recommend emphasis on searches for hidden effects that may have significant consequences on specified time scales (e.g., time scales that may be specified as important from the standpoint of exposure of the biosphere to radiation). One example of a hidden effect is the time scale for the "incubation period" of solutioning feedback.

As examples of application of simulation techniques to other forms of analysis, we recommend exploration as a tool for generating statistical populations of undersirable consequences with associated time scales. This might be approached from the standpoint of Monte Carlo series calculated from fairly unrestricted sets of input parameters, contrasted with other calculations from specified ranges and weighted interdependence of parameters (e.g., as might be specified for ranges of mechanical behavior limited according to deformation functions such as those described by Heard).<sup>(2A.8)</sup> These methods could provide one basis for "quick and dirty" Sensitivity Analysis; the main value of this would be to explore the relevant numerical techniques within a context that has some specific physical meaning from the standpoint of a hypothetical simulation model. It would still be understood that the results have no other specific import than possibly identifying most likely outcomes among a set that are already known in the simulation mode. For example, families of results for solutioning feedback might be illustrated this way, but the results would say nothing about triggering mechanisms not recognized in the simulation.

Another application implied by our discussions, and one we also recommend, is the use of DYNAMO and other Simulation Languages to provide the footwork to map out problems, boundary conditions, and specific questions to be more rigorously "solved" by multicell modeling techniques. The example highlighted is the relation of fracture permeability to chemical transport in the variety of regimes postulated. That is, are the paths, pressure heads, discharge rates, etc., realistic or are they artifacts of geometrical assumptions?

The statements of this report are not intended to represent alarmist or defeatist viewpoints. In fact, we feel that this sort of approach suggests some optimism for an eventual ability to characterize a repository sufficiently to greatly reduce fears that have grown from doubts raised concerning partial analysis.

Statements concerning the ultimate aims of assessing risks to the health and genetic future of mankind have been avoided in this report. For example, no position has been taken on the undesirability of release of radionuclides to active groundwater systems. Questions of dilution factors, absorption factors and path lengths are also relevant to the criteria of radiation hazards. More comprehensive systems analysis is required before geologic instabilities of the sort described can be considered categorically bad. It is suggested, however, that Systems Diagrams and Simulation Plots like those presented can also be helpful in this broader context.

Tables of DYNAMO Program Listings  
and Plots of Simulation Runs

<u>Tables</u>	<u>Figures</u>
2A.3	None relevant
2A.4	2A.10
2A.5	2A.11(a-1)
2A.6	2A.12(a & b)
2A.7	2A.13

TABLE 2A.3

## Typical Listing from a Solutioning Calculation

DYNAMO III, VERSION 3.02

```

* SIMPLE HEAT, THERMAL EXPANSION, COMPACTION AND SOLUTION SECTORS
N TIME=1. YEAR
L H.K=H.J+DT*(HINR.JK-HOUTP.JK) HEAT ABOVE ZERO TEMP CAL/GM
N H=5.2 CAL/GM INITIAL HEAT MTEMP=26C
R HINR.KL=0.047*FD.K PM POWER CAL/GM/YR 1/2 ORIGINAL
N HINR=0
A FD.K=EXP(2.303*LOGFD.K) RM DECAY FRACTION
N FD=1.0
A LOGFD.K=TABLE(FDTAB,LOGT.K,0,6,0.5) LOGTEN DECAY FRACTION
N LOGFD=0
T FDTAB=0/-0.03/-0.11/-0.38/-1.00/-1.8/-2.17/-2.51/-2.85/-3.27/
X -3.44/-4.0/-4.0 LOGTEN DECAY FRACTION TABLE REVISED 6/20/77
A LOGT.K=LOGN(TIME.K)/2.303 LOGTEN TIME (YEARS)
N LOGT=0
R SHLR.KL=25.0*(H.K-4.)/1.32E5-2.273E-4 STEADY HEAT LOSS RATE CAL/GM/YR
N SHLR=0
R HOUTP.KL=DELAYJ(SHLR.JK,DSHF) HEAT LOSS RATE CAL/GM/YR
N HOUTR=0
C DSHF=1000 YRS DELAY SURFACE HEAT FLUX
A MTEMP.K=(H.K-4.0)/3.2+20. MEAN TEMP FOR STEMP=20C
N MTEMP=26
S SURFLX.K=1.0+1.32E5*(HOUTP.JK/30) SURFACE FLUX MICROCAL/SQCM/SEC
N SURFLX=1.0
L TE.K=TE.J+DT*(TEF.JK) LINEAR THERMAL EXPANSION (CM)
N TE=0 INITIAL THERMAL REFERENCE STATE
R TEP.KL=UEC*(HINR.JK-HOUTR.JK)/0.2 LINEAR TE RATE (CM/YR)
N TEP=0.423
C UEC=0.9 CM/DEGC UNIT EXPANSION CONSTANT
S DTEMP.K=DT*(HINR.JK-HOUTP.JK)/0.2 DELTA TEMP JK DEGC
N DTEMP=0
A NEC.K=TE.K-CL.K NET EXPANSION MINUS COMPACTION (CM)
N NEC=0
A BFTMP.K=32+2*(MTEMP.K-26) APPROX BACKFILL TEMP DEGC
N BFTMP=32
L CL.K=MCL.J-LPV.J COMPACTION LENGTH (CM)
N CL=0
L LPV.K=LPV.J+DT*LPVCR.JK LINEAR PORE VOLUME (CM)
N LPV=60
R LPVCR.KL=LPV.K*EXP(-2.303*ELP*3.0E7*DT/EVISC.K)/DT-LPV.K/DT
NOTE LINEAR PORE VOLUME COMPACTION RATE (CM/YR)
A MCL.K=9MCL+ACLS.K MAX COMPACT LENGTH AT TIME (CM)
C BMCL=60 CM BACKFILL MAX COMPACT LENGTH
A ACLS.K=SQ.K/SA.K AVG COMPACT LENGTH FROM SOL (CM)
A SA.K=RA SOLUTIONING AREA (SQ.CM)
C PA=7.9E10 REPOSITORY AREA (SQ.CM.)
C ELP=1.3E8 DYNE/SQCM EFFECTIVE LOAD PRESSURE
A NECR.K=TEP.JK-LPVCR.JK NET EXPANSION MINUS COMPACT RATE (CM/YR)
A EVISC.K=TABLE(EVTAB,BFTMP.K,0,250,25) EFFECTIVE VISC (POISE)
T EVTAB=1.15E19,7.03E18,4.47E18,2.31E18,1.78E18,1.25E18,
X 8.91E17,6.61E17,5.01E17,3.4CE17,3.02E17
L SO.K=SO.J+DT*(ORSO.JK+ORSCLAS.K+ORSCLAS.JK+ORSCLAS.JK) SOLUT.OPEN.(CU.CM)
N SO=1 CU.CM. MINIMUM SOLUTION OPENINGS
R ORSD.KL=0
R ORSCUA.KL=1.0E8*MAX(NEC.K,-NEC.K) OPEN RATE FROM SOLUTION BY CONVECTION
NOTE JP AQUIFER (CU.CM./YR)
R ORSCLAS.KL=0
R ORSEDLA.KL=0
A SCDIAM.K=2.0*EXP(LNVFUNC.K) SINGLE CAVITY DIAM (CM)
A LNVFUNC.K=0.33*LOGN(SO.K)-0.45
NOTE
PPRINT CL,NEC,SO,SCDIAM,ORSCLAS,ACLS,MCL,LPV,BFTMP,TE,HINR,HOUTR
PLOT ACLS=A(0,1.0E4)/SCDIAM=0(0,2.0E4)/SO=S(0,0.0E15)/CL=C(0,1.0E4)/
X NEC=N(1.0E4,0)/PFTMP=B/TE=F/HINR=P/HOUTP=0
SPEC DT=10/LENGTH=1.0E5/PLTFR=1.0E4/PRIPER=100
RUN 10 YR DT TO 1.0E6 NEW HINR,FDTAB,ORSCLAS,ORSCLAS DS+P=1000
SFO -
FLX -
MP -
P -

```

```

1047 OF 2472 DATA LIST WORDS
127 OF 200 SYMBOL TABLE VARIABLES
9 OF 15 MACRO DEFINITIONS
11 OF 15 OUTPUT RECORDS (PLOT CARDS/PRINT LINES)

```

TABLE 2A.4

## Equation Listing for Plots in Figure 2A. 10

DYNAMO IIF, VERSION 3.02

```

*      BMCL=60, SO MIN AND ORSCUA=1.0E8...
N      TIME=1. YEAR
L      H.K=H.J*DT*(HINR.JK-HOUTR.JK) HEAT ABOVE ZERO TEMP CAL/GH
N      H=5.2 CAL/GH INITIAL HEAT MTEMP=26C
R      HINR.KL=0.094*FD.K RN POWER CAL/GH/YR
N      HINR=0
A      FD.K=EXP(2.333*LOGFD.K) RN DECAY FRACTION
N      FD=1.0
A      LOGFD.K=TABLE(FDTAB,LOGT.K,0.6,0.5) LOGTEN DECAY FRACTION
N      LOGFD=0
T      FDTAB=C/-0.03/-0.11/-0.38/-1.00/-1.80/-2.17/-2.51/-2.80/-3.28/
X      -3.34/-4.0/-4.0 LOGTEN DECAY FRACTION TABLE REVISED 6/20/77
A      LOGT.K=LOGN(TIME.K)/2.303 LOGTEN TIME (YEARS)
N      LOGT=0
R      SHLR.KL=25.0*(H.K-4.)/1.32E5-2.273E-4 STEADY HEAT LOSS RATE CAL/GH/YR
N      SHLR=0
R      HOUTP.KL=DELAY3(SHLR.JK,0.3HF) HEAT LOSS RATE CAL/GH/YR
N      HOUTR=0
C      OSWF=100
A      MTEMP.K=(H.K-4.0)/0.2+20. MEAN TEMP FOR STEMP=20C
N      MTEMP=26
S      SURFLX.K=1.0+1.32E5*(HOUTR.JK/30) SURFACE FLUX MICROCAL/SQCM/SEC
N      SURFLX=1.0
L      TE.K=TE.J*DT*(TER.JK) LINEAR THERMAL EXPANSION (CM)
N      TE=0 INITIAL THERMAL REFERENCE STATE
R      TER.KL=UEC*(HINR.JK-HOUTR.JK)/0.2 LINEAR TE RATE (CM/YR)
N      TER=0.423
C      UEC=0.9 CM/DEGC UNIT EXPANSION CONSTANT
S      DTEMP.K=DT*(HINR.JK-HOUTR.JK)/0.2 DELTA TEMP JK DEGC
N      DTEMP=0
A      BFTEMP.K=32+2*(MTEMP.K-26) APPROX BACKFILL TEMP DEGC
N      BFTEMP=32
C      BMCL=60 CM BACKFILL MAX COMPACT LENGTH
A      SA.K=RA SOLUTIONING AREA (SQ.CM)
C      RA=7.9E10 REPOSITORY AREA (SQ.CM.)
C      ELP=1.3E8 DYNE/SQCM EFFECTIVE LOAD PRESSURE
A      EVISC.K=TABLE(EVTAB,BFTEMP.K,0.250,25) EFFECTIVE VISC (POISE)
T      EVTAB=1.15E19,7.08E18,4.47E18,2.81E18,1.78E18,1.26E18,
X      8.91E17,6.61E17,5.01E17,3.85E17,3.02E17
R      ORSCU1.KL=1.0E8*MAX(NEC1.K,-NEC1.K)
A      NEC1.K=TE.K-CL1.K
N      NEC1=0
L      CL1.K=MCL1.J-LPV1.J
N      CL1=0
L      LPV1.K=LPV1.J*DT*(LPVCR1.JK)
N      LPV1=6C
R      LPVCR1.KL=LPV1.K*EXP(-2.303*ELP*3.0E7*DT/EVISC.K)/DT-LPV1.K/DT
A      MCL1.K=BMCL+ACLS1.K
A      ACLS1.K=SO1.K/SA.K
N      SO1=1 CU.CM.
L      SO1.K=SO1.J*DT*FIFGE(0,ORSCU1.JK,ACLS1.JK,1.0E4)
A      SC0IA1.K=2.0*EXP(LN1VFU1.K)
A      LN1VFU1.K=0.33*LOGN(SO1.K)-0.46
NOTE
PRINT HINR,HOUTR,SURFLX,TE,NEC1,BFTEMP,CL1,MCL1,SC0IA1,SO1,ORSCU1,ACLS1
PLDT HINR=P/HOUTR=0/SURFLX=F/TE=E/NEC1=N/(-1.0E4,0)/BFTEMP=B
X      CL1=C,MCL1=M(0,1.0E4)/SC0IA1=0(0,2.0E4)
SPEC DT=1/LENGTH=1.0E4/PLTPER=100/PRTPER=100
RUN ORSCUA CONSTANT BUT NOTHING ELSE

```

```

ISED -
MP

```

```

-----
1030 OF 2472 DATA LIST #0-05
123 OF 203 SYMBOL TABLE VARIABLES
9 OF 15 MACRO DEFINITIONS
11 OF 15 OUTPUT RECORDS (PLOT CARDS/PRINT LINES)
-----

```

TABLE 2A.5

Equation Listing for Plots in Figure 2A.11 (a - 1)

DYNAMO IIF..VERSION 3.02

```

* ... SIMPLE HEAT AND COMPACTION SECTION
* ... SOLUTIONING BY DIFFUSION
* ... SOLUTIONING BY CONVECTION
N ... TIME=1. YEAR
A ... FD.K=EXP(2.303*LOGFD.K) ... RN DECAY FRACTION
N ... FD=1.0
A ... LOGFD.K=TABLE(FDTAB,LOGT.K,0.6,0.5) ... LOGTEN DECAY FRACTION
N ... LOGFD=0
T ... FDTAB=1/-0.03/-0.11/-0.33/-1.00/-1.80/-2.17/-2.51/-2.80/-3.26/
X ... -3.84/-4.0/-4.0 LOGTEN DECAY FRACTION TABLE REVISED 6/20/77
A ... LOGT.K=LOGN(TIME,K)/2.303 ... LOGTEN TIME (YEARS)
N ... LOGT=0
A ... FDX.K=EXP(2.303*LOGFDX.K) ... RN DECAY FRACTION
N ... FDX=1.0
A ... LOGFDX.K=TABLE(FDXTAB,LOGT.K,0.6,0.5) ... LOGTEN DECAY FRACTION
N ... LOGFDX=0
T ... FDXTAB=0/-0.12/-0.29/-0.51/-0.80/-1.12/
X ... -1.48/-1.83/-2.18/-2.50/-3.22/-3.22/-3.22 LOGTEN DECAY FRACTION TABLE
C ... ELP=1.3E6 DYNE/CMCH EFFECTIVE LOAD PRESSURE
T ... EVTAB=1.15E19,7.04E18,4.47E18,2.81E18,1.78E18,1.25E18,
X ... 8.91E17,6.61E17,5.11E17,3.80E17,3.02E17
* ... SIMPLE HEAT SECTION
R ... HINR1.KL=0.094*FD.K
N ... HINR1=0
R ... HINR2.KL=0.108*FD.K
N ... HINR2=0
R ... HINR3.KL=0.047*FD.K
N ... HINR3=0
R ... HINRX.KL=0.094*FDX.K
N ... HINRX=0
R ... SHLR1.KL=12.5*(H2.K-4.0)/1.32E5-2.273E-4
N ... SHLR1=0
R ... SHLR2.KL=25.0*(H3.K-4.0)/1.32E5-2.273E-4
N ... SHLR2=0
C ... OSHF1=5000
C ... OSHF2=1000
C ... OSHF3=200
L ... H1.K=H1.J+DT*(HINR1.JK-HOUTR1.JK)
N ... H1=5.2
R ... HOUTR1.KL=DELAY3(HINR1.JK,OSHF1)
N ... HOUTR1=0
A ... MTEMP1.K=(H1.K-4.0)/0.2+20
S ... SURFL1.K=1.0+1.32E5*(HOUTR1.JK/30)
L ... H2.K=H2.J+DT*(HINR1.JK-HOUTR2.JK)
N ... H2=5.2
R ... HOUTR2.KL=DELAY3(HINR1.JK,OSHF2)
N ... HOUTR2=0
A ... MTEMP2.K=(H2.K-4.0)/0.2+20
S ... SURFL2.K=1.0+1.32E5*(HOUTR2.JK/30)
L ... H3.K=H3.J+DT*(HINR1.JK-HOUTR3.JK)
N ... H3=5.2
R ... HOUTR3.KL=DELAY3(HINR1.JK,OSHF3)
N ... HOUTR3=0
A ... MTEMP3.K=(H3.K-4.0)/0.2+20
S ... SURFL3.K=1.0+1.32E5*(HOUTR3.JK/30)
L ... H4.K=H4.J+DT*(HINR2.JK-HOUTR4.JK)
N ... H4=5.2
R ... HOUTR4.KL=DELAY3(HINR2.JK,OSHF1)
N ... HOUTR4=0
A ... MTEMP4.K=(H4.K-4.0)/0.2+20
S ... SURFL4.K=1.0+1.32E5*(HOUTR4.JK/30)
L ... H5.K=H5.J+DT*(HINR3.JK-HOUTR5.JK)
N ... H5=5.2
R ... HOUTR5.KL=DELAY3(HINR3.JK,OSHF1)
N ... HOUTR5=0
A ... MTEMP5.K=(H5.K-4.0)/0.2+20
S ... SURFL5.K=1.0+1.32E5*(HOUTR5.JK/30)
L ... H6.K=H6.J+DT*(HINR1.JK-HOUTR6.JK)
N ... H6=5.2
R ... HOUTR6.KL=DELAY3(HINR1.JK,OSHF1)
N ... HOUTR6=0
A ... MTEMP6.K=(H6.K-4.0)/0.2+20
S ... SURFL6.K=1.0+1.32E5*(HOUTR6.JK/30)
L ... H7.K=H7.J+DT*(HINR1.JK-HOUTR7.JK)
N ... H7=5.2
R ... HOUTR7.KL=DELAY3(SHLR1.JK,OSHF1)
N ... HOUTR7=0
A ... MTEMP7.K=(H7.K-4.0)/0.2+20
S ... SURFL7.K=1.0+1.32E5*(HOUTR7.JK/30)

```

TABLE 2A.5 (Cont)

R	HOUTR5.KL=DELAY3(HINR3.JK,DSHF1)
N	HOUTR5=0
A	MTEMP5.K=(H5.K-4.0)/0.2+20
S	SURFL5.K=1.0+1.32E5*(HOUTR5.JK/30)
L	H6.K=H6.J+DT*(HINR1.JK-HOUTR5.JK)
N	H6=5.2
R	HOUTR6.KL=DELAY1(HINR1.JK,DSHF1)
N	HOUTR6=0
A	MTEMP6.K=(H6.K-4.0)/0.2+20
S	SURFL6.K=1.0+1.32E5*(HOUTR6.JK/30)
L	H7.K=H7.J+DT*(HINR1.JK-HOUTR6.JK)
N	H7=5.2
R	HOUTR7.KL=DELAY3(SHLR1.JK,DSHF1)
N	HOUTR7=0
A	MTEMP7.K=(H7.K-4.0)/0.2+20
S	SURFL7.K=1.0+1.32E5*(HOUTR7.JK/30)
L	H8.K=H8.J+DT*(HINR1.JK-HOUTR7.JK)
N	H8=5.2
R	HOUTR8.KL=DELAY3(SHLR2.JK,DSHF1)
N	HOUTR8=0
A	MTEMP8.K=(H8.K-4.0)/0.2+20
S	SURFL8.K=1.0+1.32E5*(HOUTR8.JK/30)
L	H9.K=H9.J+DT*(HINR1.JK-HOUTR8.JK)
N	H9=5.2
R	HOUTR9.KL=DELAY1(SHLR1.JK,DSHF3)
N	HOUTR9=0
A	MTEMP9.K=(H9.K-4.0)/0.2+20
S	SURFL9.K=1.0+1.32E5*(HOUTR9.JK/30)
C	UEC=0.9
L	TE1.K=TE1.J+DT*(TER1.JK)
N	TE1=0
R	TER1.KL=UEC*(HINR1.JK-HOUTR1.JK)/0.2
L	TE2.K=TE2.J+DT*(TER2.JK)
N	TE2=0
R	TER2.KL=UEC*(HINR1.JK-HOUTR2.JK)/0.2
L	TE3.K=TE3.J+DT*(TER3.JK)
N	TE3=0
R	TER3.KL=UEC*(HINR1.JK-HOUTR3.JK)/0.2
L	TE4.K=TE4.J+DT*(TER4.JK)
N	TE4=0
R	TER4.KL=UEC*(HINR2.JK-HOUTR4.JK)/0.2
L	TE5.K=TE5.J+DT*(TER5.JK)
N	TE5=0
R	TER5.KL=UEC*(HINR3.JK-HOUTR5.JK)/0.2
L	TE6.K=TE6.J+DT*(TER6.JK)
N	TE6=0
R	TER6.KL=UEC*(HINR1.JK-HOUTR6.JK)/0.2
L	TE7.K=TE7.J+DT*(TER7.JK)
N	TE7=0
R	TER7.KL=UEC*(HINR1.JK-HOUTR7.JK)/0.2
L	TE8.K=TE8.J+DT*(TER8.JK)
N	TE8=0
R	TER8.KL=UEC*(HINR1.JK-HOUTR8.JK)/0.2
L	TE9.K=TE9.J+DT*(TER9.JK)
N	TE9=0
R	TER9.KL=UEC*(HINR1.JK-HOUTR9.JK)/0.2
A	EVISC1.K=TABLE(EVTAB,BFT1.K,0,250,25)
A	BFT1.K=32+2*(MTEMP1.K-26)
A	EVISC2.K=TABLE(EVTAB,BFT2.K,0,250,25)
A	BFT2.K=32+2*(MTEMP2.K-26)
A	EVISC3.K=TABLE(EVTAB,BFT3.K,0,250,25)
A	BFT3.K=32+2*(MTEMP3.K-26)
A	EVISC4.K=TABLE(EVTAB,BFT4.K,0,250,25)
A	BFT4.K=32+2*(MTEMP4.K-26)
A	EVISC5.K=TABLE(EVTAB,BFT5.K,0,250,25)
A	BFT5.K=32+2*(MTEMP5.K-26)
A	EVISC6.K=TABLE(EVTAB,BFT6.K,0,250,25)
A	BFT6.K=32+2*(MTEMP6.K-26)
A	EVISC7.K=TABLE(EVTAB,BFT7.K,0,250,25)
A	BFT7.K=32+2*(MTEMP7.K-26)
A	EVISC8.K=TABLE(EVTAB,BFT8.K,0,250,25)
A	BFT8.K=32+2*(MTEMP8.K-26)
A	EVISC9.K=TABLE(EVTAB,BFT9.K,0,250,25)
A	BFT9.K=32+2*(MTEMP9.K-26)
NOTE: SAMPLE TREAT AND COMPACTION SECTIONS WITH SLOTTED TONING OR CONNECTIONS	
A	NECSCL.K=TEL.K-CLSC1.K
N	NECSCL=0
L	CLSC1.K=CLSC1.J-LPVSC1.J
N	CLSC1=0
L	LPVSC1.K=LPVSC1.J+DT*LPVRC1.JK
N	LPVSC1=0
R	LPVRC1.KL=LPVSC1.K*EXP(-2.303*ELP*3.0E7*DT/EVISC1.K)/DT-LP*SC1.K/DT
A	MCLSC1.K=60+ACLSC1.K

TABLE 2A.5 (Cont)

```

A      BFI3,K=1.0/2.0*(MILMPY,K-20)
NOTE: SIMPLIFIED AND COMPACTION SECTORS WITH SOLUTIONING BY CONNECTION
A      NECSC1,K=TE1,K-CLSC1,K
N      NECSC1=C
L      CLSC1,K=MCLSC1,J-LPVSC1,J
N      CLSC1=C
L      LPVSC1,K=LPVSC1,J+DT*LPVRC1,JK
N      LPVSC1=60
R      LPVRC1,KL=LPVSC1,K*EXP(-2.303*ELP*3.0E7*DT/EVISC1,K)/DT-LPVSC1,K/DT
A      MCLSC1,K=60+ACLSC1,K
A      ACLSC1,K=SOC1,K/7.9E10
L      SOC1,K=SOC1,J+DT*(ORSC1,JK) SOL OPEN BY CONV
N      SOC1=1
R      ORSC1,KL=1.0E8*MAX(NECSC1,K,-NECSC1,K)
A      SCOC1,K=2.0*EXP(LNVFC1,K)
A      LNVFC1,K=0.33*LCGN(SOC1,K)-0.46
A      NECSC2,K=TE2,K-CLSC2,K
N      NECSC2=C
L      CLSC2,K=MCLSC2,J-LPVSC2,J
N      CLSC2=C
L      LPVSC2,K=LPVSC2,J+DT*LPVRC2,JK
N      LPVSC2=60
R      LPVRC2,KL=LPVSC2,K*EXP(-2.303*ELP*3.0E7*DT/EVISC2,K)/DT-LPVSC2,K/DT
A      MCLSC2,K=60+ACLSC2,K
A      ACLSC2,K=SOC2,K/7.9E10
L      SOC2,K=SOC2,J+DT*(ORSC2,JK) SOL OPEN BY CONV
N      SOC2=1
R      ORSC2,KL=1.0E8*MAX(NECSC2,K,-NECSC2,K)
A      SCOC2,K=2.0*EXP(LNVFC2,K)
A      LNVFC2,K=0.33*LCGN(SOC2,K)-0.46
A      NECSC3,K=TE3,K-CLSC3,K
N      NECSC3=C
L      CLSC3,K=MCLSC3,J-LPVSC3,J
N      CLSC3=C
L      LPVSC3,K=LPVSC3,J+DT*LPVRC3,JK
N      LPVSC3=60
R      LPVRC3,KL=LPVSC3,K*EXP(-2.303*ELP*3.0E7*DT/EVISC3,K)/DT-LPVSC3,K/DT
A      MCLSC3,K=60+ACLSC3,K
A      ACLSC3,K=SOC3,K/7.9E10
L      SOC3,K=SOC3,J+DT*(ORSC3,JK) SOL OPEN BY CONV
N      SOC3=1
R      ORSC3,KL=1.0E8*MAX(NECSC3,K,-NECSC3,K)
A      SCOC3,K=2.0*EXP(LNVFC3,K)
A      LNVFC3,K=0.33*LCGN(SOC3,K)-0.46
A      NECSC4,K=TE4,K-CLSC4,K
N      NECSC4=C
L      CLSC4,K=MCLSC4,J-LPVSC4,J
N      CLSC4=C
L      LPVSC4,K=LPVSC4,J+DT*LPVRC4,JK
N      LPVSC4=60
R      LPVRC4,KL=LPVSC4,K*EXP(-2.303*ELP*3.0E7*DT/EVISC4,K)/DT-LPVSC4,K/DT
A      MCLSC4,K=60+ACLSC4,K
A      ACLSC4,K=SOC4,K/7.9E10
L      SOC4,K=SOC4,J+DT*(ORSC4,JK) SOL OPEN BY CONV
N      SOC4=1
R      ORSC4,KL=1.0E8*MAX(NECSC4,K,-NECSC4,K)
A      SCOC4,K=2.0*EXP(LNVFC4,K)
A      LNVFC4,K=0.33*LCGN(SOC4,K)-0.46
A      NECSC5,K=TE5,K-CLSC5,K
N      NECSC5=C
L      CLSC5,K=MCLSC5,J-LPVSC5,J
N      CLSC5=C
L      LPVSC5,K=LPVSC5,J+DT*LPVRC5,JK
N      LPVSC5=60
R      LPVRC5,KL=LPVSC5,K*EXP(-2.303*ELP*3.0E7*DT/EVISC5,K)/DT-LPVSC5,K/DT
A      MCLSC5,K=60+ACLSC5,K
A      ACLSC5,K=SOC5,K/7.9E10
L      SOC5,K=SOC5,J+DT*(ORSC5,JK) SOL OPEN BY CONV
N      SOC5=1
R      ORSC5,KL=1.0E8*MAX(NECSC5,K,-NECSC5,K)
A      SCOC5,K=2.0*EXP(LNVFC5,K)
A      LNVFC5,K=0.33*LCGN(SOC5,K)-0.46
A      NECSC6,K=TE6,K-CLSC6,K
N      NECSC6=C
L      CLSC6,K=MCLSC6,J-LPVSC6,J
N      CLSC6=C
L      LPVSC6,K=LPVSC6,J+DT*LPVRC6,JK
N      LPVSC6=60
R      LPVRC6,KL=LPVSC6,K*EXP(-2.303*ELP*3.0E7*DT/EVISC6,K)/DT-LPVSC6,K/DT
A      MCLSC6,K=60+ACLSC6,K
A      ACLSC6,K=SOC6,K/7.9E10
L      SOC6,K=SOC6,J+DT*(ORSC6,JK) SOL OPEN BY CONV
N      SOC6=1
R      ORSC6,KL=1.0E8*MAX(NECSC6,K,-NECSC6,K)

```

TABLE 2A.5 (Cont)

```

A      1CLSC5.K=6J*ACLS5.K
A      ACLSC5.K=SOC5.K/7.9E10
L      SOC5.K=SOC5.J+DT*(ORSC5.JK) SOL OPEN BY CONV
N      SOC5=1
R      ORSC5.KL=1.0E8*MAX(NECSC5.K,-NECSC5.K)
A      SCOC5.K=2.0*EXP(LNVFC5.K)
A      LNVFC5.K=0.33*LCGN(SOC5.K)-0.46
A      NECSC6.K=TE6.K-CLSC6.K
N      NECSC6=0
L      CLSC6.K=MCLSC6.J-LPVSC6.J
N      CLSC6=0
L      LPVSC6.K=LPVSC5.J+DT*LPVRC6.JK
N      LPVSC6=60
R      LPVRC6.KL=LPVSC6.K*EXP(-2.303*ELP*3.0E7*DT/EVISC6.K)/DT-LPVSC6.K/DT
A      MCLSC6.K=60*ACLS6.K
A      ACLSC6.K=SOC6.K/7.9E10
L      SOC6.K=SOC6.J+DT*(ORSC6.JK) SOL OPEN BY CONV
N      SOC6=1
R      ORSC6.KL=1.0E8*MAX(NECSC6.K,-NECSC6.K)
A      SCOC6.K=2.0*EXP(LNVFC6.K)
A      LNVFC6.K=0.33*LCGN(SOC6.K)-0.46
A      NECSC7.K=TE7.K-CLSC7.K
N      NECSC7=0
L      CLSC7.K=MCLSC7.J-LPVSC7.J
N      CLSC7=0
L      LPVSC7.K=LPVSC6.J+DT*LPVRC7.JK
N      LPVSC7=60
R      LPVRC7.KL=LPVSC7.K*EXP(-2.303*ELP*3.0E7*DT/EVISC7.K)/DT-LPVSC7.K/DT
A      MCLSC7.K=60*ACLS7.K
A      ACLSC7.K=SOC7.K/7.9E10
L      SOC7.K=SOC7.J+DT*(ORSC7.JK) SOL OPEN BY CONV
N      SOC7=1
R      ORSC7.KL=1.0E8*MAX(NECSC7.K,-NECSC7.K)
A      SCOC7.K=2.0*EXP(LNVFC7.K)
A      LNVFC7.K=0.33*LCGN(SOC7.K)-0.46
A      NECSC8.K=TE8.K-CLSC8.K
N      NECSC8=0
L      CLSC8.K=MCLSC8.J-LPVSC8.J
N      CLSC8=0
L      LPVSC8.K=LPVSC7.J+DT*LPVRC8.JK
N      LPVSC8=60
R      LPVRC8.KL=LPVSC8.K*EXP(-2.303*ELP*3.0E7*DT/EVISC8.K)/DT-LPVSC8.K/DT
A      MCLSC8.K=60*ACLS8.K
A      ACLSC8.K=SOC8.K/7.9E10
L      SOC8.K=SOC8.J+DT*(ORSC8.JK) SOL OPEN BY CONV
N      SOC8=1
R      ORSC8.KL=1.0E8*MAX(NECSC8.K,-NECSC8.K)
A      SCOC8.K=2.0*EXP(LNVFC8.K)
A      LNVFC8.K=0.33*LCGN(SOC8.K)-0.46
A      NECSC9.K=TE9.K-CLSC9.K
N      NECSC9=0
L      CLSC9.K=MCLSC9.J-LPVSC9.J
N      CLSC9=0
L      LPVSC9.K=LPVSC8.J+DT*LPVRC9.JK
N      LPVSC9=60
R      LPVRC9.KL=LPVSC9.K*EXP(-2.303*ELP*3.0E7*DT/EVISC9.K)/DT-LPVSC9.K/DT
A      MCLSC9.K=60*ACLS9.K
A      ACLSC9.K=SOC9.K/7.9E10
L      SOC9.K=SOC9.J+DT*(ORSC9.JK) SOL OPEN BY CONV
N      SOC9=1
R      ORSC9.KL=1.0E8*MAX(NECSC9.K,-NECSC9.K)
A      SCOC9.K=2.0*EXP(LNVFC9.K)
A      LNVFC9.K=0.33*LCGN(SOC9.K)-0.46
NDRE
PLOT NECSC1=1,NECSC2=2,NECSC3=3,NECSC4=4,NECSC5=5,NECSC6=6,
     NECSC7=7,NECSC8=8,NECSC9=9(-1.0E4,0)
PLOT SCOC1=1,SCOC2=2,SCOC3=3,SCOC4=4,SCOC5=5,SCOC6=6,
     SCOC7=7,SCOC8=8,SCOC9=9(0,2.0E4)
PRINT NECSC1,NECSC2,NECSC3,NECSC4,NECSC5,NECSC6,NECSC7,NECSC8,NECSC9
PRINT CLSC1,CLSC2,CLSC3,CLSC4,CLSC5,CLSC6,CLSC7,CLSC8,CLSC9
PRINT LPVSC1,LPVSC2,LPVSC3,LPVSC4,LPVSC5,LPVSC6,LPVSC7,LPVSC8,LPVSC9
PRINT LPVRC1,LPVRC2,LPVRC3,LPVRC4,LPVRC5,LPVRC6,LPVRC7,LPVRC8,LPVRC9
PRINT ACLSC1,ACLSC2,ACLSC3,ACLSC4,ACLSC5,ACLSC6,ACLSC7,ACLSC8,ACLSC9
PRINT SOC1,SCOC2,SOC3,SCOC4,SOC5,SCOC6,SOC7,SCOC8,SOC9
PRINT ORSC1,ORSC2,ORSC3,ORSC4,ORSC5,ORSC6,ORSC7,ORSC8,ORSC9
PRINT SCOC1,SCOC2,SCOC3,SCOC4,SCOC5,SCOC6,SCOC7,SCOC8,SCOC9
SPEC DT=10/LENGTH=1.0E4/PLTPEP=100/PRTPEP=100
RUN SOLUTICING BY CONVECTION

```

E0

X

L1

L2

L3



TABLE 2A.6

Equation Listing for Plots in Figure 2A.12 (a - b)

DYNAMO IIF, VERSION 3.C2

```

* TEST OF CHANGE IN ORSCUA CONSTANT
N TIME=1. YEAR
L H.K=H.J+DT*(HINR.JK-HOUTR.JK) HEAT ABOVE ZERO TEMP CAL/GM
N H=5.2 CAL/GM INITIAL HEAT MTEMP=26C
R HINR.KL=0.094*FO.K RN POWER CAL/GM/YR
N HINR=0
A FO.K=EXP(12.303*LOGFO.K) RN DECAY FRACTION
N FO=1.0
A LOGFO.K=TABLE(FCTA9,LOGT.K,0.6,0.5) LOGTEN DECAY FRACTION
N LCGFO=0
T FDTAB=((-0.03/-0.11/-0.34/-1.00/-1.40/-2.17/-2.51/-2.80/-3.29/-
X -3.84/-4.07/-4.0 LOGTEN DECAY FRACTION TABLE REVISED 6/20/77
A LOGT.K=LCGM(TIME.K)/2.303 LOGTEN TIME (YEARS)
N LOGT=C
R SHLR.KL=25.0*(H.K-4.)/1.32E5-2.273E-4 STEADY HEAT LOSS RATE CAL/GM/YR
N SHLR=C
R HOUTR.KL=DELAY3(SHLR.JK,DSHF) HEAT LOSS RATE CAL/GM/YR
N HOUTR=0
C DSHF=1000 YRS DELAY SURFACE HEAT FLUX
A MTEMP.K=(H.K-4.)/0.2+20. MEAN TEMP FOR STEMP=26C
N MTEMP=26
S SURFLX.K=1.0+1.32E5*(HOUTR.JK/30) SURFACE FLUX MICROCAL/SQCM/SEC
N SURFLX=1.0
L TE.K=TE.J+DT*(TER.JK) LINEAR THERMAL EXPANSION (CM)
N TE=0 INITIAL THERMAL REFERENCE STATE
R TEP.KL=UEC*THINA.JK-HOUTR.JK/70.2 LINEAR TE RATE (CM/YR)
N TEP=0.423
C UEC=0.9 CM/DEGC UNIT EXPANSION CONSTANT
S DTEMP.K=DT*(HINR.JK-HOUTR.JK)/0.2 DELTA TEMP JK DEGC
N DTEMP=0
A BFTEMP.K=32+2*(MTEMP.K-26) APPROX BACKFILL TEMP DEGC
N BFTEMP=32
C BMCL=60 CM BACKFILL MAX COMPACT LENGTH
A SA.K=RA SOLUTIONING AREA (SQ.CM)
C RA=7.9E10 REPOSITORY AREA (SQ.CM)
C FLF=1.3E8 DYNE/SQCM EFFECTIVE LOAD PRESSURE
A EVISC.K=TABLE(EVTAB,BFTEMP.K,0.250,25) EFFECTIVE VISC (POISE)
T EVTAB=1.15E19,7.05E18,4.47E18,2.81E18,1.78E18,1.26E18,
X 8.91E17,6.61E17,5.01E17,3.80E17,3.02E17
R ORSCU1.KL=1.0E8*MAX(NEC1.K,-NEC1.K)
A NEC1.K=TE.K-CL1.K
N NEC1=0
L CL1.K=PCL1.J-LPV1.J
N CL1=C
L LPV1.K=LPV1.J+DT*(LPVCR1.JK)
N LPV1=60
R LPVCR1.KL=LPV1.K*EXP(-2.303*ELP*3.0E7*DT/EVISC.K)/DT-LPV1.K/DT
A MCL1.K=BMCL*ACLS1.K
A ACLS1.K=S01.K/SA.K
N S01=1 CL.CM
L S01.K=S01.J+DT*FIFGE(0,ORSCU1.JK,ACLS1.K,1.0E4)
A SCOA1.K=2.0*EXP(LNVFU1.K)
A LNVFU1.K=0.33*LCGM(S01.K)-0.46
R ORSCU2.KL=1.0E7*MAX(NEC2.K,-NEC2.K)
A NEC2.K=TE.K-CL2.K
N NEC2=0
L CL2.K=PCL2.J-LPV2.J
N CL2=0
L LPV2.K=LPV2.J+DT*(LPVCR2.JK)
N LPV2=50
R LPVCR2.KL=LPV2.K*EXP(-2.303*ELP*3.0E7*DT/EVISC.K)/DT-LPV2.K/DT
A MCL2.K=BMCL*ACLS2.K
A ACLS2.K=S02.K/SA.K
N S02=1 CL.CM
L S02.K=S02.J+DT*FIFGE(0,ORSCU2.JK,ACLS2.K,1.0E4)
A SCOA2.K=2.0*EXP(LNVFU2.K)
A LNVFU2.K=0.33*LCGM(S02.K)-0.46
R ORSCU3.KL=1.0E6*MAX(NEC3.K,-NEC3.K)
A NEC3.K=TE.K-CL3.K
N NEC3=0
L CL3.K=PCL3.J-LPV3.J
N CL3=0
L LPV3.K=LPV3.J+DT*(LPVCR3.JK)
N LPV3=60
R LPVCR3.KL=LPV3.K*EXP(-2.303*ELP*3.0E7*DT/EVISC.K)/DT-LPV3.K/DT
A MCL3.K=BMCL*ACLS3.K
A ACLS3.K=S03.K/SA.K
N S03=1 CL.CM

```

TABLE 2A.6 (Cont)

```

N NEC1=0
L CL1.K=PCL1.J-LPV1.J
N CL1=0
L LPV1.K=LPV1.J+DT*(LPVCR1.JK)
N LPV1=60
R LPVCR1.KL=LPV1.K*EXP(-2.303*ELP*3.0E7*DT/EVISC.K)/DT-LPV1.K/DT
A PCL1.K=BMCL+ACLS1.K
A ACLS1.K=S01.K/SA.K
N S01=1 CU.CM.
L S01.K=SC1.J+DT*FIFGE(0,ORSCU1.JK,ACLS1.JK,1.0E4)
A SC0IA1.K=2.0*EXP(LNVFU1.K)
A LNVFU1.K=0.33*LCGN(S01.K)-0.46
R ORSCU2.KL=1.0E7*MAX(NEC2.K,-NEC2.K)
A NEC2.K=TE.K-CL2.K
N NEC2=0
L CL2.K=PCL2.J-LPV2.J
N CL2=0
L LPV2.K=LPV2.J+DT*(LPVCR2.JK)
N LPV2=60
R LPVCR2.KL=LPV2.K*EXP(-2.303*ELP*3.0E7*DT/EVISC.K)/DT-LPV2.K/DT
A PCL2.K=BMCL+ACLS2.K
A ACLS2.K=S02.K/SA.K
N S02=1 CU.CM.
L S02.K=SC2.J+DT*FIFGE(0,ORSCU2.JK,ACLS2.JK,1.0E4)
A SC0IA2.K=2.0*EXP(LNVFU2.K)
A LNVFU2.K=0.33*LCGN(S02.K)-0.46
R ORSCU3.KL=1.0E6*MAX(NEC3.K,-NEC3.K)
A NEC3.K=TE.K-CL3.K
N NEC3=0
L CL3.K=PCL3.J-LPV3.J
N CL3=0
L LPV3.K=LPV3.J+DT*(LPVCR3.JK)
N LPV3=60
R LPVCR3.KL=LPV3.K*EXP(-2.303*ELP*3.0E7*DT/EVISC.K)/DT-LPV3.K/DT
A PCL3.K=BMCL+ACLS3.K
A ACLS3.K=S03.K/SA.K
N S03=1 CU.CM.
L S03.K=SC3.J+DT*FIFGE(0,ORSCU3.JK,ACLS3.JK,1.0E4)
A SC0IA3.K=2.0*EXP(LNVFU3.K)
A LNVFU3.K=0.33*LCGN(S03.K)-0.46
R ORSCU4.KL=1.0E5*MAX(NEC4.K,-NEC4.K)
A NEC4.K=TE.K-CL4.K
N NEC4=0
L CL4.K=PCL4.J-LPV4.J
N CL4=0
L LPV4.K=LPV4.J+DT*(LPVCR4.JK)
N LPV4=60
R LPVCR4.KL=LPV4.K*EXP(-2.303*ELP*3.0E7*DT/EVISC.K)/DT-LPV4.K/DT
A PCL4.K=BMCL+ACLS4.K
A ACLS4.K=S04.K/SA.K
N S04=1 CU.CM.
L S04.K=SC4.J+DT*(ORSCU4.JK)
A SC0IA4.K=2.0*EXP(LNVFU4.K)
A LNVFU4.K=0.33*LCGN(S04.K)-0.46
R ORSCU5.KL=1.0E4*MAX(NEC5.K,-NEC5.K)
A NEC5.K=TE.K-CL5.K
N NEC5=0
L CL5.K=PCL5.J-LPV5.J
N CL5=0
L LPV5.K=LPV5.J+DT*(LPVCR5.JK)
N LPV5=60
R LPVCR5.KL=LPV5.K*EXP(-2.303*ELP*3.0E7*DT/EVISC.K)/DT-LPV5.K/DT
A PCL5.K=BMCL+ACLS5.K
A ACLS5.K=S05.K/SA.K
N S05=1 CU.CM.
L S05.K=SC5.J+DT*(ORSCU5.JK)
A SC0IA5.K=2.0*EXP(LNVFU5.K)
A LNVFU5.K=0.33*LCGN(S05.K)-0.46
NOTE
PRINT ACLS1,ACLS2,ACLS3,ACLS4,ACLS5,SC0IA1,SC0IA2,SC0IA3,SC0IA4,SC0IA5,
X MTEMP,CLFFLX
PLOT ACLS1=1,ACLS2=2,ACLS3=3(0,1.0E4)/ACLS4=4/ACLS5=5/
X MTEMP=M/SURFLX=F
PLOT SC0IA1=6,SC0IA2=7,SC0IA3=8,SC0IA4=9,SC0IA5=0(0,2.0E4)/
X MTEMP=M/SURFLX=F
SPEC DT=100/LFNGTH=1.0E6/PLTPER=1.0E3/PRTPER=1.0E3
RUN VARYING THE ORSCUA CONSTANT
SEC -
4P

```

1625 OF 2472 DATA LIST WORDS  
163 OF 200 SYMBOL TABLE VARIABLES

TABLE 2A.7

## Equation Listing for Plots in Figure 2A.13

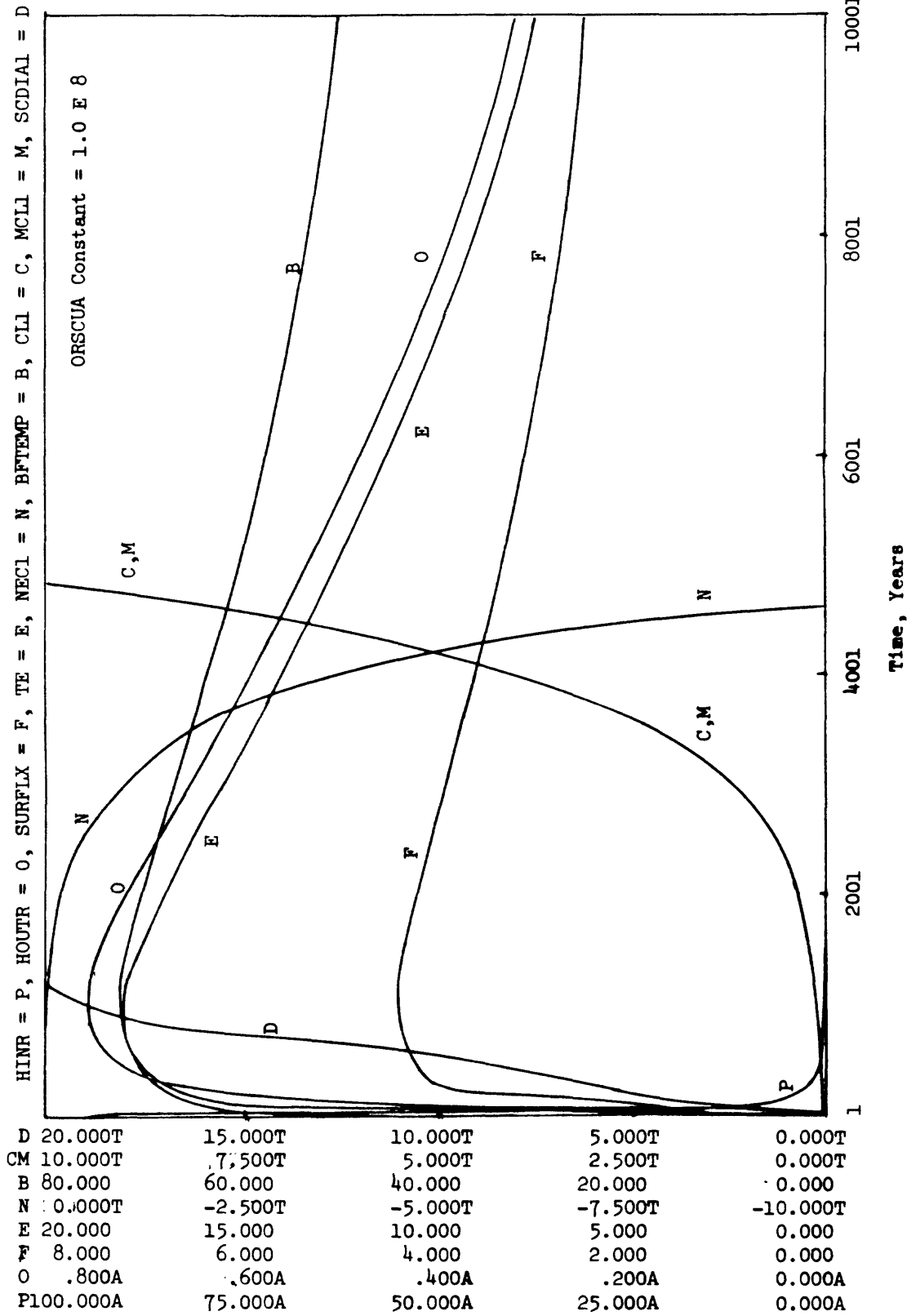
DYNAMO IIF, VERSION 3.02

```

*      HMCL=20, SO MIN AND ORSCUA=1.019...
N      TIME=1. YEAR
L      H.K=H.C+DT*(HINR.JK-HOUT.JK) HEAT ABOVE ZPD TEMP CAL/GM
N      H=5.2 CAL/GM INITIAL HEAT MTEMP=260
R      HINR.KL=C.047*FC.K 11 POWER CAL/GM/YR 1/2 ORIGINAL
N      HINR=C
A      FD.K=EXP(2.303*LOGFD.K) PM DECAY FRACTION
N      FC=1.0
A      LOGFD.K=TABLE(FC*TA3,LOGT.<.0,5,0.5) LOGTEN DECAY FRACTION
N      LOGFD=C
T      FDTAB=C/-0.03/-0.11/-0.33/-1.00/-1.93/-2.17/-2.51/-2.93/-3.23/
X      -3.94/-4.0/-4.0 LOGTEN DECAY FRACTION TABLE REVISED 6/20/77
A      LOGT.K=LOGN(TIME.K)/2.303 LOGTEN TIME (YEARS)
N      LOGT=C
R      SHLR.KL=25.0*(1.K-1.)/1.32E5-2.273E-4 STEADY HEAT LOSS RATE CAL/GM/YR
N      SHLR=C
R      HOUTP.KL=DELAY3(SHLR.JK,DSHF) HEAT LOSS RATE CAL/GM/YR
N      HOUTP=C
C      DSHF=1000 YRS DELAY SURFACE HEAT FLUX
A      MTEMP.K=(H.K-4.C)/3.2*20. MEAN TEMP FOR STEMP=200
N      MTEMP=20
S      SURFLX.K=1.0*1.32E5*(HOUTP.JK/30) SURFACE FLUX MICROCAL/CM/SEC
N      SURFLX=1.0
L      TE.K=TE.J+DT*(TER.JK) LINEAR THERMAL EXPANSION (CM)
N      TE=C INITIAL THERMAL REFERENCE STATE
R      TER.KL=CFC*(HINR.JK-HOUTP.JK)/0.2 LINEAR TE RATE (CM/YR)
N      TER=C.423
C      CEC=C.9 CM/DEGC UNIT EXPANSION CONSTANT
S      DTEMP.K=DT*(HINR.JK-HOUTP.JK)/0.2 DELTA TEMP JK DEGC
N      DTEMP=C
A      JFTEMP.K=32+2*(MTEMP.K-26) APPROX BACKFILL TEMP DEGC
N      JFTEMP=32
C      HMCL=20
A      SA.K=RA SOLUTIONING AREA (SQ.CM)
C      PA=7.9E10 REPOSITORY AREA (SQ.CM)
C      ELP=1.3E3 DYNE/SQCM EFFECTIVE LOAD PRESSURE
A      EVISC.K=TABLE(EVTAB,JFTEMP.K,0.250,25) EFFECTIVE VISC (POISE)
T      EVTAB=1.15E19,7.0E18,4.47E18,2.4E18,1.78E18,1.26E18,
X      8.61E17,6.61E17,5.01E17,3.80E17,3.02E17
R      ORSCU1.KL=1.0E9*MAX(NEC1.K,-NEC1.K)
A      NEC1.K=TE.K-CL1.K
N      NEC1=C
L      CL1.K=PC1.J-LPV1.J
N      CL1=C
L      LPV1.K=LPV1.J+DT*(LPVCR1.JK)
N      LPV1=20
R      LPVCR1.KL=LPV1.K*EXP(-2.303*ELP*3.0E7*DT/EVISC.K)/DT-LPV1.K/DT
A      PC1.K=B*CL+ACLS1.K
A      ACLS1.K=SO1.K/SA.K
N      SO1=1 CC.CM.
L      SO1.K=SO1.J+DT*FIFGE(0,ORSCU1.JK,ACLS1.JK,1.0E4)
A      SC01A1.K=2.0*EXP(LNMFU1.K)
A      LNMFU1.K=C.33*LOGN(SO1.K)-0.46
NOTE
PRINT HINR,HOUTP,SURFLX,TE,NEC1,JFTEMP,CL1,MCL1,SC01A1,SO1,ORSCU1,ACLS1
PLOT HINR=P/HOUTP=C/SURFLX=P/TE=B/NEC1=N/(-1.CE4,DT/JFTEMP=B
X CL1=C,MCL1=M(0,1.0E4)/SC01A1=D(0,2.0E4)
SPEC CT=1/LENCT4=1.0E4/PLTPR=100/PRTPER=100
RUN OPSCUA CONSTANT BUT NOTHING ELSE

```

USE C =  
END



Units: See Table  
T = 1.0 E 3, A = 1.0 E-3

Figure 2A.10. Simple Heat, Thermal Expansion, Compaction and Solution Sectors

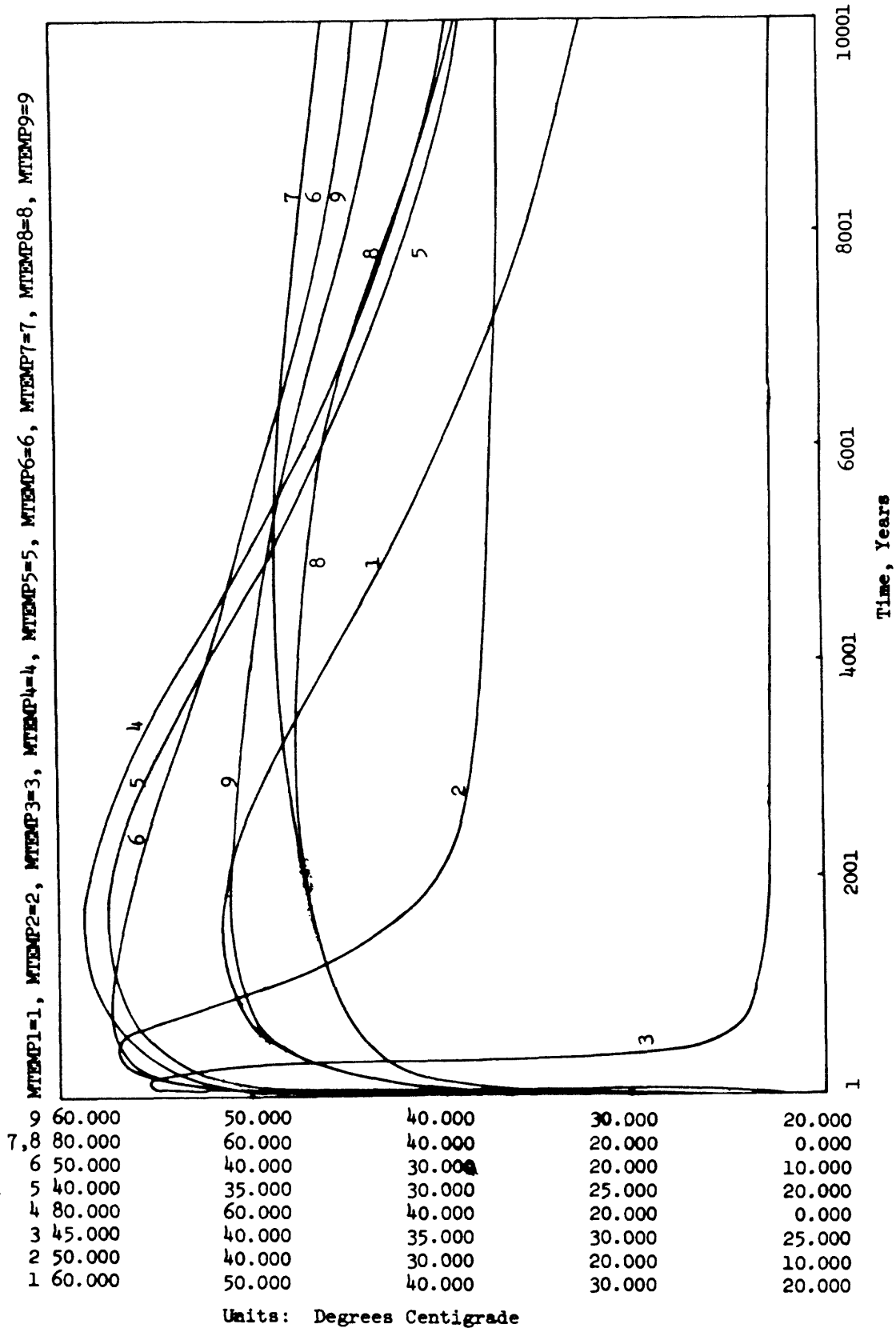


Figure 2A.11a. Examples of Heat and Compaction Sectors

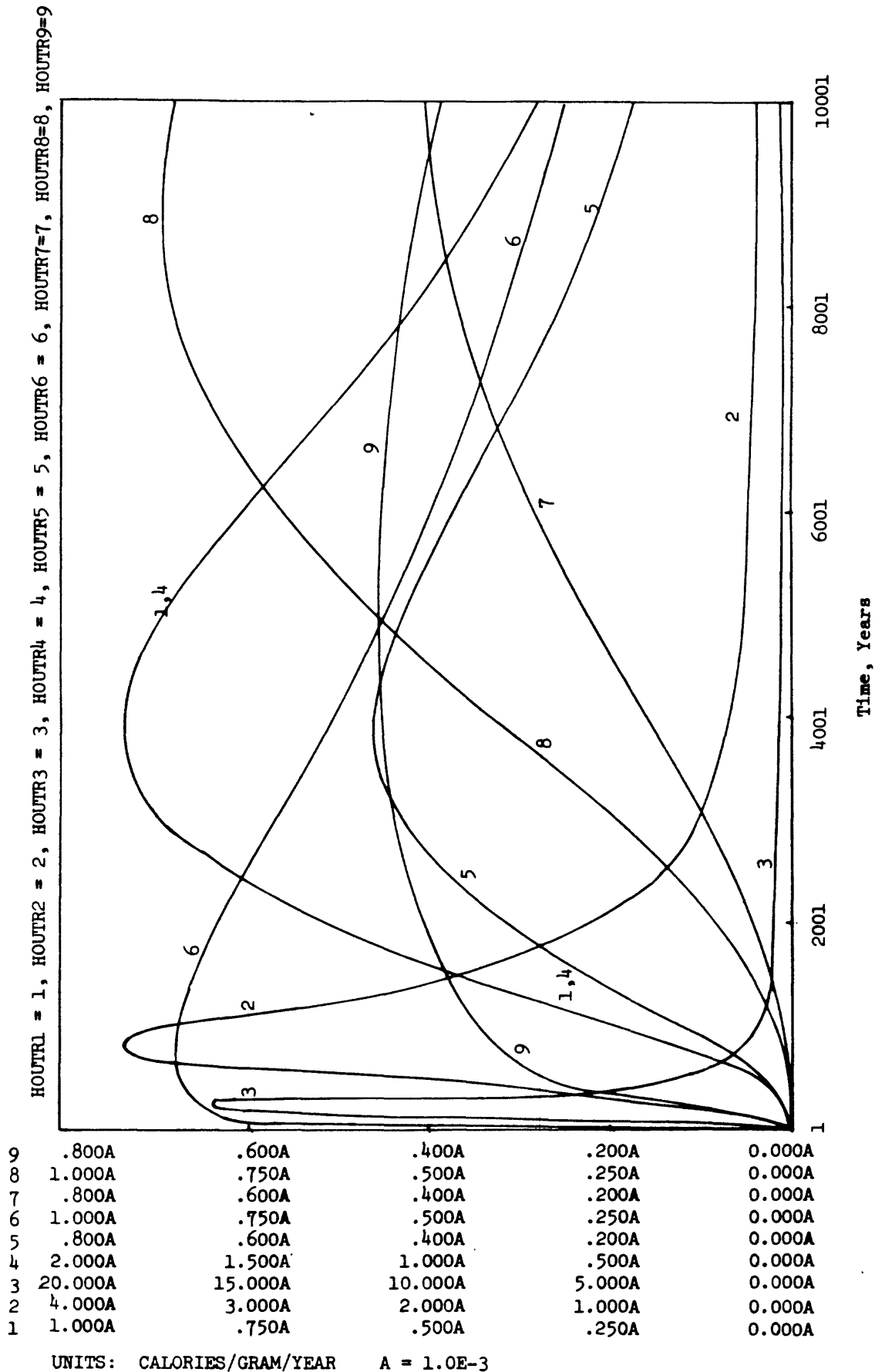


Figure 2A.11b. Examples of Heat and Compaction Sectors

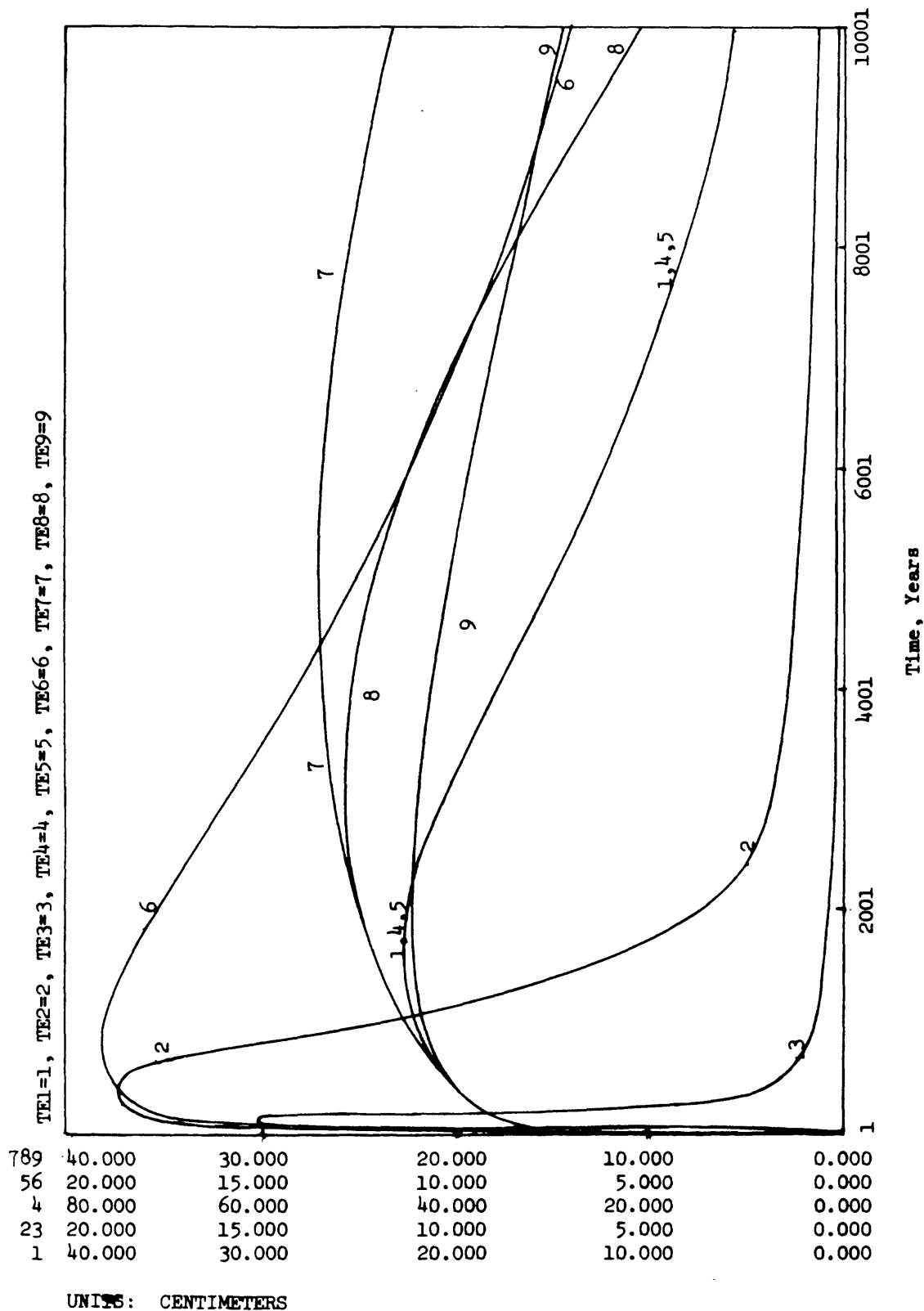


Figure 2A.11c. Examples of Heat and Compaction Sectors

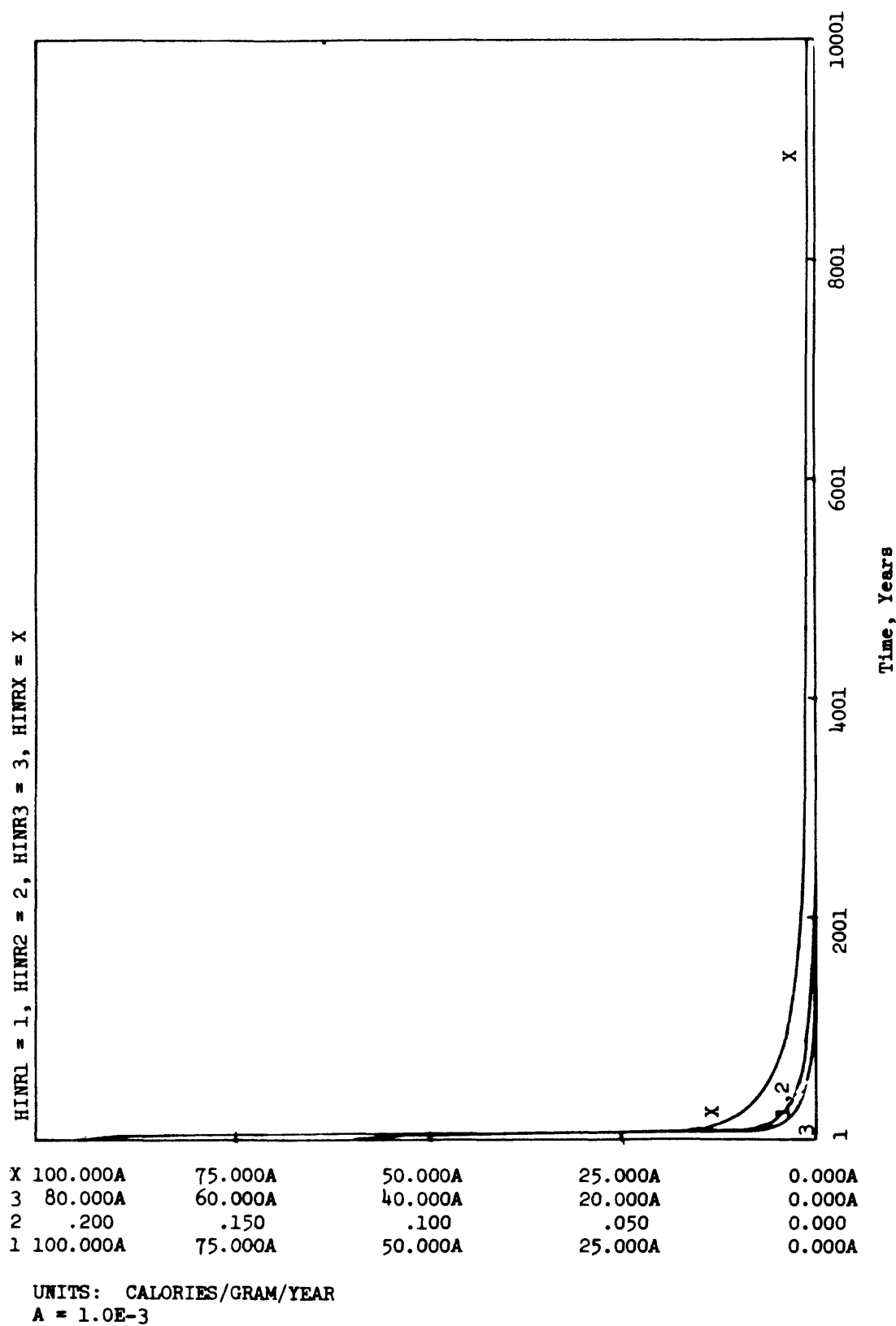


Figure 2A.11d. Examples of Heat and Compaction Sectors



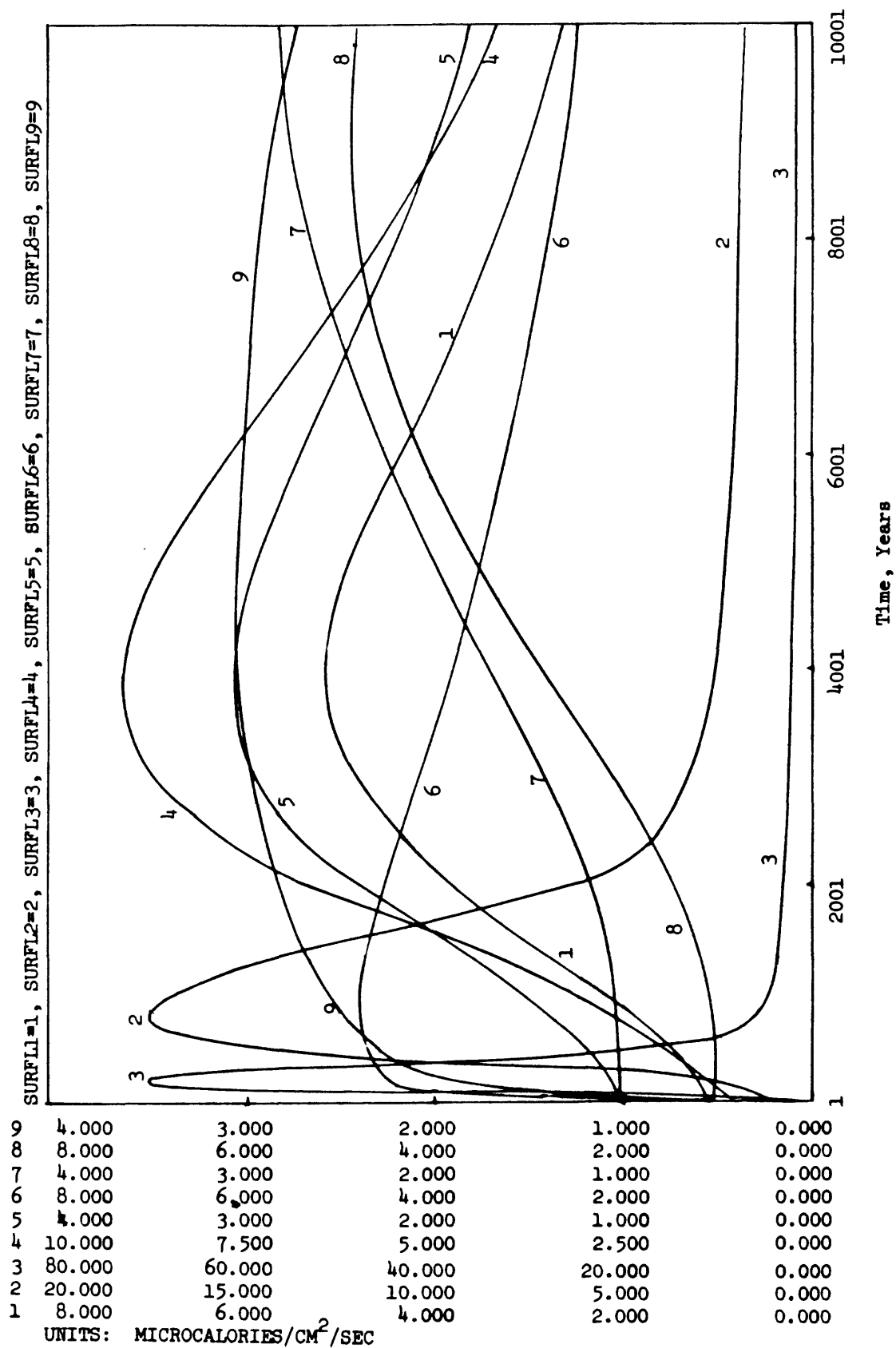


Figure 2A.11e. Examples of Heat and Compaction Sectors

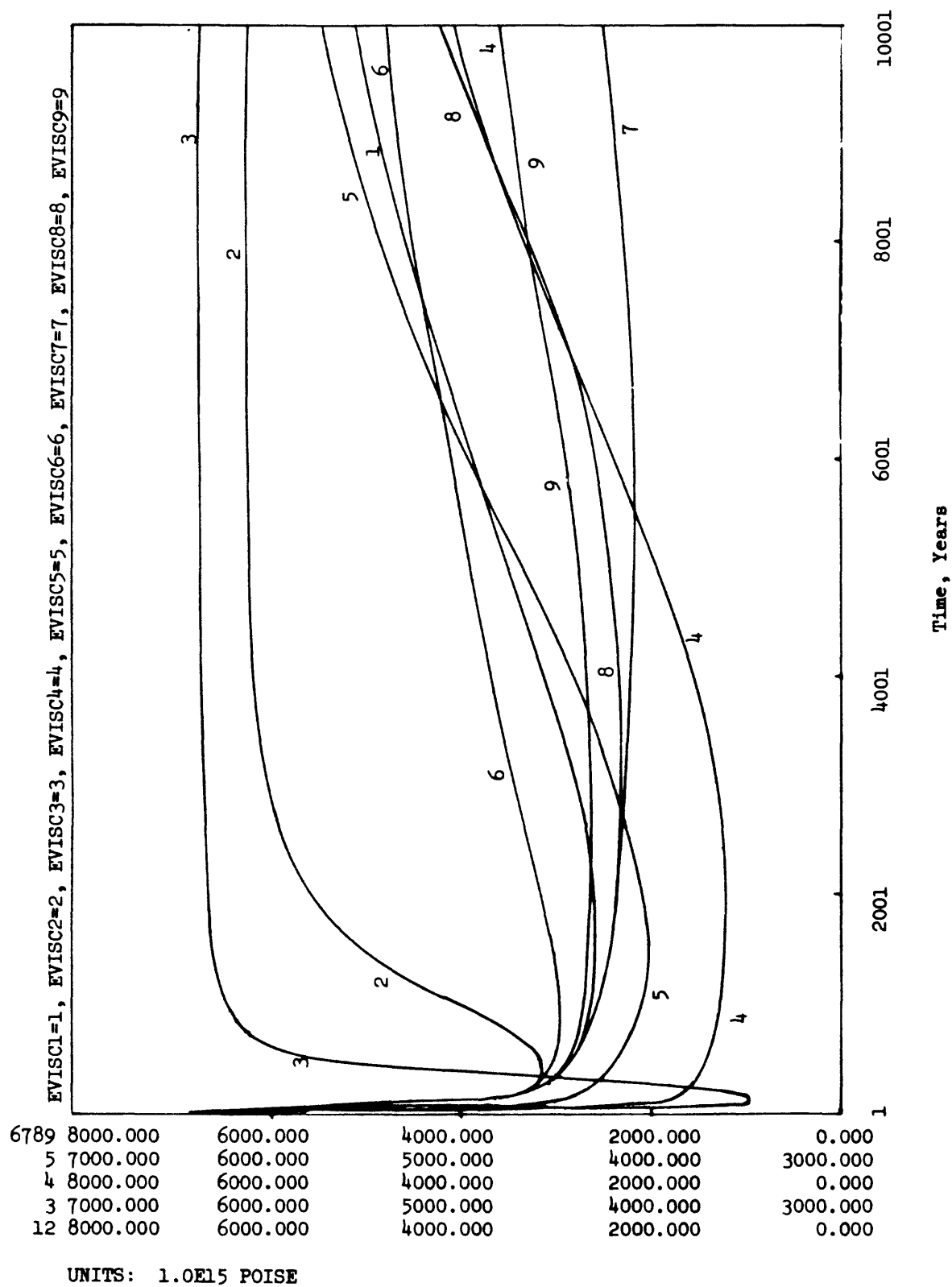


Figure 2A.11f. Examples of Heat and Compaction Sectors

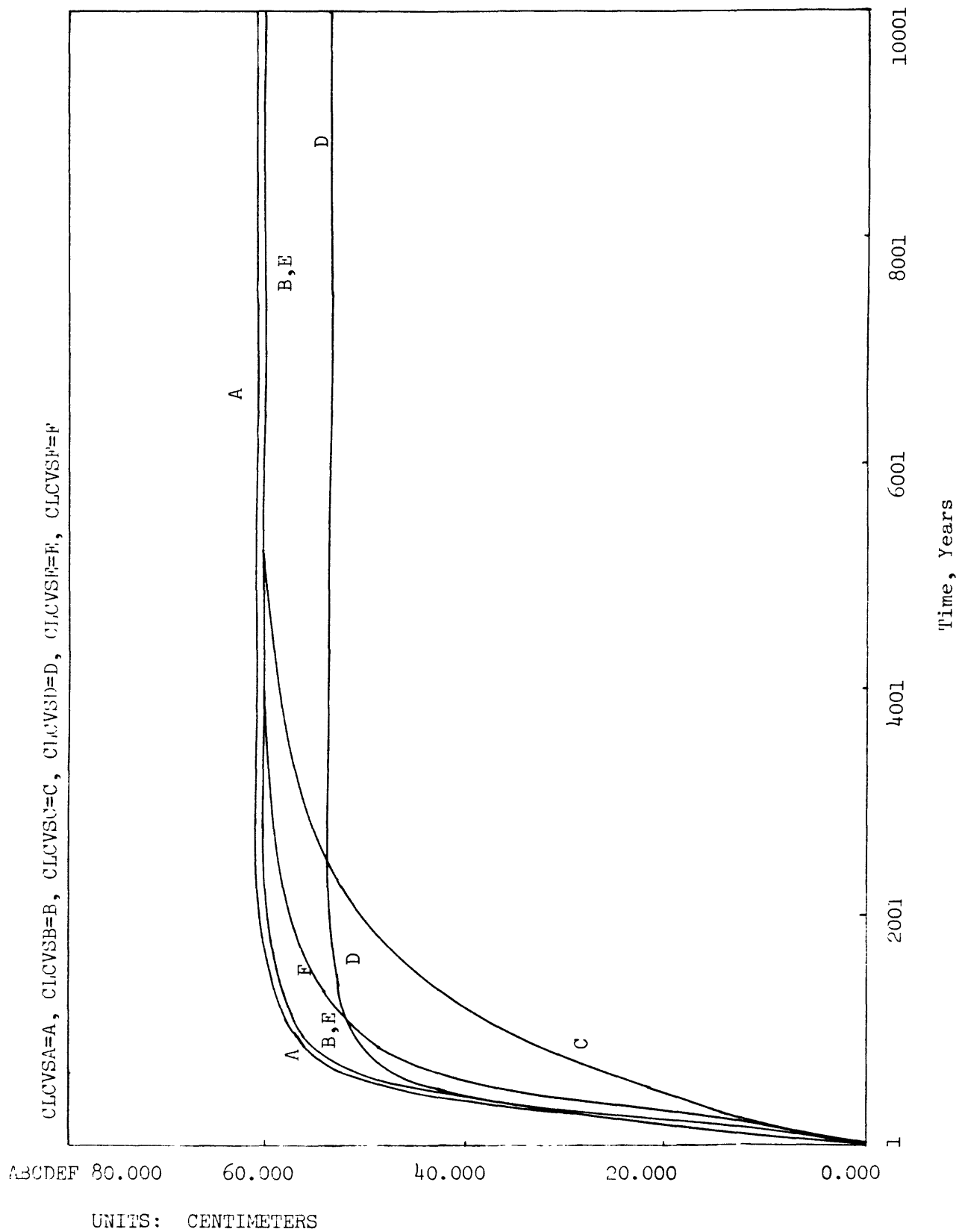


Figure 2A.11g. Examples of Heat and Compaction Sectors

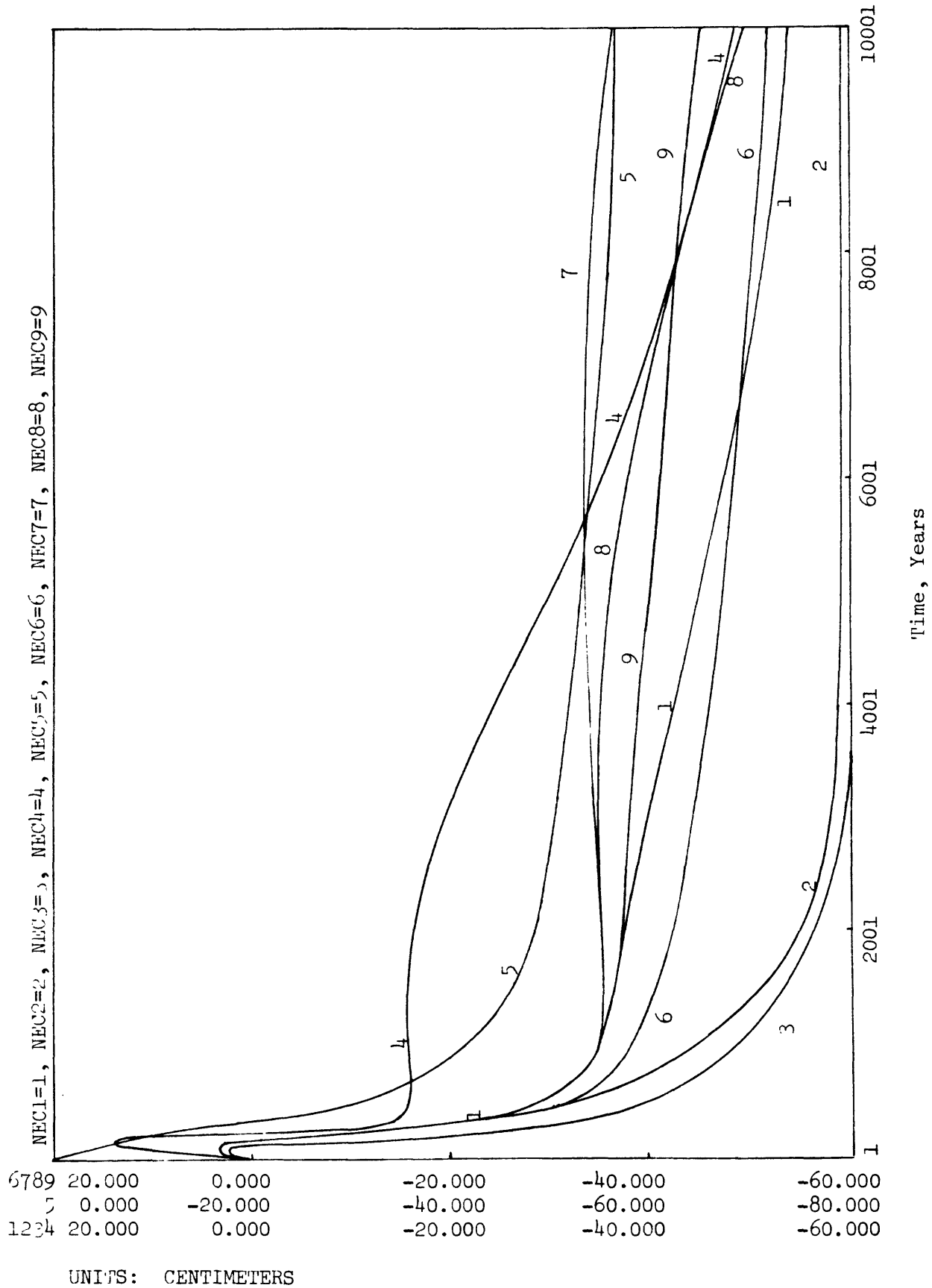


Figure 2A.11h. Examples of Heat and Compaction Sectors

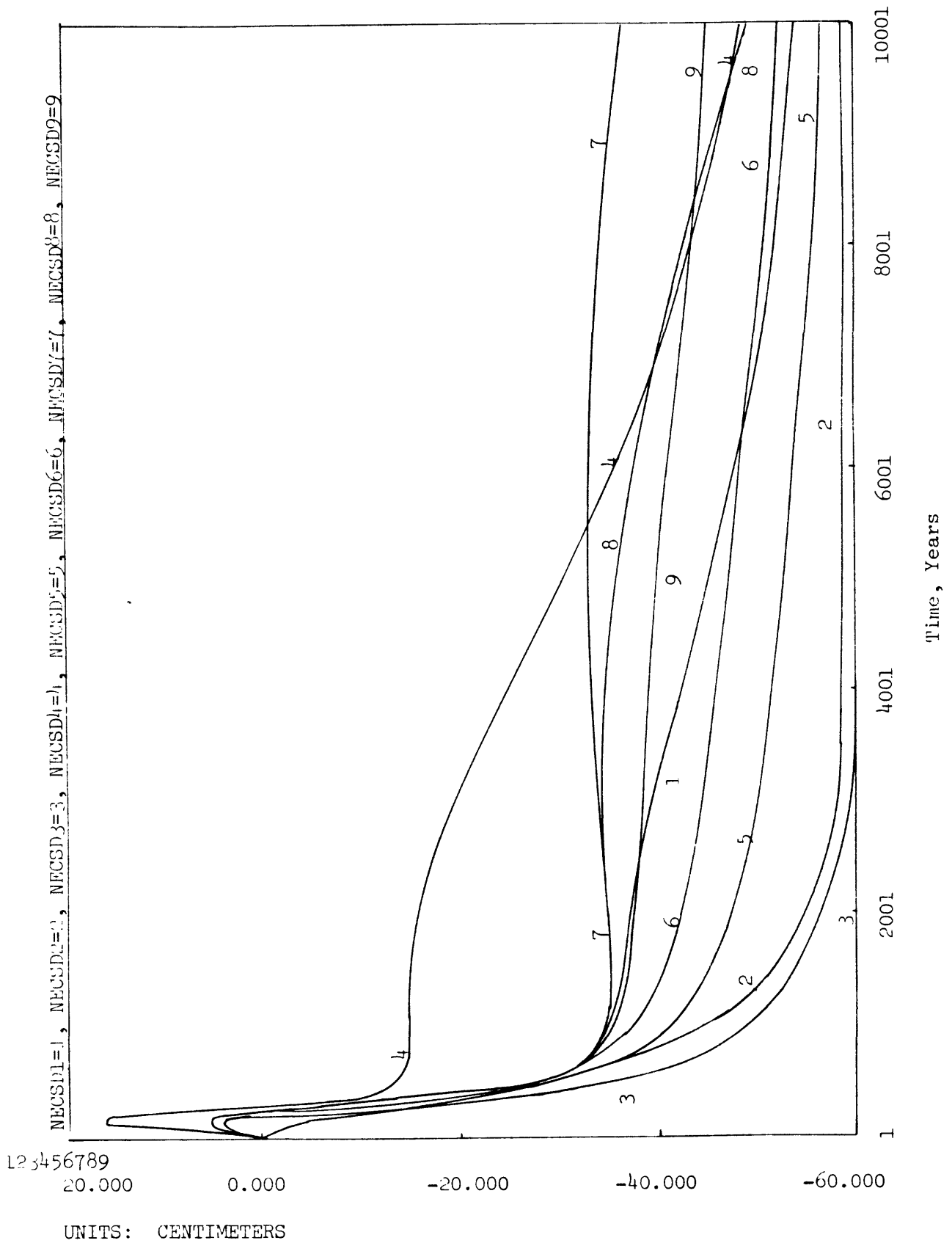


Figure 2A.11i. Solutioning by Diffusion

123456789  
4.000T

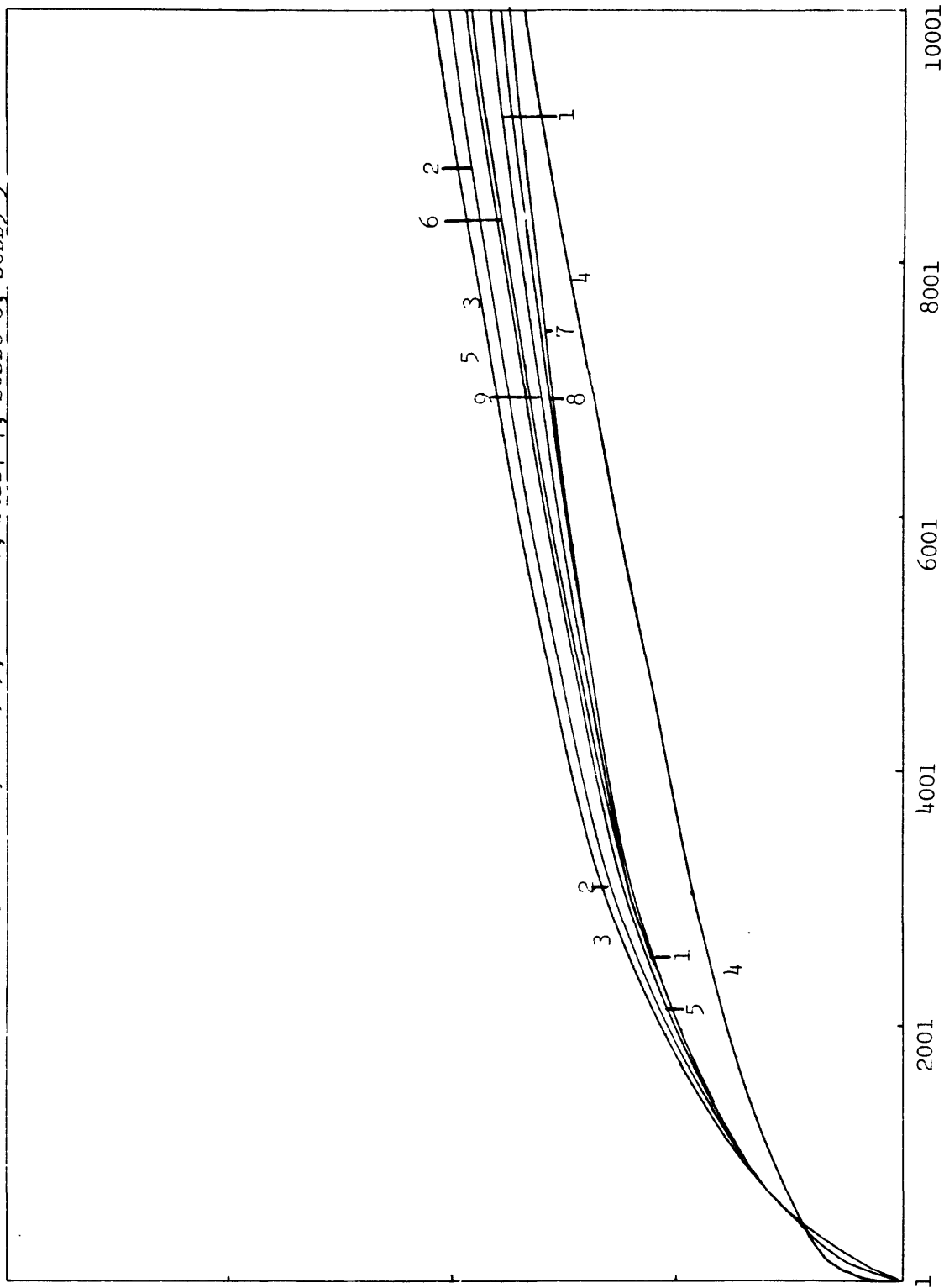
3.000T

2.000T

1.000T

0.000T

SCDD1=1, SCDD2=2, SCDD3=3, SCDD4=4, SCDD5=5, SCDD6=6, SCDD7=7, SCDD8=8, SCDD9=9



Time, Years

Figure 2A.11j. Solutioning by Diffusion

UNITS: CENTIMETERS  
T = 1.0E3

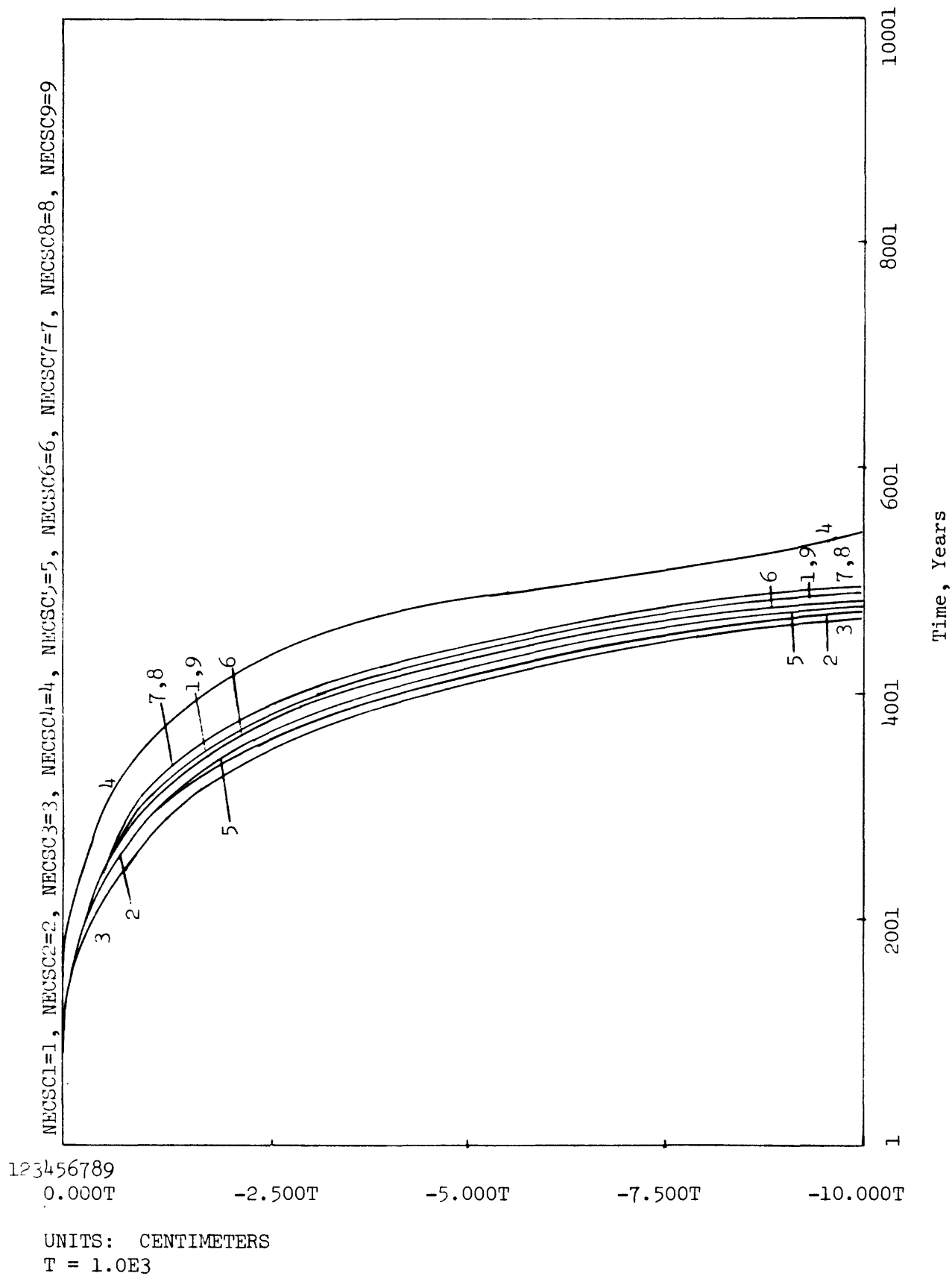


Figure 2A.11k. Solutioning by Convection

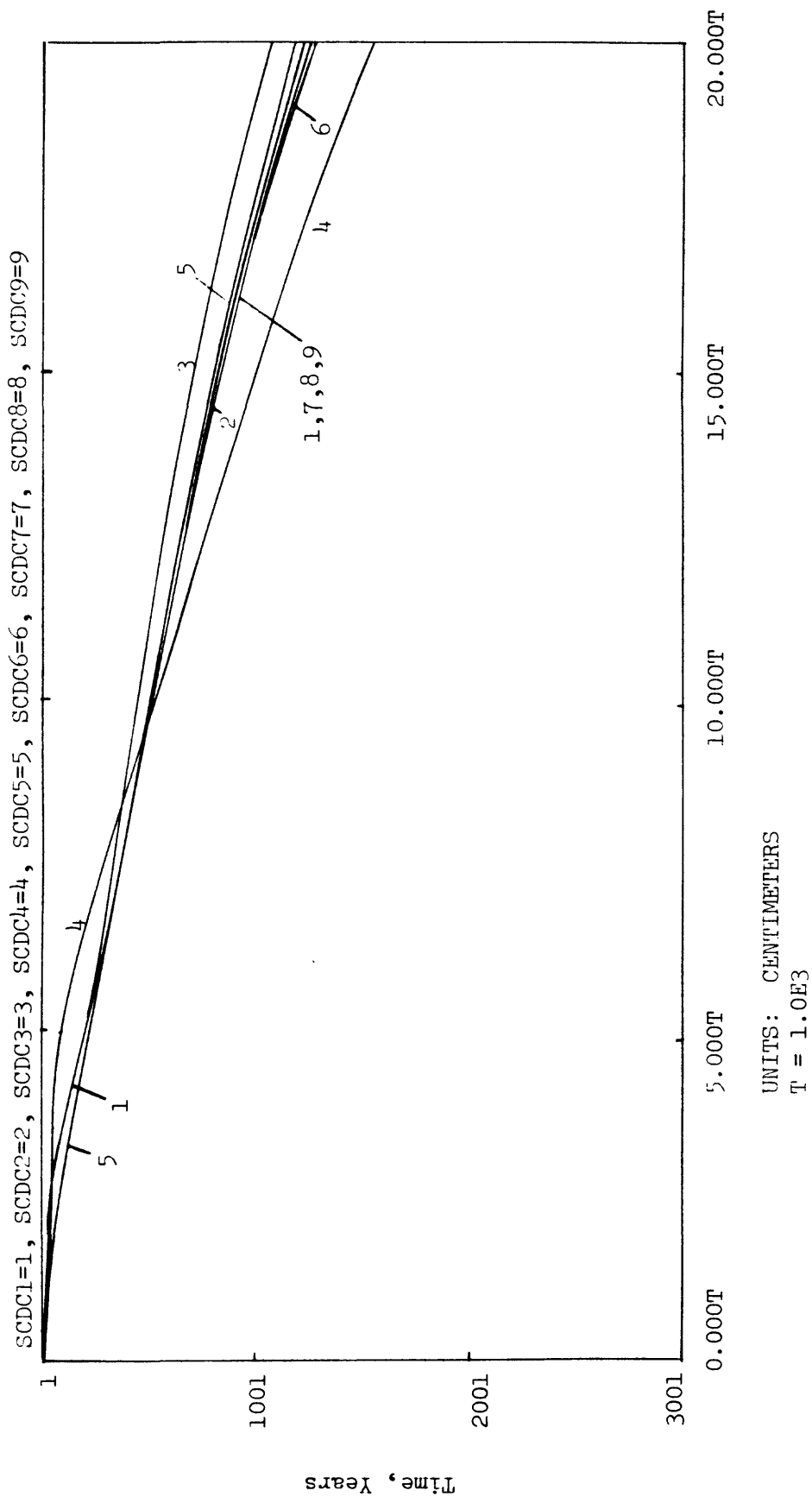


Figure 2A.11ℓ. Solutioning by Convection



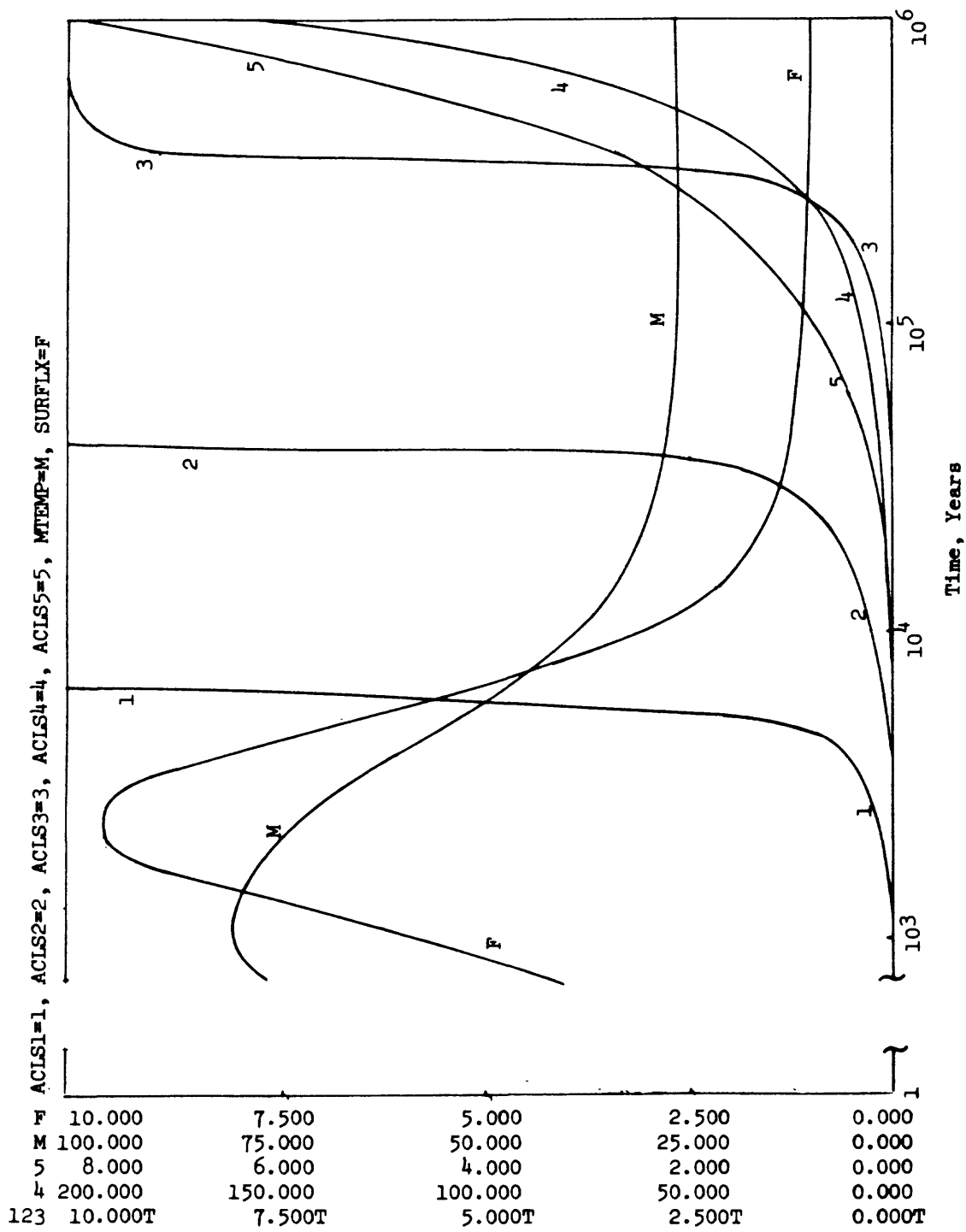


Figure 2A.12a. Varying the ORSCUA Constant

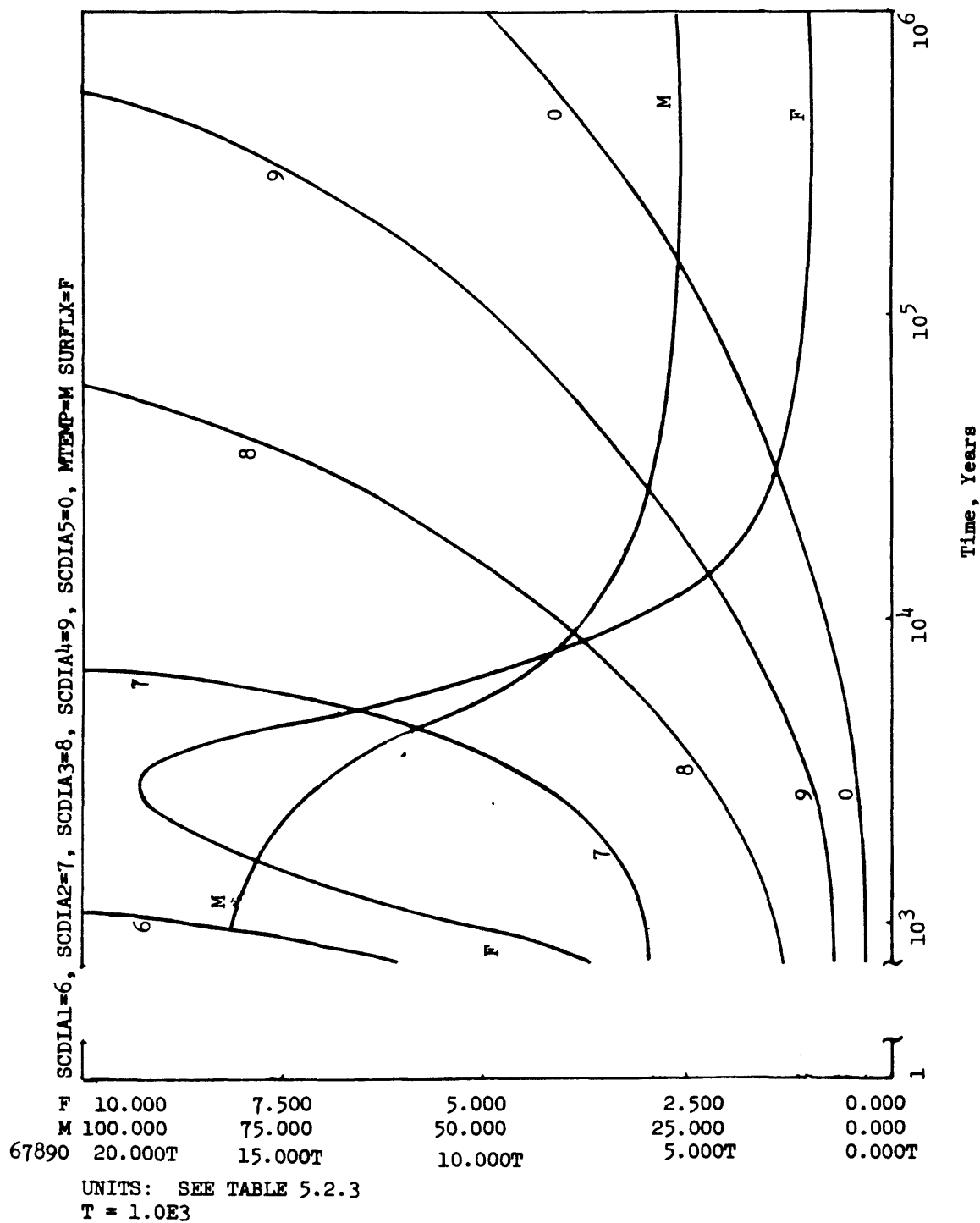


Figure 2A.12b. Varying the ORSCUA Constant

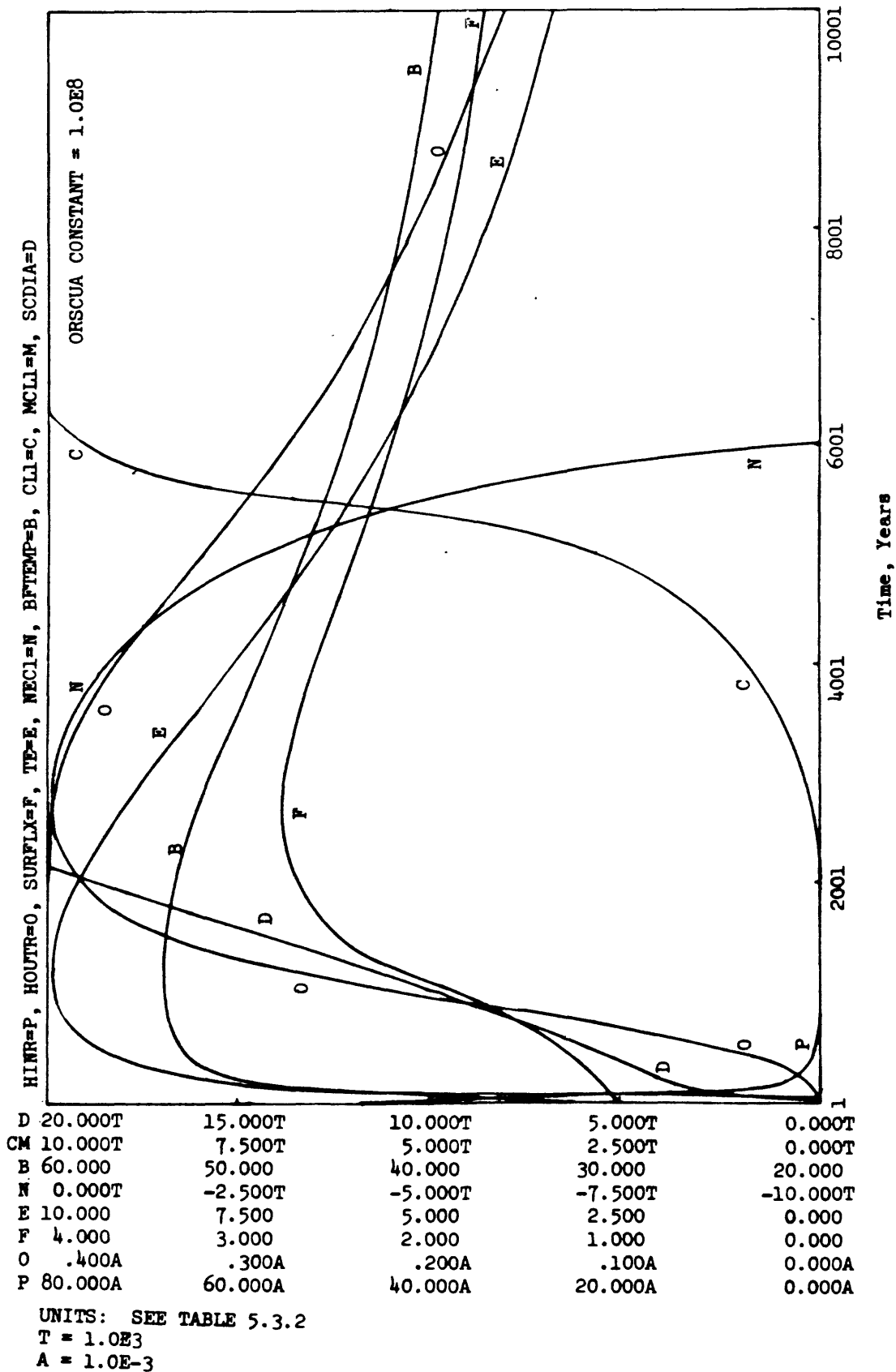


Figure 2A.13. Solutioning Feedback with Half of Original Thermal Load

References  
Appendix 2A

- 2A.1 R. E. Barlow and H. E. Lambert, 1975, "Introduction to Fault Tree Analysis: in Reliability and Fault Tree Analysis; Theoretical and Applied Aspects of System Reliability and Safety Assessment," SIAM, Philadelphia, PA, p. 7-35.
- 2A.2 R. L. Bradshaw and W. C. McClain (eds.), 1971, Project Salt Vault: A Demonstration of the Disposal of High-Activity Solidified Wastes in Underground Salt Mines, ORNL-4555, 360 p.
- 2A.3 D. G. Brookins, 1976, "Shale as a Repository for Radioactive Waste: The Evidence from Oklo," Environmental Geology, Vol. 1, pp. 255-259.
- 2A.4 J. W. Forrester, 1961, Industrial Dynamics, Cambridge, Mass., M.I.T. Press, 464 p.
- 2A.5 J. W. Forrester, 1971, World Dynamics, Cambridge, Mass., Wright-Allen Press.
- 2A.6 I. J. Gruntfest, 1963, "Thermal Feedback in Liquid Flow; Plane Shear at Constant Stress," Trans. Soc. Rheology, Vol. 7, pp. 195-207.
- 2A.7 I. J. Gruntfest, 1968, The Role of Energy in Deformation, NASA Contractors Report CR-1039.
- 2A.8 H. C. Heard, 1976, "Comparison of the Flow Properties of Rocks at Crustal Conditions," Phil. Trans. Royl. Soc. Lond., A., Vol. 283, pp. 173-186.
- 2A.9 D. L. Meadows and D. H. Meadows, 1973, Toward Global Equilibrium: Collected Papers, Cambridge, Mass., Wright-Allen Press, 358 p.
- 2A.10 A. A. B. Pritsker, 1974, The GASP IV Simulation Language, New York, Wiley and Sons, 451 p.
- 2A.11 A. L. Pugh III, 1973, DYNAMO II User's Manual, 4th Edition Including DYNAMO II<sub>F</sub>, Cambridge, Mass., M.I.T. Press, 92 p.
- 2A.12 H. R. Shaw, 1969, "Rheology of Basalt in the Melting Range," Jour. Petrology, Vol. 10, pp. 510-535.
- 2A.13 H. R. Shaw, 1965, "Comments on Viscosity, Crustal Settling and Convection in Granitic Magma," Amer. Jour. Sci., Vol. 263, pp. 120-152.
- 2A.14 H. R. Shaw and D. A. Swanson, 1970, "Eruption and Flow Rates of Flood Basalts; in E. H. Gilmour and D. Stradling (eds.) Proceedings of the Second Columbia River Basalt Symposium, Eastern Wash. State College Press, Cheney, WA, pp. 271-299.
- 2A.15 H. P. Taylor, J. R., 1975, "Stable Isotope Geochemistry," Revs. Geophys. and Space Phys., Vol. 13, pp. 102-107; pp. 159-163.

# Table AR.3.2

## ANNOTATED LIST OF EQUATIONS FOR DISSW/WOCC

L	H.K=H.J+DT*(HINR.JK-HOUTR.JK)	HEAT ABOVE 0 TEMPERATURE (CAL/GM)	THIS LEVEL EVALUATES THE HEAT CONTENT OF THE SYSTEM RELATIVE TO A VALUE AT ZERO TEMPERATURE, TAKEN TO BE ZERO BY CONVENTION.
N	H=5.2	INITIAL HEAT; MTMP=26°C (CAL/GM)	THE INITIAL HEAT CONTENT AT A MEAN TEMPERATURE OF 26°C. THE MEAN TEMPERATURE IS AVERAGED OVER THE TOTAL CONTROL VOLUME OF THE DEPOSITORY.
R	HINR.KL=DCP*FD.K	RADIONUCLIDE POWER (CAL/GM/YR)	THE RATE HEAT IS GENERATED BY THE RADIOACTIVE WASTE INVENTORY.
N	HINR=0	HEATING RATE AT START	
C	DCP=0.094	DIMENSIONAL COEFFICIENT FOR THERMAL POWER (CAL/GM/YR)	THIS COEFFICIENT GIVES AN INITIAL HEATING RATE EQUIVALENT TO 60kw/acre AND IS THE VALUE USED IN THE INTERIM REPORT( Risk Methodology for Geologic Disposal of Radioactive Waste: Interim Report, Campbell and others, October 1978); VALUES AS HIGH AS 150kw/acre HAVE APPEARED IN DESIGN REPORTS.
A	FD.K=EXP(2.303*LOGFD.K)	RADIONUCLIDE DECAY FRACTION	THE DECAY FRACTION REPRESENTS THE FRACTION OF THE ORIGINAL RADIOACTIVE INVENTORY THAT REMAINS ACTIVE AS A HEAT SOURCE AT A GIVEN VALUE OF TIME.
N	FD=1.	INITIAL RADIONUCLIDE DECAY FRACTION	THIS IS THE INITIAL DECAY FRACTION; PRESUMABLY, SMALLER FRACTIONS COULD BE ASSIGNED FOR PRE-AGED WASTE INVENTORIES(See Interim Report, 1978).
A	LOGFD.K=TABLE(FDTAB,LOGT.K,0,8,0.5)	LOGTEN DECAY FRACTION	SAMPLE OF TABLE VALUES AT INTERVALS OF 0.5 LOG UNITS OVER 8 DECADES; i.e. TO 100 MILLION YEARS.
N	LOGFD=0	INITIAL VALUE OF LOGFD	TO BE CONSISTENT WITH N FD=1.
T	FDTAB=0/-0.03/-0.11/-0.38/-1.00/-1.80/-2.17/-2.51/-2.80/-3.28/-3.84/-4.0/-4.0/-4.0/-4.0/-4.0/-4.0	TABLE VALUES OF LOGFD	TABLE VALUES ARE BASED ON THE TOTAL RADIONUCLIDE INVENTORY AS DEFINED IN THE INTERIM REPORT(1978), CHAPTER 1.4.
A	LOGT.K=LOGN(TIME.K)/2.303	LOGTEN TIME (YEARS)	TIME FUNCTION FOR TABLE VALUES OF LOGFD.
N	TIME=1.	TIME (YEARS)	AN INITIAL VALUE OF THE BUILT-IN FUNCTION TIME IS REQUIRED SO THAT IT CAN BE USED AS AN EQUATION VARIABLE IN FUNCTIONS INVOLVING LOG TIME.
N	LOGT=0	INITIAL VALUE OF LOGT	STARTING TIME IS 1 YEAR.
R	HOUTR.KL=DELAY3(SHLR.JK,DSHF)	HEAT LOSS RATE (CAL/GM/YR)	THE HEAT LOSS OVER AND ABOVE THE GEOTHERMAL FLUX. THE THIRD ORDER DELAY HAS BEEN USED TO SIMULATE TIME TO APPROACH AQUAST-STEADY BALANCE WITH HEAT GENERATION RATE. THE DELAY TIME DSHF IS A SORT OF THERMAL "SOAKING" TIME.

C	DSHF=100	DELAY SURFACE HEAT FLUX (YEARS)	THIRD ORDER DELAY CONSTANT. SEE Industrial Dynamics, Forrester, Chapter 9, 1961.
N	HOUTR=0	INITIAL HEAT OUTPUT RATE (CAL/CM/YR)	
R	SHLR.KL=25.*(H.K-4.0)/-2.4E-4	STEADY HEAT LOSS RATE (CAL/CM/YR)	THIS INCLUDES FACTORS FOR THERMAL CONDUCTIVITY, INDUCED TEMPERATURE GRADIENT AND ORIGINAL GEOTHERMAL GRADIENT. THESE FACTORS MUST BE BALANCED IF THE COEFFICIENT 25 IS MODIFIED (See Interim Report).
N	SHLR=0	INITIAL VALUE STEADY HEAT LOSS RATE (CAL/CM/YR)	THE INITIAL VALUE IS ZERO BECAUSE GEOTHERMAL FLUX IS A STEADY STATE.
N	TER.KL=UEC*(HINR.JK-HOUTR.JK)/0.2	LINEAR THERMAL EXPANSION RATE (CM/YR)	THE THERMAL EXPANSION RATE IS BASED ON THE AVERAGE PROPERTIES OF THE REFERENCE DEPOSITORY(See Interim Report, Table 2A.1).
C	UEC=0.9	UNIT EXPANSION CONSTANT (CM/DEG C)	THIS CONSTANT IS EQUIVALENT TO A THERMAL EXPANSION COEFFICIENT OF 1E-5 per °C OVER A DEPTH INTERVAL OF 900 M (DEPTH TO DEPOSITORY LEVEL IS -600 M).
N	TER=0.423	INITIAL VALUE THERMAL EXPANSION RATE (CM/YR)	
L	TE.K=TE.J+DT*(TER.JK)	LINEAR THERMAL EXPANSION (CM)	THE CUMULATIVE EXPANSION IS BASED ON THE CHOICE OF THE THERMAL EXPANSION COEFFICIENT, UEC.
N	TE=0	INITIAL THERMAL EXPANSION STATE (CM)	THE INITIAL VALUE OF ZERO ASSUMES A CONSTANT HEAT BALANCE ACROSS THE REFERENCE VOLUME.
L	CL.K=MCL.J-LPV.J	COMPACTION LENGTH (CM)	THIS IS THE ACTUAL OBSERVED VERTICAL SUBSIDENCE OR COMPACTION AT A GIVEN TIME.
N	CL=1.	INITIAL VALUE CL (CM)	
A	LPV.K=BMCL+PVPS.K-PVDC.K	LINEAR PORE VOLUME (CM)	THIS IS THE UNCOLLAPSED PORE VOLUME AT A GIVEN TIME.
C	BMCL=60.	BACKFILL MAXIMUM COMPACTION LENGTH (CM)	THIS IS EQUIVALENT TO 6 METERS OF BACKFILL HORIZON WITH 10 % POROSITY; THE POSSIBLE RANGE IS FROM 0-30 %.
L	PVPS.K=PVPS.J+DT*(BDRUA.JK)/DA	(LINEAR) PORE VOLUME PRODUCED BY SOLUTIONING (CM)	THE PORE SPACE CALCULATED FROM DISSOLUTIONING FEED-BACK THAT IS AVERAGED OVER THE DEPOSITORY VOLUME.
N	PVPS=0	INITIAL (LINEAR) PORE VOLUME PRODUCED BY SOLUTIONING (CU CM)	THIS ASSUMES THERE ARE NO CAVITIES ALREADY EXISTING IN THE DEPOSITORY.
R	BDRUA.KL=FIFGE(MBFA,ACDR.K,ACDR.K,MBFA)	BRINE DISCHARGE RATE TO UPPER AQUIFER (CU CM/YR)	THIS EQUATION GIVES THE RATE THAT VARIES AS ACDR UNTIL THE MAXIMUM IS REACHED; THEN IT IS CONSTANT AT MBFA.
C	MBFA=3E12	MAXIMUM BRINE FLOW IN AQUIFER (CU CM /YR)	THIS IS BASED ON A MAXIMUM OF 4 % OF THE AQUIFER CAPACITY FOR THE REFERENCE DEPOSITORY ( See Interim Report).

A	ACDR.K=RCVR.K*NC.K	(TOTAL) APPARENT CRACK DISCHARGE RATE (CU CM /YR)	THIS IS THE FLOW RATE THROUGH THE CRACK CONDUITS FOR A CONSTANT HEAD. THE ACTUAL RATES ARE LIMITED BY THE BRINE CONCENTRATION IN THE AQUIFER, GIVEN BY MBFA.
A	RCVR.K=(3E7*BFPH*RCW*RCW*CTL)/(12.*BV*CPL)	REFERENCE CRACK VOLUME RATE (CU CM /YR)	THIS IS BASED ON THE EQUATION OF FLOW IN TABULAR SLOTS; THE CONSTANTS BPH, RCW, CTL AND CPL COULD BE MADE VARIABLE TO SIMULATE CHANGING CRACK DIMENSIONS. AS STATED THE SIMULATION VARIES THE NUMBER OF "CONSTANT" CRACKS.
C	BPH=2E6	BRINE PRESSURE HEAD (DYNE/SQ CM)	THIS IS BASED ON THE U-TUBE PATH, AND THE HEAD DIFFERENCE DISCUSSED IN THE INTERIM REPORT( Appendix 2A, p. 123).
A	ACDR.K=DCBPH.K*NBPH*NC.K/(1.+DCBPHA.K*DCBPHB.K*NC.K)	APPARENT CRACK DISCHARGE RATE (CU CM/YR)	ACDR ADJUSTED FOR DECAY OF BRINE PRESSURE HEAD.
A	DCBPHA.K=(3E7*RCW*RCW*RCW*CTL)/(12.*BV*CPL)	DIMENSIONAL CONSTANT FOR BRINE PRESSURE HEAD (SQ CM/DYNE)*(CU CM/YR)	DIMENSIONAL COEFFICIENTS THAT NORMALIZE THE APPARENT CRACK DISCHARGE RATE TO VALUES THAT RANGE BETWEEN ACDR.K*NC.K AT SMALL VALUES OF NC.K TO THE LIMIT MBFA AT LARGE VALUES OF NC.K.
A	DCBPHB.K=NBPH/MBFA	BRINE PRESSURE FLOW RATIO (DYNE/SQ CM)/(CU CM /YR)	
C	NBPH=2E6	INITIAL BRINE PRESSURE HEAD (DYNE/SQ CM)	BASED ON A DIFFERENCE IN ELEVATION OF 20 METERS BETWEEN THE UPPER AND LOWER ENDS OF THE U-TUBE AND CONSTANT DENSITY IN THE FLOW PATH.
C	RCW=1E-3	REFERENCE CRACK WIDTH (CM)	THIS IS THE VALUE USED IN THE INTERIM REPORT.
C	CTL=6E5	CRACK TRACE LENGTH (CM)	THIS IS EQUIVELANT TO TWO CRACKS AS LONG AS THE DEPOSITORY DIAMETER, ONE AT THE UPSTREAM EDGE OF THE DEPOSITORY, THE OTHER AT THE DOWNSTREAM EDGE.
C	CPL=1E4	CRACK PATH LENGTH (CM)	THIS LENGTH IS BASED ON DOUBLE THE SINGLE THICKNESS OF THE DEPOSITORY; THIS ASSUMES THERE IS NO RESISTANCE BETWEEN SALT-SHALE INTERFACE. CPL MAY RANGE UP TO 3E5 IF A HORIZONTAL PATH IS INCLUDED.
C	BV=1E-2	BRINE VISCOSITY (POISE)	THE BRINE VISCOSITY IS ASSUMED ROUGHLY TO BE THE SAME AS WATER.
A	NC.K=CC*FIRCE(1E4,AVNEC.K,AVNEC.K,1E4)	NUMBER OF CRACKS; FROM NET VERTICAL DISPLACEMENT	THE NUMBER IS PROPORTIONAL TO AVNEC WITH LIMITS OF 1E4 CRACKS.
C	CC=5.	CRACK COEFFICIENT (PER CM)	THIS IS THE COEFFICIENT USED IN THE INTERIM REPORT. CONCEIVABLY IT VARIES BETWEEN 0 AND 10.
N	NC=1.	INITIAL NUMBER OF CRACKS	IN SOME INSTANCES IT MAY BE DESIRABLE TO ASSUME A PRIOR DISTRIBUTION OF CRACKS.
A	NC.K=DA*PVDC.K/(RCW*CTL*CPL)	NUMBER OF CRACKS; FROM VOLUME OF REFERENCE CRACKS	NOTE: NC.K IS GIVEN IN TWO FORMS; RESULTS WILL BE CHECKED BOTH WAYS.

A	AVNEC.K=MAX(NEC.K,-NEC.K)	ABSOLUTE VALUE OF NEC (CM)	THIS FUNCTION HAS BEEN USED TO ELIMINATE THE SIGN OF VERTICAL DISPLACEMENT.
A	NEC.K=TE.K-CL.K	NET EXPANSION MINUS COMPACTION (CM)	THIS REPRESENTS THE SIMPLE ALGEBRAIC SUMMATION OF THERMAL EXPANSION AND COMPACTION.
N	NEC=-1.	INITIAL NEC (CM)	THIS IS THE PORE VOLUME REMOVED BY VISCOUS COLLAPSE OF CAVITIES.
L	PVDC.K=PVDC.J-DT*(1.PVCR.K)	PORE VOLUME DESTROYED BY COMPACTION (CM)	NO COMPACTION HAS BEEN TAKEN INTO ACCOUNT DURING THE PREPARATION AND BEFORE THE CLOSURE OF THE DEPOSITORY.
N	PVDC=0	INITIAL VALUE OF PVDC (CM)	THE RATE OF VISCOUS COLLAPSE OF VOID SPACE ACCORDING TO AN EMPIRICAL RELATION GIVEN BY SHAW AND SWANSON(1970).
R	LPVCR.KL=LPV.K*EXP(-2.303*ELP*3E7*DT/EVISC.K)/DT-LPV.K/DT	LINEAR PORE VOLUME COMPACTION RATE (CM/YR)	THIS IS BASED ON A MEAN DENSITY OF $2.2\text{gm/cm}^3$ AND A DEPTH OF 600 METERS.
C	ELP=1.3E8	EFFECTIVE LOAD PRESSURE (DYNE/SQ CM)	THE EFFECTIVE VISCOSITY IS TABULATED AT INTERVALS OF $25^\circ\text{C}$ FROM 0 TO $250^\circ\text{C}$ .
A	EVISC.K=TABLE(EVTAB,BFTEMP.K,0,250,25)	EFFECTIVE VISCOSITY (POISE)	THESE DATA ARE BASED ON REFERENCE 2A.8 IN THE INTERIM REPORT, ADJUSTED FOR OBSERVED COMPACTION RATES IN SALT(See Interim Report, Ref. 2A.2).
T	EVTAB=1.15E19,7.08E18,4.47E18,2.81E18,1.78E18,1.26E18,8.91E17,6.61E17,5.01E17,3.80E17,3.02E17	TABLE VALUES OF EVISC (POISE)	THIS TEMPERATURE IS BASED ON ASSUMED LINEAR GRADIENT BETWEEN THE SURFACE AND THE BACKFILL HORIZON (~600 M DEPTH) EQUIVALENT TO MEAN TEMPERATURE.
A	BFTEMP.K=32.+2.*(MTEMP.K-26.)	BACKFILL TEMPERATURE (DEG C)	THE TEMPERATURE EQUIVALENT TO MEAN TEMPERATURE OF $26^\circ\text{C}$ AND BACKFILL HORIZON AT ~600 M DEPTH.
N	BFTEMP=32.	INITIAL VALUE OF BFTEMP (DEG C)	THE MEAN TEMPERATURE IS COMPUTED ON THE BASIS OF THE HEAT CONTENT OF THE REFERENCE VOLUME, THE HEAT CAPACITY AND THE SURFACE TEMPERATURE.
A	MTEMP.K=(H.K-4.0)/0.2+STEMP	MEAN TEMPERATURE FOR STEMP= $20^\circ\text{C}$ (DEG C)	THIS IS THE SURFACE TEMPERATURE AT GROUND LEVEL.
C	STEMP=20.	SURFACE TEMPERATURE (DEG C)	THE MEAN TEMPERATURE OF THE DEPOSITORY.
N	MTEMP=26.	INITIAL VALUE OF MTEMP (DEG C)	THE MAXIMUM CREATED VOLUME FROM ANY SOURCE, REGARDLESS OF THE COMPACTION STATE.
A	MCL.K=BMCL+ACLS.K	MAXIMUM COMPACTION LENGTH (CM)	THE POTENTIAL COMPACTION LENGTH IS EQUIVALENT TO THE TOTAL DISSOLVED VOLUME AVERAGED OVER THE DEPOSITORY AREA.
A	ACLS.K=SO.K/SA.K	AVERAGE COMPACTION LENGTH FROM SOLUTIONING (CM)	THE EQUATION REPRESENTS THE TOTAL VOLUME DISSOLVED.
L	SO.K=SO.J+DT*BDUA.JK	SOLUTION OPENINGS (CU CM)	TAKEN TO BE THE TOTAL HORIZONTAL AREA OF THE DEPOSITORY PLANE.
A	SA.K=DA	SOLUTIONING AREA (SQ CM)	THE HORIZONTAL AREA BASED ON DESIGN IN THE INTERIM REPORT.
C	DA=7.9E10	DEPOSITORY AREA (SQ CM)	



N	SO=1.	INITIAL VALUE OF SO (CU CM)	
A	LNVFU.K=0.33*LOGN(SO.K)-0.46	NATURAL LOG SINGLE CAVITY VOLUME FUNCTION (CU CM)	
A	SCDIA.K=2.0*EXP(LNVFU.K)	SINGLE CAVITY DIAMETER (CM)	CALCULATED AS THE DIAMETER OF A HYPOTHETICAL SPHERE EQUAL IN VOLUME TO THE TOTAL DISSOLVED SALT EXPRESSED BY SO AND SOC.
L	CLC.K=MCLC.J-LPVC.J	COMPACTION LENGTH; WITH CLOSURE (CM)	THIS IS THE ACTUAL OBSERVED VERTICAL SUBSIDENCE, OR COMPACTION AT A GIVEN TIME.
N	CLC=1.	INITIAL VALUE OF CLC (CM)	
A	LPVC.K=BMCL+PVPSC.K-PVDCC.K	LINEAR PORE VOLUME NORMALIZED BY CLOSURE (CM)	
L	PVPSC.K=PVPSC.J+DT*(BDRUAC.JK)/DA	(LINEAR) PORE VOLUME PRODUCED BY SOLUTIONING; WITH CLOSURE (CM)	SAME AS PVPSC WITH CLOSURE.
N	PVPSC=0	INITIAL VALUE PVPSC (CM)	
R	BDRUAC.KL=FIFGE(MBFA,ACDRC.K,ACDRC.K,MBFA)	BRINE DISCHARGE RATE TO UPPER AQUIFER; WITH CLOSURE (CU CM/YR)	SAME AS BDRUA WITH CLOSURE.
A	ACDRC.K=PVOR.K*ANCC.K	APPARENT CRACK DISCHARGE RATE; WITH CLOSURE (CU CM/YR)	THIS IS THE FLOW RATE THROUGH THE DIMINISHED NUMBER OF CRACKS.
A	ACDRC.K=DCBPHA.K*NBPH*ANCC.K/(1.+(DCBPHA.K*DCBPHB.K*ANCC.K))	APPARENT NUMBER OF CRACKS REDUCED BY CLOSURE	
S	RCVRC.K=ACDRC.K/NCC.K	REFERENCE CRACK VOLUME RATE (CU CM/YR)	SAME AS RCVR WITH CLOSURE.
A	ANCC.K=(LPVC.K/MCLC.K)*NCC.K	ACTIVE NUMBER OF CRACKS; REDUCED BY CLOSURE	THIS IS BASED ON THE ASSUMPTION THAT THE NUMBER OF CRACKS IS PROPORTIONAL TO LPV RATHER THAN BY THE COMPACTION LENGTH. THE RATIO LPVC/MCLC RANGES FROM UNITY TO ZERO. ZERO CORRESPONDS TO COMPACTION THAT HAS COMPENSATED PREVIOUS DISSOLUTIONING.
A	NCC.K=CC*FIFGE(IE4,AVNECC.K,AVNECC.K,IE4)	NUMBER OF CRACKS FROM VERTICAL DISPLACEMENT; WITH CLOSURE	SAME AS NC WITH CLOSURE.
N	NCC=1.	INITIAL NUMBER OF CRACKS; WITH CLOSURE	
A	NCC.K=DA*PVDCC.K/(RCW*CTL*CPL)	NUMBER OF CRACKS CALCULATED FROM VOLUME OF REFERENCE CRACK; WITH CLOSURE	NOTE: NCC IS GIVEN IN TWO FORMS.
A	AVNECC.K=MAX(NECC.K-NECC.K)	ABSOLUTE VALUE NEC; WITH CLOSURE (CM)	THE ABSOLUTE VALUE OF NEC ADJUSTED FOR CLOSURE.
A	NECC.K=TE.K-CLC.K	NET EXPANSION MINUS COMPACTION; WITH CLOSURE (CM)	
N	NECC=-1.	INITIAL VALUE NEC (CM)	
L	PVDCC.K=PVDCC.J-DT*(LPVRCRC.JK)	(LINEAR) PORE VOLUME DESTROYED BY COMPACTION; WITH CLOSURE (CM)	SAME AS PVDCC WITH CLOSURE.

N	PVDCC=0	INITIAL VALUE PVDCC (CM)	
R	LPVCRCL=LPVC.K*EXP(-2.303*ELP *3E7*DT/EVISC.K)/DT-LPVC.K/DT	LINEAR PORE VOLUME COMPACTION RATE; WITH CLOSURE (CM/YR)	SAME AS LPVC WITH CLOSURE.
A	MCLC.K=BMCL+ACLSC.K	MAXIMUM COMPACTION LENGTH; WITH CLOSURE (CM)	MCL ADJUSTED FOR NEGATIVE FEEDBACK.
A	ACLSC.K=SOC.K/SA.K	AVERAGE COMPACTION LENGTH FROM SOLUTION; WITH CLOSURE (CM)	SAME AS ACLS WITH CLOSURE.
L	SOC.K=SOC.J+DT*BDRUAC.JK	SOLUTION OPENINGS; WITH CLOSURE (CU CM)	ADJUSTED SO WITH CLOSURE.
N	SOC=1.	INITIAL VALUE SOC (CU CM)	
A	LNVC.K=0.33*LOGN(SOC.K)-0.46	NATURAL LOG SINGLE CAVITY VOLUME FUNCTION; WITH CLOSURE (CU CM)	
A	SCDIAC.K=2.0*EXP(LNVFC.K)	SINGLE CAVITY DIAMETER; WITH CLOSURE (CM)	SAME AS SCDIA WITH CLOSURE.
S	BDRAT.K=(1.+BDRUAC.K)/(1.+ BDRUA.K)	BRINE DISCHARGE RATIO TO UPPER AQUIFER; WITH AND WITHOUT CLOSURE	RATIO OF BRINE DISCHARGE RATE INTO THE UPPER AQUIFER WITH CLOSURE TO THAT WITHOUT CLOSURE.
S	PVRAT.K=PVDC.K/MCLC.K	(LINEAR) PORE VOLUME RATIO	THE RATIO OF ACTUAL COMPACTIONED VOLUME TO MAXIMUM AVAILABLE VOLUME FOR COMPACTION.
S	PVRATC.K=PVDCC.K/MCLC.K	(LINEAR) PORE VOLUME RATIO; WITH CLOSURE	SAME AS PVRAT WITH CLOSURE.

(6)

```

*****
*****
* REFERENCE SET 1-DISSCC WORKING LIST FOR OPTION 1 NC,NCC
* DATE OF RUN RUN IDENTIFICATION
* DCP= (CAL/GM/YR)
* BMCL= (CM)
* RCW= (CM)
* MBFA=3E12 (CAL/GM/YR)
* BPH=3E6 (DYNE/SQ CM)
* DT=
* LENGTH=
* PRTPER=
* PLTPER=
* OVERRUN TIME AT
* OPTION 1 FOR NC
* OPTION 1 FOR NCC
* DISSOLUTION WITH AND WITHOUT CRACK CLOSURE (DISSCC WORKING LIST-OPTION 1 FOR NC AND NCC)
*****
*****
L H.K=H.J+DT*(HINR.JK-HOUTR.JK) HEAT ABOVE 0 TEMPERATURE (CAL/GM)
N H=5.2 INITIAL HEAT; MTEMP=26C (CAL/GM)
R HINR.KL=DCP*FD.K RADIONUCLIDE POWER (CAL/GM/YR)
N HINR=0 HEATING RATE AT START (CAL/GM/YR)
C DCP=0.094 DIMENSIONAL COEFFICIENT FOR THERMAL POWER (CAL/GM/YR)
A FD.K=EXP(2.303*LOGFD.K) RADIONUCLIDE DECAY FRACTION
N FD=1 INITIAL DECAY FRACTION
A LOGFD.K=TABLE(FDTAB,LOGT.K,0,8,0.5) LOGTEN DECAY FRACTION
N LOGFD=0 INITIAL LOGFD
T FDTAB=0/-0.03/-0.11/-0.38/-1.00/-1.80/-2.17/-2.51/-2.80/-3.28/
X -3.84/-4.0/-4.0/-4.0/-4.0/-4.0/-4.0/-4.0 TABLE VALUES OF LOGFD
A LOGT.K=LOGN(TIME.K)/2.303 LOGTEN TIME (YEARS)
N TIME=1 INITIAL VALUE OF TIME (YEARS)
N LOGT=0 INITIAL VALUE OF LOG TIME
R HOUTR.KL=DELAY3(SHLR.JK,DSHF) HEAT OUTPUT RATE (CAL/GM/YR)
N HOUTR=0 INITIAL HEAT OUTPUT RATE (CAL/GM/YR)
R SHLR.KL=2E-4*(H.K-4.0)-2.4E-4 STEADY HEAT LOSS RATE (CAL/GM/YR)
N SHLR=0 INITIAL VALUE STEADY HEAT LOSS (CAL/GM/YR)
C DSHF=100 DELAY SURFACE HEAT FLUX (YEARS)
R TER.KL=UEC*(HINR.JK-HOUTR.JK)/0.2 (LINEAR) THERMAL EXPANSION RATE (CM/YR)
C UEC=0.9 UNIT EXPANSION CONSTANT (CM/DEG C)
N TER=0.423 INITIAL VALUE OF TER (CM/YR)
L TE.K=TE.J+DT*(TER.JK) (LINEAR) THERMAL EXPANSION (CM)
N TE=0 INITIAL THERMAL EXPANSION STATE (CM)
L CL.K=MCL.J-LPV.J COMPACTION LENGTH (CM)
N CL=1 INITIAL VALUE CL (CM)
A LPV.K=BMCL+PVPS.K-PVDC.K LINEAR PORE VOLUME (CM)
C BMCL=60 BACKFILL MAXIMUM COMPACTION LENGTH (CM)
L PVPS.K=PVPS.J+DT*(BDRUA.JK)/DA (LINEAR) PORE VOLUME PRODUCED BY SOLUTIONING (CM)
N PVPS=0 INITIAL (LINEAR) PORE VOLUME PRODUCED BY SOLUTIONING (CU CM)
R BDRUA.KL=FIGE(MBFA,ACDR.K,ACDR.K,MBFA) BRINE DISCHARGE RATE TO UPPER AQUIFER (CU CM/YR)
C MBFA=3E12 MAXIMUM BRINE FLOW IN AQUIFER (CU/CM/YR)
A ACDR.K=RCVR.K*NC.K (TOTAL) APPARENT CRACK DISCHARGE RATE(CU CM/YR)
R RCVR.K=(3E7*BPH*RCW*RCW*CTL)/(12*BV*CPL) REFERENCE CRACK VOLUME RATE (CU CM/YR)
C BPH=2E6 BRINE PRESSURE HEAD (DYNE/SQ CM)
C RCW=1E-3 REFERENCE CRACK WIDTH (CM)
C CTL=6E5 CRACK TRACE LENGTH (CM)
C BV=1E-2 BRINE VISCOSITY (POISE)
C CPL=1E4 CRACK PATH LENGTH (CM)
A NC.K=DA*PVDC.K/(RCW*CTL*CPL) NUMBER OF CRACKS FROM VOLUME OF REFERENCE CRACK
N NC=1 INITIAL NUMBER OF CRACKS
A AVNEC.K=MAX(NEC.K,-NEC.K) ABSOLUTE VALUE OF NEC (CM)
A NEC.K=TE.K-CL.K NET EXPANSION MINUS COMPACTION (CM)
N NEC=-1. INITIAL NEC (CM)
L PVDC.K=PVDC.J-DT*(LPVCR.JK) (LINEAR) PORE VOLUME DESTROYED BY COMPACTION (CM)
N PVDC=0 INITIAL VALUE OF PVDC (CM)
R LPVCR.KL=LPV.K*EXP(-2.303*ELP*3E7*DT/EVISC.K)/DT-LPV.K/DT LINEAR PORE VOLUME COMPACTION RATE (CM/YR)
C ELP=1.3E8 EFFECTIVE LOAD PRESSURE (DYNE/SQ CM)
A EVISC.K=TABLE(EVTAB,BTEMP.K,0,250,25) EFFECTIVE VISCOSITY (POISE)
T EVTAB=1.15E19,7.08E18,4.47E18,2.81E18,1.78E18,1.26E18,
X 8.91E17,6.61E17,5.01E17,3.80E17,3.02E17 TABLE VALUES OF EVISC (POISE)
A BTEMP.K=32+2*(MTEMP.K-26) BACKFILL TEMPERATURE (DEG C)
N BTEMP=32 INITIAL VALUE BTEMP (DEG C)
A MTEMP.K=(H.K-4.0)/0.2+STEMP MEAN TEMPERATURE FOR STEMP=20C (DEG C)
N MTEMP=26 INITIAL VALUE OF MTEMP (DEG C)
C STEMP=20 SURFACE TEMPERATURE (DEG C)
A MCL.K=BMCL+ACLS.K MAXIMUM COMPACTION LENGTH (CM)
A ACLS.K=SO.F/SA.K AVERAGE COMPACTION LENGTH FROM SOLUTIONING (CM)
L SO.K=SO.J+DT*BDRUA.JK SOLUTION OPENINGS (CU CM)
A SA.K=DA SOLUTIONING AREA (SQ CM)
C DA=7.9E10 DEPOSITORY AREA (SQ CM)
N SO=1 INITIAL VALUE OF SO ( CU CM)
A LNVFU.K=0.33*LOGN(SO.K)-0.46 NATURAL LOG SINGLE CAVITY VOLUME FUNCTION (CU CM)
A SCDIA.K=2.0*EXP(LNVFU.K) SINGLE CAVITY DIAMETER (CM)
L CLC.K=MCLC.J-LPVC.J COMPACTION LENGTH; WITH CLOSURE (CM)
N CLC=1 INITIAL VALUE CLC (CM)
A LPVC.K=BMCL+PVPS.C.K-PVDC.C.K (LINEAR) PORE VOLUME; WITH CLOSURE (CM)
L PVPS.C.K=PVPS.C.J+DT*(BDRUA.C.K)/DA (LINEAR) PORE VOLUME PRODUCED BY SOLUTIONING; WITH CLOSURE (CM)
N PVPS.C=0 INITIAL VALUE PVPS.C (CM)
R BDRUA.C.KL=FIGE(MBFA,ACDR.C.K,ACDR.C.K,MBFA) BRINE DISCHARGE RATE TO UPPER AQUIFER; WITH CLOSURE (CU CM/YR)
A ACDR.C.K=RCVR.C.K*ANCC.K APPARENT CRACK DISCHARGE RATE; WITH CLOSURE (CU CM/YR)
A ANCC.K=(LPVC.C.K/MCLC.C.K)*NCC.K ACTIVE NUMBER OF CRACKS; REDUCED BY CLOSURE
A NCC.K=DA*PVDC.C.K/(RCW*CTL*CPL) NUMBER OF CRACKS CALCULATED FROM VOLUME OF REFERENCE CRACK; WITH CLOSURE
N NCC=1 INITIAL NUMBER OF CRACKS; WITH CLOSURE
A AVNECC.K=MAX(NECC.K,-NECC.K) ABSOLUTE VALUE OF NEC; WITH CLOSURE (CM)
A NECC.K=TE.C.K-CLC.C.K NET EXPANSION MINUS COMPACTION; WITH CLOSURE (CM)
N NECC=-1. INITIAL VALUE NECC (CM)
L PVDC.C.K=PVDC.C.J-DT*(LPVCR.C.K) (LINEAR) PORE VOLUME DESTROYED BY COMPACTION; WITH CLOSURE (CM)
N PVDC.C=0 INITIAL VALUE PVDC.C (CM)
R LPVCR.C.KL=LPVC.C.K*EXP(-2.303*ELP*3E7*DT/EVISC.C.K)/DT-LPV.C.K/DT LINEAR PORE VOLUME COMPACTION RATE; WITH CLOSURE (CM/YR)
A MCLC.K=BMCL+ACLS.C.K MAXIMUM COMPACTION LENGTH; WITH CLOSURE (CM)
A ACLSC.K=SOC.K/SA.K AVERAGE COMPACTION LENGTH FROM SOLUTIONING; WITH CLOSURE (CM)
L SOC.K=SOC.J+DT*BDRUA.C.K SOLUTION OPENINGS; WITH CLOSURE (CU CM)
N SOC=1 INITIAL VALUE SOC (CU CM)
A LNVFC.K=0.33*LOGN(SOC.K)-0.46 NATURAL LOG SINGLE CAVITY VOLUME FUNCTION; WITH CLOSURE (CU CM)
A SCDIAC.K=2.0*EXP(LNVFC.C.K) SINGLE CAVITY DIAMETER; WITH CLOSURE (CM)
S BDRAT.K=(1.+BDRUA.C.K)/(1.+BDRUA.K) BRINE DISCHARGE RATE; WITH AND WITHOUT CLOSURE
S PVRAT.K=PVDC.C.K/MCLC.K (LINEAR) PORE VOLUME RATIO
S PVRATC.K=PVDC.C.K/MCLC.K (LINEAR) PORE VOLUME RATIO; WITH CLOSURE
NOTE
PRINT H,HINR,HOUTR,SHLR,TER,TE,CL,LPV,PVPS,BDRUA,
X ACDR,NC,AVNEC,NEC,PVDC,LPVCR,EVISC,BTEMP,
X MTEMP,MCL,ACLS,SO,LNVFU,SCDIA,CLC,LPVC,PVPS,
X BDRUA,ACDR,ANCC,NCC,AVNECC,NECC,PVDC,LPVCR,
X MCLC,ACLS,SOC,LNVFC,SCDIAC,BDRAT,PVRAT,PVRATC
PLOT NC/NANCC/AVNEC=V(0,1.0E4)/AVNECC=A(0,1.0E4)/SCDIA=D(0,1.0E4)/
X SCDIAC=S(0,1.0E4)/BDRAT=B/PVRAT=P/RCVR=R
SPEC DT=1/LENGTH=1.0E4/PLTPER=1.0E2/PRTPER=1.0E2
RUN "DISS WITH AND WITHOUT CC"----"DISSOLUTION WITH AND WITHOUT CRACK CLOSURE"
EOI ENCOUNTERED.
/

```

# Table AR.3.4B

```

*****
*****
*   DATE OF RUN           RUN IDENTIFICATION
*   REFERENCE SET 2-DISSCC WORKING LIST FOR OPTION 1 NC,NCC WITH DECAY OF BPH
*   DCP=                   (CAL/GM/YR)
*   BMCL=                  (CM)
*   RCW=                   (CM)
*   MBFA=3E12              (CU CM/YR)
*   NBPH=2E6               (DYNE/SQ CM)
*   DT=
*   LENGTH=
*   PRTPER=
*   PLTPER=
*   OVERRUN TIME AT
*   OPTION 1 FOR NC WITH DECAY OF BPH
*   OPTION 1 FOR NCC WITH DECAY OF BPH
*   DISSOLUTION WITH AND WITHOUT CRACK CLOSURE (DISSCC WORKING LIST-OPTION 1 FOR NC AND NCC WITH DECAY OF BPH)
*****
*****
L   H.K=H.J+DT*(HINR.JK-HOUTR.JK)      HEAT ABOVE 0 TEMPERATURE (CAL/GM)
N   H=5.2                              INITIAL HEAT; MTEMP=26C (CAL/GM)
R   HINR.KL=DCP*FD.K                   RADIONUCLIDE POWER (CAL/GM/YR)
N   HINR=0                             HEATING RATE AT START (CAL/GM/YR)
C   DCP=0.094                          DIMENSIONAL COEFFICIENT FOR THERMAL POWER (CAL/GM/YR)
A   FD.K=EXP(2.303*LOGFD.K)            RADIONUCLIDE DECAY FRACTION
N   FD=1.                              INITIAL DECAY FRACTION
A   LOGFD.K=TABLE(FDTAB,LOGT.K,0,8,0.5) LOGTEN DECAY FRACTION
N   LOGFD=0                            INITIAL LOGFD
T   FDTAB=0/-0.03/-0.11/-0.38/-1.00/-1.80/-2.17/-2.51/-2.80/-3.28/
X   -3.84/-4.0/-4.0/-4.0/-4.0/-4.0/-4.0/-4.0/      TABLE VALUES OF LOGFD
A   LOGT.K=LOGN(TIME.K)/2.303          LOGTEN TIME (YEARS)
N   TIME=1.                            INITIAL VALUE OF TIME (YEARS)
N   LOGT=0                             INITIAL VALUE OF LOG TIME
R   HOUTR.KL=DELAY3(SHLR.JK,DSHF)      HEAT OUTPUT RATE (CAL/GM/YR)
N   HOUTR=0                            INITIAL HEAT OUTPUT RATE (CAL/GM/YR)
R   SHLR.KL=2E-4*(H.K-4.0)-2.4E-4     STEADY HEAT LOSS RATE (CAL/GM/YR)
N   SHLR=0                             INITIAL VALUE STEADY HEAT LOSS (CAL/GM/YR)
C   DSHF=100                           DELAY SURFACE HEAT FLUX (YEARS)
R   TER.KL=UEC*(HINR.JK-HOUTR.JK)/0.2 (LINEAR) THERMAL EXPANSION RATE (CM/YR)
C   UEC=0.9                            UNIT EXPANSION CONSTANT (CM/DEG C)
N   TER=0.423                          INITIAL VALUE OF TER (CM/YR)
L   TE.K=TE.J+DT*(TER.JK)             (LINEAR) THERMAL EXPANSION (CM)
N   TE=0                               INITIAL THERMAL EXPANSION STATE (CM)
L   CL.K=MCL.J-LPV.J                  COMPACTION LENGTH (CM)
N   CL=1.                              INITIAL VALUE CL (CM)
A   LPV.K=BMCL+PVPS.K-PVDC.K          LINEAR PORE VOLUME (CM)
C   BMCL=60                           BACKFILL MAXIMUM COMPACTION LENGTH (CM)
L   PVPS.K=PVPS.J+DT*(BDRUA.JK)/DA    (LINEAR) PORE VOLUME PRODUCED BY SOLUTIONING (CM)
N   PVPS=0                             INITIAL (LINEAR) PORE VOLUME PRODUCED BY SOLUTIONING (CU CM)
R   BDRUA.KL=FIGE(MBFA,ACDR.K,ACDR.K,MBFA) BRINE DISCHARGE RATE TO UPPER AQUIFER (CU CM/YR)
C   MBFA=3E12                          MAXIMUM BRINE FLOW IN AQUIFER (CU CM/YR)
A   ACDR.K=DCBPHA.K*NBPH*NC.K/(1.+(DCBPHA.K*DCBPHB.K*NC.K)) (TOTAL) APPARENT CRACK DISCHARGE RATE (CU CM/YR)
S   RCVR.K=ACDR.K/NC.K                 REFERENCE CRACK VOLUME RATE (CU CM/YR)
A   DCBPHA.K=(3E7*RCW*RCW*CTL)/(12*BV*CPL) DIMENSIONAL CONSTANT BRINE PRESSURE HEAD (SQ CM/DYNE)*(CU CM/YR)
R   DCBPHB.K=NBPH/MBFA                BRINE PRESSURE FLOW RATIO (DYNE/SQ CM)/(CU CM/YR)
C   NBPH=2E6                           INITIAL BRINE PRESSURE HEAD (DYNE/SQ CM)
C   RCW=1E-3                           REFERENCE CRACK WIDTH (CM)
C   CTL=6E5                             CRACK TRACE LENGTH (CM)
C   BV=1E-2                             BRINE VISCOSITY (POISE)
C   CPL=1E4                             CRACK PATH LENGTH (CM)
A   NC.K=DA*PVDC.K/(RCW*CTL*CPL)      NUMBER OF CRACKS FROM VOLUME OF REFERENCE CRACK
N   NC=1.                              INITIAL NUMBER OF CRACKS
A   AVNEC.K=MAX(NEC.K,-NEC.K)          ABSOLUTE VALUE OF NEC (CM)
A   NEC.K=TE.K-CL.K                   NET EXPANSION MINUS COMPACTION (CM)
N   NEC=-1.                            INITIAL NEC (CM)
L   PVDC.K=PVDC.J-DT*(LPVCR.JK)        (LINEAR) PORE VOLUME DESTROYED BY COMPACTION (CM)
N   PVDC=1.                            INITIAL VALUE OF PVDC (CM)
C   LPVCR.KL=LPV.K*EXP(-2.303*ELP*3E7*DT/EVISC.K)/DT-LPV.K/DT LINEAR PORE VOLUME COMPACTION RATE (CM/YR)
R   ELP=1.3E8                          EFFECTIVE LOAD PRESSURE (DYNE/SQ CM)
C   EVISC.K=TABLE(EVTAB,BFTEMP.K,0,250,25) EFFECTIVE VISCOSITY (POISE)
T   EVTAB=1.15E19,7.08E18,4.47E18,2.81E18,1.78E18,1.26E18,
X   8.91E17,6.61E17,5.01E17,3.80E17,3.02E17      TABLE VALUES OF EVISC (POISE)
A   BFTEMP.K=32+2*(MTEMP.K-26)         BACKFILL TEMPERATURE (DEG C)
N   BFTEMP=32.                         INITIAL VALUE BFTEMP (DEG C)
A   MTEMP.K=(H.K-4.0)/0.2+STEMP        MEAN TEMPERATURE FOR STEMP=20C (DEG C)
N   MTEMP=26.                          INITIAL VALUE OF MTEMP (DEG C)
C   STEMP=20.                          SURFACE TEMPERATURE (DEG C)
A   MCL.K=BMCL+ACLS.K                 MAXIMUM COMPACTION LENGTH (CM)
A   ACLS.K=SO.K/SA.K                  AVERAGE COMPACTION LENGTH FROM SOLUTIONING (CM)
L   SO.K=SO.J+DT*BDRUA.JK             SOLUTION OPENINGS (CU CM)
A   SA.K=DA                           SOLUTIONING AREA (SQ CM)
C   DA=7.9E10                         DEPOSITORY AREA (SQ CM)
N   SO=1.                              INITIAL VALUE OF SO ( CU CM)
A   LNVFU.K=0.33*LOGN(SO.K)-0.46       NATURAL LOG SINGLE CAVITY VOLUME FUNCTION (CU CM)
A   SCDIA.K=2.0*EXP(LNVFU.K)           SINGLE CAVITY DIAMETER (CM)
L   CLC.K=MCLC.J-LPVC.J               COMPACTION LENGTH; WITH CLOSURE (CM)
N   CLC=1.                             INITIAL VALUE CLC (CM)
A   LPVC.K=BMCL+PVPS.K-PVDC.C.K        (LINEAR) PORE VOLUME; WITH CLOSURE (CM)
L   PVPS.C.K=PVPS.C.J+DT*(BDRUA.C.K)/DA (LINEAR) PORE VOLUME PRODUCED BY SOLUTIONING; WITH CLOSURE (CM)
N   PVPS.C=0                           INITIAL VALUE PVPS (CM)
R   BDRUA.C.KL=FIGE(MBFA,ACDR.C,K,ACDR.C,K,MBFA) BRINE DISCHARGE RATE TO UPPER AQUIFER; WITH CLOSURE (CU CM/YR)
A   ACDR.C.K=DCBPHA.K*NBPH*ANCC.K/(1.+(DCBPHA.K*DCBPHB.K*ANCC.K)) APPARENT NUMBER OF CRACKS REDUCED BY CLOSURE
S   RCVR.C.K=ACDR.C.K/NC.C.K           REFERENCE CRACK VOLUME RATE (CU CM/YR)
A   ANCC.K=(LPVC.C.K/MCLC.C.K)*NC.C.K  ACTIVE NUMBER OF CRACKS; REDUCED BY CLOSURE
A   NC.C.K=DA*PVDC.C.K/(RCW*CTL*CPL)  NUMBER OF CRACKS FROM VOLUME OF REFERENCE CRACK; WITH CLOSURE
N   NC.C=1.                            INITIAL NUMBER OF CRACKS; WITH CLOSURE
A   AVNECC.K=MAX(NECC.K,-NECC.K)       ABSOLUTE VALUE OF NEC; WITH CLOSURE (CM)
A   NECC.K=TE.C-K-CLC.C.K             NET EXPANSION MINUS COMPACTION; WITH CLOSURE (CM)
N   NECC=-1.                           INITIAL VALUE NECC (CM)
L   PVDC.C.K=PVDC.C.J-DT*(LPVCR.C.K)   (LINEAR) PORE VOLUME DESTROYED BY COMPACTION; WITH CLOSURE (CM)
N   PVDC.C=1.                          INITIAL VALUE PVDC (CM)
R   LPVCR.C.KL=LPVC.C.K*EXP(-2.303*ELP*3E7*DT/EVISC.C.K)/DT-LPV.C.K/DT LINEAR PORE VOLUME COMPACTION RATE; WITH CLOSURE (CM/YR)
A   MCLC.K=BMCL+ACLS.C.K               MAXIMUM COMPACTION LENGTH; WITH CLOSURE (CM)
A   ACLS.C.K=SO.C.K/SA.C.K             AVERAGE COMPACTION LENGTH FROM SOLUTIONING; WITH CLOSURE (CM)
L   SOC.K=SOC.J+DT*BDRUA.C.K          SOLUTION OPENINGS; WITH CLOSURE (CU CM)
N   SOC=1.                             INITIAL VALUE SOC (CU CM)
A   LNVFC.K=0.33*LOGN(SOC.K)-0.46       NATURAL LOG SINGLE CAVITY VOLUME FUNCTION; WITH CLOSURE (CU CM)
A   SCDIAC.K=2.0*EXP(LNVFC.C.K)         SINGLE CAVITY DIAMETER; WITH CLOSURE (CM)
S   BDRAT.K=(1.+(BDRUA.C.K)/(1.+(BDRUA.C.K)) BRINE DISCHARGE RATE; WITH AND WITHOUT CLOSURE
S   PV RAT.K=PVDC.C.K/MCLC.C.K         (LINEAR) PORE VOLUME RATIO
S   PV RATC.K=PVDC.C.K/MCLC.C.K        (LINEAR) PORE VOLUME RATIO; WITH CLOSURE
NOTE
PRINT H,HINR,HOUTR,SHLR,TER,TE,CL,LPV,PVPS,BDRUA,ACDR,
X   NC,AVNEC,NEC,PVDC,LPVCR,EVISC,BFTEMP,MTEMP,MCL,
X   ACLS,SO,LNVFU,SCDIA,CLC,LPVC,PVPS,C,BDRUA,C,ACDR,C,
X   ANCC,NCC,AVNECC,NECC,PVDC,C,LPVCR,C,MCLC,ACLS,C,SOC,
X   LNVFC,SCDIAC,BDRAT,PVRAT,PVRATC
PLOT NC=N/ANCC=C/AVNEC=V(0,1.0E4)/AVNECC=A(0,1.0E4)/SCDIA=D(0,1.0E4)/
X   SCDIAC=S(0,1.0E4)/BDRAT=B/PVRAT=P/RCVR=R/RCVRC=H
SPEC DT=1/LENGTH=1.0E4/PLTPER=1.0E2/PRTPER=1.0E2

```

# Table AR.3.4C

```

*****
* DATE OF RUN RUN IDENTIFICATION
* REFERENCE SET 3-DISSCC WORKING LIST FOR OPTION 2 NC,NCC
* RCW= (CM)
* BMCL= (CM)
* DCP= (CAL/GM/YR)
* CC= (PER CM)
* MBFA=3E12 (CU CM/YR)
* BPH=2E6 (DYNE/SQ CM)
* DT=
* LENGTH=
* PRTPER=
* PLTPER=
* OVERRUN TIME AT
* OPTION 2 FOR NC
* OPTION 2 FOR NCC
* DISSOLUTION WITH AND WITHOUT CRACK CLOSURE (DISSCC WORKING LIST-OPTION 2 FOR NC AND NCC)
*****
L H.K=H.J+DT*(HINR.JK-HOUTR.JK) HEAT ABOVE 0 TEMPERATURE (CAL/GM)
N H=5.2 INITIAL HEAT; MTEMP=26C (CAL/GM)
R HINR.KL=DCP*FD.K RADIONUCLIDE POWER (CAL/GM/YR)
N HINR=0 HEATING RATE AT START (CAL/GM/YR)
C DCP=0.094 DIMENSIONAL COEFFICIENT FOR THERMAL POWER (CAL/GM/YR)
A FD.K=EXP(2.303*LOGFD.K) RADIONUCLIDE DECAY FRACTION
N FD=1 INITIAL DECAY FRACTION
A LOGFD.K=TABLE(FDTAB,LOGT.K,0,8,0.5) LOGTEN DECAY FRACTION
N LOGFD=0 INITIAL LOGFD
T FDTAB=0/-0.03/-0.11/-0.38/-1.00/-1.80/-2.17/-2.51/-2.80/-3.28/
X -3.84/-4.0/-4.0/-4.0/-4.0/-4.0/-4.0/-4.0/-4.0/-4.0 TABLE VALUES OF LOGFD
A LOGT.K=LOGN(TIME.K)/2.303 LOGTEN TIME (YEARS)
N TIME=1 INITIAL VALUE OF TIME (YEARS)
N LOGT=0 INITIAL VALUE OF LOG TIME
R HOUTR.KL=DELAY3(SHLR.JK,DSHF) HEAT OUTPUT RATE (CAL/GM/YR)
N HOUTR=0 INITIAL HEAT OUTPUT RATE (CAL/GM/YR)
R SHLR.KL=2E-4*(H.K-4.0)-2.4E-4 STEADY HEAT LOSS RATE (CAL/GM/YR)
N SHLR=0 INITIAL VALUE STEADY HEAT LOSS (CAL/GM/YR)
C DSHF=100 DELAY SURFACE HEAT FLUX (YEARS)
R TER.KL=UEC*(HINR.JK-HOUTR.JK)/0.2 (LINEAR) THERMAL EXPANSION RATE (CM/YR)
C UEC=0.9 UNIT EXPANSION CONSTANT (CM/DEG C)
N TER=0.423 INITIAL VALUE OF TER (CM/YR)
L TE.K=TE.J+DT*(TER.JK) (LINEAR) THERMAL EXPANSION (CM)
N TE=1 INITIAL THERMAL EXPANSION STATE (CM)
L CL.K=MCL.J-LPV.J COMPACTION LENGTH (CM)
N CL=1 INITIAL VALUE CL (CM)
A LPV.K=BMCL+PVPS.K-PVDC.K LINEAR PORE VOLUME (CM)
C BMCL=60 BACKFILL MAXIMUM COMPACTION LENGTH (CM)
L PVPS.K=PVPS.J+DT*(BDRUA.JK)/DA (LINEAR) PORE VOLUME PRODUCED BY SOLUTIONING (CM)
N PVPS=0 INITIAL (LINEAR) PORE VOLUME PRODUCED BY SOLUTIONING (CU CM)
R BDRUA.KL=FIFGE(MBFA,ACDR.K,ACDR.K,MBFA) BRINE DISCHARGE RATE TO UPPER AQUIFER (CU CM/YR)
C MBFA=3E12 MAXIMUM BRINE FLOW IN AQUIFER (CU CM/YR)
A ACDR.K=RCVR.K*NCC.K (TOTAL) APPARENT CRACK DISCHARGE RATE(CU CM/YR)
R RCVR.K=(3E7*BPH*RCW*RCW*RCW*CTL)/(12*BV*CPL) REFERENCE CRACK VOLUME RATE (CU CM/YR)
C BPH=2E6 BRINE PRESSURE HEAD (DYNE/SQ CM)
C RCW=1E-3 REFERENCE CRACK WIDTH (CM)
C CTL=6E5 CRACK TRACE LENGTH (CM)
C BV=1E-2 BRINE VISCOSITY (POISE)
C CPL=1E4 CRACK PATH LENGTH (CM)
A NC.K=CC*FIFGE(1E4,AVNEC.K,AVNEC.K,1E4) NUMBER OF CRACKS FROM NET VERTICAL DISPLACEMENT
C CC=5 CRACK COEFFICIENT; PROPORTIONAL TO NET VERTICAL DISPLACEMENT
N NC=1 INITIAL NUMBER OF CRACKS
A AVNEC.K=MAX(NEC.K,-NEC.K) ABSOLUTE VALUE OF NEC (CM)
N NEC.K=TE.K-CL.K NET EXPANSION MINUS COMPACTION (CM)
N NEC=-1 INITIAL NEC (CM)
L PVDC.K=PVDC.J-DT*(LPVCR.JK) (LINEAR) PORE VOLUME DESTROYED BY COMPACTION (CM)
N PVDC=0 INITIAL VALUE OF PVDC (CM)
R LPVCR.KL=LPV.K*EXP(-2.303*ELP*3E7*DT/EVISC.K)/DT-LPV.K/DT LINEAR PORE VOLUME COMPACTION RATE (CM/YR)
C ELP=1.3E8 EFFECTIVE LOAD PRESSURE (DYNE/SQ CM)
A EVISC.K=TABLE(EVTAB,BFTEMP.K,0,250,25) EFFECTIVE VISCOSITY (POISE)
T EVTAB=1.15E19,7.08E18,4.47E18,2.81E18,1.78E18,1.26E18,
X 8.91E17,6.61E17,5.01E17,3.80E17,3.02E17 TABLE VALUES OF EVISC (POISE)
A BFTEMP.K=32+2*(MTEMP.K-26) BACKFILL TEMPERATURE (DEG C)
N BFTEMP=32 INITIAL VALUE BFTEMP (DEG C)
A MTEMP.K=(H.K-4.0)/0.2+STEMP MEAN TEMPERATURE FOR STEMP=20C (DEG C)
N MTEMP=26 INITIAL VALUE OF MTEMP (DEG C)
C STEMP=20 SURFACE TEMPERATURE (DEG C)
A MCL.K=BMCL+ACLS.K MAXIMUM COMPACTION LENGTH (CM)
A ACLS.K=SO.K/SA.K AVERAGE COMPACTION LENGTH FROM SOLUTIONING (CM)
L SO.K=SO.J+DT*BDRUA.JK SOLUTION OPENINGS (CU CM)
A SA.K=DA SOLUTIONING AREA (SQ CM)
C DA=7.9E10 DEPOSITORY AREA (SQ CM)
N SO=1 INITIAL VALUE OF SO ( CU CM)
A LNVFU.K=0.33*LOGN(SO.K)-0.46 NATURAL LOG SINGLE CAVITY VOLUME FUNCTION (CU CM)
A SCDIA.K=2.0*EXP(LNVFU.K) SINGLE CAVITY DIAMETER (CM)
L CLC.K=MCLC.J-LPVC.J COMPACTION LENGTH; WITH CLOSURE (CM)
N CLC=1 INITIAL VALUE CLC (CM)
A LPVC.K=BMCL+PVPS.K-PVDC.C (LINEAR) PORE VOLUME; WITH CLOSURE (CM)
L PVPS.C=PVPS.C+DT*(BDRUA.C)/DA (LINEAR) PORE VOLUME PRODUCED BY SOLUTIONING; WITH CLOSURE (CM)
N PVPS.C=0 INITIAL VALUE PVPS (CM)
R BDRUA.C.KL=FIFGE(MBFA,ACDR.C,ACDR.C,MBFA) BRINE DISCHARGE RATE TO UPPER AQUIFER; WITH CLOSURE (CU CM/YR)
A ACDRC.K=RCVR.K*ANCC.K APPARENT CRACK DISCHARGE RATE; WITH CLOSURE (CU CM/YR)
A ANCC.K=(LPVC.K/MCLC.K)*NCC.K ACTIVE NUMBER OF CRACKS; REDUCED BY CLOSURE
N NCC.K=CC*FIFGE(1E4,AVNECC.K,AVNECC.K,1E4) NUMBER OF CRACKS FROM NET VERTICAL DISPLACEMENT
N NCC=1 INITIAL NUMBER OF CRACKS; WITH CLOSURE
A AVNECC.K=MAX(NECC.K,-NECC.K) ABSOLUTE VALUE OF NEC; WITH CLOSURE (CM)
N NECC.K=TE.K-CLC.K NET EXPANSION MINUS COMPACTION; WITH CLOSURE (CM)
N NECC=-1 INITIAL VALUE NECC (CM)
L PVDC.C.K=PVDC.C-DT*(LPVCR.C.K) (LINEAR) PORE VOLUME DESTROYED BY COMPACTION; WITH CLOSURE (CM)
N PVDC.C=0 INITIAL VALUE PVDC.C (CM)
R LPVCR.C.KL=LPVC.K*EXP(-2.303*ELP*3E7*DT/EVISC.K)/DT-LPV.C/DT LINEAR PORE VOLUME COMPACTION RATE; WITH CLOSURE (CM/YR)
A MCLC.K=BMCL+ACLS.C MAXIMUM COMPACTION LENGTH; WITH CLOSURE (CM)
A ACLSC.K=SOC.K/SA.K AVERAGE COMPACTION LENGTH FROM SOLUTIONING; WITH CLOSURE (CM)
L SOC.K=SOC.J+DT*BDRUA.C.K SOLUTION OPENINGS; WITH CLOSURE (CU CM)
N SOC=1 INITIAL VALUE SOC (CU CM)
A LNVFC.K=0.33*LOGN(SOC.K)-0.46 NATURAL LOG SINGLE CAVITY VOLUME FUNCTION; WITH CLOSURE (CU CM)
A SCDIAC.K=2.0*EXP(LNVFC.K) SINGLE CAVITY DIAMETER; WITH CLOSURE (CM)
S BDRAT.K=(1.+BDRUA.C.K)/(1.+BDRUA.K) BRINE DISCHARGE RATE; WITH AND WITHOUT,CLOSURE
S PVRAT.K=PVDC.C.K/MCLC.K (LINEAR) PORE VOLUME RATIO
S PVRATC.K=PVDC.C.K/MCLC.K (LINEAR) PORE VOLUME RATIO; WITH CLOSURE
NOTE
PRINT H,HINR,HOUTR,SHLR,TER,TE,CL,LPV,PVPS,BDRUA,ACDR,
X NC,AVNEC,NEC,PVDC,LPVCR,EVISC,BFTEMP,MTEMP,MCL,
X ACLS,SO,LNVFU,SCDIA,CLC,LPVC,PVPS,C,BDRUA,C,ACDR,C,
X ANCC,NCC,AVNECC,NECC,PVDC,C,LPVCR,C,MCLC,ACLS,C,SOC,
X LNVFC,SCDIAC,BDRAT,PVRAT,PVRATC
PLOT NC=N/ANCC=C/AVNEC=V(0,1.0E4)/AVNECC=A(0,1.0E4)/SCDIA=D(0,1.0E4)/
X SCDIAC=S(0,1.0E4)/BDRAT=B/PVRAT=P/RCVR=R
SPEC DT=1/LENGTH=1.0E4/PLTPER=1.0E2/PRTPER=1.0E2
RUN "DISS WITH AND WITHOUT CC"---"DISSOLUTION WITH AND WITHOUT CRACK CLOSURE"
EOI ENCOUNTERED.

```

# Table AR.3.4D

```

*****
*****
* DATE OF RUN RUN IDENTIFICATION
* REFERENCE SET 4-DISSCC WORKING LIST FOR OPTION 2 NC, NCC WITH DECAY OF BPH
* DCP= (CAL/GM/YR)
* BMCL= (CM)
* RCW= (CM)
* CC= (PER CM)
* MBFA= 3E12 (CU CM /YR)
* NBPH=2E6 (DYNE/SQ CM)
* DT=
* LENGTH=
* PRIPR=
* PLTPR=
* OVERRUN TIME AT
* OPTION 2 FOR NC WITH DECAY OF BPH
* OPTION 2 FOR NCC WITH DECAY OF BPH
* DISSOLUTION WITH AND WITHOUT CRACK CLOSURE (DISSCC WORKING LIST-OPTION 2 FOR NC AND NCC WITH DECAY OF BPH)
*****
*****
L H.K=H.J+DT*(HINR.JK-HOUTR.JK) HEAT ABOVE 0 TEMPERATURE (CAL/GM)
N H=5.2 INITIAL HEAT; MTEMP=26C (CAL/GM)
R HINR.KL=DCP*FD.K RADIONUCLIDE POWER (CAL/GM/YR)
N HINR=0 HEATING RATE AT START (CAL/GM/YR)
C DCP=0.094 DIMENSIONAL COEFFICIENT FOR THERMAL POWER (CAL/GM/YR)
A FD.K=EXP(2.303*LOGFD.K) RADIONUCLIDE DECAY FRACTION
N FD=1. INITIAL DECAY FRACTION
A LOGFD.K=TABLE(FDTAB,LOGT.K,0,8,0.5) LOGTEN DECAY FRACTION
N LOGFD=0 INITIAL LOGFD
T FDTAB=0/-0.03/-0.11/-0.38/-1.00/-1.80/-2.17/-2.51/-2.80/-3.28/
X -3.84/-4.0/-4.0/-4.0/-4.0/-4.0/-4.0/-4.0 TABLE VALUES OF LOGFD
A LOGT.K=LOGN(TIME.K)/2.303 LOGTEN TIME (YEARS)
N TIME=1. INITIAL VALUE OF TIME (YEARS)
N LOGT=0 INITIAL VALUE OF LOG TIME
R HOUTR.KL=DELAY3(SHLR.JK,DSHF) HEAT OUTPUT RATE (CAL/GM/YR)
N HOUTR=0 INITIAL HEAT OUTPUT RATE (CAL/GM/YR)
N SHLR=0 INITIAL VALUE STEADY HEAT LOSS (CAL/GM/YR)
R SHLR.KL=2E-4*(H.K-4.0)-2.4E-4 STEADY HEAT LOSS RATE (CAL/GM/YR)
C DSHF=100 DELAY SURFACE HEAT FLUX (YEARS)
R TER.KL=UEC*(HINR.JK-HOUTR.JK)/0.2 (LINEAR) THERMAL EXPANSION RATE (CM/YR)
C UEC=0.9 UNIT EXPANSION CONSTANT (CM/DEG C)
N TER=0.423 INITIAL VALUE OF TER (CM/YR)
L TE.K=TE.J+DT*(TER.JK) (LINEAR) THERMAL EXPANSION (CM)
N TE=0 INITIAL THERMAL EXPANSION STATE (CM)
L CL.K=MCL.J-LPV.J COMPACTION LENGTH (CM)
N CL=1. INITIAL VALUE CL (CM)
A LPV.K=BMCL+PVPS.K-PVDC.K LINEAR PORE VOLUME (CM)
C BMCL=60 BACKFILL MAXIMUM COMPACTION LENGTH (CM)
L PVPS.K=PVPS.J+DT*(BDRUA.JK)/DA (LINEAR) PORE VOLUME PRODUCED BY SOLUTIONING (CM)
N PVPS=0 INITIAL (LINEAR) PORE VOLUME PRODUCED BY SOLUTIONING (CU CM)
R BDRUA.KL=FIFGE(MBFA,ACDR.K,ACDR.K,MBFA) BRINE DISCHARGE RATE TO UPPER AQUIFER (CU CM/YR)
C MBFA=3E12 MAXIMUM BRINE FLOW IN AQUIFER (CU CM/YR)
A ACDR.K=DCBPHA.K*NBPH*NC.K/(1.+(DCBPHA.K*DCBPHB.K*NC.K)) (TOTAL) APPARENT CRACK DISCHARGE RATE (CU CM/YR)
S RCVR.K=ACDR.K/NC.K REFERENCE CRACK VOLUME RATE (CU CM/YR)
A DCBPHA.K=(3E7*RCW*RCW*CTL)/(12*BV*CPL) DIMENSIONAL CONSTANT BRINE PRESSURE HEAD (SQ CM/DYNE)*(CU CM/YR)
C DCBPHB.K=NBPH/MBFA BRINE PRESSURE FLOW RATIO (DYNE/SQ CM)/(CU CM/YR)
C NBPH=2E6 INITIAL BRINE PRESSURE HEAD (DYNE/SQ CM)
C RCW=1E-3 REFERENCE CRACK WIDTH (CM)
C CTL=6E5 CRACK TRACE LENGTH (CM)
C BV=1E-2 BRINE VISCOSITY (POISE)
C CPL=1E4 CRACK PATH LENGTH (CM)
A NC.K=CC*FIFGE(1E4,AVNEC.K,AVNEC.K,1E4) NUMBER OF CRACKS FROM NET VERTICAL DISPLACEMENT
C CC=5. CRACK COEFFICIENT; PROPORTIONAL TO VERTICAL DISPLACEMENT (CM)
N NC=1. INITIAL NUMBER OF CRACKS
A AVNEC.K=MAX(NEC.K,-NEC.K) ABSOLUTE VALUE OF NEC (CM)+1E-3
A NEC.K=TE.K-CL.K NET EXPANSION MINUS COMPACTION (CM)
N NEC=-1. INITIAL NEC (CM)
L PVDC.K=PVDC.J-DT*(LPVCR.JK) (LINEAR) PORE VOLUME DESTROYED BY COMPACTION (CM)
N PVDC=0 INITIAL VALUE OF PVDC (CM)
R LPVCR.KL=LPV.K*EXP(-2.303*ELP*3E7*DT/EVISC.K)/DT-LPV.K/DT LINEAR PORE VOLUME COMPACTION RATE (CM/YR)
C ELP=1.3E8 EFFECTIVE LOAD PRESSURE (DYNE/SQ CM)
A EVISC.K=TABLE(EVTAB,BFTEMP.K,0,250,25) EFFECTIVE VISCOSITY (POISE)
T EVTAB=1.15E19,7.08E18,4.47E18,2.81E18,1.78E18,1.26E18,
X 8.91E17,6.61E17,5.01E17,3.80E17,3.02E17 TABLE VALUES OF EVISC (POISE)
A BFTEMP.K=32+2*(MTEMP.K-26) BACKFILL TEMPERATURE (DEG C)
N BFTEMP=32. INITIAL VALUE BFTEMP (DEG C)
A MTEMP.K=(H.K-4.0)/0.2+STEMP MEAN TEMPERATURE FOR STEMP=20C (DEG C)
N MTEMP=26. INITIAL VALUE OF MTEMP (DEG C)
C STEMP=20. SURFACE TEMPERATURE (DEG C)
A MCL.K=BMCL+ACLS.K MAXIMUM COMPACTION LENGTH (CM)
A ACLS.K=SO.K/SA.K AVERAGE COMPACTION LENGTH FROM SOLUTIONING (CM)
L SO.K=SO.J+DT*BDRUA.JK SOLUTION OPENINGS (CU CM)
A SA.K=DA SOLUTIONING AREA (SQ CM)
C DA=7.9E10 DEPOSITORY AREA (SQ CM)
N SO=1. INITIAL VALUE OF SO ( CU CM)
A LNVFU.K=0.33*LOGN(SO.K)-0.46 NATURAL LOG SINGLE CAVITY VOLUME FUNCTION (CU CM)
A SCDIA.K=2.0*EXP(LNVFU.K) SINGLE CAVITY DIAMETER (CM)
L CLC.K=MCLC.J-LPVC.J COMPACTION LENGTH; WITH CLOSURE (CM)
N CLC=1. INITIAL VALUE CLC (CM)
A LPVC.K=BMCL+PVPS.C.K-PVDC.C.K (LINEAR) PORE VOLUME; WITH CLOSURE (CM)
L PVPS.C.K=PVPS.C.J+DT*(BDRUA.C.JK)/DA (LINEAR) PORE VOLUME PRODUCED BY SOLUTIONING; WITH CLOSURE (CM)
N PVPS.C=0 INITIAL VALUE PVPS.C (CM)
R BDRUA.C.KL=FIFGE(MBFA,ACDR.C,K,ACDR.C,K,MBFA) BRINE DISCHARGE RATE TO UPPER AQUIFER; WITH CLOSURE (CU CM/YR)
A ACDR.C.K=DCBPHA.K*NBPH*ANCC.K/(1.+(DCBPHA.K*DCBPHB.K*ANCC.K)) APPARENT NUMBER OF CRACKS REDUCED BY CLOSURE
S RCVR.C.K=ACDR.C.K/NC.C.K REFERENCE CRACK VOLUME RATE (CU CM/YR)
A ANCC.K=(LPVC.K/MCLC.K)*NC.C.K ACTIVE NUMBER OF CRACKS; REDUCED BY CLOSURE
A NC.C.K=CC*FIFGE(1E4,AVNECC.K,AVNECC.K,1E4) NUMBER OF CRACKS FROM VERTICAL DISPLACEMENT; WITH CLOSURE
N NC=1. INITIAL NUMBER OF CRACKS; WITH CLOSURE
A AVNECC.K=MAX(NECC.K,-NECC.K) ABSOLUTE VALUE OF NEC; WITH CLOSURE (CM)
A NECC.K=TE.K-CLC.K NET EXPANSION MINUS COMPACTION; WITH CLOSURE (CM)
N NECC=-1. INITIAL VALUE NECC (CM)
L PVDC.C.K=PVDC.C.J-DT*(LPVCR.C.JK) (LINEAR) PORE VOLUME DESTROYED BY COMPACTION; WITH CLOSURE (CM)
N PVDC.C=0 INITIAL VALUE PVDC.C (CM)
R LPVCR.C.KL=LPVC.C.K*EXP(-2.303*ELP*3E7*DT/EVISC.K)/DT-LPVC.C.K/DT LINEAR PORE VOLUME COMPACTION RATE; WITH CLOSURE (CM/YR)
A MCLC.K=BMCL+ACLS.C.K MAXIMUM COMPACTION LENGTH; WITH CLOSURE (CM)
A ACLS.C.K=SO.C.K/SA.K AVERAGE COMPACTION LENGTH FROM SOLUTIONING; WITH CLOSURE (CM)
L SO.C.K=SO.C.J+DT*BDRUA.C.JK SOLUTION OPENINGS; WITH CLOSURE (CU CM)
N SO=1. INITIAL VALUE SO.C (CU CM)
A LNVFC.K=0.33*LOGN(SO.C.K)-0.46 NATURAL LOG SINGLE CAVITY VOLUME FUNCTION; WITH CLOSURE (CU CM)
A SCDIAC.K=2.0*EXP(LNVFC.K) SINGLE CAVITY DIAMETER; WITH CLOSURE (CM)
S BDRAT.K=(1.4*BDRUA.C.K)/(1.4+BDRUA.C.K) BRINE DISCHARGE RATE; WITH AND WITHOUT CLOSURE
S PVRAT.K=PVDC.C.K/MCLC.K (LINEAR) PORE VOLUME RATIO
S PVRATC.K=PVDC.C.K/MCLC.K (LINEAR) PORE VOLUME RATIO; WITH CLOSURE
NOTE
PRINT H,HINR,HOUTR,SHLR,TER,TE,CL,LPV,PVPS,BDRUA,ACDR,
X NC,AVNEC,NEC,PVDC,LPVCR,EVISC,BFTEMP,MTEMP,MCL,
X ACLS,SO,LNVFC,SCDIA,CLC,LPVC,PVPS,C,BDRUA,C,ACDR,C,
X ANCC,NCC,AVNECC,NECC,PVDC,C,LPVCR,C,MCLC,ACLS,C,SOC,
X LNVFU,SCDIAC,BDRAT,PVRAT,PVRATC
PLOT NC=N/ANCC=C/AVNEC=V(0,1.0E4)/AVNECC=A(0,1.0E4)/SCDIA=D(0,1.0E4)/
X SCDIAC=C(0,1.0E4)/BDRAT=B/PVRAT=P/RCVR=R/RCVRC=H

```

## Table AR.5.3

DCP	=	0.094 CAL/GM/YR
DSHF	=	100 YEARS
UEC	=	0.9 CM/DEG C
BMCL	=	60 CM
MBFA	=	3E12 CU CM/YR
BPH	=	2E6 DYNE/SQ CM
CTL	=	6E5 CM
BV	=	1E-2 POISE
CPL	=	1E4 CM
ELP	=	1.3E8 DYNE/SQ CM
STEMP	=	20 DEG C
DA	=	7.9E10 SQ CM
CC	=	5

80-705

# Table AR.5.4A

		RCM=1E-2 CM	RCM=1E-3 CM	RCM=1E-4 CM	RCM=1E-5 CM
RFST1	PT	SCDIA	13 years(L)	15 years(L)	66 years(L)
		SCDIAC	13 years(L)	14 years(L)	69 years(L)
	TCT	AVNEC	@601 years	@601 years	950 years(L)
		AVNECC	@601 years	@601 years	@1001 years
	OT	SO	286 years(L)	@301 years	650 years(L)
RFST2		SOC	286 years(L)	@301 years	750 years(L)
	TDT		not achieved ANCC#0	not achieved ANCC#0	not achieved ANCC#0
	PT	SCDIA	13 years(L)	15 years(L)	63 years(L)
		SCDIAC	13 years(L)	15 years(L)	63 years(L)
	TCT	AVNEC	584 years(L)	@601 years	@1101 years
RFST3		AVNECC	584 years(L)	@601 years	@1201 years
	OT	SO	286 years(L)	@301 years	@801 years
		SOC	286 years(L)	@301 years	@901 years
	TDT		not achieved ANCC#0	not achieved ANCC#0	not achieved ANCC#0
	PT	SCDIA	17 years(L)	@501 years	not achieved
RFST4		SCDIAC	17 years(L)	@801 years	not achieved
	TCT	AVNEC	@601 years	@5001 years	not achieved
		AVNECC	@601 years(L)	not achieved	not achieved
	OT	SO	367 years(L)	@2901 years	not achieved
		SOC	367 years(L)	not achieved	not achieved
RFST5	TDT		not achieved ANCC#0	not achieved ANCC#0	not achieved ANCC#0
	PT	SCDIA	20 years(L)	@501 years	not achieved
		SCDIAC	20 years(L)	@501 years	not achieved
	TCT	AVNEC	680 years(L)	@5201 years	not achieved
		AVNECC	680 years(L)	not achieved	not achieved
RFST6	OT	SO	379 years(L)	@4801 years	not achieved
		SOC	380 years(L)	not achieved	not achieved
	TDT		not achieved ANCC#0	not achieved ANCC#0	not achieved ANCC#0
	PT	SCDIA	20 years(L)	@501 years	not achieved
		SCDIAC	20 years(L)	@501 years	not achieved
RFST7	TCT	AVNEC	680 years(L)	@5201 years	not achieved
		AVNECC	680 years(L)	not achieved	not achieved
	OT	SO	379 years(L)	@4801 years	not achieved
		SOC	380 years(L)	not achieved	not achieved
	TDT		not achieved ANCC#0	not achieved ANCC#0	not achieved ANCC#0

DT=1.0 yr LENGTH=1.0E4 yrs PLTPER=1.0E2 yrs PRTPER=1.0E2 yrs



# Table AR.5.4B

		RCW=1E-5 CM			
		RCW=1E-2 CM		RCW=1E-3 CM	
		RCW=1E-4 CM		RCW=1E-5 CM	
RFST1	PT SCDIA	62 years(L)	63 years(L)	63 years(L)	728 years(L)
	SCDIAC	62 years(L)	63 years(L)	63 years(L)	not achieved
	TCT AVNEC	390 years(L)	400 years(L)	400 years(L)	@13000 years
	AVNECC	390 years(L)	400 years(L)	400 years(L)	not achieved
	OT SO	250 years(L)	300 years(L)	300 years(L)	@13000 years
	SOC	250 years(L)	300 years(L)	300 years(L)	not achieved
	TDT	not achieved ANCC#0	not achieved ANCC#0	not achieved ANCC#0	ANCC=0 @7000 years
RFST2	PT SCDIA	62 years(L)	63 years(L)	63 years(L)	725 years(L)
	SCDIAC	62 years(L)	63 years(L)	63 years(L)	not achieved
	TCT AVNEC	385 years(L)	407 year(L)	407 years(L)	13250 years(L)
	AVNECC	385 years(L)	407 years(L)	407 years(L)	not achieved
	OT SO	250 years(L)	363 years(L)	363 years(L)	@13000 years(L)
	SOC	250 years(L)	363 years(L)	363 years(L)	not achieved
	TDT	not achieved ANCC#0	not achieved ANCC#0	not achieved ANCC#0	ANCC=0 @7000 years
RFST3	PT SCDIA	63 years(L)	535 years(L)	535 years(L)	not achieved
	SCDIAC	63 years(L)	@1000 years	@1000 years	not achieved
	TCT AVNEC	413 years(L)	@5000 years	@5000 years	not achieved
	AVNECC	413 years(L)	@68000 years	@68000 years	not achieved
	OT SO	260 years(L)	4500 years(L)	4500 years(L)	not achieved
	SOC	260 years(L)	@67000 years	@67000 years	not achieved
	TDT	not achieved ANCC#0	ANCC=0 @7000 years	ANCC=0 @7000 years	ANCC=0 @7000 years
RFST4	PT SCDIA	63 years(L)	530 years(L)	530 years(L)	not achieved
	SCDIAC	63 years(L)	@1000 years	@1000 years	not achieved
	TCT AVNEC	437 years(L)	5532 years(L)	5532 years(L)	not achieved
	AVNECC	439 years(L)	@66000 years	@66000 years	not achieved
	OT SO	280 years(L)	@4800 years	@4800 years	not achieved
	SOC	280 years(L)	@65000 years	@65000 years	not achieved
	TDT	not achieved ANCC#0	ANCC=0 @7000 years	ANCC=0 @7000 years	ANCC=0 @6000 years

DT=10 yrs LENGTH=1.0E5 yrs PLTPER=1.0E3 yrs PRTPER=1.0E3 yrs

# Table AR.5.4C

		RCM=1E-2 CM	RCM=1E-3 CM	RCM=1E-4 CM	RCM=1E-5 CM
RFST1	PT	SCDIA	290 years(L)	290 years(L)	294 years(L)
		SCDIAC	290 years(L)	290 years(L)	295 years(L)
	TCT	AVNEC	280 years(L)	285 years(L)	298 years(L)
		AVNECC	280 years(L)	284 years(L)	306 years(L)
	OT	SO	265 years(L)	266 years(L)	277 years(L)
RFST2		SOC	266 years(L)	266 years(L)	280 years(L)
	TOT		not achieved ANCC#0	not achieved ANCC#0	not achieved ANCC#0
	PT	SCDIA	290 years(L)	291 years(L)	297 years(L)
		SCDIAC	290 years(L)	291 years(L)	305 years(L)
	TCT	AVNEC	280 years(L)	285 years(L)	303 years(L)
RFST3		AVNECC	280 years(L)	285 years(L)	331 years(L)
	OT	SO	263 years(L)	267 years(L)	283 years(L)
		SOC	263 years(L)	267 years(L)	309 years(L)
	TOT		not achieved ANCC#0	not achieved ANCC#0	not achieved ANCC#0
	PT	SCDIA	290 years(L)	450 years(L)	@80000 years
RFST4		SCDIAC	290 years(L)	@10000 years	not achieved
	TCT	AVNEC	280 years(L)	1136 years(L)	not achieved
		AVNECC	280 years(L)	95000 years(L)	not achieved
	OT	SO	260 years(L)	1000 years(L)	not achieved
		SOC	260 years(L)	95000 years(L)	not achieved
RFST5	TOT		ANCC=0 @4.9E5 years	not achieved ANCC#0	not achieved ANCC#0
	PT	SCDIA	290 years(L)	512 years(L)	not achieved
		SCDIAC	290 years(L)	@10000 years	not achieved
	TCT	AVNEC	290 years(L)	1667 years(L)	not achieved
		AVNECC	290 years(L)	95000 years(L)	not achieved
RFST6	OT	SO	260 years(L)	1482 years(L)	not achieved
		SOC	270 years(L)	95000 years(L)	not achieved
	TOT		not achieved ANCC#0	ANCC=0 @10000 years	ANCC=0 @10000 years

OT=100 yrs LENGTH=1.0E6 yrs PLTPER=1.0E4 yrs PRTPER=1.0E4 yrs

Table AR.5.5A

LATIN HYPERCUBE SAMPLE VECTORS															
RUN NO.	X(1)	X(2)	X(3)	X(4)	PENETRATION TIME		TOTAL COLLAPSE TIME		OVERRUN TIME		TERMINATION				
					SCDIA	SCDIAC	AVNEC	AVNECC	S0	S0C	DISSOLUTION TIME				
1.	7.770E-2	107.	.395	1.852E-4	35 yrs(L)	36 yrs(L)	780 yrs(L)	781 yrs(L)	450 yrs(L)	450 yrs(L)	ANCC#0				
2.	1.556E-2	109.	2.77	4.136E-4	18 yrs(L)	18 yrs(L)	0001 yrs	0001 yrs	350 yrs(L)	350 yrs(L)	ANCC#0				
3.	2.309E-2	95.5	.661	6.238E-4	15 yrs(L)	15 yrs(L)	0701 yrs	0701 yrs	0301 yrs	0301 yrs	ANCC#0				
4.	7.881E-4	28.6	.172	2.968E-4	40 yrs(L)	41 yrs(L)	0901 yrs	0901 yrs	430 yrs(L)	430 yrs(L)	ANCC#0				
5.	.278	315.	1.46	2.131E-3	13 yrs(L)	13 yrs(L)	390 yrs(L)	390 yrs(L)	314 yrs(L)	314 yrs(L)	ANCC#0				
6.	7.055E-2	7.75	1.969E-2	1.206E-3	15 yrs(L)	15 yrs(L)	681 yrs(L)	681 yrs(L)	0301 yrs	0301 yrs	ANCC#0				
7.	5.934E-2	52.9	4.00	1.383E-4	57 yrs(L)	59 yrs(L)	895 yrs(L)	979 yrs(L)	520 yrs(L)	510 yrs(L)	ANCC#0				
8.	5.240E-2	45.5	4.66	1.111E-4	70 yrs(L)	73 yrs(L)	1079 yrs(L)	1090 yrs(L)	614 yrs(L)	733 yrs(L)	ANCC#0				
9.	4.167E-2	34.7	3.20	1.331E-2	14 yrs(L)	14 yrs(L)	668 yrs(L)	668 yrs(L)	275 yrs(L)	275 yrs(L)	ANCC#0				
10.	7.391E-2	18.0	1.73	6.844E-4	18 yrs(L)	18 yrs(L)	683 yrs(L)	683 yrs(L)	342 yrs(L)	343 yrs(L)	ANCC#0				
11.	9.496E-2	70.9	.558	7.774E-3	12 yrs(L)	12 yrs(L)	585 yrs(L)	585 yrs(L)	274 yrs(L)	274 yrs(L)	ANCC#0				
12.	8.580E-2	166.	9.796E-2	1.942E-3	14 yrs(L)	14 yrs(L)	589 yrs(L)	589 yrs(L)	273 yrs(L)	273 yrs(L)	ANCC#0				
13.	.167	77.6	.254	2.959E-3	14 yrs(L)	14 yrs(L)	486 yrs(L)	486 yrs(L)	273 yrs(L)	273 yrs(L)	ANCC#0				
14.	8.276E-2	24.2	1.652E-3	3.333E-4	33 yrs(L)	34 yrs(L)	692 yrs(L)	693 yrs(L)	371 yrs(L)	372 yrs(L)	ANCC#0				
15.	5.003E-2	146.	.290	5.634E-3	14 yrs(L)	14 yrs(L)	680 yrs(L)	680 yrs(L)	274 yrs(L)	274 yrs(L)	ANCC#0				
16.	6.697E-2	485.	.748	9.472E-4	14 yrs(L)	14 yrs(L)	594 yrs(L)	594 yrs(L)	272 yrs(L)	272 yrs(L)	ANCC#0				
17.	9.232E-2	171.	.836	4.323E-3	13 yrs(L)	13 yrs(L)	585 yrs(L)	585 yrs(L)	273 yrs(L)	273 yrs(L)	ANCC#0				
18.	2.994E-2	132.	.541	1.265E-3	14 yrs(L)	14 yrs(L)	690 yrs(L)	690 yrs(L)	273 yrs(L)	273 yrs(L)	ANCC#0				
19.	.129	58.8	.974	3.912E-3	13 yrs(L)	13 yrs(L)	0501 yrs	0501 yrs	273 yrs(L)	273 yrs(L)	ANCC#0				
20.	6.105E-2	138.	4.302E-2	2.270E-4	26 yrs(L)	28 yrs(L)	0701 yrs	736 yrs(L)	370 yrs(L)	372 yrs(L)	ANCC#0				

RFS11 DT=1.0yr LENGTH=1.0E4 yrs PLTPER=1.0E2 yrs PRTPER=1.0E2 yrs

# Table AR.5.5B

## LATIN HYPERCUBE SAMPLE VECTORS

RUN NO.	X(1)	X(2)	X(3)	X(4)	PENETRATION TIME		TOTAL COLLAPSE TIME		OVERRUN TIME		TERMINATION	
					SCDIA	SCDIAC	AVNEC	AVNECC	SO	SOC	DISSOLUTION TIME	
1.	7.770E-2	107.	.395	1.852E-4	35 yrs(L)	36 yrs(L)	8801 yrs	880 yrs(L)	490 yrs(L)	8501 yrs	ANCC#0	
2.	1.556E-2	109.	2.77	4.136E-4	21 yrs(L)	22 yrs(L)	8801 yrs	8801 yrs	387 yrs(L)	389 yrs(L)	ANCC#0	
3.	2.309E-2	95.5	.661	6.238E-4	17 yrs(L)	17 yrs(L)	783 yrs(L)	784 yrs(L)	368 yrs(L)	373 yrs(L)	ANCC#0	
4.	7.881E-4	28.6	.172	2.968E-4	34 yrs(L)	35 yrs(L)	983 yrs(L)	488 yrs(L)	488 yrs(L)	492 yrs(L)	ANCC#0	
5.	.278	315.	1.46	2.131E-3	14 yrs(L)	14 yrs(L)	390 yrs(L)	390 yrs(L)	288 yrs(L)	288 yrs(L)	ANCC#0	
6.	7.055E-2	7.75	1.969E-2	1.206E-3	15 yrs(L)	15 yrs(L)	678 yrs(L)	679 yrs(L)	8301 yrs	8301 yrs	ANCC#0	
7.	5.934E-2	52.9	4.00	1.383E-4	53 yrs(L)	55 yrs(L)	995 yrs(L)	1084 yrs(L)	683 yrs(L)	8701 yrs	ANCC#0	
8.	5.240E-2	45.5	4.66	1.111E-4	65 yrs(L)	68 yrs(L)	1192 yrs(L)	1281 yrs(L)	795 yrs(L)	888 yrs(L)	ANCC#0	
9.	4.167E-2	34.7	3.20	1.331E-2	13 yrs(L)	13 yrs(L)	683 yrs(L)	683 yrs(L)	286 yrs(L)	286 yrs(L)	ANCC#0	
10.	7.391E-2	18.0	1.73	6.844E-4	17 yrs(L)	17 yrs(L)	684 yrs(L)	684 yrs(L)	373 yrs(L)	373 yrs(L)	ANCC#0	
11.	9.496E-2	70.9	.558	7.774E-3	13 yrs(L)	13 yrs(L)	584 yrs(L)	584 yrs(L)	286 yrs(L)	286 yrs(L)	ANCC#0	
12.	8.580E-2	166.	9.796E-2	1.942E-3	14 yrs(L)	14 yrs(L)	589 yrs(L)	589 yrs(L)	290 yrs(L)	290 yrs(L)	ANCC#0	
13.	.167	77.6	.254	2.959E-3	14 yrs(L)	14 yrs(L)	486 yrs(L)	486 yrs(L)	289 yrs(L)	289 yrs(L)	ANCC#0	
14.	8.276E-2	24.2	1.652E-3	3.333E-4	29 yrs(L)	30 yrs(L)	8701 yrs	778 yrs(L)	466 yrs(L)	466 yrs(L)	ANCC#0	
15.	5.003E-2	146.	.290	5.634E-3	13 yrs(L)	13 yrs(L)	680 yrs(L)	680 yrs(L)	287 yrs(L)	287 yrs(L)	ANCC#0	
16.	6.697E-2	485.	.748	9.472E-4	14 yrs(L)	14 yrs(L)	8601 yrs	8601 yrs	294 yrs(L)	294 yrs(L)	ANCC#0	
17.	9.232E-2	171.	.836	4.323E-3	13 yrs(L)	13 yrs(L)	585 yrs(L)	585 yrs(L)	287 yrs(L)	287 yrs(L)	ANCC#0	
18.	2.994E-2	132.	.541	1.265E-3	14 yrs(L)	14 yrs(L)	692 yrs(L)	692 yrs(L)	294 yrs(L)	294 yrs(L)	ANCC#0	
19.	.129	58.8	.947	3.912E-3	14 yrs(L)	14 yrs(L)	8501 yrs	8501 yrs	287 yrs(L)	287 yrs(L)	ANCC#0	
20.	6.105E-2	138.	4.302E-2	2.270E-4	28 yrs(L)	28 yrs(L)	791 yrs(L)	795 yrs(L)	479 yrs(L)	484 yrs(L)	ANCC#0	

RFST2 DT=1.0 yr LENGTH=1.0E4 yrs PLTPER=1.0E2 yrs PRTPER=1.0E2 yrs

# Table AR.5.5C

## LATIN HYPERCUBE SAMPLE VECTORS

RUN NO.	X(1)		X(2)	X(3)	X(4)	PENETRATION TIME			TOTAL COLLAPSE TIME			OVERRUN TIME		TERMINATION	
	DCP	BMCL		CC	RCW	SCDIA	SCDIAC		AVNEC	AVNECC		S0	SOC		DISSOLUTION TIME
1.	7.770E-2	107.		.395	1.852E-4	@81000 yrs	not achieved		not achieved	not achieved		not achieved	not achieved		@73000 yrs
2.	1.556E-2	109.		2.77	4.136E-4	not achieved	not achieved		not achieved	not achieved		not achieved	not achieved		@7000 yrs
3.	2.309E-2	95.5		.661	6.238E-4	@3000 yrs	not achieved		@82000 yrs	not achieved		@81000 yrs	not achieved		@9000 yrs
4.	7.881E-4	28.6		.172	2.968E-4	not achieved	not achieved		not achieved	not achieved		not achieved	not achieved		@10000 yrs
5.	.278	315.		1.46	2.131E-3	311 yrs(L)	458 yrs(L)		1256 yrs(L)	19530 yrs(L)		1200 yrs(L)	17300 yrs(L)		@39000 yrs
6.	7.055E-2	7.75		1.969E-2	1.206E-3	not achieved	not achieved		not achieved	not achieved		not achieved	not achieved		@5000 yrs
7.	5.934E-2	52.9		4.00	1.383E-4	@40000 yrs	not achieved		not achieved	not achieved		not achieved	not achieved		@6000 yrs
8.	5.240E-2	45.5		4.66	1.111E-4	@74000 yrs	not achieved		not achieved	not achieved		not achieved	not achieved		@7000 yrs
9.	4.167E-2	34.7		3.20	1.331E-2	63 yrs(L)	63 yrs(L)		510 yrs(L)	513 yrs(L)		250 yrs(L)	250 yrs(L)		ANCC#0
10.	7.391E-2	18.0		1.73	6.844E-4	@6000 yrs	not achieved		@37000 yrs	not achieved		@39000 yrs	not achieved		@8000 yrs
11.	9.496E-2	70.9		.558	7.774E-3	70 yrs(L)	71 yrs(L)		650 yrs(L)	708 yrs(L)		33 yrs(L)	330 yrs(L)		@53000 yrs
12.	8.580E-2	166.		9.796E-2	1.942E-3	695 yrs(L)	not achieved		@19000 yrs	not achieved		@18000 yrs	not achieved		@7000 yrs
13.	.167	77.6		.245	2.959E-3	406 yrs(L)	@33000 yrs		3476 yrs(L)	@51000 yrs		3300 yrs(L)	@50000 yrs		@72000 yrs
14.	8.276E-2	24.2		1.652E-3	3.333E-4	not achieved	not achieved		not achieved	not achieved		not achieved	not achieved		@7000 yrs
15.	5.003E-2	146.		.290	5.634E-3	96 yrs(L)	130 yrs(L)		1320 yrs(L)	1423 yrs(L)		@1000 yrs	1250 yrs(L)		@27000 yrs
16.	6.697E-2	485.		.748	9.472E-4	497 yrs(L)	764 yrs(L)		@16000 yrs	not achieved		@15000 yrs	not achieved		@7000 yrs
17.	9.232E-2	171.		.836	4.323E-3	79 yrs(L)	91 yrs(L)		1231 yrs(L)	1269 yrs(L)		500 yrs(L)	@1000 yrs		ANCC#0
18.	2.994E-2	132.		.541	1.265E-3	678 yrs(L)	@10000 yrs		@14000 yrs	not achieved		13400 yrs(L)	not achieved		@10000 yrs
19.	.129	58.8		.974	3.912E-3	94 yrs(L)	166 yrs(L)		1257 yrs(L)	1392 yrs(L)		@1000 yrs	1230 yrs(L)		@78000 yrs
20.	6.105E-2	138.		4.302E-2	2.270E-4	not achieved	not achieved		not achieved	not achieved		not achieved	not achieved		@7000 yrs

RFST3 DT=10yrs LENGTH=1.0E5yrs PLTPER=1.0E3yrs PRTPER=1.0E3yrs

# Table AR.5.5D

## LATIN HYPERCUBE SAMPLE VECTORS

RUN NO.	DCP	X(1)	X(2)	X(3)	X(4)	PENETRATION TIME			TOTAL COLLAPSE TIME			OVERRUN TIME		TERMINATION	
						SCG1A	SCD1AC	AVNEC	AVNECC	S0	SOC				
1.	7.770E-2	107.	.395	1.852E-4	.081000 yrs	not achieved	not achieved	not achieved	not achieved	not achieved	not achieved	not achieved	not achieved	@6000 yrs	@6000 yrs
2.	1.556E-2	109.	2.77	4.136E-4	1908 yrs(L)	not achieved	not achieved	65978 yrs(L)	not achieved	@65000 yrs	not achieved	@65000 yrs	not achieved	@10000 yrs	@10000 yrs
3.	2.309E-2	95.5	.661	6.238E-4	@3000 yrs	not achieved	not achieved	@82000 yrs	not achieved	@81000 yrs	not achieved	@10000 yrs	not achieved	@10000 yrs	@10000 yrs
4.	7.881E-4	28.6	.172	2.968E-4	not achieved	not achieved	not achieved	not achieved	not achieved	not achieved	not achieved	not achieved	not achieved	@10000 yrs	@10000 yrs
5.	.278	315.	1.46	2.131E-3	125 yrs(L)	462 yrs(L)	1448 yrs(L)	@20000 yrs	not achieved	1500 yrs(L)	19500 yrs(L)	@52000 yrs	not achieved	@5000 yrs	@52000 yrs
6.	7.055E-2	7.75	1.969E-2	1.206E-3	@7000 yrs	not achieved	not achieved	not achieved	not achieved	not achieved	not achieved	@6000 yrs	not achieved	@6000 yrs	@6000 yrs
7.	5.934E-2	52.9	4.00	1.383E-4	@39000 yrs	not achieved	not achieved	not achieved	not achieved	not achieved	not achieved	@7000 yrs	not achieved	@7000 yrs	@7000 yrs
8.	5.240E-2	45.5	4.66	1.111E-4	@72000 yrs	not achieved	not achieved	not achieved	not achieved	not achieved	not achieved	not achieved	not achieved	not achieved	not achieved
9.	4.167E-2	34.7	3.20	1.331E-2	64 yrs(L)	64 yrs(L)	544 yrs(L)	547 yrs(L)	330 yrs(L)	330 yrs(L)	330 yrs(L)	330 yrs(L)	330 yrs(L)	330 yrs(L)	330 yrs(L)
10.	7.391E-2	18.0	1.73	6.844E-4	@6000 yrs	not achieved	not achieved	@40000 yrs	not achieved	@39000 yrs	not achieved	@6000 yrs	not achieved	@6000 yrs	@6000 yrs
11.	9.496E-2	70.9	.558	7.774E-3	74 yrs(L)	78 yrs(L)	834 yrs(L)	@1000 yrs	not achieved	500 yrs(L)	500 yrs(L)	500 yrs(L)	500 yrs(L)	500 yrs(L)	500 yrs(L)
12.	8.580E-2	166.	9.796E-2	1.942E-3	688 yrs(L)	not achieved	@19000 yrs	not achieved	not achieved	@18000 yrs	not achieved	@7000 yrs	not achieved	@7000 yrs	@7000 yrs
13.	.167	77.6	.254	2.959E-3	405 yrs(L)	@3000 yrs	3725 yrs(L)	@50000 yrs	not achieved	3500 yrs(L)	49500 yrs(L)	@76000 yrs	not achieved	@76000 yrs	@76000 yrs
14.	8.276E-2	24.2	1.652E-3	3.333E-4	not achieved	not achieved	not achieved	not achieved	not achieved	not achieved	not achieved	@6000 yrs	not achieved	@6000 yrs	@6000 yrs
15.	5.003E-2	146.	.290	5.634E-3	114 yrs(L)	142 yrs(L)	1459 yrs(L)	1717 yrs(L)	1300 yrs(L)	1800 yrs(L)	1800 yrs(L)	@71000 yrs	not achieved	@71000 yrs	@71000 yrs
16.	6.697E-2	485.	.748	9.472E-4	497 yrs(L)	764 yrs(L)	@16000 yrs	not achieved	not achieved	@15000 yrs	not achieved	@7000 yrs	not achieved	@7000 yrs	@7000 yrs
17.	9.232E-2	171.	.836	4.323E-3	92 yrs(L)	111 yrs(L)	1300 yrs(L)	1428 yrs(L)	1300 yrs(L)	300 yrs(L)	1300 yrs(L)	ANCC#0	not achieved	ANCC#0	ANCC#0
18.	2.994E-2	132.	.541	1.265E-3	675 yrs(L)	@10000 yrs	14768 yrs(L)	not achieved	not achieved	13660 yrs(L)	not achieved	@10000 yrs	not achieved	@10000 yrs	@10000 yrs
19.	.129	58.8	.974	3.912E-3	112 yrs(L)	177 yrs(L)	1345 yrs(L)	1705 yrs(L)	1330 yrs(L)	1500 yrs(L)	1500 yrs(L)	ANCC#0	not achieved	ANCC#0	ANCC#0
20.	6.105E-2	138.	4.302E-2	2.270E-4	not achieved	not achieved	not achieved	not achieved	not achieved	not achieved	not achieved	@7000 yrs	not achieved	@7000 yrs	@7000 yrs

RFS14 DT=10yrs LENGTH=1.0E5yrs PLTPER=1.0E3yrs PRTPER=1.0E3yrs

# Table AR.5.5E

LATIN HYPERCUBE SAMPLE VECTORS

RUN NO.	DCP	X(1)	X(2)	X(3)	X(4)	PENETRATION TIME		TOTAL COLLAPSE TIME		OVERRUN TIME		TERMINATION
						SCDIA	SCDIAC	AVREC	AVNECC	SO	SOC	
1.	7.70E-2	107.		.395	1.852E-5	not achieved	not achieved	not achieved	not achieved	not achieved	not achieved	@10000 yrs
2.	1.556E-2	109.		2.77	4.136E-5	@9.9E5 yrs	not achieved	not achieved	not achieved	not achieved	not achieved	@10000 yrs
3.	2.309E-2	95.5		.661	6.238E-5	not achieved	not achieved	not achieved	not achieved	not achieved	not achieved	@10000 yrs
4.	7.881E-4	28.6		.172	2.968E-5	not achieved	not achieved	not achieved	not achieved	not achieved	not achieved	@10000 yrs
5.	.278	315.		1.46	2.131E-4	3700 yrs(L)	not achieved	@6.6E5 yrs	not achieved	@6.6E5 yrs	not achieved	@10000 yrs
6.	7.055E-2	7.75		1.969E-2	1.206E-4	not achieved	not achieved	not achieved	not achieved	not achieved	not achieved	@10000 yrs
7.	5.934E-2	52.9		4.00	1.383E-5	not achieved	not achieved	not achieved	not achieved	not achieved	not achieved	@10000 yrs
8.	5.240E-2	45.5		4.66	1.111E-5	not achieved	not achieved	not achieved	not achieved	not achieved	not achieved	@10000 yrs
9.	4.167E-2	34.7		3.20	1.331E-3	500 yrs(L)	6000 yrs(L)	1250 yrs(L)	20320 yrs(L)	1050 yrs(L)	13300 yrs(L)	@50000 yrs
10.	7.391E-2	18.0		1.73	6.844E-5	not achieved	not achieved	not achieved	not achieved	not achieved	not achieved	@10000 yrs
11.	9.496E-2	70.9		.558	7.774E-4	5150 yrs(L)	not achieved	58060 yrs(L)	not achieved	56600 yrs(L)	not achieved	@10000 yrs
12.	8.580E-2	166.		9.796E-2	1.942E-4	@1.9E5 yrs	not achieved	not achieved	not achieved	not achieved	not achieved	@10000 yrs
13.	.167	77.6		.254	2.959E-4	@5.0E4 yrs	not achieved	not achieved	not achieved	not achieved	not achieved	@10000 yrs
14.	8.276E-2	24.2		1.652E-3	3.333E-5	not achieved	not achieved	not achieved	not achieved	not achieved	not achieved	@10000 yrs
15.	5.003E-2	146.		.290	5.634E-4	6800 yrs(L)	not achieved	@2.3E5 yrs	not achieved	@2.3E5 yrs	not achieved	@10000 yrs
16.	6.697E-2	485.		.784	9.472E-5	@8.0E4 yrs	not achieved	not achieved	not achieved	not achieved	not achieved	@10000 yrs
17.	9.232E-2	171.		.836	4.323E-4	6000 yrs(L)	not achieved	1700 yrs(L)	not achieved	@1.7E5 yrs	not achieved	@10000 yrs
18.	2.994E-2	132.		.541	1.265E-4	@1.5E5 yrs	not achieved	not achieved	not achieved	not achieved	not achieved	@10000 yrs
19.	.129	58.8		.974	3.912E-4	17500 yrs(L)	not achieved	@2.5E5 yrs	not achieved	@2.5E5 yrs	not achieved	@10000 yrs
20.	6.105E-2	138.		4.302E-2	2.270E-5	not achieved	not achieved	not achieved	not achieved	not achieved	not achieved	@10000 yrs

REST4 DT=100 yrs LENGTH=1.0E6 yrs PLTPER=1.0E4 yrs PRTPER=1.0E4 yrs

# Table AR.5.5F

LATIN HYPERCUBE SAMPLE VECTORS											
RUN NO.	X(1)	X(2)	X(3)	X(4)	PENETRATION TIME		TOTAL COLLAPSE TIME		OVERRUN TIME		TERMINATION
					SCDIA	SCDIAC	AVNEC	AVNECC	S0	SOC	DISSOLUTION TIME
1.	7.770E-2	107.	.395	1.852E-5	382 yrs(L)*	595 yrs(L)*	5820 yrs(L)*	66900 yrs(L)*	6293 yrs(L)*	70540 yrs(L)*	ANCC#0*
2.	1.556E-2	109.	2.77	4.136E-5	167 yrs(L)	171 yrs(L)	2392 yrs(L)	3094 yrs(L)	@1901 yrs	2950 yrs(L)	ANCC#0
3.	2.309E-2	95.5	.661	5.238E-5	81 yrs(L)	84 yrs(L)	1695 yrs(L)	1988 yrs(L)	1289 yrs(L)	@1501 yrs	ANCC#0
4.	7.831E-4	28.6	.172	2.968E-5	@301 yrs	394 yrs(L)	4093 yrs(L)	@6401 yrs	3588 yrs(L)	5794 yrs(L)	ANCC#0
5.	.278	315.	1.46	2.131E-4	20 yrs(L)	21 yrs(L)	486 yrs(L)	492 yrs(L)	385 yrs(L)	393 yrs(L)	ANCC#0
6.	7.055E-2	7.75	1.969E-2	1.205E-4	85 yrs(L)	90 yrs(L)	1185 yrs(L)	1283 yrs(L)	875 yrs(L)	970 yrs(L)	ANCC#0
7.	6.934E-2	52.9	4.00	1.383E-5	623 yrs(L)*	927 yrs(L)*	9725 yrs(L)*	not achieved*	9550 yrs(L)*	not achieved*	@15000 yrs*
8.	5.240E-2	45.5	4.66	1.111E-5	775 yrs(L)*	@5000 yrs*	13720 yrs(L)*	not achieved*	1357 yrs(L)*	not achieved*	@11000 yrs*
9.	4.167E-2	34.7	3.20	1.331E-3	14 yrs(L)	15 yrs(L)	688 yrs(L)	688 yrs(L)	295 yrs(L)	295 yrs(L)	ANCC#0
10.	7.391E-2	18.0	1.73	6.844E-5	172 yrs(L)	179 yrs(L)	1596 yrs(L)	1895 yrs(L)	1292 yrs(L)	1587 yrs(L)	ANCC#0
11.	9.496E-2	70.9	.558	7.774E-4	16 yrs(L)	16 yrs(L)	594 yrs(L)	594 yrs(L)	364 yrs(L)	364 yrs(L)	ANCC#0
12.	8.580E-2	166.	9.796E-2	1.942E-4	29 yrs(L)	30 yrs(L)	787 yrs(L)	7894 yrs(L)	486 yrs(L)	491 yrs(L)	ANCC#0
13.	.167	77.6	.254	2.959E-4	23 yrs(L)	24 yrs(L)	586 yrs(L)	589 yrs(L)	392 yrs(L)	395 yrs(L)	ANCC#0
14.	8.276E-2	24.2	1.652E-3	3.333E-5	29 yrs(L)	30 yrs(L)	@701 yrs	778 yrs(L)	466 yrs(L)	469 yrs(L)	ANCC#0
15.	5.003E-2	146.	.290	5.634E-4	17 yrs(L)	17 yrs(L)	691 yrs(L)	692 yrs(L)	371 yrs(L)	372 yrs(L)	ANCC#0
16.	6.697E-2	485.	.748	9.472E-5	36 yrs(L)	37 yrs(L)	984 yrs(L)	@1001 yrs	675 yrs(L)	@701 yrs	ANCC#0
17.	9.232E-2	171.	.836	4.323E-4	18 yrs(L)	18 yrs(L)	778 yrs(L)	779 yrs(L)	376 yrs(L)	378 yrs(L)	ANCC#0
18.	2.994E-2	132.	.541	1.265E-4	45 yrs(L)	47 yrs(L)	1088 yrs(L)	@1101 yrs	686 yrs(L)	@801 yrs	ANCC#0
19.	.129	58.3	.974	3.912E-4	21 yrs(L)	21 yrs(L)	592 yrs(L)	596 yrs(L)	384 yrs(L)	386 yrs(L)	ANCC#0
20.	6.105E-2	138.	4.302E-2	2.270E-5	304 yrs(L)*	446 yrs(L)*	4700 yrs(L)*	@14000 yrs*	6880 yrs(L)*	14782 yrs(L)*	ANCC#0
RFST2											

DT=1.0 yr    LENGTH=1.0E4 yrs    PLTPER=1.0E2 yrs    PRTPER=1.0E2 yrs  
 \*DT=10 yrs    LENGTH=1.0E5 yrs    PLTPER=1.0E3 yrs    PRTPER=1.0E3 yrs



# Table AR.5.5G

## LATIN HYPERCUBE SAMPLE VECTORS

RUN NO.	X(1) DCP	X(2) BMCL	X(3) CC	X(4) RCW	PENETRATION TIME		TOTAL COLLAPSE TIME		OVERRUN TIME		TERMINATION	
					SCDIA	SCDIAC	AVNEC	AVNECC	SO	SOC	DISSOLUTION TIME	
1.	7.770E-2	107.	.395	1.852E-4	@9.0E4 yrs	not achieved	not achieved	not achieved	not achieved	not achieved	not achieved	ANCC#0
2.	1.556E-2	109.	2.77	4.136E-4	4450 yrs(L)	not achieved	67960 yrs(L)	not achieved	67900 yrs(L)	not achieved	67900 yrs(L)	@10000 yrs
3.	2.309E-2	95.5	.661	6.238E-4	5100 yrs(L)	not achieved	8690 yrs(L)	not achieved	82900 yrs(L)	not achieved	82900 yrs(L)	@10000 yrs
4.	7.831E-4	28.6	.172	2.968E-4	@1.6E4 yrs	not achieved	not achieved	not achieved	not achieved	not achieved	not achieved	@10000 yrs
5.	.278	315.	1.46	2.131E-3	304 yrs(L)	4860 yrs(L)	320 yrs(L)	21660 yrs(L)	260 yrs(L)	20100 yrs(L)	20100 yrs(L)	@50000 yrs
6.	7.055E-2	7.75	1.969E-2	1.205E-3	@7.0E4 yrs	not achieved	@5.7E4 yrs	not achieved	@5.7E4 yrs	not achieved	not achieved	ANCC#0
7.	6.934E-2	52.9	4.00	1.383E-4	@5.0E4 yrs	not achieved	not achieved	not achieved	not achieved	not achieved	not achieved	ANCC#0
8.	5.240E-2	45.5	4.66	1.111E-4	@8.0E4 yrs	not achieved	not achieved	not achieved	not achieved	not achieved	not achieved	ANCC#0
9.	4.167E-2	34.7	3.20	1.331E-2	300 yrs(L)	300 yrs(L)	300 yrs(L)	300 yrs(L)	2500 yrs(L)	2500 yrs(L)	2500 yrs(L)	@77000 yrs
10.	7.931E-2	18.0	1.73	6.844E-4	6250 yrs(L)	not achieved	43300 yrs(L)	not achieved	@4.0E4 yrs	not achieved	not achieved	ANCC#0
11.	9.496E-2	70.9	.558	7.774E-3	294 yrs(L)	294 yrs(L)	294 yrs(L)	296 yrs(L)	2500 yrs(L)	2500 yrs(L)	2500 yrs(L)	@70000 yrs
12.	8.580E-2	166.	9.796E-2	1.942E-3	1900 yrs(L)	not achieved	8500 yrs(L)	not achieved	16300 yrs(L)	not achieved	not achieved	ANCC#0
13.	.167	77.6	.254	2.959E-3	400 yrs(L)	7100 yrs(L)	700 yrs(L)	64000 yrs(L)	6000 yrs(L)	61000 yrs(L)	61000 yrs(L)	@90000 yrs
14.	8.276E-2	24.2	1.652E-3	3.333E-4	not achieved	not achieved	not achieved	not achieved	1667 yrs(L)	not achieved	not achieved	ANCC#0
15.	5.003E-2	146.	.290	5.634E-3	300 yrs(L)	400 yrs(L)	320 yrs(L)	700 yrs(L)	3000 yrs(L)	680 yrs(L)	680 yrs(L)	ANCC#0
16.	6.697E-2	405.	.748	9.472E-4	1400 yrs(L)	ot achieved	15000 yrs(L)	not achieved	15000 yrs(L)	not achieved	not achieved	ANCC#0
17.	9.232E-2	171.	.836	4.323E-3	300 yrs(L)	425 yrs(L)	304 yrs(L)	890 yrs(L)	2341 yrs(L)	852 yrs(L)	852 yrs(L)	ANCC#0
18.	2.994E-2	132.	.541	1.265E-3	1481 yrs(L)	not achieved	13190 yrs(L)	740 yrs(L)	2890 yrs(L)	not achieved	not achieved	ANCC#0
19.	.129	53.8	.974	3.912E-3	300 yrs(L)	428 yrs(L)	305 yrs(L)	1370 yrs(L)	2870 yrs(L)	1335 yrs(L)	1335 yrs(L)	ANCC#0
20.	6.105E-2	138.	4.302E-2	2.270E-4	@3.1E5 yrs	not achieved	not achieved	not achieved	not achieved	not achieved	not achieved	ANCC#0

RFST4 DT=100 yrs LENGTH=1.0E6 yrs PLTPER=1.0E4 yrs PRTPER=1.0E4 yrs

Table AR.5.7

```

*****
* DATE OF RUN          RUN IDENTIFICATION
* CLTST-CL LOOP TEST PROGRAM
* BMCL=                (CM)
* BCU=                 (CM)
* MBFA=3E12            (CU CM/YR)
* MBPH=2E6             (DYNE/SQ CM)
* DT=
* LENGTH=
* PRTPER=
* PLTPER=
* DVERRUN TIME AT
* OPTION 1 FOR BC WITH DECAY OF BPH
* OPTION 1 FOR MCC WITH DECAY OF BPH
* DISSOLUTION WITH AND WITHOUT CRACK CLOSURE (DISSEC WORKING LIST-OPTION 1 FOR BC AND MCC WITH DECAY OF BPH)
*****
A  TE=TEC
C  TEC=0
L  CL=K*BMCL-J-LPV.J          COMPACTION LENGTH (CM)
N  CL=0                        INITIAL VALUE CL (CM)
A  LPV=K*BMCL-PVPS.K-PVDC.K    LINEAR PORE VOLUME (CM)
C  BMCL=0                      BACKFILL MAXIMUM COMPACTION LENGTH (CM)
L  PVPS=K*PVPS.J-DT*(BDRUA.JK)/DA (LINEAR) PORE VOLUME PRODUCED BY SOLUTIONING (CM)
N  PVPS=0                      INITIAL (LINEAR) PORE VOLUME PRODUCED BY SOLUTIONING (CU CM)
B  BDRUA=KL*FIFGE(MBFA,ACDR.K,ACDR.K,MBFA) BRINE DISCHARGE RATE TO UPPER AQUIFER (CU CM/YR)
C  MBFA=3E12                    MAXIMUM BRINE FLOW IN AQUIFER (CU CM/YR)
A  ACDRC=K*DCBPHA.K*MBPH*NC.K/(1.-(DCBPHA.K*DCBPHB.K*NC.K)) (TOTAL) APPARENT CRACK DISCHARGE RATE (CU CM/YR)
B  DCBPHB=K*(3ET*BCU*RCU*BMCL*CTL)/(12*BV*CPL) DIMENSIONAL CONSTANT BRINE PRESSURE HEAD (SQ CM/DYNE)*(CU CM/YR)
A  DCBPHB=K*MBPH/MBFA          BRINE PRESSURE FLOW RATIO (DYNE/SQ CM)/(CU CM/YR)
C  MBPH=2E6                    INITIAL BRINE PRESSURE HEAD (DYNE/SQ CM)
N  BCU=1E-3                    REFERENCE CRACK WIDTH (CM)
C  CTL=6E5                     CRACK TRACE LENGTH (CM)
C  BV=1E-2                     BRINE VISCOSITY (POISE)
C  CPL=1E4                     CRACK PATH LENGTH (CM)
A  NC=K*NCN+DA*AVNEC.K/(RCU*CTL*CPL) NUMBER OF CRACKS FROM VOLUME OF REFERENCE CRACK
C  NCN=0                       INITIAL NUMBER OF CRACKS
A  AVNEC=K*MAX(NEC.K,-NEC.K)    ABSOLUTE VALUE OF NEC (CM)
A  NEC=K*TE.K-CLC.K            NET EXPANSION MINUS COMPACTION (CM)
N  NEC=0                       INITIAL NEC (CM)
L  PVDC=K*PVDC.J-DT*(LPVCR.JK) (LINEAR) PORE VOLUME DESTROYED BY COMPACTION (CM)
N  PVDC=0                       INITIAL VALUE OF PVDC (CM)
B  LPVCR=KL*LPV.K*EXP(-2.303*ELP*3E7*DT/EVISC.K)/DT-LPV.K/DT LINEAR PORE VOLUME COMPACTION RATE (CM/YR)
C  ELP=1.3E8                    EFFECTIVE LOAD PRESSURE (DYNE/SQ CM)
A  EVISC=K*TABLE(EVTAB,BTEMP.K,0.250,25) EFFECTIVE VISCOSITY (POISE)
T  EVTAB=1.15E19,7.08E18,0.47E18,2.81E18,1.78E18,1.26E18,
X  8.91E17,6.61E17,5.01E17,3.80E17,3.02E17 TABLE VALUES OF EVISC (POISE)
C  BTEMP=20.                    SURFACE TEMPERATURE (DEG C)
A  BTEMP=K*BTEMPC
C  BTEMPC=32.
A  MCL=K*BMCL-ACLS.K          MAXIMUM COMPACTION LENGTH (CM)
A  ACLS=K*SO.K/SA.K           AVERAGE COMPACTION LENGTH FROM SOLUTIONING (CM)
L  SO=K*SO.J-DT*BDRUA.JK      SOLUTION OPENINGS (CU CM)
A  SA=K*DA                    SOLUTIONING AREA (SQ CM)
C  DA=7.9E10                  DEPOSITORY AREA (SQ CM)
N  SO=0                        INITIAL VALUE OF SO (CU CM)
A  SCDIA=K*2.0*EXP(LNVFC.K)    SINGLE CAVITY DIAMETER (CM)
L  CLC=K*BMCL-J-LPVC.J        COMPACTION LENGTH; WITH CLOSURE (CM)
N  CLC=0                       INITIAL VALUE CLC (CM)
A  LPVC=K*BMCL-PVPS.C-K-PVDC.C (LINEAR) PORE VOLUME, WITH CLOSURE (CM)
L  PVPS.C=K*PVPS.C-J-DT*(BDRUA.CJK)/DA (LINEAR) PORE VOLUME PRODUCED BY SOLUTIONING; WITH C
N  PVPS.C=0                    INITIAL VALUE PVPS.C (CM)
B  BDRUA.C=KL*FIFGE(MBFA,ACDR.C,ACDR.C,MBFA) BRINE DISCHARGE RATE TO UPPER AQUIFER, WITH CLOSURE (CU CM/YR)
A  ACDRC.C=K*DCBPHA.K*MBPH*ANCC.K/(1.-(DCBPHA.K*DCBPHB.K*ANCC.K)) APPARENT NUMBER OF CRACKS REDUCED BY CLOSURE
B  ANCC=K*NCN+DA*AVNECC.K/(RCU*CTL*CPL) NUMBER OF CRACKS FROM VOLUME OF REFERENCE CRACK; WITH CLOSURE
C  NCN=0                       INITIAL NUMBER OF CRACKS, WITH CLOSURE
A  AVNECC=K*MAX(NECC.K,-NECC.K) ABSOLUTE VALUE OF NEC; WITH CLOSURE (CM)
A  NECC=K*TE.K-CLC.C          NET EXPANSION MINUS COMPACTION; WITH CLOSURE (CM)
N  NECC=0                      INITIAL VALUE NECC (CM)
L  PVDC.C=K*PVDC.C-J-DT*(LPVCR.CJK) (LINEAR) PORE VOLUME DESTROYED BY COMPACTION; WITH CLOSURE (CM)
N  PVDC.C=0                    INITIAL VALUE PVDC.C (CM)
B  LPVCR.C=KL*LPVC.K*EXP(-2.303*ELP*3E7*DT/EVISC.K)/DT-LPV.C.K/DT LINEAR PORE VOLUME COMPACTION RATE; WITH CLOSURE (CM/YR)
A  MCLC=K*BMCL-ACLSC.K        MAXIMUM COMPACTION LENGTH; WITH CLOSURE (CM)
A  ACLSC=K*SO.C/SA.C          AVERAGE COMPACTION LENGTH FROM SOLUTIONING; WITH CLOSURE (CM)
L  SO.C=K*SO.C-J-DT*BDRUA.CJK SOLUTION OPENINGS, WITH CLOSURE (CU CM)
N  SO.C=0                      INITIAL VALUE SOC (CU CM)
A  SCDIAC=K*2.0*EXP(LNVFC.C)   SINGLE CAVITY DIAMETER; WITH CLOSURE (CM)
B  BDRAT=K*(1.-(BDRUA.CK)/(1.-(BDRUA.K)) BRINE DISCHARGE RATE; WITH AND WITHOUT CLOSURE
NOTE
PRINT TE,CL,LPV,PVPS,BDRUA,ACDR,
X  NC,AVNEC,NEC,PVDC,LPVCR,EVISC,BTEMP,MCL,
X  ACLS,SO,SCDIA,CLC,LPVC,PVPS,C,BDRUA,C,ACDR,C,
X  ANCC,NEC,AVNECC,NECC,PVDC,C,LPVCR,C,MCLC,ACLSC,SOC,
X  SCDIAC,BDRAT
PLOT NC=N/ANCC,C/AVNECC,V(0,1.0E4)/AVNECC+A(0,1.0E4)/SCDIA*D(0,1.0E4)/
X  SCDIAC*S(0,1.0E4)/BDRAT*B
SPEC DT=0.1/LENGTH=1.0E3/PLTPER=10/PRTPER=20
RUN  *DISS WITH AND WITHOUT CC*-----*DISSOLUTION WITH AND WITHOUT CRACK CLOSURE*
EOI ENCOUNTERED.
/

```

### Figure AR.5.1

[illegible]

```
*****
DATE OF RUN OCT 16/79 RUN IDENTIFICATION 10-16-79-3
REFERENCE SET 2-DISSC WORKING LIST FOR OPTION 1 NCC WITH DECAY OF BPH
DCP= 0.094 (CAL/GM/YR)
BMCL=60 (CM)
RCW= 1E-3 (CM)
MGRF=3E12 (CU CM/YR)
NBPH=2E6 (DYNE/SQ CM)
DT= 1
LENGTH= 1.0E4
PTRPER= 1.0E2
PLTPER= 1.0E2
OVERRUN TIME AT
OPTION 1 FOR NC WITH DECAY OF BPH
OPTION 1 FOR NCC WITH DECAY OF BPH
DISSOLUTION WITH AND WITHOUT CRACK CLOSURE (DISSC WORKING LIST-OPTION 1 FOR NC AND NCC WITH DECAY OF BPH)
*****
```

NC=N, ANCC=C, AVNEC=V, AVNECC=A, SCDIA=D, SCDIAC=S, BDRAT=B, PRAT=P  
RCVR=R, RCVRC=H

```
*****
DATE OF RUN OCT 17, 1979 RUN IDENTIFICATION 10-17-79-1
REFERENCE SET 4-DISSCC WORKING LIST FOR OPTION 2 NC, NCC WITH DECAY OF BPH
DCP= 0.094 (CAL/GM/YR)
BMCL= 60 (CM)
RCM= 1E-3 (CM)
CC= 5 (PER CM)
MAFA= 3E12 (CU CM /YR)
NBPH=2E6 (DYNE/SQ CM)
DT= 1
LENGTH= 1.0E4
PTRPER= 1.0E2
PLTPER= 1.0E2
OVERRUN TIME AT
OPTION 2 FOR NC WITH DECAY OF BPH
OPTION 2 FOR NCC WITH DECAY OF BPH
DISSOLUTION WITH AND WITHOUT CRACK CLOSURE (DISSCC WORKING LIST-OPTION 2 FOR NC AND NCC WITH DECAY OF BPH)
*****
```



NC=N, ANCC=C, AVNEC=V, AVNECC=A, SCDIA=D, SCDIAC=S, BDRAT=B, PVRAT=P  
RCVR=R, RCVRC=H

Figure AR.5.3A

0.00M	200.00M	400.00M	600.00M	800.00M	N
0.00M	10.00M	20.00M	30.00M	40.00M	C
0.00T	2.50T	5.00T	7.50T	10.00T	VADS
.98	.98	.99	.99	1.00	B
0.00	.25	.50	.75	1.00	P
0.00B	1.00B	2.00B	3.00B	4.00B	RH
1.0NP-	- - B -	- - - - - R -	- - - - -	- - - - -	. NCVADS, RH
NCV	P	.	.	.	B VA, NRH
N C	V P.	.	.	.	B VA, NRH
N	C	P V	.	.	B VA, NRH
N	C	.	P	.	B VA, NRH
RN	C	.	.	V	B VA, RH
RN	C	.	P	.	B RH
RN	C	.	P	.	B RH
RN	C	.	P	.	B RH
R N	C	.	P	.	B RH
1001.0R	N - - - - C -	- - - - - P -	- - - - -	- - - - -	B RH
R N	.	.	P	.	B RH
R N	.	.	P	.	B RH
R N	.	.	P	.	B RH
R N	.	.	P	.	B RH
R N	.	.	P	.	B RH
R N	.	.	P	.	B RH
R N	.	.	P	.	B RH
R N	.	.	P	.	B RH
2001.0R	- - N - - - C -	- - - - -	- - - - -	- - - - -	B RH
R N	.	.	P	.	B RH
R N	.	.	P	.	B RH
R N	.	.	P	.	B RH
R N	.	.	P	.	B RH
R N	.	.	P	.	B RH
R N	.	.	P	.	B RH
R N	.	.	P	.	B RH
R N	.	.	P	.	B RH
3001.0R	- - N - - - C -	- - - - -	- - - - -	- - - - -	B RH
R N	.	.	P	.	B RH
R N	.	.	P	.	B RH
R N	.	.	P	.	B RH
R N	.	.	P	.	B RH
R N	.	.	P	.	B RH
R N	.	.	P	.	B RH
R N	.	.	P	.	B RH
R N	.	.	P	.	B RH
4001.0R	- - N - - - C -	- - - - -	- - - - -	- - - - -	B RH
R N	.	.	P	.	B RH
R N	.	.	P	.	B RH
R N	.	.	P	.	B RH
R N	.	.	P	.	B RH
R N	.	.	P	.	B RH
R N	.	.	P	.	B RH
R N	.	.	P	.	B RH
R N	.	.	P	.	B RH
5001.0R	- - N - - - C -	- - - - -	- - - - -	- - - - -	B RH

\*\*\*\*\*  
 DATE OF RUN 12 Dec 1979 RUN IDENTIFICATION December 12, 1979-1  
 REFERENCE SET 2-DISSCC WORKING LIST FOR OPTION 1 NC,NCC WITH DECAY OF BPH  
 DCP= 0.094 (CAL/GM/YR)  
 BMCL= 60 (CM)  
 RCW= 1E-2 (CM)  
 MBFA=3E12 (CU CM/YR)  
 NBPH=2E6 (DYNE/SQ CM)  
 DT= 1  
 LENGTH= 1.0E4  
 PRTPER= 1.0E2  
 PLTPER= 1.0E2  
 OVERRUN TIME AT  
 OPTION 1 FOR NC WITH DECAY OF BPH  
 OPTION 1 FOR NCC WITH DECAY OF BPH  
 DISSOLUTION WITH AND WITHOUT CRACK CLOSURE (DISSCC WORKING LIST-OPTION 1 FOR NC AND NCC WITH DECA  
 \*\*\*\*\*

NC=N, ANCC=C, AVNEC=V, AVNECC=A, SCDIA=D, SCDIAC=S, BDRAT=B, PVRAT=P  
RCVR=R, RCVRC=H

Figure AR.5.3B

	0.00B	2.00B	4.00B	6.00B	8.00B N
0.00M	100.00M	200.00M	300.00M	400.00M C	
0.00T	2.50T	5.00T	7.50T	10.00T VADS	
.98	.98	.99	.99	1.00 B	
0.00	.25	.50	.75	1.00 P	
0.00M	10.00M	20.00M	30.00M	40.00M RH	
1.0NP-	-B-	-HR-	-B-	-NCVADS	
NV	P	.	.	B	. NC,VARH
N C	V P	.	.	B	. VA,NRH
N C	.	V	.	B	. VAP,NRH
N C	.	P	.	B	. VA,NRH
RN	C	.	V	B	. VA,RH
RN	C	P	.	B	. RH
RN	C	P	.	B	. RH
RN	C	P	.	B	. RH
RN	C	P	.	B	. RH
RN	C	P	.	B	. RH
1001.0R	N	-C-	-P-	-B.	RH
R	N	. C	P	B.	RH
R	N	. C	P	B.	RH
R	N	. C	P	B.	RH
R	N	. C	P	B.	RH
R	N	. C	P	B.	RH
R	N	. C	P	B.	RH
R	N	. C	P	B.	RH
R	N	. C	P	B.	RH
2001.0R	N	-C-	-P-	-B.	RH
R	N	. C	P	B.	RH
R	N	. C	P	B.	RH
R	N	. C	P	B.	RH
R	N	. C	P	B.	RH
R	N	. C	P	B.	RH
R	N	. C	P	B.	RH
R	N	. C	P	B.	RH
R	N	. C	P	B.	RH
3001.0R	N	-C-	-P-	-B.	RH
R	N	. C	P	B.	RH
R	N	. C	P	B.	RH
R	N	. C	P	B.	RH
R	N	. C	P	B.	RH
R	N	. C	P	B.	RH
R	N	. C	P	B.	RH
R	N	. C	P	B.	RH
R	N	. C	P	B.	RH
4001.0R	N	-C-	-P-	-B.	RH
R	N	. C	P	B.	RH
R	N	. C	P	B.	RH
R	N	. C	P	B.	RH
R	N	. C	P	B.	RH
R	N	. C	P	B.	RH
R	N	. C	P	B.	RH
R	N	. C	P	B.	RH
R	N	. C	P	B.	RH
5001.0R	N	-C-	-P-	-B.	RH

DATE OF RUN 12 Dec 1979 RUN IDENTIFICATION December 12, 1979-2  
REFERENCE SET 2-DISSCC WORKING LIST FOR OPTION 1 NC,NCC WITH DECAY OF BPH  
DCP= 0.094 (CAL/GM/YR)  
BMCL= 60 (CM)  
RCW= 1E-3 (CM)  
MBFA=3E12 (CU CM/YR)  
NBPH=2E6 (DYNE/SQ CM)  
DT= 1  
LENGTH= 1.0E4  
PRTPER= 1.0E2  
PLTPER= 1.0E2  
OVERRUN TIME AT  
OPTION 1 FOR NC WITH DECAY OF BPH  
OPTION 1 FOR NCC WITH DECAY OF BPH  
DISSOLUTION WITH AND WITHOUT CRACK CLOSURE (DISSCC WORKING LIST-OPTION 1 FOR NC AND NCC WITH DECAY

### Figure AR.5.3C

```

*****
*****
*   DATE OF RUN 12 Dec 1979RUN IDENTIFICATION December 12, 1979-3
*   REFERENCE SET 2-DISSCC WORKING LIST FOR OPTION 1 NC,NCC WITH DECAY OF BPH
*   DCP= 0.094 (CAL/GM/YR)
*   BMCL= 60 (CM)
*   RCW= 1E-4 (CM)
*   MBFA=3E12 (CU CM/YR)
*   NBPH=2E6 (DYNE/SQ CM)
*   DT= 1
*   LENGTH= 1.0E4
*   PRTPER= 1.0E2
*   PLTPER= 1.0E2
*   OVERRUN TIME AT
*   OPTION 1 FOR NC WITH DECAY OF BPH
*   OPTION 1 FOR NCC WITH DECAY OF BPH
*   DISSOLUTION WITH AND WITHOUT CRACK CLOSURE (DISSCC WORKING LIST-OPTION 1 FOR NC AND NCC WITH DECAY
*****
*****

```



NC=N,ANCC=C,AVNEC=V,AVNECC=A,SCDIA=D,SCDIAC=S,BDRAT=B,PVRAT=P  
RCVR=R,RCVRC=H

Figure AR.5.3D

0.00B	1.00B	2.00B	3.00B	4.00B	N
0.00M	10.00M	20.00M	30.00M	40.00M	C
0.00T	2.50T	5.00T	7.50T	10.00T	VADS
0.00	.25	.50	.75	1.00	BP
28.00	28.50	29.00	29.50	30.00	R
0.00	10.00	20.00	30.00	40.00	H
1.0NPC	-	-	-	-	-BR NVADS
N	P	C	H	B	R NVA,CDS
N	.	P	HC	D	R NVA,CS
VN	.	H	B	S	R VA
VN	H	B	C	P	R VA
VN	H	B	C	PS	R VA
VN	H	B	C	PS	R VA
VN	HB	C	.	S	R VA,SP
VN	HB	C	.	S	R VA,SP
VN	B	C	.	S	R VA,SP,BH
1001.0VN-B	-C-	.	.	-S-	R VA,SP,BH
VNB	C	.	.	PS	R VA,BH
VNB	C	.	.	PS	R VA,NBH
VN	C	.	.	PS	R VA,NBH
VN	C	.	.	PS	R VA,NBH
VNC	.	.	.	PS	R VAB,CH
VNC	.	.	.	PS	R VABH
VNC	.	.	.	PS	R VABH
2001.0VCN	-	-	-	-PS-	R VABH
VCN	.	.	.	PS	R VABH
C N	.	.	.	PS	R CVABH
CVN	.	.	.	PS	R CABH
CVN	.	.	.	PS	R CABH
CVN	.	.	.	PS	R CABH
CVN	.	.	.	PS	R CABH
CVN	.	.	.	PS	R CABH
CV N	.	.	.	PS	R CABH
3001.0CV-N	-	-	-	-PS-	R CABH
CV N	.	.	.	PS	R CABH
CV N	.	.	.	PS	R CABH
CV N	.	.	.	PS	R CABH
CV N	.	.	.	PS	R CABH
CV N	.	.	.	PS	R CABH
CV N	.	.	.	PS	R CABH
CV N	.	.	.	PS	R CABH
CV N	.	.	.	PS	R CABH
4001.0CV-N	-	-	-	-PS-	R CABH
CV N	.	.	.	PS	R CABH
CV N	.	.	.	PS	R CABH
CV N	.	.	.	PS	R CABH
CV N	.	.	.	PS	R CABH
CV N	.	.	.	PS	R CABH
CV N	.	.	.	PS	R CABH
CV N	.	.	.	PS	R CABH
CV N	.	.	.	PS	R CABH
5001.0CV-N	-	-	-	-PS-	R CABH
CV N	.	.	.	PS	R CABH
CV N	.	.	.	PS	R CABH
CV N	.	.	.	PS	R CABH
CV N	.	.	.	PS	R CABH
CV N	.	.	.	PS	R CABH
CV N	.	.	.	PS	R CABH
CV N	.	.	.	PS	R CABH
CV N	.	.	.	PS	R CABH
6001.0CV-N	-	-	-	-PS-	R CABH,SR
CV N	.	.	.	PS	R CABH,SR
CV N	.	.	.	PS	R CABH,SR
CV N	.	.	.	PS	R CABH,SR
CV N	.	.	.	PS	R CABH,SR
CV N	.	.	.	PS	R CABH,SR
CV N	.	.	.	PS	R CABH,SR
CV N	.	.	.	PS	R CABH,SR
7001.0CV-N	-	-	-	-PS-	R CABH,PR
CV N	.	.	.	PS	R CABH,PR
CV N	.	.	.	PS	R CABH,PR
CV N	.	.	.	PS	R CABH,PR
CV N	.	.	.	PS	R CABH,PR
CV N	.	.	.	PS	R CABH,PR
CV N	.	.	.	PS	R CABH,PR
CV N	.	.	.	PS	R CABH,PR
8001.0CV-N	-	-	-	-PS-	R CABH
CV N	.	.	.	PS	R CABH
CV N	.	.	.	PS	R CABH
CV N	.	.	.	PS	R CABH
CV N	.	.	.	PS	R CABH
CV N	.	.	.	PS	R CABH
CV N	.	.	.	PS	R CABH
CV N	.	.	.	PS	R CABH
CV N	.	.	.	PS	R CABH

\*\*\*\*\*  
 DATE OF RUN 12 Dec 1979 RUN IDENTIFICATION December 12, 1979-4  
 REFERENCE SET 2-DISSCC WORKING LIST FOR OPTION 1 NC,NCC WITH DECAY OF BPH  
 DCP=0.094 (CAL/GM/YR)  
 BMCL= 60 (CM)  
 RCM= 1E-5 (CM)  
 MBFA=3E12 (CU CM/YR)  
 NBPH=2E6 (DYNE/SQ CM)  
 DT= 1  
 LENGTH= 1.0E4  
 PRTER= 1.0E2  
 PLTER= 1.0E2  
 OVERRUN TIME AT  
 OPTION 1 FOR NC WITH DECAY OF BPH  
 OPTION 1 FOR NCC WITH DECAY OF BPH  
 DISSOLUTION WITH AND WITHOUT CRACK CLOSURE (DISSCC WORKING LIST-OPTION 1 FOR NC AND NCC WITH DECAY OF BPH)  
 \*\*\*\*\*

### Figure AR.5.3E

```

*****
DATE OF RUN 12 Dec 1979 RUN IDENTIFICATION December 12, 1979-5
REFERENCE SET 4-DISSCC WORKING LIST FOR OPTION 2 NC, NCC WITH DECAY OF BPH
DCP= 0.094 (CAL/GM/YR)
BMCL= 60 (CM)
RCW= 1E-2 (CM)
CC= 5 (PER CM)
MBFA= 3E12 (CU CM /YR)
NBPH=2E6 (DYNE/SQ CM)
DT= 1
LENGTH= 1.0E4
PRTPER= 1.0E2
PLTPER= 1.0E2
OVERRUN TIME AT
OPTION 2 FOR NC WITH DECAY OF BPH
OPTION 2 FOR NCC WITH DECAY OF BPH
DISSOLUTION WITH AND WITHOUT CRACK CLOSURE (DISSCC WORKING LIST-OPTION 2 FOR NC AND NCC WITH DECAY
*****

```

**Figure AR.5.3F**

	0.00T	20.00T	40.00T	60.00T	80.00T	
0.00	20.00	40.00	60.00	80.00	C	
0.00T	2.50T	5.00T	7.50T	10.00T	VADS	
0.00	.25	.50	.75	1.00	B	
0.00	.25	.50	.75	1.00	P	
20.00M	22.50M	25.00M	27.50M	30.00M	R	
0.00M	10.00M	20.00M	30.00M	40.00M	H	
1.0N	-C-	-	-	-	-	B NVADSP, BR
N	C	P	.	.	B	R NVA, DS
N	.	.	H	.	R	R NVA
N	.	H	SD	B	R	R NVA
N	.	H	CB.P	S	R	R NVA
N	H	B	.	P	R	R NVA
N	H.B	.	C	P	R	R NVA
N	H	.	C	.	R	R NVA
N	HB	.	C	P	S	R NVA, SR
N	B	.	C	P	R	R NVA, BH
N	B	.	C	P	R	R NVA, BH
1001.0N	-BH	-	-	-	-	R NVA
N	B	.	.	P	R	R NVA, BH
N	BH	C	.	P	R	R NVA
N	B	C	.	P	R	R NVA, BH
NVH	C	.	.	P	R	R NA, VB
NVH	C	.	.	P	R	R NA, VB
NV	C	.	.	P	R	R NA, VBH
AN	C	.	.	P	R	R NVBH
AN	C	.	.	P	R	R NVH, AB
AN	C	.	.	P	R	R NVH, AB
2001.0AN	-C	-	-	-	-	R NVH, AB
AN	C	.	.	P	R	R NVH, AB
ANVC	.	.	.	P	R	R AB, NH
ANVC	.	.	.	P	R	R AB, NH
ANC	.	.	.	P	R	R CV, ABH
ANC	.	.	.	P	R	R CV, ABH
A NV	.	.	.	P	R	R NC, ABH
A NV	.	.	.	P	R	R NC, ABH
A NV	.	.	.	P	R	R NC, ABH
ACN V	.	.	.	P	R	R ABH
3001.0AC	-NV	-	-	-	-	R ABH
AC N V	.	.	.	P	R	R ABH
AC N V	.	.	.	P	R	R ABH
AC N V	.	.	.	P	R	R ABH
AC N V	.	.	.	P	R	R ABH
AC N V	.	.	.	P	R	R ABH
AC N V	.	.	.	P	R	R ABH
AC N V	.	.	.	P	R	R ABH, PR
AC N V	.	.	.	P	R	R ABH
4001.0AC	-N	-	-	-	-	R ABH
C	N	V	.	R	P	R CABH
C	N	V	.	R	P	R CABH
C	N	V	.	R	P	R CABH
C	N	V	.	R	P	R CABH, VR
C	N	V	.	R	P	R CABH, NR
C	N	V	.	R	P	R CABH
C	N	V	.	R	P	R CABH, VP
C	N	V	.	R	P	R CABH
5001.0C	-R	-	-	-	-	R CABH
C	R	.	.	N	P	R CABH
C	.	.	.	N	P	R CABRH
C	.	.	.	N	P	R CABRH

NC=N, ANCC=C, AVNEC=V, AVNECC=A, SCDIA=D, SCDIAC=S, BDRAT=B, PVRAT=P  
RCVR=R, RCVRC=H

Figure AR.5.3G

	0.00	100.00	200.00	300.00	400.00	N
0.00	10.00	20.00	30.00	40.00	C	
0.00T	2.50T	5.00T	7.50T	10.00T	VADS	
0.00	.25	.50	.75	1.00	BP	
0.00T	10.00T	20.00T	30.00T	40.00T	RH	
1.0VN-	- C -	- - -	- - -	- - -	B VADSP, RH	
V N	P .C		H	R B	. VA, NDS	
V DN	.	P H C	B	R	. VA, DS	
V SD	N	H B. P	R	C	. VA	
V SD	.N	B	P	R C	. VA, NH	
V SD	H .B	N	PR	C	. VA	
V S DH B	.	N	C P	P	. VA, CR	
V S D	.	N	C	R P	. VA, DB, SH	
V HS D	.	N C.	R	P	. VA, SB	
V HBS D	.	C N.	R	P	. VA	
1001.0V	HB-S- -D-	C - - -	-N- - - -	-R- - - -	-P-	
V B S	D C.		N	R	P . VA, BH	
VHB S	CD	.	N	R	P . VA	
VB SC	D	.	N	R	P . VA, BH	
VB C	D	.	N	R	P . VA, CS, BH	
VB CS	D	.	N	R	P . VA, BH	
VB C S	D.	.	N	R	P . VAH	
V C S	D.	.	N	R	P VABH	
V C S	D.	.	N	R	P VABH	
VC S	D	.	N	R	P VABH	
2001.0VC-	-S- - -	-D- - - -	-N- - - -	-R- - - -	-P-	
VC S	D	.	N	R	P VABH	
VC S	D	.	N	R	P VABH	
C S	.D	.	N	R	P CVABH	
C S	.D	.	N	R	P CVABH	
C S	.D	.	N	R	P CVABH	
C S	.D	.	N	R	P CVABH	
C S	.D	.	N	R	P CVABH	
C S	.D	.	N	R	P CVABH	
C S	.D	.	N	R	P CVABH	
C S	.D	.	N	R	P CVABH	
3001.0C	-S- - -	-D- - - -	-N- - - -	-R- - - -	-P-	
C S	.D	.	N	R	P CVABH	
C S	.D	.	N	R	P CVABH	
C S	.D	.	N	R	P CVABH	
C S	.D	.	N	R	P CVABH	
C S	.D	.	N	R	P CVABH	
C S	.D	.	N	R	P CVABH	
C S	.D	.	N	R	P CVABH	
C S	.D	.	N	R	P CVABH	
C S	.D	.	N	R	P CVABH	
4001.0C	-S- - -	-D- - - -	-N- - - -	-R- - - -	-P-	
C S	.D	.	N	R	P CVABH	
C S	.D	.	N	R	P CVABH	
C S	.D	.	N	R	P CVABH	
C S	.D	.	N	R	P CVABH	
C S	.D	.	N	R	P CVABH	
C S	.D	.	N	R	P CVABH	
C S	.D	.	N	R	P CVABH	
C S	.D	.	N	R	P CVABH	
C S	.D	.	N	R	P CVABH	
5001.0C	-S- - -	-D- - - -	-N- - - -	-R- - - -	-P-	

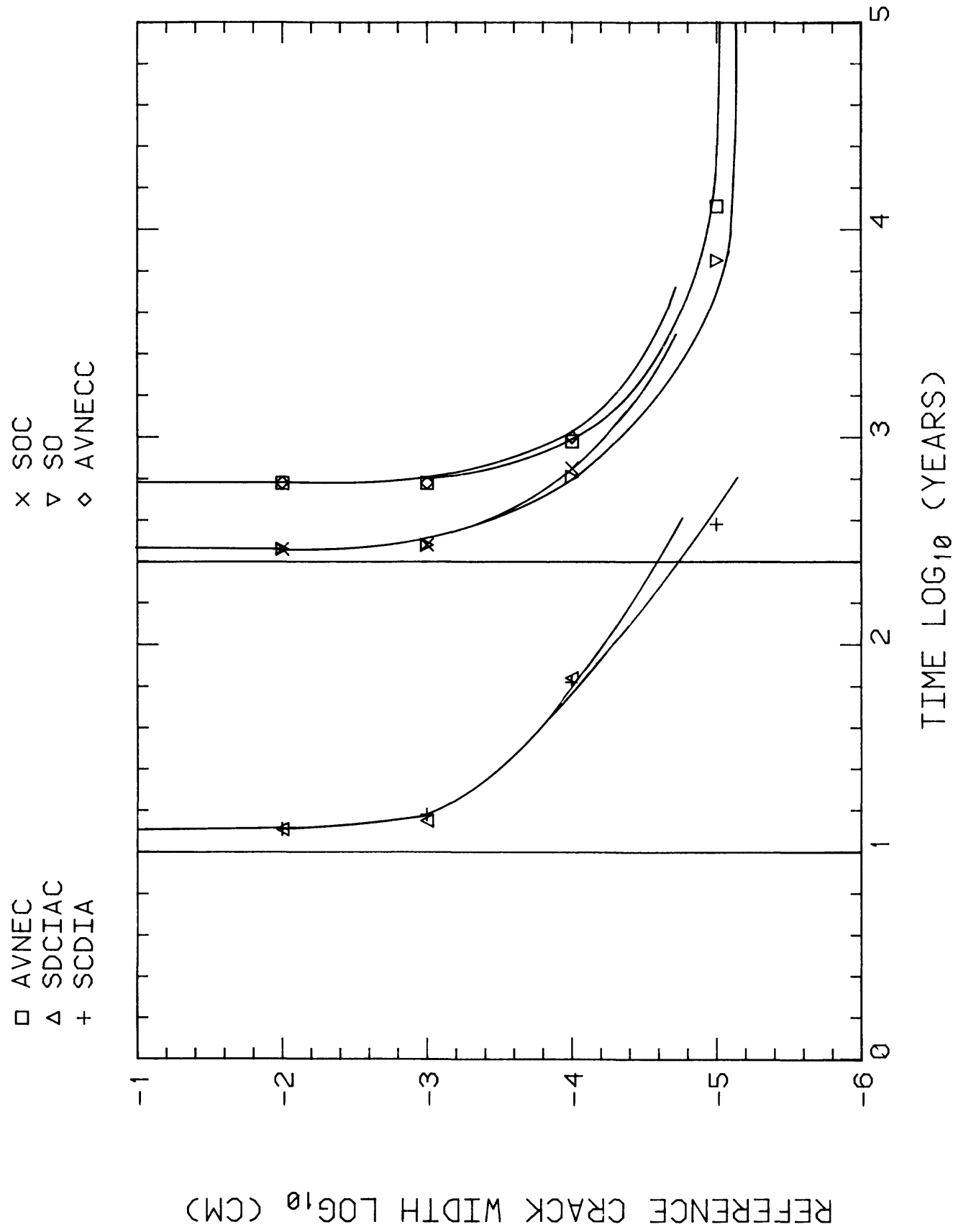
DATE OF RUN 12 Dec 1979 RUN IDENTIFICATION December 12, 1979-7  
REFERENCE SET 4-DISSCC WORKING LIST FOR OPTION 2 NC, NCC WITH DECAY OF BPH  
DCP= 0.094 (CAL/GM/YR)  
BMCL= 60 (CM)  
RCW= 1E-4 (CM)  
CC= 5 (PER CM)  
MBFA= 3E12 (CU CM /YR)  
NBPH=2E6 (DYNE/SQ CM)  
DT= 1  
LENGTH= 1.0E4  
PRTPER= 1.0E2  
PLTPER= 1.0E2  
OVERRUN TIME AT  
OPTION 2 FOR NC WITH DECAY OF BPH  
OPTION 2 FOR NCC WITH DECAY OF BPH  
DISSOLUTION WITH AND WITHOUT CRACK CLOSURE (DISSCC WORKING LIST-OPTION 2 FOR NC AND NCC WITH DECAY

**Figure AR.5.3H**

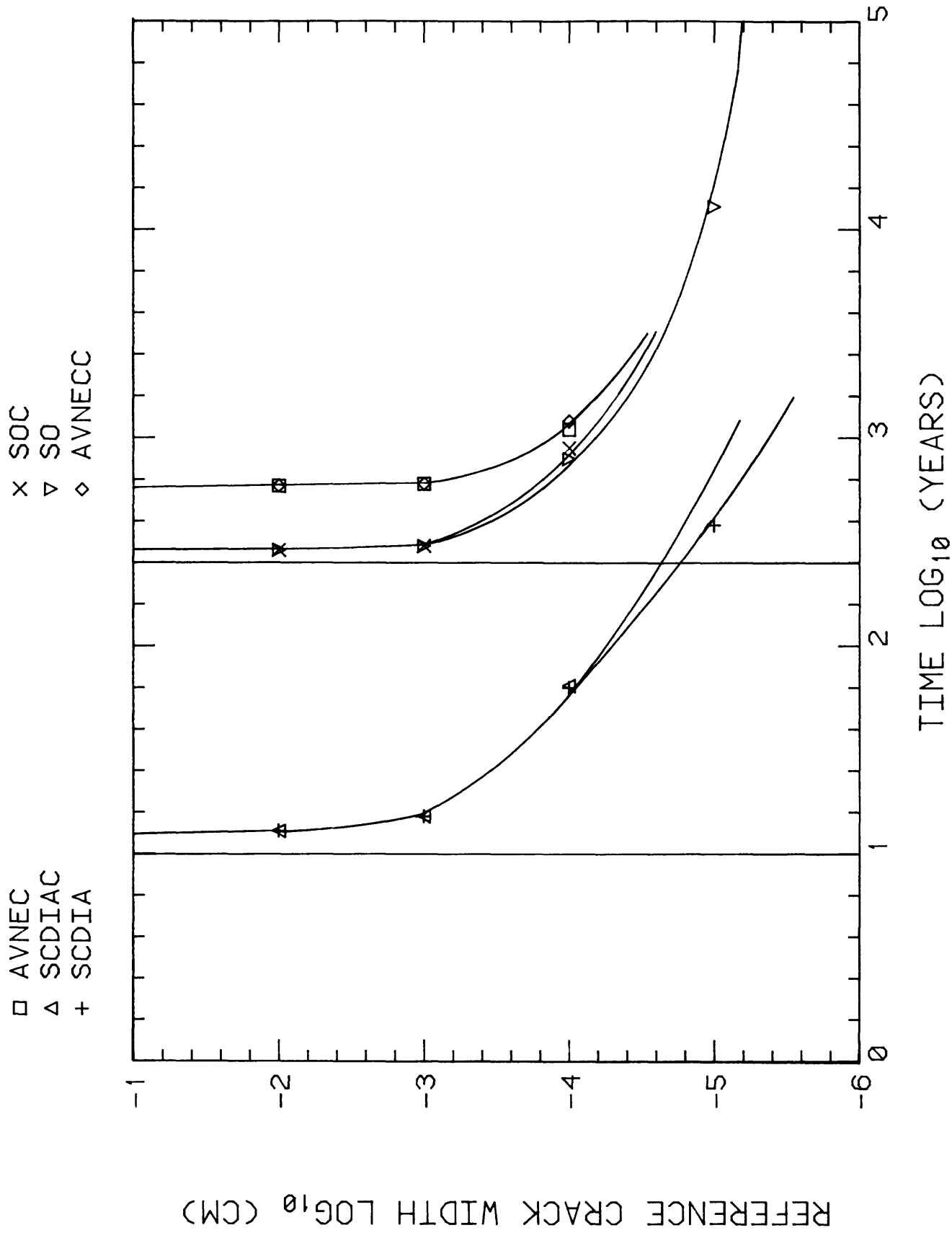
1

DISSOLUTION WITH AND WITHOUT CRACK CLOSURE (DISSCC WORKING LIST-OPTION 2 FOR NC AND NCC WITH DECAY

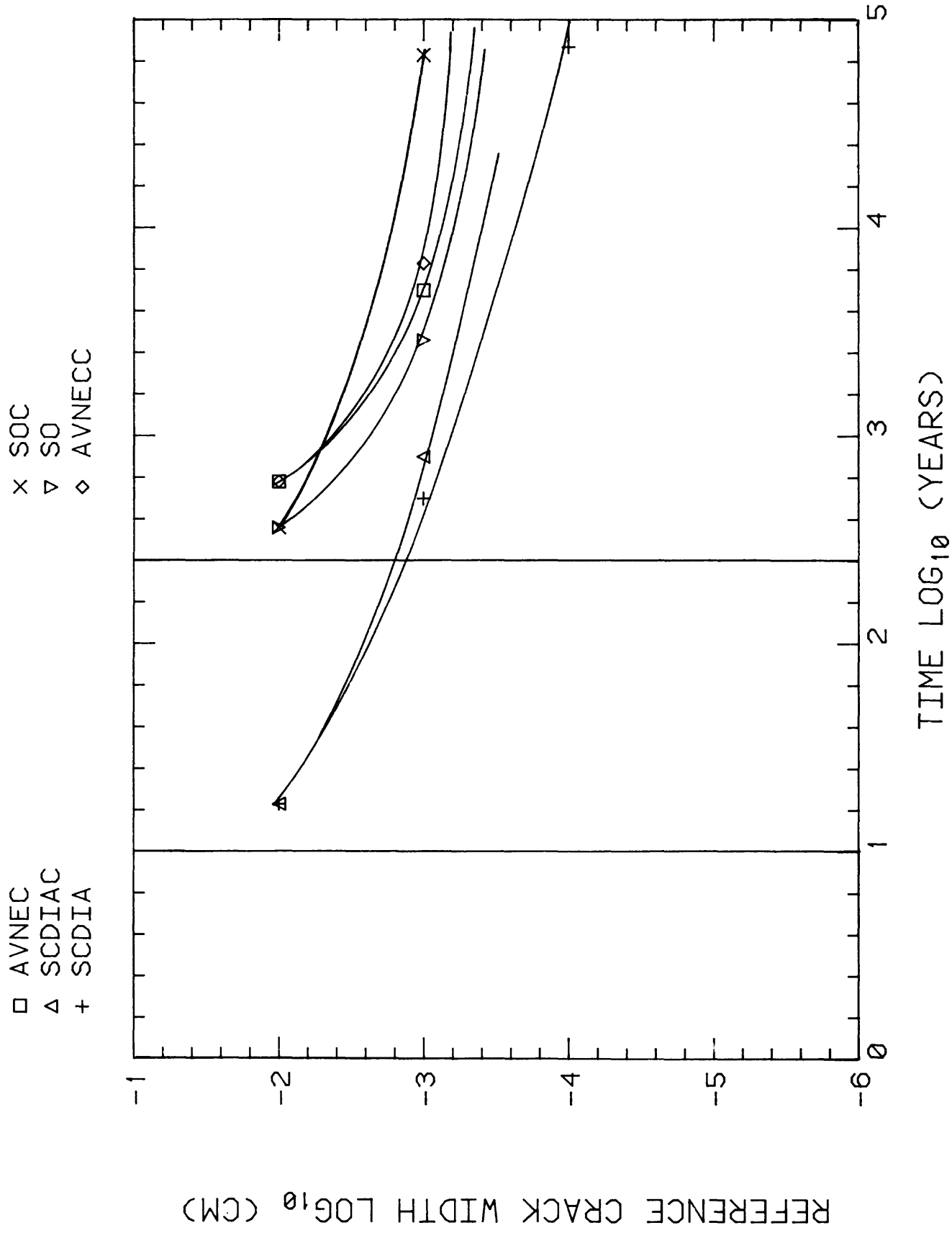
# RESULTS OF REFERENCE CALCULATIONS (RFST1)



# RESULTS OF REFERENCE CALCULATIONS (RFST2)

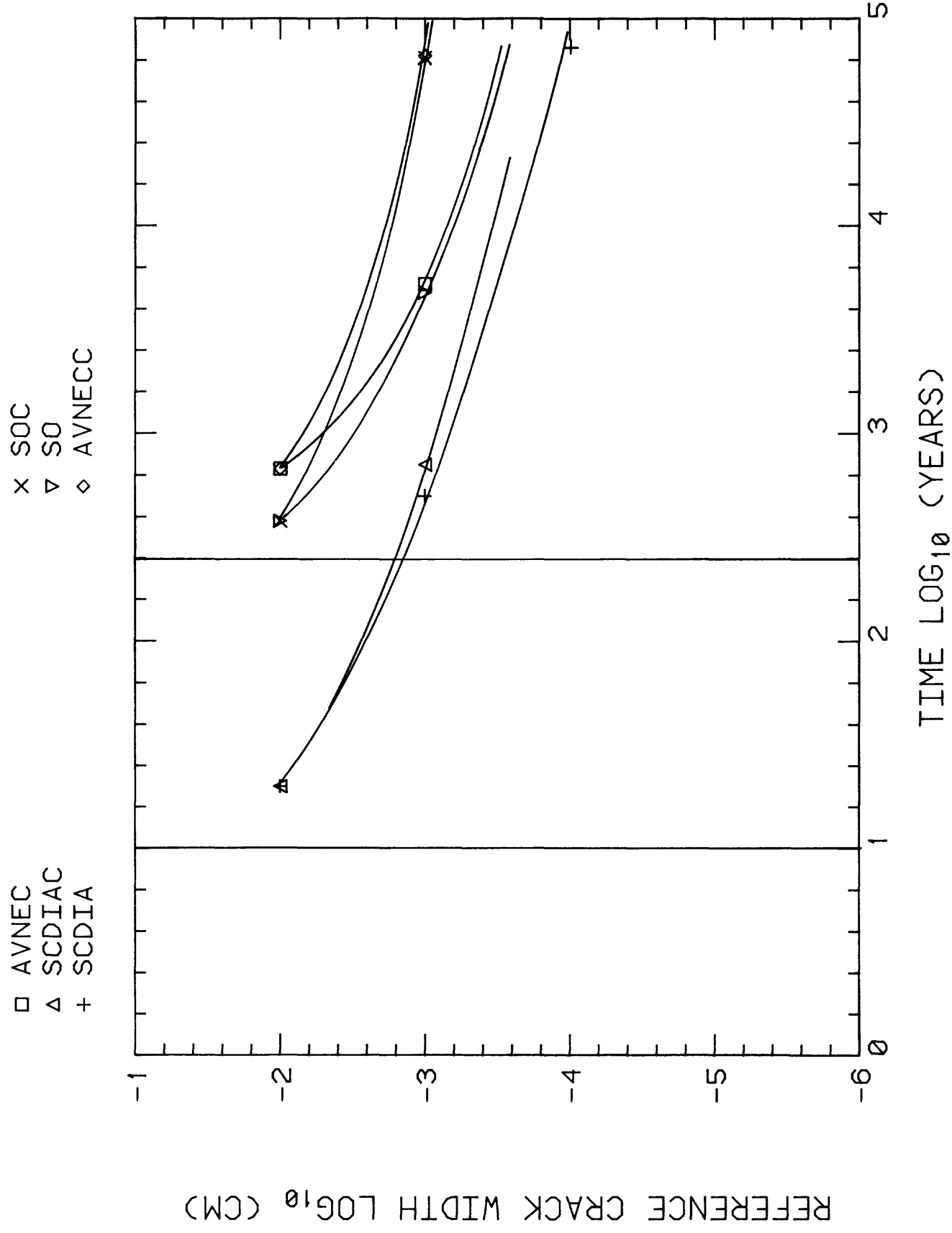


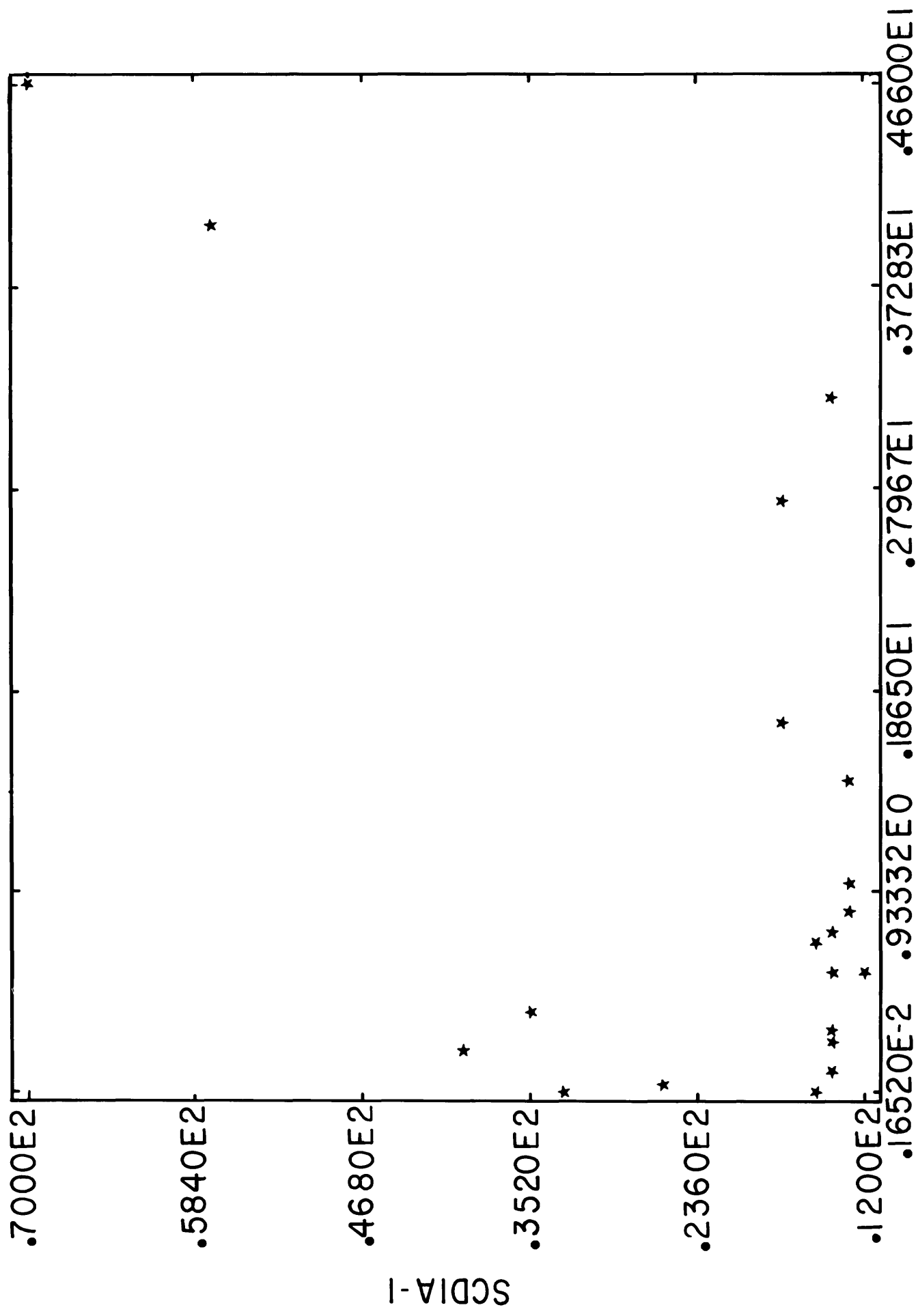
# RESULTS OF REFERENCE CALCULATIONS (RFST3)

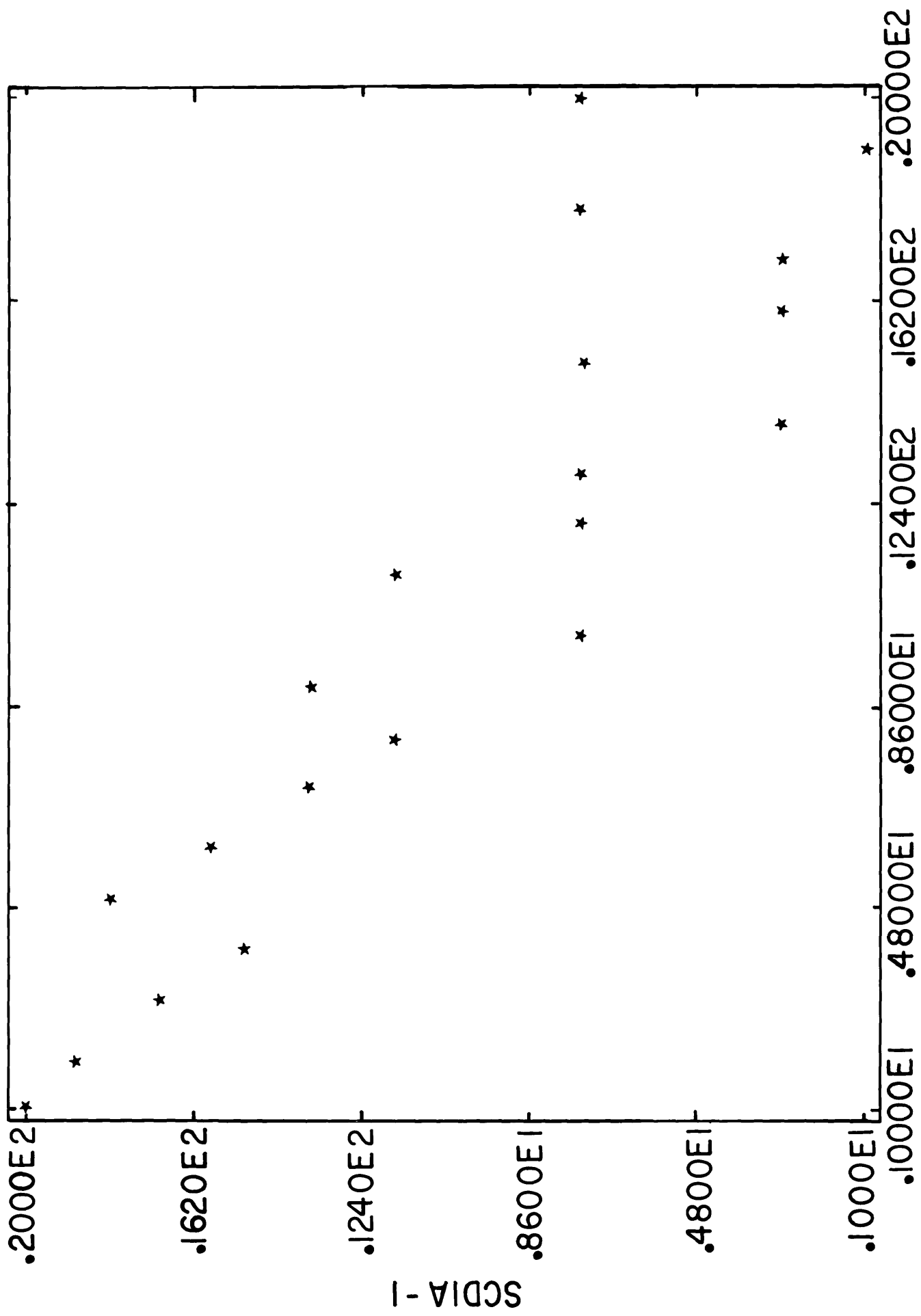




# RESULTS OF REFERENCE CALCULATIONS (RFST4)







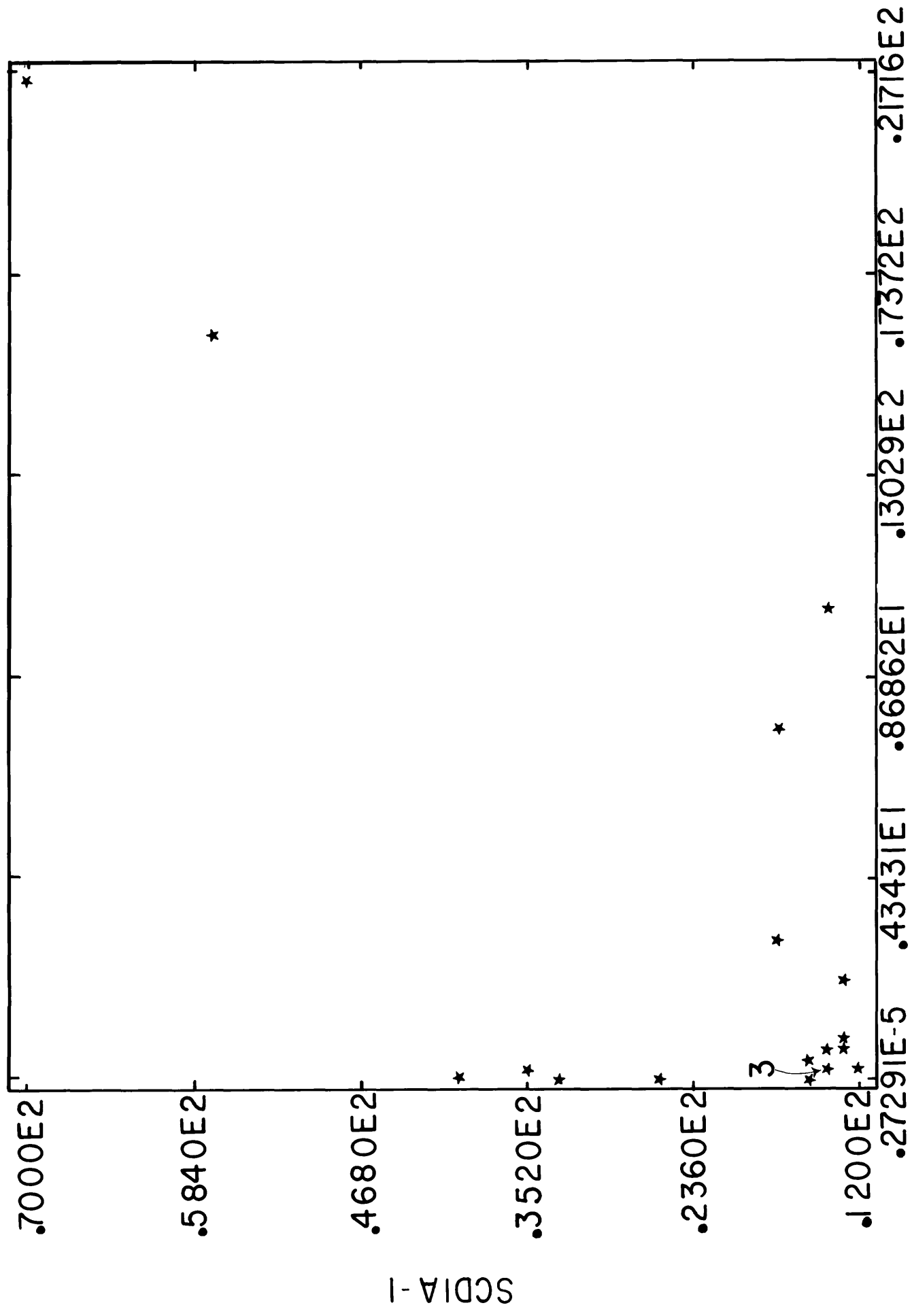


**Figure AR.5.7A**

## SENSITIVITY ANALYSIS -- RAW DATA

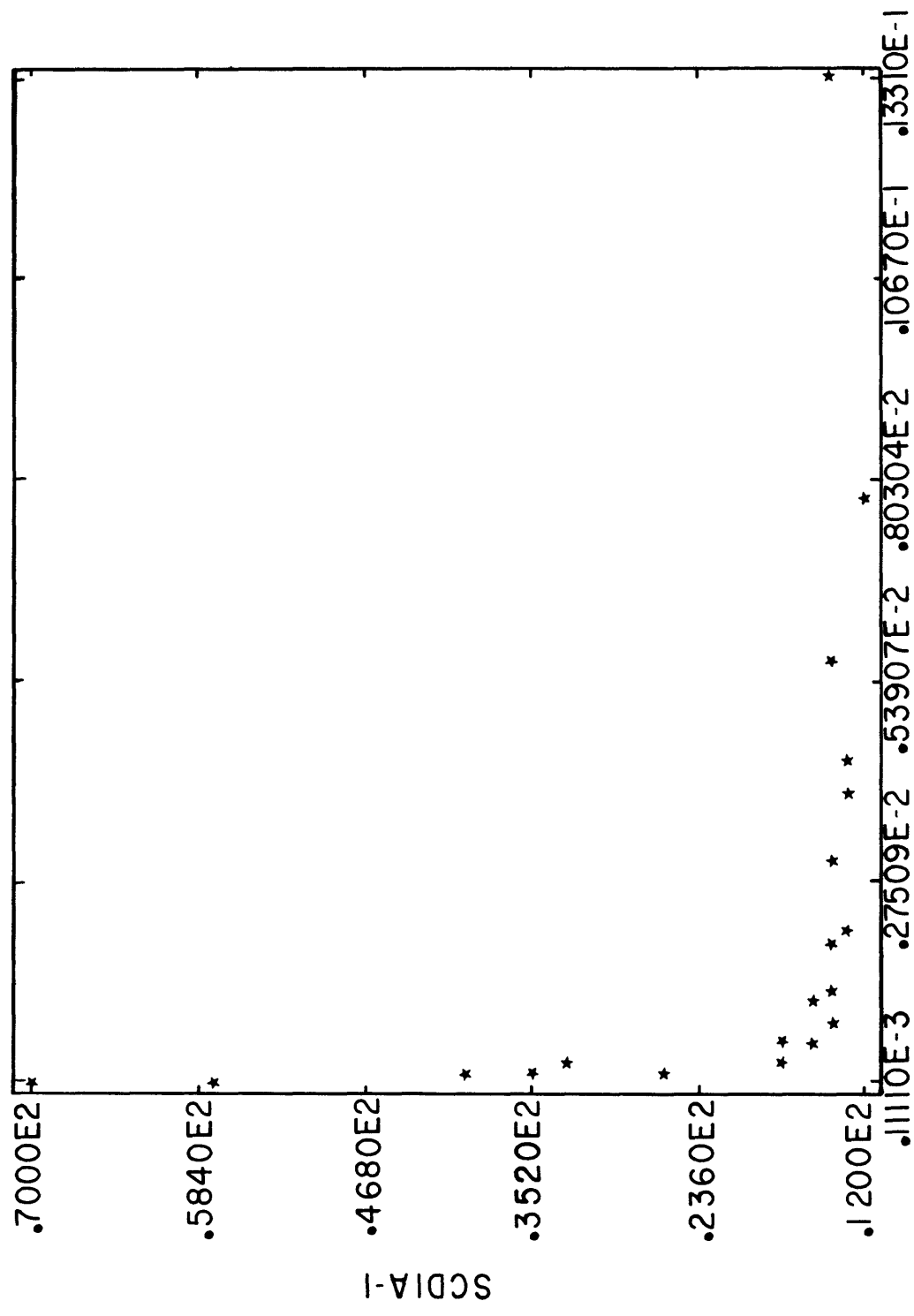


Figure AR.5.7B

SENSITIVITY ANALYSIS -- RANKS

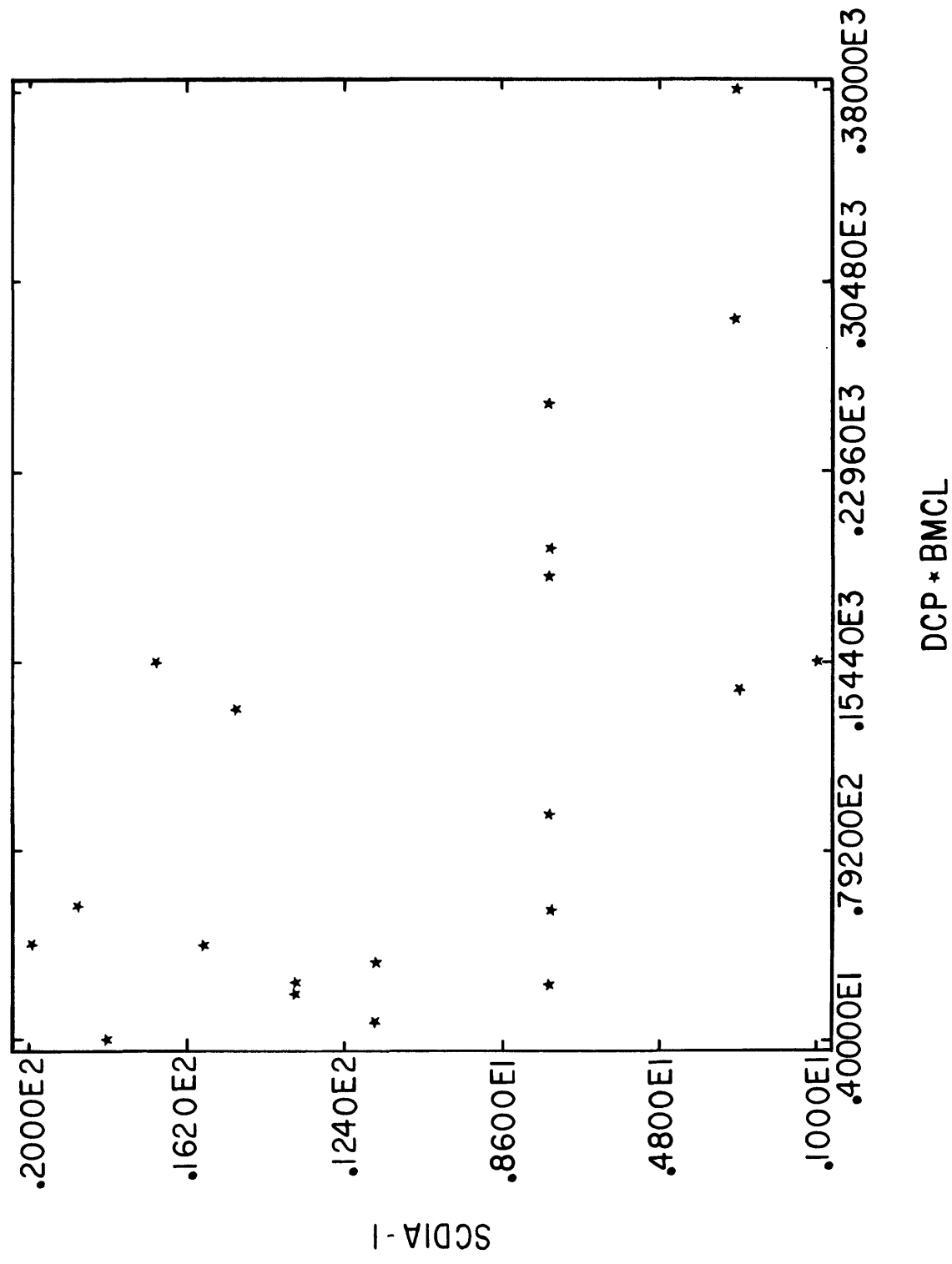


Figure AR.5.8A

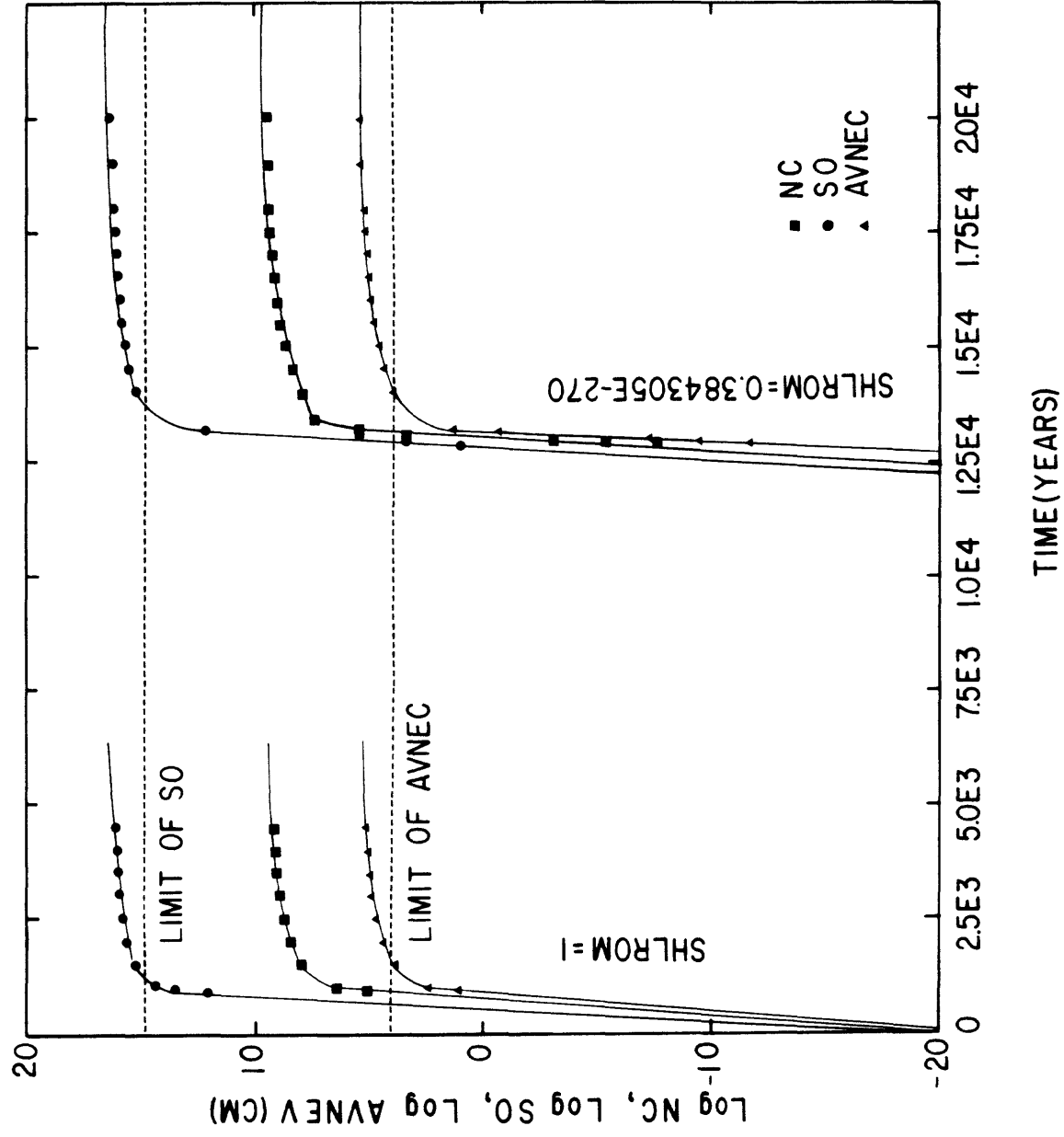


Figure AR.5.8B

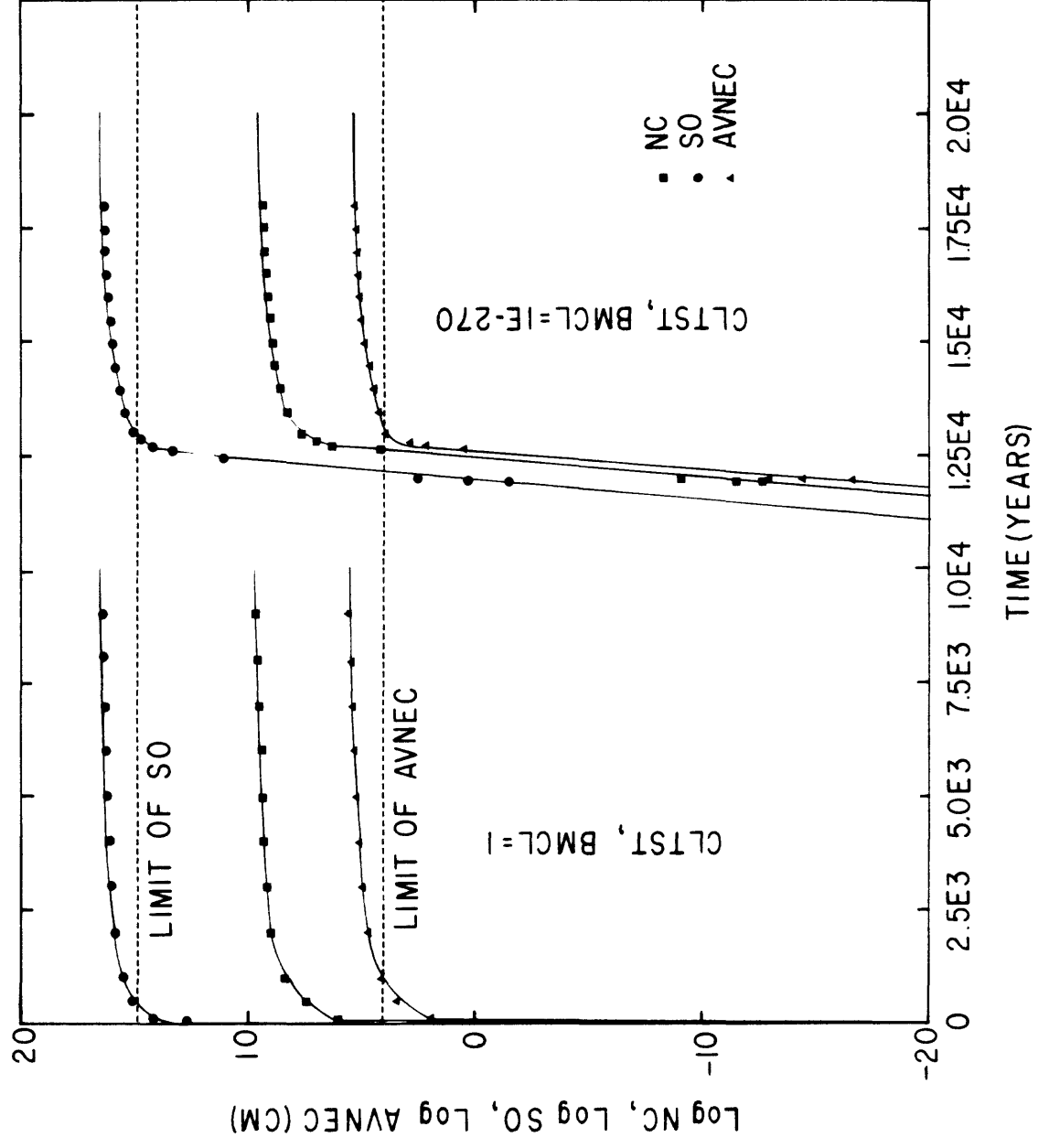
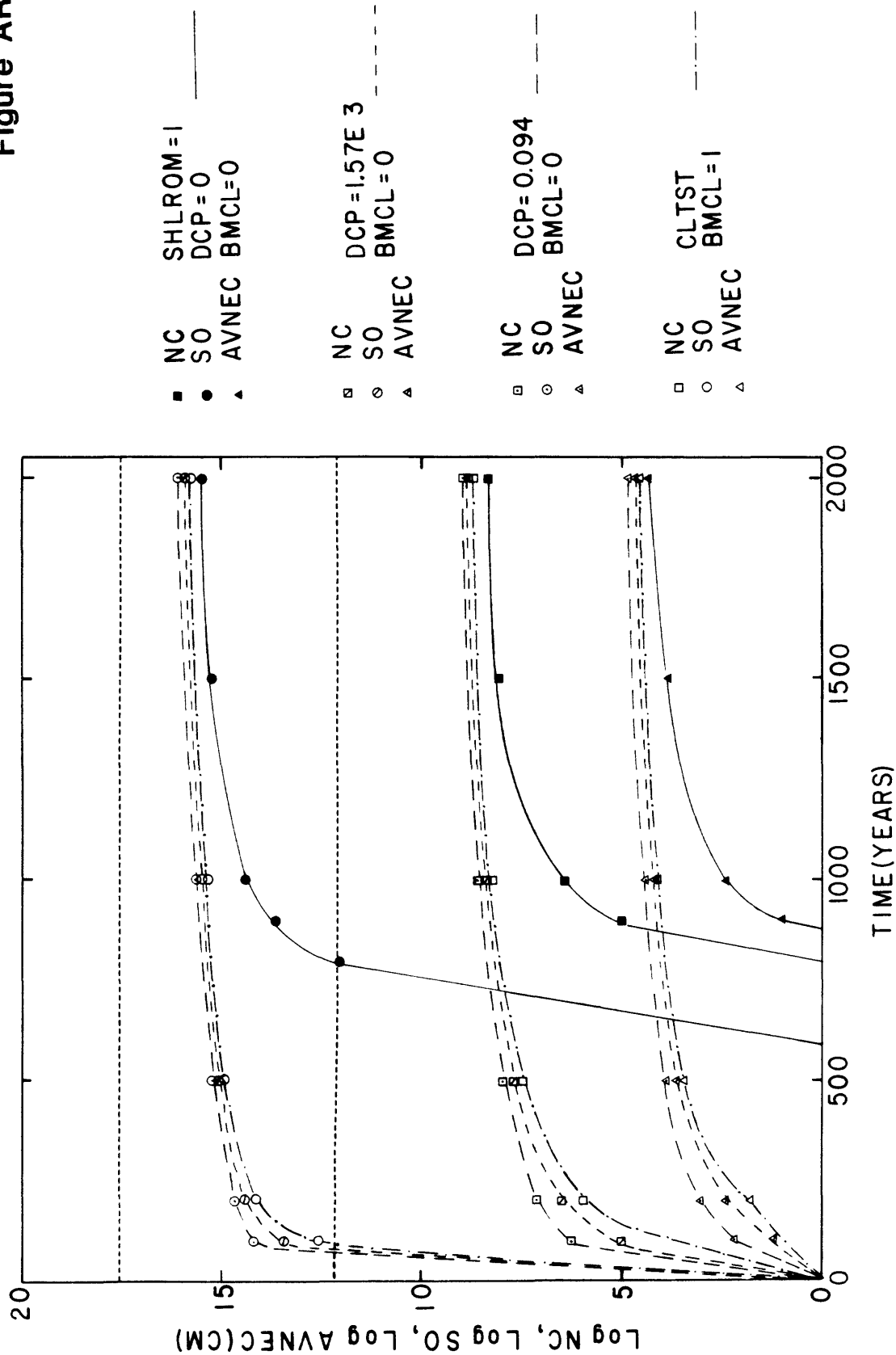
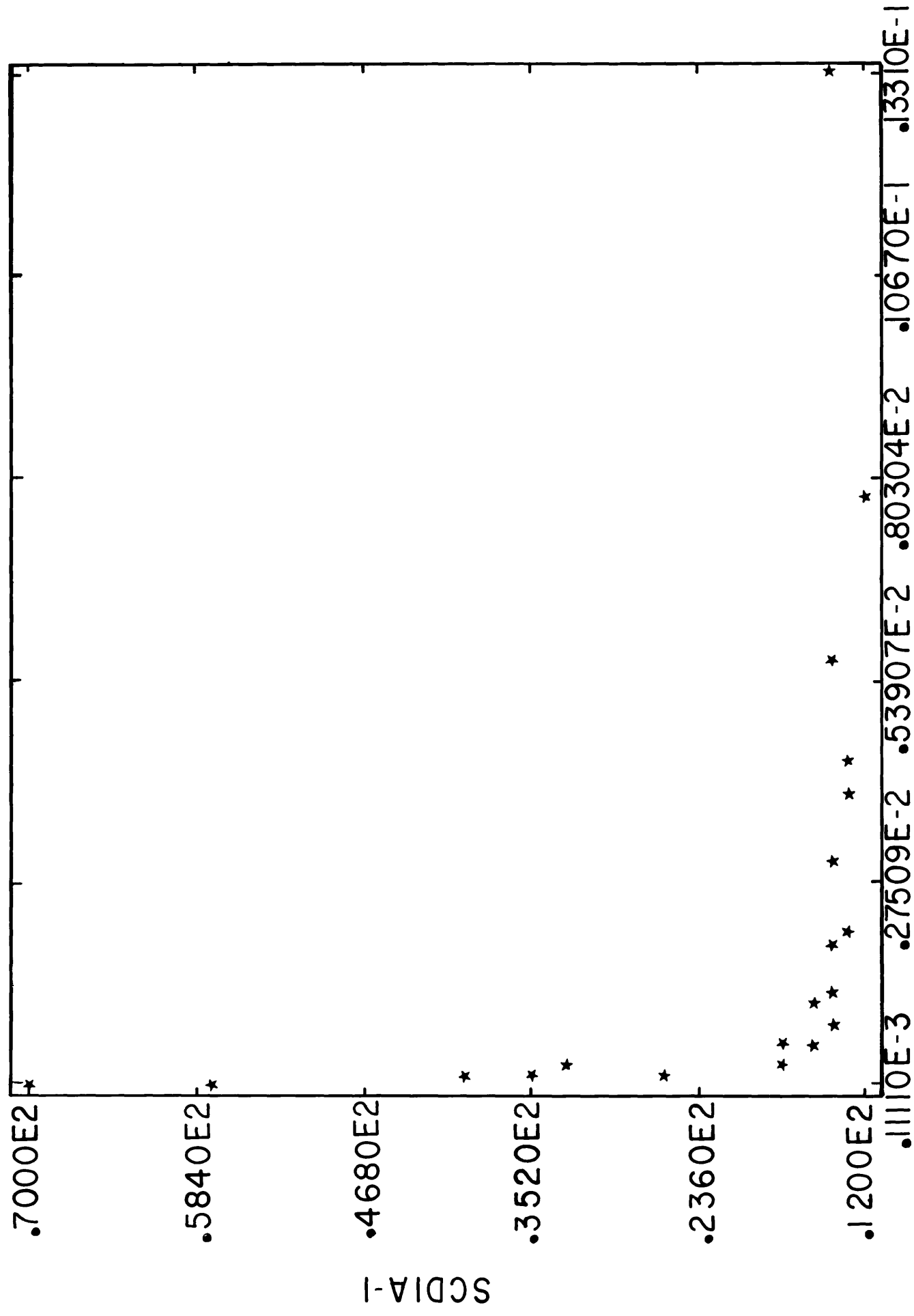




Figure AR.5.8C



**Figure AR.5.7A**



## Figure 11.5.7B

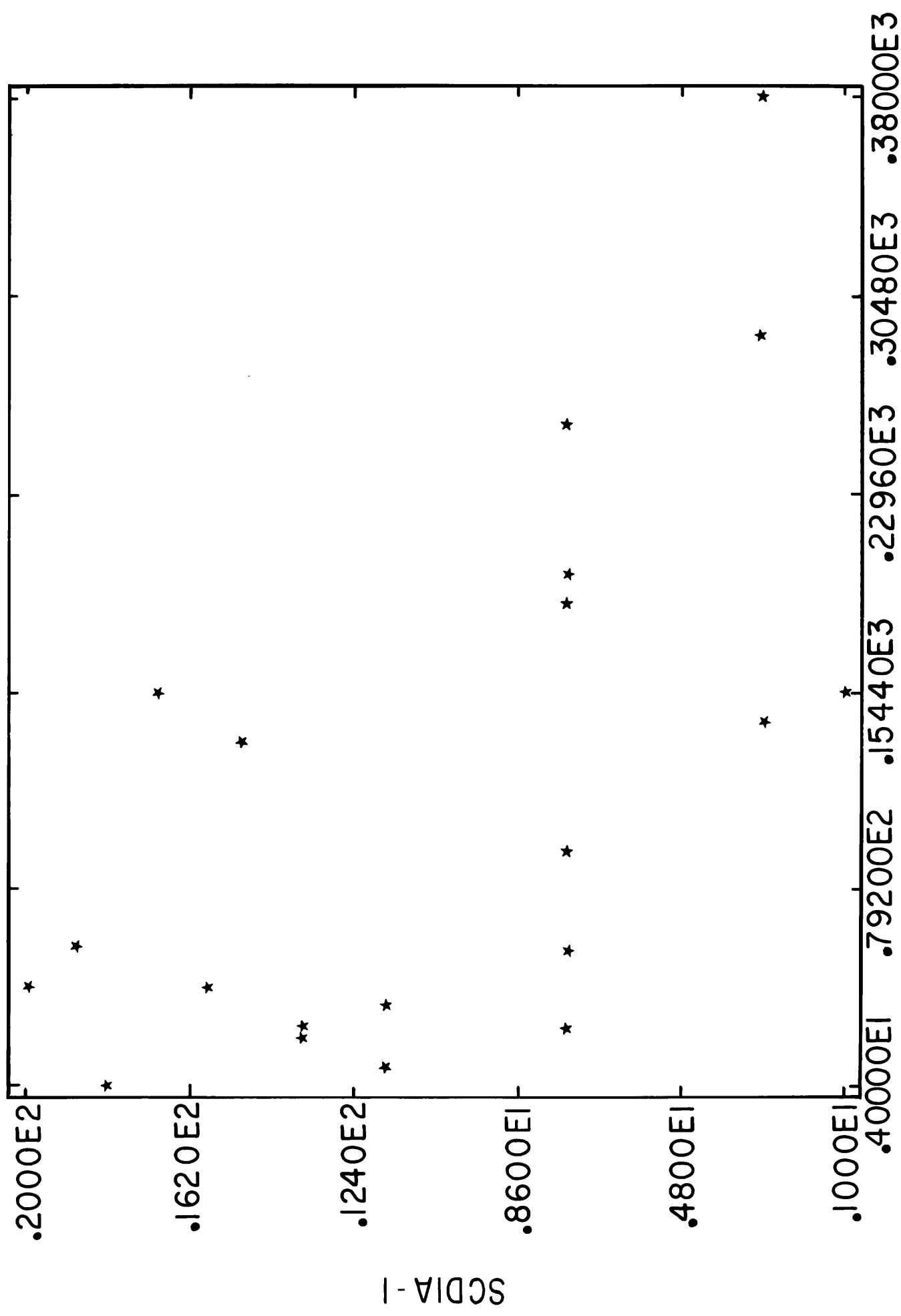


Figure AR.5.8A

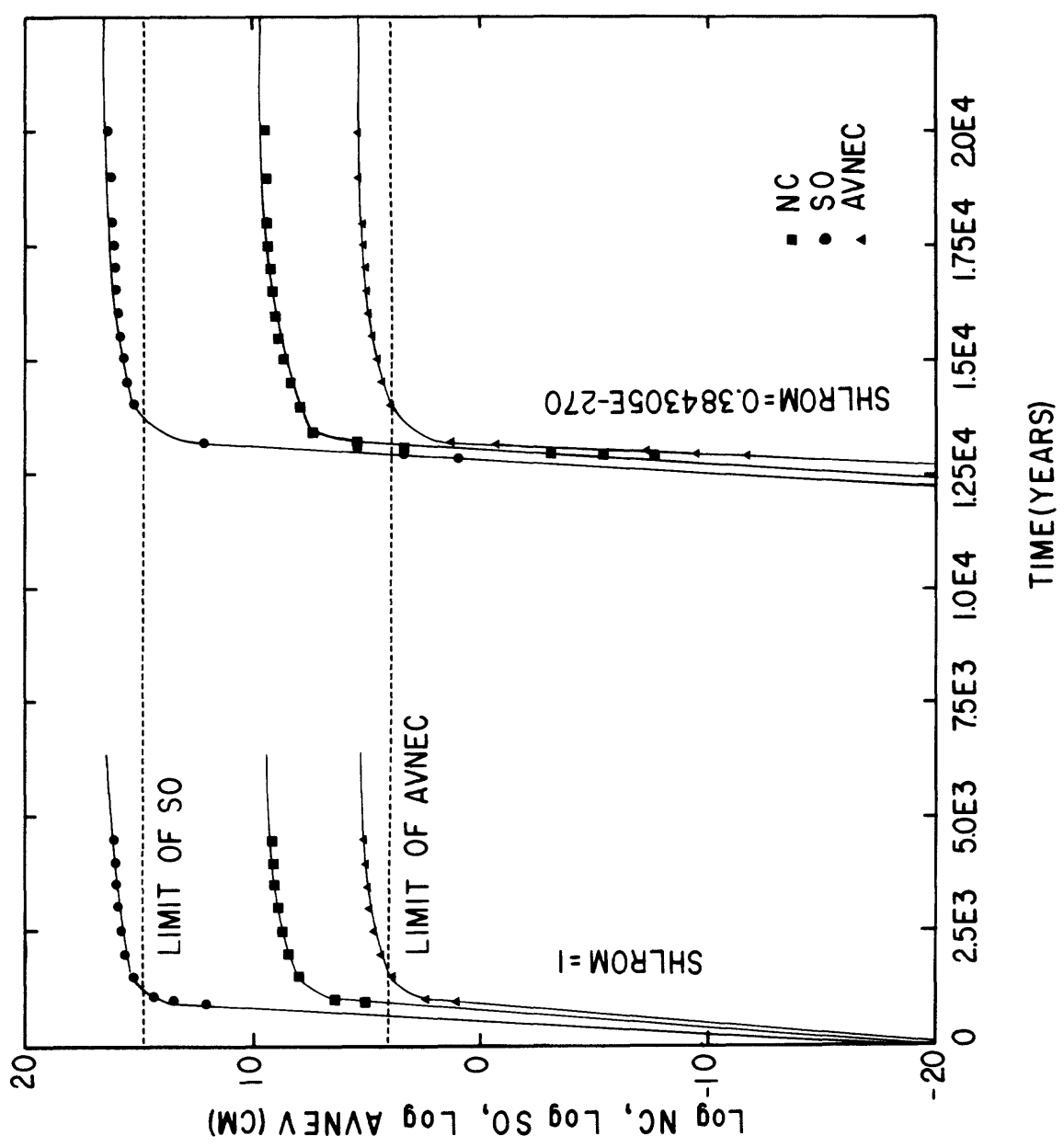


Figure AR.5.8B

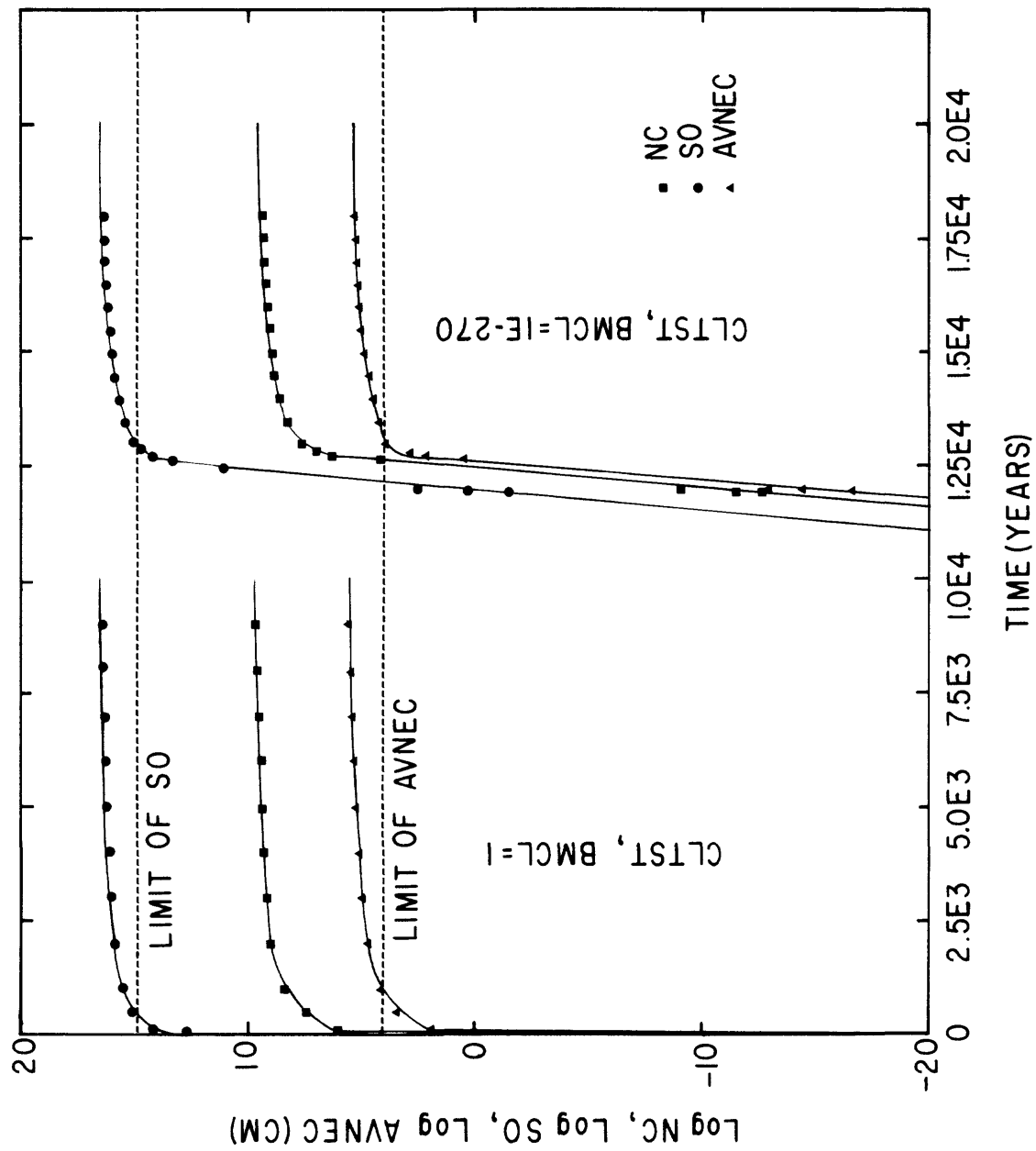
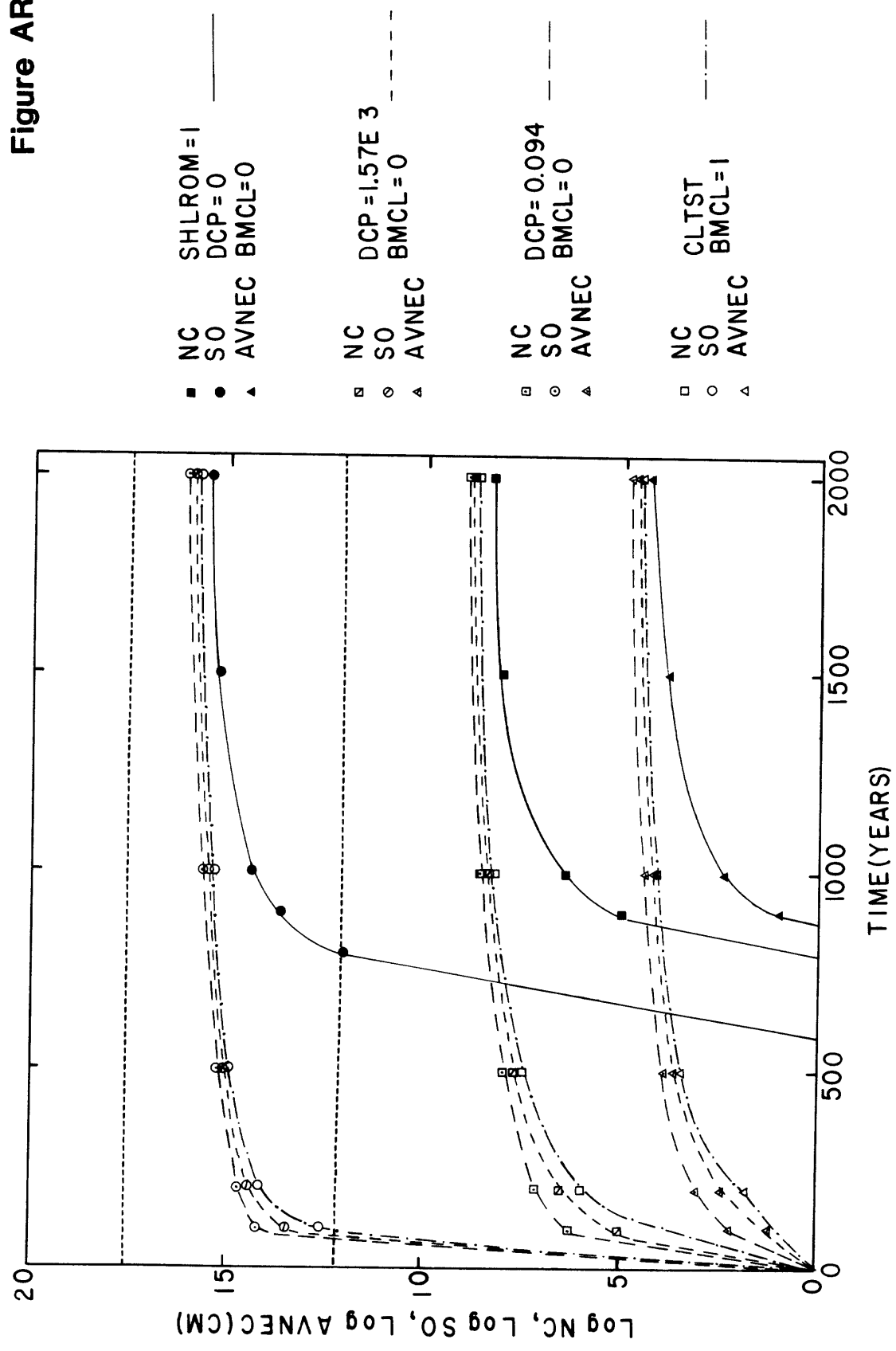


Figure AR.5.8C



```

*****
DATE OF RUN          RUN IDENTIFICATION
TEST LIST-DISSCC WORKING LIST FOR OPTION 1(THERMAL EXPANSION FEEDBACK)NC,NCC WITH DECAY OF BPH
DCP=                (CAL/GM/YR)
BMCL=              (CM)
RCW=              (CM)
MBFA=3E12         (CU CM/YR)
MBPH=2E6         (DYNE/SQ CM)
DT=
LENGTH=
PRTPER=
PLTPER=
OPTION 1(TEF)FOR NC WITH DECAY OF BPH
OPTION 1(TEF)FOR NCC WITH DECAY OF BPH
DISSOLUTION WITH AND WITHOUT CRACK CLOSURE (DISSCC WORKING LIST-OPTION 1(TEF)FOR NC AND NCC WITH DECAY OF BPH)
*****
L  H.K=H.J+DT*(HINR.JK-HOUTR.JK)      HEAT ABOVE 0 TEMPERATURE (CAL/GM)
N  H=5.2000                          INITIAL HEAT; MTEMP=26C (CAL/GM)
R  HINR.KL=DCP*FD.K                  RADIONUCLIDE POWER (CAL/GM/YR)
N  HINR=0                            HEATING RATE AT START (CAL/GM/YR)
C  DCP=0                             DIMENSIONAL COEFFICIENT FOR THERMAL POWER (CAL/GM/YR)
A  FD.K=EXP(2.303*LOGFD.K)           RADIONUCLIDE DECAY FRACTION
N  FD=1.                             INITIAL DECAY FRACTION
A  LOGFD.K=TABLE(FDTAB,LOGT.K,0,8,0.5) LOGTEN DECAY FRACTION
M  LOGFD=0                          INITIAL LOGFD
T  FDTAB=0/-0.03/-0.11/-0.38/-1.00/-1.80/-2.17/-2.51/-2.80/-3.28/
X  -3.84/-4.0/-4.0/-4.0/-4.0/-4.0    TABLE VALUES OF LOGFD
A  LOGT.K=LOGN(TIME.K)/2.303        LOGTEN TIME (YEARS)
N  TIME=1.                          INITIAL VALUE OF TIME (YEARS)
N  LOGT=0                          INITIAL VALUE OF LOG TIME
R  HOUTR.KL=DELAY3(SHLR.JK,DSHF)    HEAT OUTPUT RATE (CAL/GM/YR)
N  HOUTR=0                          INITIAL HEAT OUTPUT RATE (CAL/GM/YR)
★R  SHLR.KL=(2E-4*(H.K-4.0000)-2.4000E-4)*SHLROM    STEADY HEAT LOSS RATE (CAL/GM/YR)
★C  SHLROM=(as specified)          MULTIPLIER CONSTANT
C  DSHF=100                        DELAY SURFACE HEAT FLUX (YEARS)
R  TER.KL=UEC*(HINR.JK-HOUTR.JK)/0.2 (LINEAR) THERMAL EXPANSION RATE (CM/YR)
C  UEC=0.9                        UNIT EXPANSION CONSTANT (CM/DEG C)
N  TER=0.423                      INITIAL VALUE OF TER (CM/YR)
L  TE.K=TE.J+DT*(TER.JK)          (LINEAR) THERMAL EXPANSION (CM)
N  TE=0                          INITIAL THERMAL EXPANSION STATE (CM)
L  CL.K=MCL.J-LPV.J              COMPACTION LENGTH (CM)
N  CL=0                          INITIAL VALUE CL (CM)
A  LPV.K=BMCL+PVPS.K-PVDC.K       LINEAR PORE VOLUME (CM)
C  BMCL=0                        BACKFILL MAXIMUM COMPACTION LENGTH (CM)
L  PVPS.K=PVPS.J+DT*(BDRUA.JK)/DA (LINEAR) PORE VOLUME PRODUCED BY SOLUTIONING (CM)
N  PVPS=0                        INITIAL (LINEAR) PORE VOLUME PRODUCED BY SOLUTIONING (CU CM)
R  BDRUA.KL=FIFGE(MBFA,ACDR.K,ACDR.K,MBFA) BRINE DISCHARGE RATE TO UPPER AQUIFER (CU CM/YR)
C  MBFA=3E12                      MAXIMUM BRINE FLOW IN AQUIFER (CU CM/YR)
A  ACDR.K=DCBPHA.K*NBPH*NC.K/(1.+(DCBPHA.K*DCBPHB.K*NC.K)) (TOTAL) APPARENT CRACK DISCHARGE RATE (CU CM/YR)
A  DCBPHA.K=(3E7*RCW*RCW*RCW*CTL)/(12*BV*CPL) DIMENSIONAL CONSTANT BRINE PRESSURE HEAD (SQ CM/DYNE)*(CU CM/YR)
A  DCBPHB.K=NBPH/MBFA            BRINE PRESSURE FLOW RATIO (DYNE/SQ CM)/(CU CM/YR)
C  NBPH=2E6                      INITIAL BRINE PRESSURE HEAD (DYNE/SQ CM)
C  RCW=1E-3                      REFERENCE CRACK WIDTH (CM)
C  CTL=6E5                      CRACK TRACE LENGTH (CM)
C  BV=1E-2                      BRINE VISCOSITY (POISE)
C  CPL=1E4                      CRACK PATH LENGTH (CM)
★A  NC.K=NCN+DA*AVNEC.K/(RCW*CTL*CPL) NUMBER OF CRACKS FROM VOLUME OF REFERENCE CRACK
★C  NCN=0                        INITIAL NUMBER OF CRACKS
A  AVNEC.K=MAX(NEC.K,-NEC.K)      ABSOLUTE VALUE OF NEC (CM)
A  NEC.K=TE.K-CL.K              NET EXPANSION MINUS COMPACTION (CM)
N  NEC=-1.                      INITIAL NEC (CM)
L  PVDC.K=PVDC.J-DT*(LPVCR.JK)    (LINEAR) PORE VOLUME DESTROYED BY COMPACTION (CM)
N  PVDC=0                        INITIAL VALUE OF PVDC (CM)
R  LPVCR.KL=LPV.K*EXP(-2.303*ELP*3E7*DT/EVISC.K)/DT-LPV.K/DT LINEAR PORE VOLUME COMPACTION RATE (CM/YR)
C  ELP=1.388                    EFFECTIVE LOAD PRESSURE (DYNE/SQ CM)
A  EVISC.K=TABLE(EVTAB,BFTEMP.K,0,250,25) EFFECTIVE VISCOSITY (POISE)
T  EVTAB=1.15E19,7.08E18,4.47E18,2.81E18,1.78E18,1.26E18,
X  8.91E17,6.61E17,5.01E17,3.80E17,3.02E17 TABLE VALUES OF EVISC (POISE)
A  BFTEMP.K=32+2*(MTEMP.K-26)    BACKFILL TEMPERATURE (DEG C)
N  BFTEMP=32.                  INITIAL VALUE BFTEMP (DEG C)
A  MTEMP.K=(H.K-4.0)/0.2+STEMP    MEAN TEMPERATURE FOR STEM=20C (DEG C)
N  MTEMP=26.                  INITIAL VALUE OF MTEMP (DEG C)
C  STEMP=20.                  SURFACE TEMPERATURE (DEG C)
A  MCL.K=BMCL+ACLS.K            MAXIMUM COMPACTION LENGTH (CM)
A  ACLS.K=SO.K/SA.K            AVERAGE COMPACTION LENGTH FROM SOLUTIONING (CM)
L  SO.K=SO.J+DT*BDRUA.JK        SOLUTION OPENINGS (CU CM)
A  SA.K=DA                     SOLUTIONING AREA (SQ CM)
C  DA=7.9E10                  DEPOSITORY AREA (SQ CM)
N  SO=0                       INITIAL VALUE OF SO ( CU CM)
A  SCDIA.K=2.0*EXP(LNVFU.K)     SINGLE CAVITY DIAMETER (CM)
L  CLC.K=MCLC.J-LPVC.J          COMPACTION LENGTH; WITH CLOSURE (CM)
N  CLC=0                      INITIAL VALUE CLC (CM)
A  LPVC.K=BMCL+PVPS.K-PVDC.C.K (LINEAR) PORE VOLUME; WITH CLOSURE (CM)
L  PVPS.C.K=PVPS.C.J+DT*(BDRUAC.JK)/DA (LINEAR) PORE VOLUME PRODUCED BY SOLUTIONING; WITH CLOSURE (CM)
N  PVPS.C=0                   INITIAL VALUE PVPS.C (CM)
R  BDRUAC.KL=FIFGE(MBFA,ACDR.C.K,ACDR.C.K,MBFA) BRINE DISCHARGE RATE TO UPPER AQUIFER; WITH CLOSURE (CU CM/YR)
A  ACDRC.K=DCBPHA.K*NBPH*ANCC.K/(1.+(DCBPHA.K*DCBPHB.K*ANCC.K)) APPARENT NUMBER OF CRACKS REDUCED BY CLOSURE
★C  NCC.K=NCCN+DA*AVNECC.K/(RCW*CTL*CPL) NUMBER OF CRACKS FROM VOLUME OF REFERENCE CRACK; WITH CLOSURE
★A  NCCN=0                     INITIAL NUMBER OF CRACKS; WITH CLOSURE
A  AVNECC.K=MAX(NECC.K,-NECC.K) ABSOLUTE VALUE OF NEC; WITH CLOSURE (CM)
A  NECC.K=TE.K-CLC.K          NET EXPANSION MINUS COMPACTION; WITH CLOSURE (CM)
N  NECC=-1.                   INITIAL VALUE NECC (CM)
L  PVDC.C.K=PVDC.C.J-DT*(LPVCR.C.JK) (LINEAR) PORE VOLUME DESTROYED BY COMPACTION; WITH CLOSURE (CM)
N  PVDC.C=0                   INITIAL VALUE PVDC.C (CM)
R  LPVCR.C.KL=LPVC.K*EXP(-2.303*ELP*3E7*DT/EVISC.K)/DT-LPVC.K/DT LINEAR PORE VOLUME COMPACTION RATE; WITH CLOSURE (CM/YR)
A  MCLC.K=BMCL+ACLSC.K        MAXIMUM COMPACTION LENGTH; WITH CLOSURE (CM)
A  ACLSC.K=SOC.K/SA.K        AVERAGE COMPACTION LENGTH FROM SOLUTIONING; WITH CLOSURE (CM)
L  SOC.K=SOC.J+DT*BDRUAC.JK    SOLUTION OPENINGS; WITH CLOSURE (CU CM)
N  SOC=0                     INITIAL VALUE SOC (CU CM)
A  SCDIAC.K=2.0*EXP(LNVFC.K)   SINGLE CAVITY DIAMETER; WITH CLOSURE (CM)
S  BDRAT.K=(1.+BDRUAC.K)/(1.+BDRUA.K) BRINE DISCHARGE RATE; WITH AND WITHOUT,CLOSURE
NOTE
PRINT H,HINR,HOUTR,SHLR,TER,TE,CL,LPV,PVPS,BDRUA,ACDR,
X  NC,AVNEC,NEC,PVDC,LPVCR,EVISC,BFTEMP,MTEMP,MCL,
X  ACLS,SO,SCDIA,CLC,LPVC,PVPS,C,BDRUAC,ACDR,
X  ANCC,NCC,AVNECC,NECC,PVDC,C,LPVCR,C,MCLC,ACLSC,SOC,
X  SCDIAC,BDRAT
PLOT NC=N/ANCC=C/AVNECC=V(0,1.0E4)/AVNECC=A(0,1.0E4)/SCDIA=D(0,1.0E4)/
X  SCDIAC=S(0,1.0E4)/BDRAT=B
SPEC DT=0.1/LENGTH=1.0E3/PLTPER=10/PRTPER=20
RUN "DISS WITH AND WITHOUT CC"-----"DISSOLUTION WITH AND WITHOUT CRACK CLOSURE"
EOI ENCOUNTERED.

```



Table AR.5.2B

\*\*\*\*\*  
DATE OF RUN OCT 17, 1979 RUN IDENTIFICATION 10-17-79-2  
REFERENCE SET 4-DISSCC WORKING LIST FOR OPTION 2, WITH DECAY OF BPH  
DCP= 0.094 (CAL/GM/YR)  
BMCL= 60 (CM)  
RCW= 1E-3 (CM)  
CC= 5 (PER CM)  
MBFA= 3E12 (CU CM /YR)  
MBPH=2E6 (DYNE/SQ CM)  
DT= 10  
LENGTH= 1.0E5  
PRTPE= 1.0E3  
PLTPE= 1.0E3  
OVERRUN TIME AT  
OPTION 2 FOR MC WITH DECAY OF BPH  
OPTION 2 FOR MCC WITH DECAY OF BPH  
DISSOLUTION WITH AND WITHOUT CRACK CLOSURE (DISSCC WORKING LIST)  
\*\*\*\*\*  
PAGE 1

TIME	H PVDC ACDRC PVRATC	HINR LPVCR ANCC	HOUTR EIVSC NCC	SHLR BTEMP AVNECC	TER MTEPP NECC	TE MCL PVDCC	CL ACL LPVCR	LPV SO MCLC	PVPS LMVFC ACLSC	BDRUA SCDIA SOC	ACDR CLC LNVFU	MC LPVC SCDIAC	AVNEC PVPSC BDRAT	NEC BDRUAC PVRAT
E 03	E-00 E 03 E 09 E-00	E-03 E-00 E-00 E-00	E-06 E 15 E-00 E-00	E-06 E-00 E-00 E-00	E-03 E-00 E-00 E-00	E-00 E 03 E-00 E-00	E 03 E 03 E-00 E-00	E-00 E 12 E-00 E-00	E 03 E-00 E-00 E-00	E 09 E 03 E 12 E-00	E 09 E-00 E-00 E-00	E-00 E-00 E 03 E-00	E 03 E-00 E-00 E-00	E 03 E 09 E-03 E-03
	.00 0.0 .15 0.0000	5.2000 94.000 -1.084 5.0	0.00 6349.2 5. 5.	-1.00 32.000 1. 1.	423.00 26.000 -1. -1.	0.000 1. 0. 0.	.0 0 -0.0843 60.	60.0 0. 60. 60.	0.0 -1.460 0. 0.	.1 1. 1. 0.	.1 1. 1. -1.460	5. 60.0 1.000 1.000	.0 0. 1.000 1.000	-1.0 .15 0.00 0.00
1.00	9.4911 .1 .56 .9168	.635 -1.092 18.8 226.	862.12 2815.9 226. 226.	858.23 74.911 45. 45.	-1.02 47.456 -45. -45.	19.310 .1 65. 65.	.1 .1 -0.0184 70.	29.3 4. 70. 70.	.1 8.596 10. 10.	10.0 18.88 .8 9.152	10.0 64. 5.9 10.82	335. 5.9 10.82 10.82	.1 10. 10.82 10.82	-1.1 .56 748.87 748.87
2.00	9.1513 .3 .12 .9857	.397 -317 4.0 276.	798.22 3041.5 276. 276.	790.27 71.513 55. 55.	-1.81 45.757 -55. -55.	17.781 4. 73. 73.	.3 .3 -0.0031 74.	108.9 25. 74. 74.	.3 8.693 14. 14.	36.5 33.30 1.1 9.720	36.5 73. 1.1 11.92	1232. 1.1 11.92 11.92	.2 14. 14. 14.	-2 .12 710.52 710.52
3.00	8.7374 .9 .03 .9963	.301 -1.059 1.1 293.	715.80 3316.3 293. 293.	707.49 67.374 59. 59.	-1.87 43.687 -59. -59.	15.918 1.3 75. 75.	-9 1.2 -0.0007 75.	396.5 96. 75. 75.	1.2 8.712 15. 15.	123.1 51.98 1.2 10.165	123.1 75. 12.15 12.15	4279. .3 12.15 12.15	.9 15. 15. 15.	-9 .03 689.93 689.93
4.00	8.3371 2.8 .01 .9987	.253 -3.211 4 305.	635.11 3582.2 305. 305.	627.42 63.371 61. 61.	-1.72 41.686 -51. -51.	14.117 4.1 75. 75.	2.8 4.1 -0.0002 75.	1296.6 322. 75. 75.	4.1 8.717 15. 15.	367.0 77.38 1.2 10.563	367.0 75. 10.563 12.22	13940. .1 12.22 12.22	2.8 15. 15. 15.	-2.8 .01 686.08 686.08
5.00	7.9761 8.2 .01 .9995	.223 -8.022 2 314.	562.07 3821.9 314. 314.	555.22 59.761 63. 63.	-1.53 39.881 -53. -53.	12.493 11.6 75. 75.	8.1 11.6 -0.0001 75.	3454.0 914. 75. 75.	11.6 8.720 15. 15.	863.5 109.23 1.2 10.908	863.5 75. 12.24 12.24	40414. .0 12.24 12.24	8.1 15. 15. 15.	-8.1 .01 702.99 702.99
1PAGE 2														
6.00	7.6577 18.7 .00 .9997	.200 -11.900 1 321.	497.55 4033.3 321. 321.	491.55 56.577 64. 64.	-1.34 38.289 -64. -64.	11.060 24.1 75. 75.	18.6 24.0 -0.0000 75.	5433.3 1893. 75. 75.	24.0 8.721 15. 15.	1000.0 139.03 1.2 11.149	1000.0 75. 12.26 12.26	50000. .0 12.26 12.26	18.6 15. 15. 15.	-18.6 .00 775.66 775.66
7.00	7.3802 30.9 .00 .9998	.183 -12.354 1 327.	441.25 4217.6 327. 327.	436.04 53.802 65. 65.	-1.16 36.901 -65. -65.	9.811 36.7 75. 75.	30.8 36.7 -0.0000 75.	5863.2 2898. 75. 75.	36.7 8.721 15. 15.	1000.0 159.86 1.2 11.289	1000.0 75. 12.26 12.26	50000. .0 12.26 12.26	30.7 15. 15. 15.	-30.7 .00 840.43 840.43
8.00	7.1398 43.3 .00 .9999	.170 -12.432 0 333.	392.47 4377.1 333. 333.	387.97 51.393 67. 67.	-1.00 35.699 -67. -67.	8.729 49.4 75. 75.	43.2 49.3 -0.0000 75.	6120.9 3898. 75. 75.	49.3 8.722 15. 15.	1000.0 176.29 1.2 11.387	1000.0 75. 12.27 12.27	50000. .0 12.27 12.27	43.1 15. 15. 15.	-43.1 .00 876.10 876.10
9.00	6.9325 55.7 .00 .9999	.158 -12.416 0 334.	350.39 4540.4 334. 334.	346.51 49.325 68. 68.	-.86 34.663 -68. -68.	7.796 62.1 75. 75.	55.6 62.0 -0.0000 75.	6338.6 4899. 75. 75.	62.0 8.722 15. 15.	1000.0 190.09 1.2 11.462	1000.0 75. 12.27 12.27	50000. .0 12.27 12.27	55.6 15. 15. 15.	-55.6 .00 897.86 897.86
10.00	6.7541 68.1 .00 .9999	.149 -12.408 0 342.	314.16 4726.7 342. 342.	310.82 47.541 68. 68.	-.74 33.770 -68. -68.	6.993 74.7 75. 75.	68.0 74.7 -0.0000 75.	6592.1 5093. 75. 75.	74.7 8.722 15. 15.	1000.0 202.11 1.2 11.523	1000.0 75. 12.27 12.27	50000. .0 12.27 12.27	68.0 15. 15. 15.	-68.0 .00 911.77 911.77
11.00	6.5982 80.5 .00 .9999	.136 -12.433 0 345.	282.60 4889.4 345. 345.	279.65 45.982 69. 69.	-.66 32.991 -69. -69.	6.292 87.4 75. 75.	80.4 87.3 -0.0000 75.	6830.4 6898. 75. 75.	87.3 8.722 15. 15.	1000.0 212.83 1.2 11.575	1000.0 75. 12.28 12.28	50000. .0 12.28 12.28	80.4 15. 15. 15.	-80.4 .00 921.83 921.83
12.00	6.4502 93.0 .00 .9999	.125 -12.457 0 348.	254.65 5033.5 348. 348.	252.04 44.602 70. 70.	-.58 32.301 -70. -70.	5.671 100.0 75. 75.	92.9 100.0 -0.0000 75.	7043.7 7893. 75. 75.	100.0 8.722 15. 15.	1000.0 222.55 1.2 11.620	1000.0 75. 12.28 12.28	50000. .0 12.28 12.28	92.9 15. 15. 15.	-92.9 .00 929.59 929.59
13.00	6.3384 105.5 .00 .9999	.116 -12.480 0 351.	229.99 5160.7 351. 351.	227.69 43.384 70. 70.	-.51 31.692 -70. -70.	5.123 112.7 75. 75.	105.3 112.6 -0.0000 75.	7233.3 8598. 75. 75.	112.6 8.723 15. 15.	1000.0 231.48 1.2 11.659	1000.0 75. 12.28 12.28	50000. .0 12.28 12.28	105.3 15. 15. 15.	-105.3 .00 935.81 935.81
1PAGE 9														
62.00	5.1265 724.1 140.16 .8822	.021 -12.654 4901.1 42642.	25.81 6214.7 42642. 42642.	25.76 33.288 4516. 4516.	-.01 26.644 -4516. -4516.	.590 732.0 4951. 4951.	724.0 712.9 -1.5430 9644.	8019.4 9749.5 9644. 9644.	712.0 10.847 9802. 9802.	1000.0 429.47 749.6 749.6	1000.0 8537. 12.277 12.277	50000. 1109.3 102.72 102.72	724.0 9602. 11349 11349	-724.0 140.16 937.97 937.97
63.00	5.1263 736.8 159.36 .8878	.023 -12.654 5610.1 50000.	25.30 6217.4 50000. 50000.	25.25 33.263 10259. 10259.	-.01 26.631 -10259. -10259.	.568 732.0 10279. 10279.	716.7 745.5 -1.8611 11578.	8021.2 9749.5 9644. 9644.	745.5 10.907 11518. 11518.	1000.0 431.90 909.9 909.9	1000.0 10260. 12.283 12.283	50000. 1299.0 109.07 109.07	736.7 11518. 11594 11594	-736.7 159.36 908.17 908.17
64.00	5.3238 789.4 138.65 .9031	.022 -12.655 4845.8 50000.	24.81 6219.4 50000. 50000.	24.76 33.239 12161. 12161.	-.01 26.619 -12161. -12161.	.557 758.3 12180. 12180.	749.3 755.2 -1.8739 13437.	8426.9 95928. 9644. 9644.	758.2 10.957 13427. 13427.	1000.0 434.31 1060.7 1060.7	1000.0 12161. 12.208 12.208	50000. 1307.1 114.74 114.74	749.3 13427. 11389 11389	-749.3 138.65 988.36 988.36
65.00	5.1215 763.1 107.22 .9239	.022 -12.655 4700.9 90000.	24.34 6218.4 90000. 90000.	24.29 33.218 11418. 11418.	-.01 26.607 -11418. -11418.	.547 770.9 11912. 11912.	762.0 770.9 -1.5430 15000.	8010.4 9749.5 9644. 9644.	770.9 10.994 14988. 14988.	1000.0 416.60 1104.0 1104.0	1000.0 11914. 12.244 12.244	50000. 1115.9 114.98 114.98	762.0 14938. 11079 11079	-762.0 107.22 988.95 988.95
66.00	5.3192 774.7 77.72 .9468	.022 -12.655 2659.7 50000.	23.88 6224.9 50000. 50000.	23.84 33.192 15339. 15339.	-.01 26.594 -15339. -15339.	.536 770.6 15352. 15352.	774.6 783.5 -1.2356 16215.	8833.9 91893. 9644. 9644.	783.5 11.018 16155. 16155.	1000.0 419.04 1276.2 1276.2	1000.0 15342. 12.299 12.299	50000. 862.5 121.96 121.96	774.6 16155. 10780 10780	-774.6 77.72 988.73 988.73
67.00	5.3170 787.4 54.28 .9631	.021 -12.655 1842.5 50000.	23.44 6227.0 50000. 50000.	23.40 33.170 16407. 16407.	-.01 26.585 -16407. -16407.	.527 796.2 16417. 16417.	787.3 796.2 -1.8995 17045.	8837.2 92898. 9644. 9644.	796.2 11.035 16985. 16985.	1000.0 441.37 1341.8 1341.8	1000.0 16408. 12.304 12.304	50000. 628.1 123.99 123.99	787.3 16985. 10545 10545	-787.3 54.28 988.90 988.90
68.00	5.3149 800.1 37.06 .9750	.021 -12.655 1250.9 50000.	23.02 6229.3 50000. 50000.	22.98 33.149 17170. 17170.	-.01 26.574 -17170. -17170.	.517 808.9 17177. 17177.	799.9 808.8 -1.6309 17618.	8880.4 93898. 9644. 9644.	808.8 11.046 17558. 17558.	1000.0 443.68 1387.1 1387.1	1000.0 17171. 12.310 12.310	50000. 440.7 125.36 125.36	799.9 17558. 10372 10372	-799.9 37.06 989.07 989.07
69.00	5.3128 812.7 24.96 .9832	.021 -12.655 839.0 50000.	22.61 6231.4 50000. 50000.	22.57 33.128 17699. 17699.	-.01 26.564 -17699. -17699.	.508 821.6 17704. 17704.	8843.4 94898. 18006. 18006.	821.5 11.053 17946. 17946.	821.5 10.953 17946. 17946.	1000.0 445.95 1417.8 1417.8	1000.0 17700. 12.315 12.315	50000. 302.2 126.27 126.27	812.6 17946. 10251 10251	-812.6 24.96 989.29 989.29



```

=====
DATE OF SUBJECT 12-1979  NUM IDENTIFICATION 10-17-79-1
DC# 0.058  WORKING LIST FOR OPTION 2 WITH DECAY OF BBN
=====
DC# 0.058  (CAL/CM/HR)
=====
BNC1-60  (CM)
CC# 1 1-3  (NPS CM)
BFA# 3E12  (CU CM/HR)
MPP# 2E5  (OVL/50 CM)
=====
LENGTH 1.0E4
PATTERN 1.0E2
OVERSAMP TIME 10
=====
OPTION 2 FOR MC WITH DECAY OF BBN
=====
DISOLUTION WITH AND WITHOUT CERN CLOSURE (DISSEC WORKING LIST)
=====
PAGE 1
=====

```

[illegible]

Table AR.5.1

DATE OF RUN OCT 16, 1979 RUN IDENTIFICATION 10-16-79-3  
REFERENCE SET 2-DISSCC WORKING LIST FOR OPTION 1, WITH DECAY OF BPH  
DCP=0.094 (CAL/GM/YR)  
BMCL= 60 (CM)  
RCW= 1E-3 (CM)  
MBFA=3E12 (CU CM/YR)  
NBPH=2E6 (DYNE/SQ CM)  
DT= 1  
LENGTH= 1.0E4  
PRTPER= 1.0E2  
PLTPER= 1.0E2  
OVERRUN TIME AT  
OPTION 1 FOR NC WITH DECAY OF BPH  
OPTION 1 FOR NCC WITH DECAY OF BPH  
DISSOLUTION WITH AND WITHOUT CRACK CLOSURE (DISSCC WORKING LIST)

PAGE 1															
TIME	H PVDC ACDR PVRATC	HINR LPVCR ANCC	HOUTR EVISC NCC	SHLR BFTMP AVNECC	TER MTEMP NECC	TE MCL PVDCC	CL ACLS LPVCR	LPV SO MCLC	PVPS LNVFU ACLSC	BDRUA SCDIA SOC	ACDR CLC LNVFC	NC LPVC SCDIAC	AVNEC PVPSC BDRAT	NEC BDRUAC PVRAT	
E-00	E-00 E 03 E 09 E-03	E-03 E-00 E 06	E-06 E 15 E 06	E-06 E-00 E 03	E-03 E-00 E 03	E-00 E 03 E 03	E 03 E 03 E-00	E-00 E 12 E 03	E 03 E-00 E 03	E 09 E 03 E 12	E 09 E 03 E-00	E 06 E-00 E 03	E 03 E 03 E-03	E 03 E 09 E-03	
1.0	5.2000 .00 343.9 16.67	94.000 -.083 .01	0.00 6349.2 .0	-.00 32.000 .00	423.00 26.000 -.00	0.000 .06 .00	.00 .00 -.083	59. 0. .06	0.00 -.450 .00	349.0 .00 0.	349.0 .00 -.460	.0 .00 .00	.00 59. 983.33	-.00 343.9 16.67	
101.0	8.3346 .24 2899.0 88.25	9.260 -6.231 2.87	220.34 3583.8 3.1	626.92 63.346 .22	40.68 41.673 -.22	14.106 2.73 .24	.24 2.67 -6.183	2489. 211. 2.71	2.67 10.424 2.65	2909.5 67.34 209.	2909.5 .23 10.422	3.2 2470. 67.16	.22 2.65 396.67	-.22 2899.0 88.44	
201.0	8.8236 1.28 2977.8 196.94	3.079 -14.309 13.43	572.41 3259.1 16.7	724.72 68.236 1.24	11.28 44.118 -1.24	16.306 6.48 1.27	1.26 6.42 -14.249	5199. 507. 6.45	6.42 10.714 6.39	2982.3 89.93 505.	2982.3 1.26 10.712	16.8 5177. 89.79	1.25 6.39 998.50	-1.25 2977.8 197.28	
301.0	8.9810 3.03 2989.3 299.25	1.614 -20.547 28.01	708.43 3154.6 39.8	756.20 69.810 2.98	4.07 44.905 -2.93	17.015 10.26 3.02	3.01 10.20 -20.488	7227. 806. 10.23	10.20 10.867 10.17	2992.5 104.79 803.	2992.5 3.00 10.865	39.9 7206. 104.67	3.00 10.17 998.94	-3.00 2989.3 295.62	
401.0	9.0469 5.33 2993.1 378.76	1.250 -25.150 43.41	751.64 3110.9 69.9	769.37 70.469 5.26	2.24 45.234 -5.26	17.311 14.05 5.31	5.30 13.99 -25.096	8723. 1105. 14.01	13.99 10.971 13.95	2995.7 116.30 1102.	2995.7 5.28 10.970	70.1 8705. 116.20	5.28 13.95 999.12	-5.28 2993.1 379.13	
501.0	9.0857 8.02 2994.8 449.08	1.060 -28.559 57.99	768.11 3085.1 105.3	777.15 70.857 7.95	1.31 45.429 -7.95	17.496 17.84 7.99	7.99 17.78 -28.511	9824. 1405. 17.80	17.78 11.050 17.74	2997.2 125.89 1432.	2997.2 7.97 11.049	105.6 9807. 125.79	7.97 17.74 999.22	-7.97 2994.8 449.43	
PAGE 2															
601.0	9.1075 11.01 2995.8 508.30	.926 -31.055 71.06	776.51 3070.6 144.5	781.50 71.075 10.93	.67 45.538 -10.93	17.594 21.64 10.98	10.97 21.58 -31.011	10632. 1705. 21.59	21.58 11.114 21.53	2997.9 134.18 1701.	2997.9 10.95 11.113	144.9 10617. 134.09	10.96 21.53 999.28	-10.96 2995.8 508.62	
701.0	9.1171 14.21 2996.4 554.25	.827 -32.861 82.41	781.07 3054.3 186.0	783.41 71.171 14.12	.20 45.595 -14.12	17.627 25.43 14.17	14.17 25.37 -32.822	11228. 2004. 25.39	25.37 11.167 25.33	2999.4 141.95 2001.	2999.4 14.14 11.167	187.0 11214. 141.46	14.15 25.33 999.32	-14.15 2996.4 554.54	
801.0	9.1175 17.56 2996.7 600.49	.749 -34.157 92.17	783.10 3064.0 230.7	783.50 71.175 17.47	-.15 45.588 -17.47	17.529 29.23 17.52	17.52 29.17 -34.122	11667. 2304. 29.18	29.17 11.213 29.12	2998.7 143.22 2300.	2998.7 17.49 11.213	231.2 11657. 148.13	17.51 29.12 999.35	-17.51 2996.7 600.75	
901.0	9.1189 21.84 2997.0 636.36	.688 -35.102 100.46	781.26 3063.4 278.4	783.18 71.199 28.44	-.44 45.633 -28.44	17.599 21.64 17.59	17.59 21.58 -35.045	12001. 2604. 35.97	21.59 11.234 21.53	2999.9 143.22 11.234	2999.9 17.59 11.234	278.4 11657. 148.13	20.97 29.12 999.35	-20.97 2997.0 636.59	
1001.0	9.0986 24.56 2997.2 666.95	.635 -35.727 107.53	781.99 3076.5 322.9	779.73 70.986 24.47	-.66 45.493 -24.47	17.544 21.64 24.52	24.53 21.58 -35.697	12256. 2904. 35.77	35.76 11.290 36.71	2999.1 159.97 2900.	2999.1 24.49 11.289	323.4 12245. 159.90	24.51 36.71 999.38	-24.51 2997.2 667.15	
1101.0	9.0320 23.16 2997.4 693.16	.595 -36.131 113.59	779.58 3077.5 370.2	775.41 70.820 28.06	-.83 45.410 -28.06	17.469 21.62 28.11	28.11 21.58 -35.152	12455. 3204. 40.56	40.55 11.322 40.50	2999.2 165.25 3200.	2999.2 28.08 11.322	370.3 12445. 165.17	28.11 40.50 999.39	-28.11 2997.4 693.34	
1201.0	9.0620 31.80 2997.5 715.74	.561 -36.494 118.82	776.29 3100.8 418.0	772.40 70.620 31.69	-.97 45.310 -31.69	17.379 21.64 31.75	31.76 21.58 -36.467	12617. 3504. 44.35	44.35 11.352 44.29	2999.3 170.20 3499.	2999.3 31.71 11.351	418.6 12608. 170.12	31.74 44.29 999.40	-31.74 2997.5 715.91	
1301.0	9.0392 35.46 2997.6 735.31	.531 -36.708 123.39	772.31 3116.0 466.2	767.84 70.392 35.35	-1.08 45.196 -35.35	17.276 21.62 35.40	35.42 21.58 -36.682	12753. 3804. 48.15	48.15 11.379 48.09	2999.4 174.88 3799.	2999.4 35.37 11.378	466.8 12744. 174.80	35.40 48.09 999.40	-35.40 2997.6 735.46	



LEVEL EQUATIONS	INITIAL CONDITIONS AND SPECIAL FUNCTIONS	RATE EQUATIONS WITH ASSOCIATED CONSTANTS	AUXILIARY EQUATIONS WITH ASSOCIATED CONSTANTS
<b>HEAT</b> H.K=H.J+DT*(HINR.JK-ROUTR.JK)	H=5.2 HINR=0 PD=1. LOGFD=0 FDTAB=0/-0.03/-0.11/-0.38/-1.00/ -1.80/-2.17/-2.31/-2.80/ -3.28/-3.84/-4.0/-4.0/-4.0/ -4.0/-4.0/-4.0 LOCT=0 TIME=1. SHLR=0 ROUTR=0 MTEMP=26. BTEMP=32.	HINR.KL=DCP*FD.K DCP=.278/.167/.129/9.496E-2/.094/ 9.232E-2/8.580E-2/8.276E-2/ 7.770E-2/7.391E-2/7.055E-2/ 6.934E-2/6.697E-2/6.105E-2/ 5.240E-2/5.003E-2/4.167E-2/ 2.994E-2/2.309E-2/1.556E-2/ 7.831E-4 SHLR.KL=2E-4*(H.K-4.0)-2.4E-4 ROUTR.KL=DELAY3(SHLR.JK,DSHF) DSHF=100. STEMP=20.	FD.K=EXP(2.303*LOGFD.K) LOGFD.K=TABLE(FDTAB,LOCT.K,0,8,25) LOCT.K=LOGN(TIME.K)/2.303 MTEMP.K=(H.K-4.0)/0.2+STEMP BTEMP.K=32.+2*(MTEMP.K-26.)
<b>THERMAL EXPANSION</b> TE.K=TE.J+DT*(TER.JK)	TE=0 TER=0.423	TER.KL=UEC*(HINR.JK-ROUTR.JK)/0.2 UEC=0.9	
<b>CONTRACTION LENGTH</b> CL.K=MCL.J-LPV.J	CL=1.		LPV.K=MCL+PVFS.K-PVDC.K MCL.K=MCL+ACLS.K MCL=485./315./171./166./146./138./ 132./109./107./95.5/77.6/70.9/ 60./58.8/52.9/45.5/34.7/28.6/ 24.2/18.0/7.75
<b>PORE VOLUME PRODUCED BY SOLUTIONING</b> PVFS.K=PVFS.J+DT*(BDRUA.K)/DA	PVFS=0 DA=7.9E10	BDRUA.KL=PIFGE(MBFA,ACDR.K,ACDR.K, MBFA) MBFA=3E12	<b>OPTION: WITH CONSTANT BPH</b> ACDR.K=RCVR.K*NC.K RCVR.K=(3E7*BPH*RCW*RCW*CTL)/ (12.*BV*CPL) BPH=2E6 RCW=1.111E-4/1.0E-2/7.774E-3/ 5.634E-3/4.323E-3/3.912E-3/ 2.959E-3/2.131E-3/1.942E-3/ 1.265E-3/1.205E-3/1.0E-3/ 9.472E-4/6.844E-4/6.238E-4/ 4.136E-4/3.333E-4/2.968E-4/ 2.270E-4/1.852E-4/1.383E-4/ 1.111E-4/1.0E-4/1.0E-5 CTL=6E5 BV=1E-2 CPL=1E4 <b>OPTION: WITH DECAY OF BPH</b> ACDR.K=DCBPHA.K*MBPH*NC.K/(1.+ (DCBPHA.K*DCBPH.K*NC.K)) RCVR.K=ACDR.K/NC.K DCBPHA.K=(3E7*RCW*RCW*RCW*CTL)/ (12.*BV*CPL) DCBPHB.K=MBPH/MBFA MBPH=2E6 <b>OPTION 1</b> NC.K=DA*PVDC.K/(RCW*CTL*CPL) <b>OPTION 2</b> NC.K=CC*PIFGE(1E4,AVNEC.K,AVNEC.K, 1E4) AVNEC.K=MAX(NEC.K,-NEC.K) NEC.K=TE.K-CL.K BORAT.K=BDRUAC.K/BDRUA.K
<b>PORE VOLUME DESTROYED BY CONTRACTION</b> PVDC.K=PVDC.J-DT*(LPVCR.K)	PVDC=1. EVTAB=1.13E19,7.08E18,4.47E18,2.8 E18,1.78E18,1.26E18,8.91E17, 6.61E17,5.01E17,3.80E17,3.02 E17	LPVCR.KL=LPV.K*EXP(-2.303*ELP+3E7 *DT/EVISC.K)/DT-LPV.K/DT ELP=1.3E8	EVISC.K=TABLE(EVTAB,BTEMP.K,0, 250,25)
<b>SOLUTION OPENINGS</b> SO.K=SO.J+DT*BDRUA.K	SO=1.		ACLS.K=SO.K/BA.K SA.K=DA LNVFU.K=0.33*LOGN(SA.K)-0.46 SCDIA.K=2.*EXP(LNVFU.K)
<b>PORE VOLUME PRODUCED BY SOLUTIONING WITH CLOSURE</b> PVFSK.K=PVFSK.J+DT*(BDRUAC.K)/DA	PVFSK=0	BDRUAC.KL=PIFGE(MBFA,ACDRK.K, ACDRK.K,MBFA)	<b>OPTION: WITH CONSTANT BPH</b> ACDRK.K=RCVR.K*AMCC.K AMCC.K=(LPVC.K/MCLC.K)*MCC.K <b>OPTION: WITH DECAY OF BPH</b> ACDRK.K=DCBPHA.K*MBPH*AMCC.K/(1.+ (DCBPHA.K*DCBPHB.K*AMCC.K)) RCVRK.K=ACDRK.K/MCC.K <b>OPTION 1</b> MCC.K=DA*PVDCC.K/(RCW*CTL*CPL) <b>OPTION 2</b> MCC.K=CC*PIFGE(1E4,AVNECC.K, AVNECC.K,1E4) AVNECC.K=MAX(MECC.K,-MECC.K) MECC.K=TE.K-CLC.K
<b>PORE VOLUME DESTROYED BY CONTRACTION WITH CLOSURE</b> PVDCC.K=PVDCC.J-DT*(LPVCRK.K)	PVDCC=1.	LPVCRK.KL=LPVC.K*EXP(-2.303*ELP+ 3E7*DT/EVISC.K)/DT-LPVC.K/ DT	PVCRATC.K=PVDCC.K/MCLC.K
<b>SOLUTION OPENINGS WITH CLOSURE</b> SOC.K=SOC.J+DT*BDRUAC.K	SOC=1.		LNVFC.K=0.33*LOGN(SOC.K)-0.46 SCDIAC.K=2.*EXP(LNVFC.K)
<b>CONTRACTION LENGTH WITH CLOSURE</b> CLC.K=MCLC.J-LPVC.J	CLC=1.		

## LIST OF ACRONYMS AND INITIALISMS USED IN DISSCC

ACDR	(Total) Apparent Crack Discharge Rate
ACDRC	(Total) Apparent Crack Discharge Rate; with Closure
ACLS	Average Compaction Length from Solutioning
ACLSC	Average Compaction Length from Solutioning; with Closure
ANCC	Active Number of Cracks; reduced by Closure
AVNEC	Absolute Value of NEC
AVNECC	Absolute Value of NEC; with Closure
EDRAT	Brine Discharge Ratio; with and without Closure
EDRUA	Brine Discharge Rate to Upper Aquifer
EDRUAC	Brine Discharge Rate to Upper Aquifer; with Closure
BTEMP	Backfill Temperature
BMCL	Backfill Maximum Compaction Length
BPH	Brine Pressure Head(Conetant)
BV	Brine Viscosity
CC	Crack Coefficient
CL	Compaction Length
CLC	Compaction Length; with Closure
CPL	Crack Path Length
CTL	Crack Trace Length
DA	Depository Area
DCBPHA	Dimensional Conetant for EPH
DCBPHB	Brine Pressure Flow Ratio
DCP	Dimensionel Constant for thermal Power
DSHF	Delay Surface Heat Flux
ELP	Effective Load Pressure
EVISC	Effective VISCosity
EVTAB	Effective Viscosity TABulation
FD	Radionuclide Decay Fraction
FDTAB	Fraction Decay TABLE
H	Heat
HINR	Heat INput Rate
HOUTR	Heat OUTput Rate
LNVC	Natural Log single cavity Volume Function; with Closure
LNVCU	Natural Log single cavity Volume Function
LOGFD	LOGten Decay Fraction
LOGT	LOGten Time
LPV	Linear Pore Volume
LPVC	Linear Pore Volume; with Closure
LPVCR	Linear Pore Volume Compaction Rate
LPVCRG	Linear Pore Volume Compaction Rate; with Closure
MBFA	Maximum Brine Flow in Aquifer
MCL	Maximum Compaction Length
MCLC	Maximum Compaction Length; with Closure
MTEMP	Mean TEMperature for STEMP
NBPH	INITial Brine Pressure Head(Decey)
NC	Number of Cracks
NCC	Number of Cracks; with Closure
NKC	Net Expansion minus Compaction
NKCG	Net Expansion minus Compaction; with Closure
PVDC	(Linear) Pore Volume Destroyed by Compaction
PVDCG	(Linear) Pore Volume Destroyed by Compaction; with Closure
PVPS	(Linear) Pore Volume Produced by Solutioning
PVPSG	(Linear) Pore Volume Produced by Solutioning; with Closure
PVRAT	(Linear) Pore Volume RATIO
PVRATG	(Linear) Pore Volume RATIO; with Closure
RCVR	Reference Crack Volume Rate
RCVRG	Reference Crack Volume Rate; with Closure
RCW	Reference Crack Width
SA	Solutioning Area
SCDIA	Single Cavity DIAMeter
SCDIAC	Single Cavity DIAMeter; with Closure
SHLR	Steady Heat Loss Rate
SO	Solution Openings
SOC	Solution Openings; with Closure
T	Time
TE	Thermal Expansion
TER	Thermal Expansion Rate
UEC	Unit Expansion Coefficient



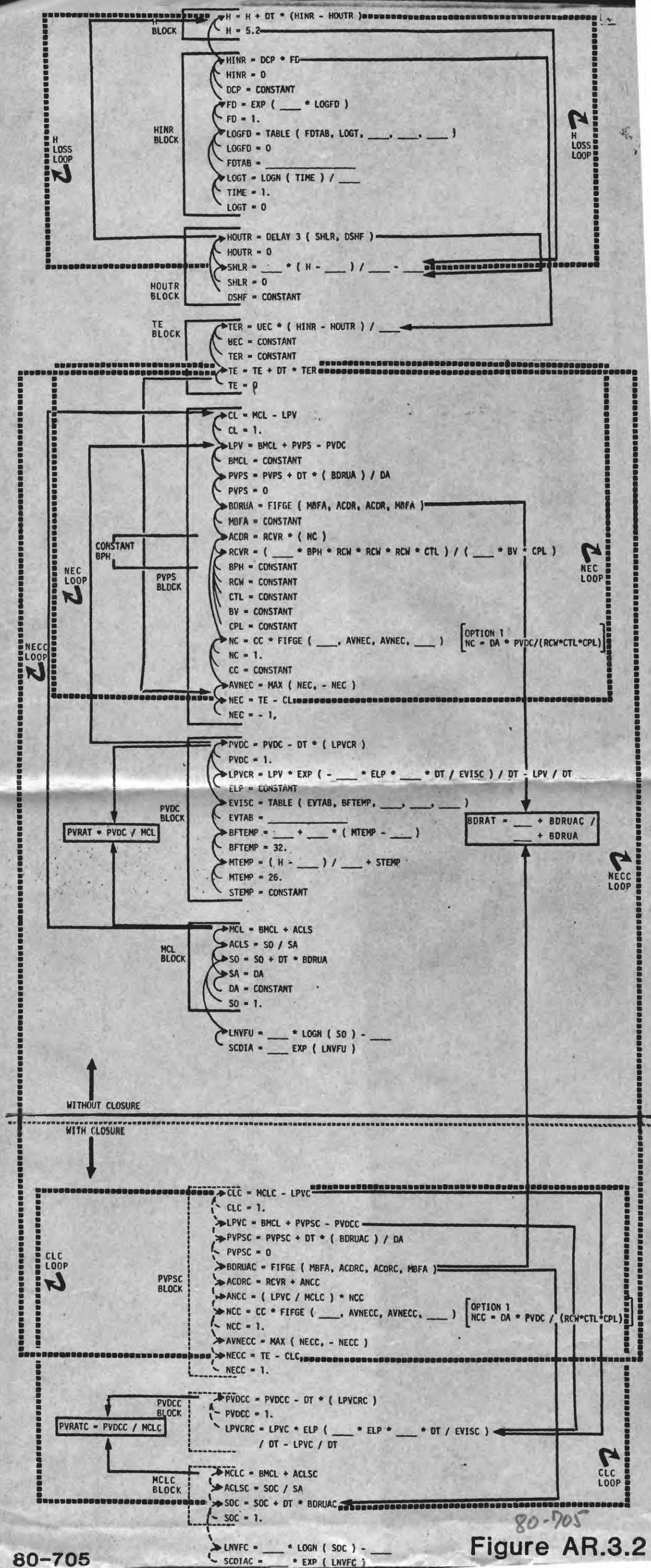


Figure AR.3.2

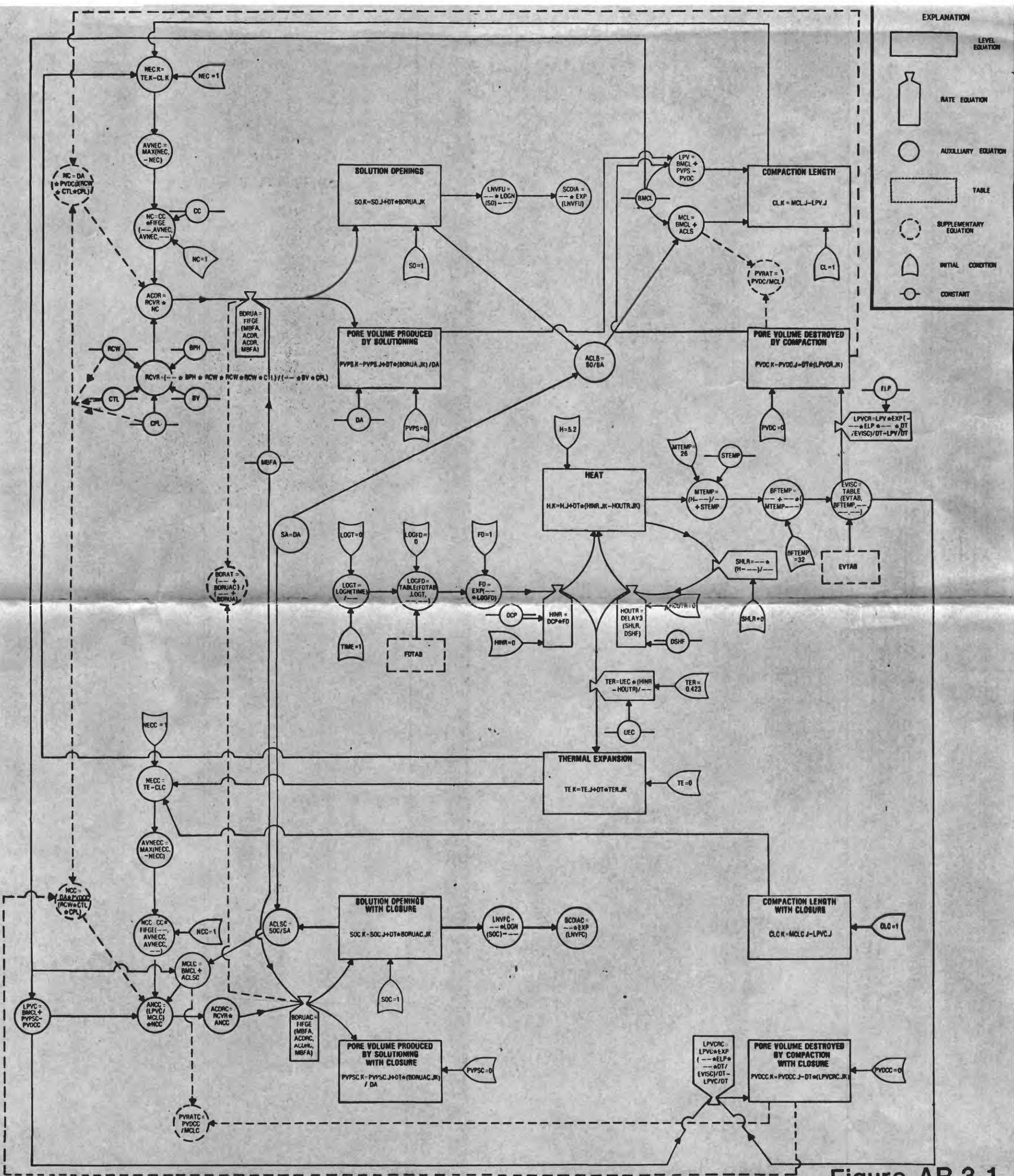


Figure AR.3.1